1. Report No.	2. Government Accession No.	3. Recipient's Catalog No.
FHWA/TX-09/0-5627-1		

4. Title and Subtitle	5. Report Date
PREDICTING ASPHALT MIXTURE SKID RESISTANCE BASED ON AGGREGATE CHARACTERISTICS	October 2008 Published: August 2009
	6. Performing Organization Code
7. Author(s)	8. Performing Organization Report No.
Eyad Masad, Arash Rezaei, Arif Chowdhury, and Pat Harris	Report 0-5627-1
9. Performing Organization Name and Address Texas Transportation Institute The Texas A&M University System College Station, Texas 77843-3135	10. Work Unit No. (TRAIS)
	11. Contract or Grant No. Project 0-5627
12. Sponsoring Agency Name and Address Texas Department of Transportation Research and Technology Implementation Office P.O. Box 5080 Austin, Texas 78763-5080	13. Type of Report and Period Covered Technical Report: September 2006 – August 2008
	14. Sponsoring Agency Code

15. Supplementary Notes

Project performed in cooperation with the Texas Department of Transportation and the Federal Highway Administration.

Project Title: Aggregate Resistance to Polishing and Its Relationship to Skid Resistance

URL: http://tti.tamu.edu/documents/ 0-5627-1.pdf

16. Abstract

The objective of this research project was to develop a method to determine the skid resistance of an asphalt mixture based on aggregate characteristics and gradation. Asphalt mixture slabs with different combinations of aggregate sources and mixture designs were fabricated in the laboratory, and their skid resistance was measured after different polishing intervals. The wheel-polishing device developed by the National Center for Asphalt Technology (NCAT) was used for polishing the slabs. Frictional characteristics of each slab were measured by sand patch method, British Pendulum, Dynamic Friction Tester (DFT), and Circular Texture Meter (CTMeter). Aggregates were characterized using a number of conventional test methods, and aggregate texture was measured using the Aggregate Imaging System (AIMS) after different polishing intervals in the Micro-Deval device. Petrographic analyses were performed using thin sections made with aggregates from each of these sources. Petrographic analyses provided the mineralogical composition of each source. The aggregate gradation was quantified by fitting the cumulative Weibull distribution function to the gradation curve. This function allows describing the gradation by using only two parameters.

The results of the analysis confirmed a strong relationship between mix frictional properties and aggregate properties. The main aggregate properties affecting the mix skid resistance were Polish Stone Value, texture change before and after Micro-Deval measured by AIMS, terminal texture after Micro-Deval measured by AIMS, and coarse aggregate acid insolubility value.

The analysis has led to the development of a model for the International Friction Index (IFI) of asphalt mixtures as a function of polishing cycles. The parameters of this model were determined as functions of (a) initial and terminal aggregate texture measured using AIMS, (b) rate of change in aggregate texture measured using AIMS after different polishing intervals, and the (c) Weibull distribution parameters describing aggregate gradation. This model allows estimating the frictional characteristics of an asphalt mixture during the mixture design stage.

17. Key Words	18. Distribution Statement
Skid Resistance, Asphalt Mixture Polishing, Aggregate Characteristics	No restrictions. This document is available to the public through NTIS: National Technical Information Service Springfield, Virginia 22161 http://www.ntis.gov No restrictions

19. Security Classif.(of this report)	20. Security Classif.(of this page)	21. No. of Pages	22. Price
Unclassified	Unclassified	226	

PREDICTING ASPHALT MIXTURE SKID RESISTANCE BASED ON AGGREGATE CHARACTERISTICS

by

Eyad Masad, Ph.D., P.E.
E.B. Snead I Associate Professor
Zachry Department of Civil Engineering
Texas A&M University

Arash Rezaei
Graduate Research Assistant
Zachry Department of Civil Engineering
Texas A&M University

Arif Chowdhury
Assistant Research Engineer
Texas Transportation Institute

and

Pat Harris
Associate Research Scientist
Texas Transportation Institute

Report 0-5627-1
Project 0-5627
Project Title: Aggregate Resistance to Polishing and Its Relationship to Skid Resistance

Performed in cooperation with the
Texas Department of Transportation
and the
Federal Highway Administration

October 2008
Published: August 2009

TEXAS TRANSPORTATION INSTITUTE
The Texas A&M University System
College Station, Texas 77843-3135

DISCLAIMER

The contents of this report reflect the views of the authors, who are responsible for the facts and accuracy of the data presented herein. The contents do not necessarily reflect the official view or policies of the Federal Highway Administration (FHWA) or the Texas Department of Transportation (TxDOT). This report does not constitute a standard, specification, or regulation. The engineer in charge was Eyad Masad P.E. #96368.

ACKNOWLEDGMENTS

The authors wish to express their appreciation to the Texas Department of Transportation personnel for their support throughout this project, as well as the Federal Highway Administration. The authors would also like to thank the project director, Ms. Caroline Herrera, and the members of the project monitoring committee, Mr. Ed Morgan and Ms. Zyna Polanski, for their constant guidance and valuable technical comments during this project.

TABLE OF CONTENTS

LIST OF FIGURES

LIST OF TABLES

CHAPTER I – INTRODUCTION

In 2005, 6.1 million traffic crashes, 43,443 traffic fatalities, and approximately 2.7 million traffic-related injuries were reported by National Highway Traffic Safety Administration (NHTSA) throughout the United States (Noyce et al., 2005).

The nationwide studies show that between 15 to 18 percent of crashes occur on wet pavements (Smith, 1976; Davis et al., 2002; Federal Highway Administration (FHWA), 1990). According to the National Transportation Safety Board and FHWA reports, approximately 13.5 percent of fatal accidents occur when pavements are wet (Chelliah et al., 2003; Kuemmel et al., 2000). Many researchers indicated that there is a relationship between wet weather accidents and pavement friction (Rizenbergs et al., 1972; Giles et al., 1962; McCullough et al., 1966; Wallman and Astron, 2001; Gandhi et al., 1991). In wet conditions, the water film covering the pavement acts as a lubricant and reduces the contact between the tires and the surface aggregate (Flintsch et al., 2005; Jayawickrama and Thomas, 1998). Hence, wet-pavement surfaces exhibit lower friction than dry-pavement surfaces. In addition to the lubricating effect of water at high speeds, certain depths of water film without any facility to drain may result in hydroplaning, which is considered the primary cause of accidents in wet weather conditions (Flintsch et al., 2005; Agrawal and Henry, 1979).

This accident rate can be reduced greatly by implementing corrective measures in hazardous areas. Safety evaluation of the roads and analyzing the different factors affecting pavement friction are necessary for future safety improvements. Research studies have shown that an increase in average pavement friction from 0.4 to 0.55 would result in a 63 percent decrease in wet-pavement crashes (Hall et al., 2006; Miller and Johnson, 1973). Research by Kamel and Gartshore also showed that by improving the skid resistance, the wet weather crashes decreased by 71 percent in intersections and 54 percent on freeways (Kamel and Gartshore, 1982; Hall et al., 2006). The Organization for Economic Cooperation and Development (OECD) revealed that there was a linear relationship between the slipperiness of the road surface and the crashes. Moreover, with an increase in slipperiness of the road surface, the rate of crashes increased (OECD, 1984; Hall et al., 2006). Roe et al. (1991) also reported that with an increase in pavement

friction, the rate of crashes decreased. Wambold et al. (1986) reported a statistically significant relationship between wet-weather crashes and the skid numbers measured with a skid trailer. Other researchers also demonstrated the relationship between pavement skid resistance and the effect of pavement friction improvement on the crash rates (Gothie, 1996; Bray, 2002; McLean, 1995; Larson, 1999; Schulze et al., 1976).

Pavement friction is primarily a function of the surface texture, which includes both microtexture and macrotexture. Pavement microtexture is defined as "a deviation of a pavement surface from a true planar surface with characteristic dimensions along the surface of less than 0.5 mm," while the pavement macrotexture is defined as "a deviation of 0.5 mm - 50 mm" (Henry, 1996; Wambold et al., 1995).

On one hand, microtexture that is primarily an aggregate surface characteristic provides a rough surface that disrupts the continuity of the water film and produces frictional resistance between the tire and pavement by creating intermolecular bonds. On the other hand, macrotexture that is an overall asphalt mixture characteristic provides surface drainage paths for water to drain faster from the contact area between the tire and pavement, prevents hydroplaning, and improves wet frictional resistance particularly at high speed areas (Fulop et al., 2000; Hanson and Prowell, 2004; Kowalski, 2007). Many factors influence the level of skid resistance on a paved road such as (Chelliah et al., 2003):

- microtexture and macrotexture,
- age of the road surface,
- seasonal variation,
- traffic intensity,
- aggregate properties, and
- road geometry.

While there is much research about increasing the life span of pavement materials, there is no direct specification for the selection and use of aggregate and mixture design to assure satisfactory frictional performance. In addition, current methods of evaluating aggregates for use in asphalt mixtures are mainly based on historical background of the aggregate performance (West et al., 2001; Goodman et al., 2006).

The high correlation between pavement skid resistance and rate of crashes demands a comprehensive material selection and mixture design system. The material characteristics including aggregate and mixture type will be studied in this project, and a relationship will be developed between aggregate characteristics and frictional properties of the pavement.

PROBLEM STATEMENT

The selection of aggregates has always been a question for the mix designers. Furthermore, frictional properties of aggregates and their ability to keep their rough texture against polishing action of the passing traffic need to be addressed carefully. Any mixture design system that does not consider these important factors may lead to additional cost for surface treatments. A comprehensive system for selecting aggregate based on a quantitative measurement of the physical properties of aggregate related to pavement skid resistance would help to reduce the cost of maintenance and rehabilitation. This system would propose the optimal pavement skid resistance by combining the effects of pavement microtexture and macrotexture. To achieve this optimization, an accelerated polishing method along with systematic test methods for measuring the frictional properties of the pavement are required. This system would facilitate the selection of aggregate type and mixture design to satisfy safety requirements.

OBJECTIVES

The purpose of this study is to investigate and develop a laboratory procedure and a testing protocol to accelerate polishing of hot mix asphalt (HMA) surfaces to evaluate changes in frictional characteristics as a function of the polishing effect.

The evaluation of aggregates with different characteristics and the study of frictional characteristics of mixtures with different aggregate types are used are other objectives of this study. Development of the relationship between mixture frictional characteristics and aggregate quantitative indices are also investigated in this research project.

SCOPE OF THE STUDY

The literature survey shows that aggregate characteristics affect frictional properties of flexible pavements to. The hypothesis behind this study is that it is possible to improve the frictional performance of the pavement surface by the selection of polish-resistant aggregates with certain shape characteristics.

The scope of this study included the investigation of the relationship between pavement skid resistance and following aggregate characteristics: aggregate shape characteristics measured by Aggregate Imaging System (AIMS), British Pendulum value, coarse aggregate acid insolubility, Los Angeles weight loss, Micro-Deval weight loss, and Magnesium sulfate weight loss. Based on laboratory measurements on three mixture types—Type C, Type D, and Porous Friction Course (PFC)—the International Friction Index (IFI), a harmonization tool for measured frictional properties across the world, was calculated and the effect of different aggregate properties on frictional characteristics was investigated. Aggregate types (crushed gravel, granite, sandstone, and two types of limestone) commonly used in HMA in the south central region of the U.S. were the focus of this research study.

Friction and texture measurements were conducted on 13 laboratory-prepared and polished HMA slabs. To obtain frictional performance curves, measurements were performed before polishing and after the application of different numbers of polishing cycles. Laboratory texture and friction tests were performed using the British Pendulum, Circular Track Meter (CTM), Dynamic Friction Tester (DFT) devices, and Sand Patch method.

ORGANIZATION OF THE REPORT

The first part of this report includes the results of the literature search. The second part includes the description of the materials and equipment used in this study. The third part presents the results and discussion. This information is followed by conclusions and recommendations extracted from data analysis.

CHAPTER II – LITERATURE REVIEW

INTRODUCTION

This section summarizes the general knowledge, and research studies have been done on characterization of the frictional properties of the pavement surface. The first part of this chapter will explain the friction mechanism and the factors affecting frictional properties of the road surface. The microtexture and macrotexture as two important parameters contributing in pavement friction will be explained in detail. Additionally, the methods currently used to measure the skid resistance will be discussed. This chapter also will discuss the different aggregate characteristics related to pavement skid resistance. Different approaches developed to model pavement friction and the concept of International Friction Index (IFI) will also be introduced and discussed.

DEFINITION OF FRICTION

Pavement surface friction is a measure of pavement riding safety and has a great role in reducing wet-pavement skid accidents (FHWA, 1980; Li et al., 2005; Lee et al., 2005). Friction force between the tire and the pavement surface is an essential part of the vehicle-pavement interaction. It gives the vehicle the ability to accelerate, maneuver, corner, and stop safely (Dewey et al., 2001).

Skid resistance is the friction force developed at the tire-pavement contact area (Noyce et al., 2005). The skid resistance is an interaction between many factors. Various characteristics of pavement surface and the tire influence the friction level. Because of the complicated nature of the tire-pavement interaction, it is very difficult to develop realistic models to predict in-situ pavement friction (Li et al., 2005).

There are many factors contributing to developing friction between rubber tires and a pavement surface including the texture of the pavement surface, vehicle speed, and the presence of water. Additionally, the characteristics of the construction materials, construction techniques, and weathering influence pavement texture (Dewey et al., 2001). Wilson and Dunn addressed several factors that affect the frictional characteristics of a tire-pavement system. These factors can be categorized as (Wilson and Dunn, 2005):

- vehicle factors:
  - vehicle speed,
  - angle of the tire to the direction of the moving vehicle,
  - the slip ratio,
  - tire characteristics (structural type, hardness, and wear), and
  - tire tread depth.
- road surface aggregate factors:
  - geological properties of the surfacing aggregate,
  - surface texture (microtexture and macrotexture), and
  - type of surfacing.
- load factors:
  - age of the surface,
  - the equivalent number of vehicle traffic loadings,
  - road geometry, and
  - traffic flow conditions.
- environmental factors:
  - temperature;
  - prior accumulation of rainfall, rainfall intensity, and duration; and
  - surface contamination.

Moore (1972) in an attempt to explain the friction phenomenon between tire and pavement, showed that frictional forces in elastomers[1] comprised primarily of adhesive and hysteresis components as shown in Figure 1 (Choubane et al., 2004). During sliding on a wet pavement, a complex interplay between adhesion and hysteresis forces contributes to vehicle stopping distance.

Intermolecular binding or adherence at the surface level creates the adhesive component of friction. As the micro-asperities or surface irregularities of the two surfaces are exposed to each other, Vander Waals or dipole forces provide an attractive force keeping the two asperities together and prevent further movement (Dewey et al., 2001; Person, 1998).

[1] An elastomer is a polymer that shows elastic behavior (e.g., rubber).

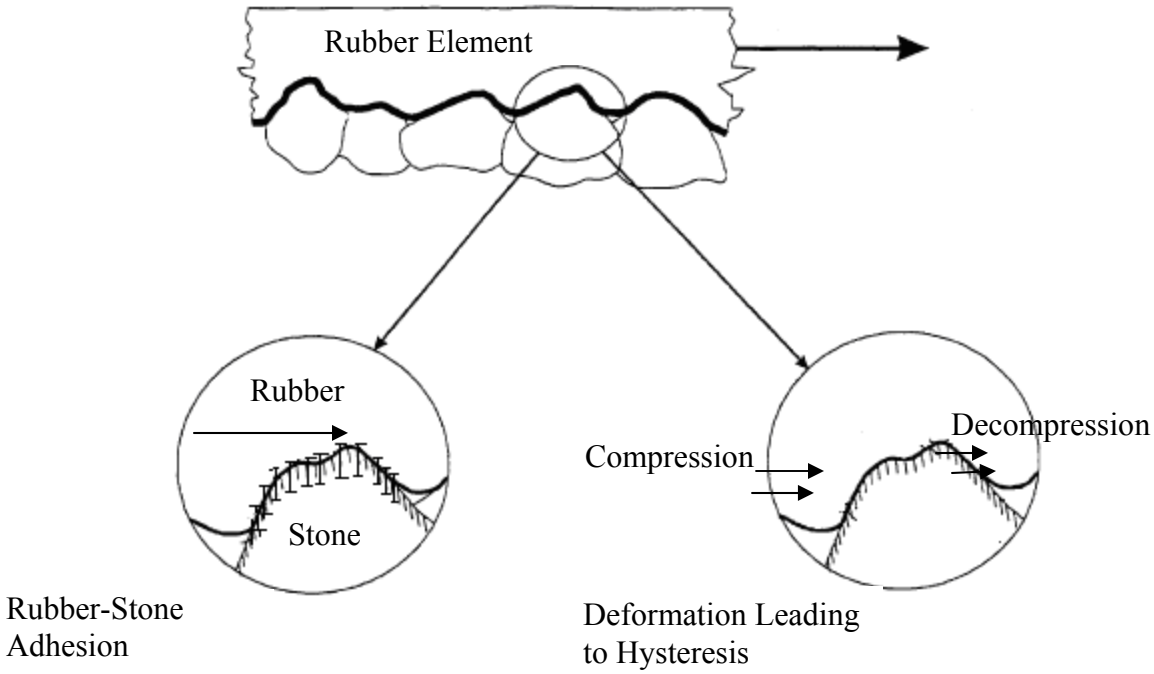

Figure 1. Schematic Plot of Hysteresis and Adhesion (Choubane et al., 2004).

The adhesion relates to the actual contact area between the tire and the traveled surface as well as the shear strength of the interface (Zimmer et al., 2003; Choubane et al., 2004). The adhesion friction is dominant until critical slip occurs. Typically, at driving speed on wet pavement, the adhesion accounts for two-thirds of the resistance force (Hogervorst, 1974).

The hysteresis component of friction arises from the energy loss due to bulk deformation of rubber around the protuberance and depression of pavement surface (Linder et al., 2004). It reflects energy losses that occur, as the rubber is alternately compressed and expanded when passing across the asperities of a rough surface pavement (Choubane et al., 2004).

Moreover, during a bulk deformation process, the friction force takes place at the interface of the moving objects. In this process, the elastomer drapes over, in, or around each macro-asperity. After passing over the asperity, the rubber returns to its initial state

but with a net loss of energy. This loss of energy contributes to the hysteresis part of friction (Linder et al., 2004).

Several researchers tried to relate the pavement texture and friction. Yandell emphasized the contribution of various texture scales to the hysteresis friction (Yandell, 1971; Yandell and Sawyer, 1994; Do et al., 2000). Forster (1981) used linear regression analysis to show that the texture shape, defined also by an average slope, explains friction satisfactorily. Roberts (1988) showed the forces and the energy dissipation between tire and pavement surface depend on the material properties and the separation velocity. Kummer (1966) showed that at high-speed sliding, the hysteresis component reaches a maximum value; while at relatively low speeds of sliding, adhesion is at a maximum value (Dewey et al., 2001).

PAVEMENT TEXTURE

As travel safety and efficiency of the road system are of increasing importance to state agencies, friction measurements have become an important tool in the management of pavement surfaces (Choubane et al., 2004). The friction-related properties of a pavement depend on its surface texture characteristics. These characteristics, as previously stated, are known as macrotexture and microtexture (Kummer and Meyer, 1963).

Macrotexture refers to the larger irregularities in the road surface (coarse-scale texture) that affect the hysteresis part of the friction. These larger irregularities are associated with voids between aggregate particles. The magnitude of this component will depend on the size, shape, and distribution of coarse aggregates used in pavement construction, the nominal maximum size of aggregates as well as the particular construction techniques used in the placement of the pavement surface layer (Noyce et al., 2005; National Asphalt Pavement Association (NAPA), 1996).

Microtexture refers to irregularities in the surfaces of the aggregate particles (fine-scale texture) that are measured at the micron scale of harshness and are known to be mainly a function of aggregate particle mineralogy (Noyce et al., 2005). These irregularities make the stone particles smooth or harsh when touched. The magnitude of microtexture depends on initial roughness on the aggregate surface and the ability of the

aggregate to retain this roughness against the polishing action of traffic and environmental factors (Noyce et al., 2005; Jayawickrama et al., 1996). Microtexture affects mainly the adhesion part of the friction (Noyce et al., 2005).

Several researchers tried to find quantitative measures to define microtexture and macrotexture and relate them to pavement friction. Moore (1975) defined three parameters for characterizing a surface texture: size, interspace or density, and shape. Taneerananon and Yandell (1981) showed that, compared with the two other parameters, the role of density is of minor importance in the water drainage mechanism. Kokkalis and Panagouli (1999) tried to explain surface texture by using fractals. They developed a model to relate surface depth and density to pavement friction.

Pavement texture generally is divided into the two size classes of microtexture and macrotexture (ASTM E 867). Surface asperities less than 0.5 mm (0.02 inch) in height are classified as microtexture, while asperities greater than 0.5 mm (0.02 inch) in size are considered as macrotexture (Dewey et al., 2001). Figure 2 shows the different categories of pavement texture.

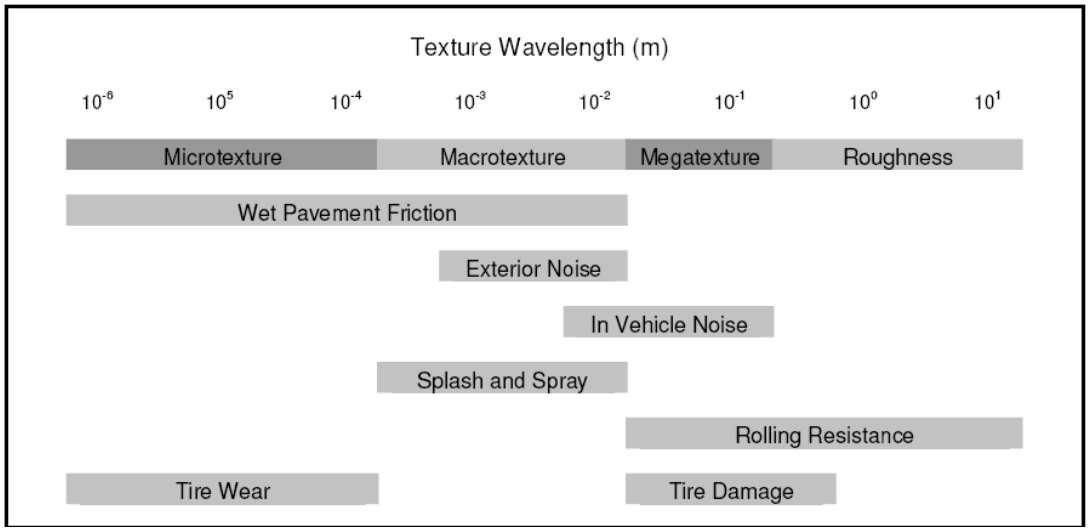

Figure 2. Pavement Wavelength and Surface Characteristics (Hall et al., 2006).

Figure 3 shows the schematic plot of the effect of micro/macrotexture on pavement friction. Adequate macrotexture is important for the quick dispersion of water accumulated on the surface of the pavement to prevent hydroplaning. Additionally, it aids for the development of the hysteresis component of friction that is related to energy loss

as the tire deforms around macroasperities and consequently increases pavement friction (Dewey et al., 2001; Forster, 1989; Ergun et al., 2005). Macrotexture of the pavements could be estimated by simulating the percentage of contact points within the area of a tire footprint on the pavement surface (Forster, 1989). Davis et al. (2002) showed that there is a significant influence of mixture parameters on the ribbed tire skid resistance measurements and laser profile mean texture depth. Moreover, they stated that it is possible to predict some of the frictional properties of the wearing surface mixes based on HMA mix design properties (Davis et al., 2002).

Bloem (1971) showed that an average texture depth of about 0.5 mm (0.02 inch) is required as the minimum to assure the desired depletion of water from under the tire (Bloem, 1971).

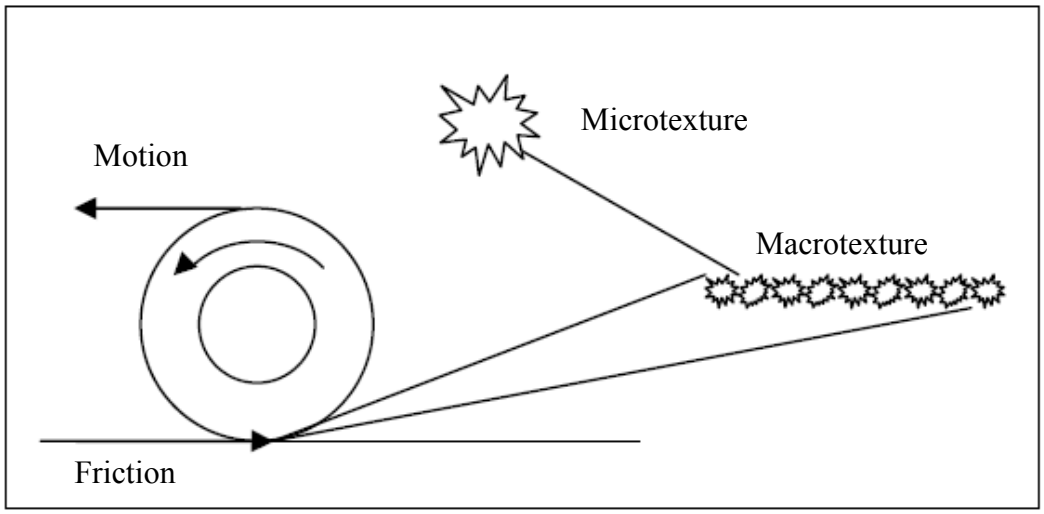

Figure 3. Schematic Plot of Microtexture/Macrotexture (Noyce et al., 2005).

Experiments conducted by Balmer (1978) showed that changes in surface textures from about (0.02 inch to 0.12 inch) 0.5 to over 3mm resulted in a difference of 16 km/h (10 mph) in the speed for the initiation of hydroplaning (Gardiner et al., 2004; Balmer, 1978).

Microtexture plays a significant role in the wet road/tire contact. The size of microasperities plays a key role in overcoming the thin water film. Existence of microtexture is essential for squeezing the thin water film present in the contact area and

generating friction forces (Do et al., 2000). Moreover, the role of microtexture is to penetrate into thin water film present on the surface of the pavement so that the intimate tire/pavement contact is maintained (Forster, 1989). Drainage is controlled by the shape of microasperities (Do et al., 2000; Rhode, 1976; Taneerananon and Yandell, 1981). Savkoor (1990) also showed that drainage of the water film between tire and pavement is a function of amplitude and number of microasperities on a surface (Do et al., 2000). Forster (1989) developed a parameter to account for microtexture. This parameter is a combination of average height and average spacing between microasperities. A study by Ong et al. (2005) showed that in the pavements comprised of coarse aggregates with high microtexture in the range of 0.2 mm to 0.5 mm, hydroplaning occurs at a 20 percent higher speed. This means that using materials with better microtexture reduces the chance of hydroplaning.

Horne (1977) also stated that pavements with a good microtexture could delay hydroplaning (Ong et al., 2005). Pelloli (1972) based his research on five different types of surfaces and found that the amount of microtexture would affect the relationship between friction coefficient and the water depth accumulated on the surface (Ong et al., 2005). Moore (1975) reported a minimum water film thickness to be expelled by microasperities in the order of 5×10^{-3} mm. Bond et al. (1976) reported the same order of magnitude from visual experiments conducted to monitor the water film between a tire and a smooth transparent plate.

Bond et al. (1976) showed how differences in surface microtexture and macrotexture of pavement surfaces influence peak brake coefficients of a standard test tire (Johnsen, 1997). Leu and Henry (1978) demonstrated how skid resistance tests taken from different pavement surfaces are different based on their microtexture and macrotexture. Horne and Buhlmann (1983), however, showed the surface friction measurements are poorly related to pavement texture measurements (Johnsen, 1997).

Hogervorst (1974) reported that the change of skid resistance with vehicle speed depends on both microtexture and macrotexture. Microtexture defines the magnitude of skid resistance, and macrotexture will control the slope of skid resistance reduction as speed increases. Moreover, macrotexture affects the skid resistance of pavements at high speed by reducing the friction-speed gradient and facilitating the drainage of water. It has

little effect on friction level at low speed. On the other hand, at low speeds, microtexture dominates and defines the level of friction (Hall et al., 2006; Rose and Gallaway, 1970; Gallaway et al., 1972) (Figure 4).

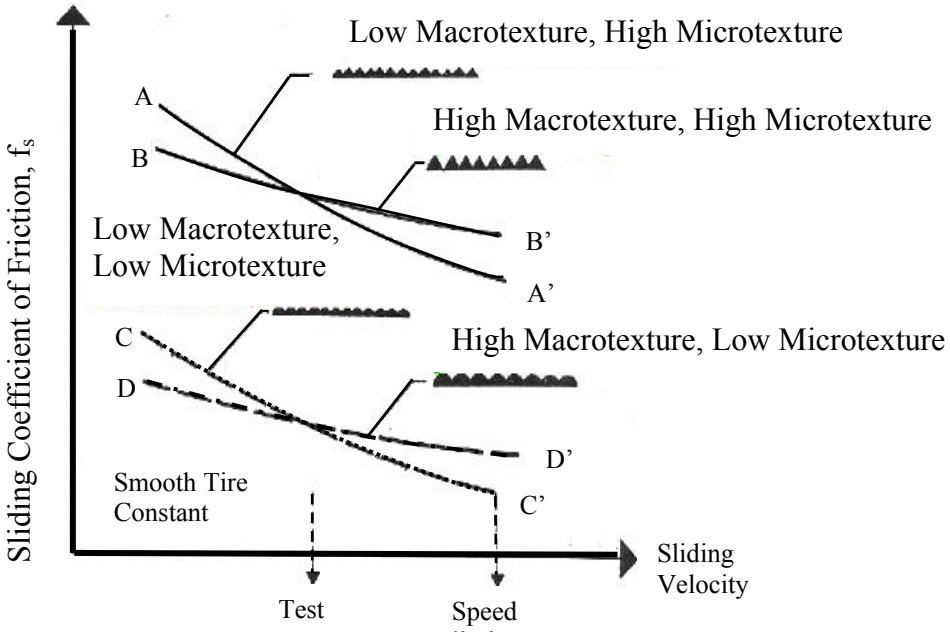

Figure 4. Schematic Plot of the Effect of Microtexture/Macrotexture on Pavement Friction (Noyce et al., 2005).

Researchers noted that both macrotexture and microtexture of pavement surface are influenced by the properties of the coarse aggregates exposed at the wearing course (Dewey et al., 2001; Forster, 1989).

TEXTURE AND FRICTION MEASUREMENT

Field skid resistance is generally measured by the force generated when a locked tire slides along a pavement surface (Cairney, 1997). These measurements should be precise, repeatable, and reproducible to reflect the real condition in the field (Kummer and Meyer, 1963). State-of-the-art friction testing comprises of applying a standard tire to pavement surfaces with controlled wheel slip (0 to 100 percent slip) while measuring

friction between a tire (on the wheel) and pavement (American Society for Testing and Materials (ASTM) E274, E303, E503, E556, E670, E707) (Johnsen, 1997).

There are four main types of skid resistance measuring approaches (Kokot, 2005; Roe et al., 1998; Permanent International Association of Road Congresses (PIARC), 1995):

- locked wheel, where the force is measured while a 100 percent slip condition is produced;
- sideway force, where the force is measured on a rotating wheel with a yaw angle of 20°;
- fixed slip, where friction is measured for wheels that are constantly slipping; and
- variable slip, where devices are designed to measure at any desired slip, sweep through a predetermined set of values, or seek the maximum friction.

In each technique, relating locked-wheel and variable-slip of tires to the rolling, braking, or cornering, friction coefficient is measured on wet pavement surfaces (Johnsen, 1997).

Pavement friction testing with the locked wheel tester can be conducted with either a standard ribbed tire or a standard smooth tire (Lee et al., 2005). The most common method is the locked-wheel braking mode, which is specified by ASTM E-274. The concept of a skid trailer was introduced in the mid-1960s to improve the safety and efficiency of friction testing operations (Choubane et al., 2004).

According to Saito et al. (1996), there are also some disadvantages associated with locked-wheel testers:

- Continuous measurement of skid resistance is not possible.
- Although Kummer and Meyer (1963) showed the cost of a locked-wheel trailer is about 90 percent of other field test methods, its initial and operating costs of the test equipment are still high.
- Tests are conducted at only one speed so that speed dependency of skid resistance cannot be determined without repeated measurements on the same sections of road and different speeds.

Other types of measurement modes comprise the fixed slip, variable slip, and the sideway force or cornering mode. In the slip mode (fixed or variable), the friction factor

is a function of the "slip" of the test wheel while rolling over the pavement. The sideway mode uses a test wheel that moves at an angle to the direction of motion. The use of this test procedure is based upon the assumption that the critical situation for skid resistance occurs in cornering (Saito et al., 1996).

These methods are categorized as field modes. Other testing modes include portable and laboratory testers. The most common tester is the British pendulum tester (BPT), which is a dynamic pendulum impact-type tester and is specified in ASTM E303. The British pendulum tester (Giles et al., 1964) is one of the simplest and cheapest instruments used in the measurement of friction characteristics of pavement surfaces. The BPT has the advantage of being easy to handle, both in the laboratory and in the field, but it provides only a measure of a frictional property at a low speed (Saito et al., 1996). Although it is widely suggested that the measurement is largely governed by the microtexture of the pavement surface, experience has shown that the macrotexture can also affect the measurements (Fwa et al., 2003; Lee et al., 2005). Moreover, Fwa et al. (2003) and Liu et al. (2004) showed that the British pendulum measurements could be affected by the macrotexture of pavement surfaces, aggregate gap width, or the number of gaps between aggregates. It can also lead to misleading results on coarse-textured test surfaces (Lee et al., 2005).Other researchers pointed out that the British pendulum tester exhibited unreliable behavior when tested on coarse-textured surfaces (Forde et al., 1976; Salt, 1977; Purushothaman et al., 1988).

The DFT is a disc-rotating-type tester that measures the friction force between the surface and three rubber pads attached to the disc. The disc rotates horizontally at a linear speed of about 20 to 80 km/hr under a constant load. It touches the surface at different speeds so the DFT can measure the skid resistance at any speed in this range (Saito et al., 1996). Studies by Saito et al. (1996) showed that there is a strong relationship between the coefficient of friction of the DFT and the British Pendulum Number (BPN) at each point for each measuring speed (Saito et al., 1996).

Measuring the pavement microtexture and macrotexture and relating these measurements to pavement skid resistance has been a major concern for pavement researchers. The practice of measuring pavement macrotexture has been a common practice in recent years (Abe et al., 2000; Henry, 2000). Yandell et al. (1983) stated that it

is desirable to predict pavement surface friction with computer models by use of laboratory measurements rather than field measurement. The use of a computer model is motivated considering that test methods are not easily repeatable and prediction methods will save time and money (Johnsen, 1997).

Macrotexture data is generally measured using a volumetric technique. Essentially, this method consists of spreading a known volume of a material (sand, glass beads, or grease) into the pavement surface and measuring the resulting area. Dividing the initial volume by the area gives Mean Texture Depth (MTD) (Ergun et al., 2005; Leland et al., 1968). It has been reported that the sand patch method, Silly Putty method, and volumetric methods are burdensome to use in routine testing (Jayawickrama et al., 1996).

Outflow Meter Test (OFT) is another method to measure pavement macrotexture (Henry and Hegmon, 1975). The outflow meter measures relative drainage abilities of pavement surfaces. It can also be used to detect surface wear and predict correction measures (Moore, 1966).

The OFT is a transparent vertical cylinder that rests on a rubber annulus placed on the pavement. Then, the water is allowed to flow into the pavement, and the required time for passing between two marked levels in the transparent vertical cylinder is recorded. This time indicates the ability of the pavement surface to drain water and shows how fast it depletes from the surface. This time is reported as the outflow time and can be related to pavement macrotexture afterwards (Abe et al., 2000).

In the past decade, significant advances have been made in laser technology and in the computational power and speed of small computers. As a result, several systems now available can measure macrotexture at traffic speeds. The profiles produced by these devices can be used to compute various profile statistics such as the Mean Profile Depth (MPD), the overall Root Mean Square (RMS) of the profile height and other parameters that reduce the profile to a single parameter (Abe et al., 2000). The Mini-Texture-Meter developed by British Transport and Road Research Laboratory (Jayawickrama et al., 1996), Selcom Laser System developed by researchers at the University of Texas at Arlington (Jayawickrama et al., 1996; Walker and Payne.,undated), and the noncontact high speed optical scanning technique developed by the researchers at Pennsylvania State

University (Jayawickrama et al., 1996; Her et al., 1984) are examples of these systems. The first two of these devices use a laser beam to scan the pavement surface and, hence, estimate pavement texture depth. The third device makes use of a strobe band of light with high infrared content to generate shadowgraphs. This equipment can collect data from a vehicle moving at normal highway speeds (Jayawickrama et al., 1996).

A relatively new device for measuring MPD called the Circular Texture Meter (CTMeter) was introduced in 1998 (Henry et al., 2000; Noyce et al., 2005). The CTMeter is a laser-based device for measuring the MPD of a pavement at a static location. The CTMeter can be used in the laboratory as well as in the field. It uses a laser to measure the profile of a circle 11.2 inch (284 mm) in diameter or 35 inch (892 mm) circumference (Abe et al., 2000). The profile is divided into eight segments of 4.4 inch (111.5 mm). The mean depth of each segment or arc of the circle is computed according to the standard practices of ASTM and the International Standard Organization (ISO) (Abe et al., 2000). Testing indicated that CTMeter produced comparable results to the ASTM E965 Sand Patch Test. Studies by Hanson and Prowell (2004) indicated that the CTMeter is more variable than the Sand Patch Test.

There are several methods for measuring the microtexture (Do et al., 2000). In research at Pennsylvania State University, it was found that there is a high correlation between the zero speed intercept of the friction-speed curve of the Penn State model and the RMS of the microtexture profile height. In addition, researchers found that the BPN values were highly correlated to this parameter. Therefore, the BPN values could be considered as the surrogate for microtexture measurements (Henry and Liu, 1978). Observations of pictures of road stones taken by means of the Scanning Electron Microscope (SEM) showed how the polishing actions, as simulated in the laboratory by the British Accelerated Polishing Test, affected the microtexture of the aggregates (Williams and Lees, 1970; Tourenq and Fourmaintraux, 1971; Do and Marsac, 2002). It should be kept in mind that the test results are highly sensitive and result in a large variability in test results. For the test results to be purely indicative of aggregate textures, other factors need to be controlled. Coupon curvature, the arrangement of aggregate particles in a coupon for heterogeneous materials such as gravel, the length of the contact path, and slider load have significant effects on the results, and any change in this

parameters would yield misleading results (Won and Fu, 1996). The aggregates are further polished or conditioned during slider swing; consequently, the degree of polishing varies from aggregate type to aggregate type (Won and Fu, 1996).

Schonfeld (1974) developed a method for the Ontario Transportation Department based on subjective assessment using photos taken from the pavement. He defined microtexture levels from road stereo photography. Despite the fact that this method is a subjective and global method, the attributed levels were related to microasperity size and shape (Do et al., 2000).

Direct measurements using optic or laser devices are gaining popularity because of their simplicity and ease of use. Forster (1981) used cameras to digitize and measure road profile images obtained from a projection device. He developed a parameter that combines measurements of the average height and average spacing of the microtexture asperities. Yandell and Sawyer (1994) developed a device using almost the same measurement principle for in-situ use. Samuels (1986) used a laser sensor to record profiles directly. The laser system, with a measuring range of 6 mm and a spot size of around 0.1 to 0.2 mm, was not able to detect significant differences in microtexture between road surfaces (Do et al., 2000).

Improvements of measuring devices in recent years make the measuring techniques faster and more reliable. New data acquisition techniques include interferometry, structured light, various 2D profiling methods, and the Scanning Laser Position Sensor (SLPS). Figure 5 is a chart of topographic data acquisition techniques operating near the target scales that could be used in pavement (Johnsen, 1997).

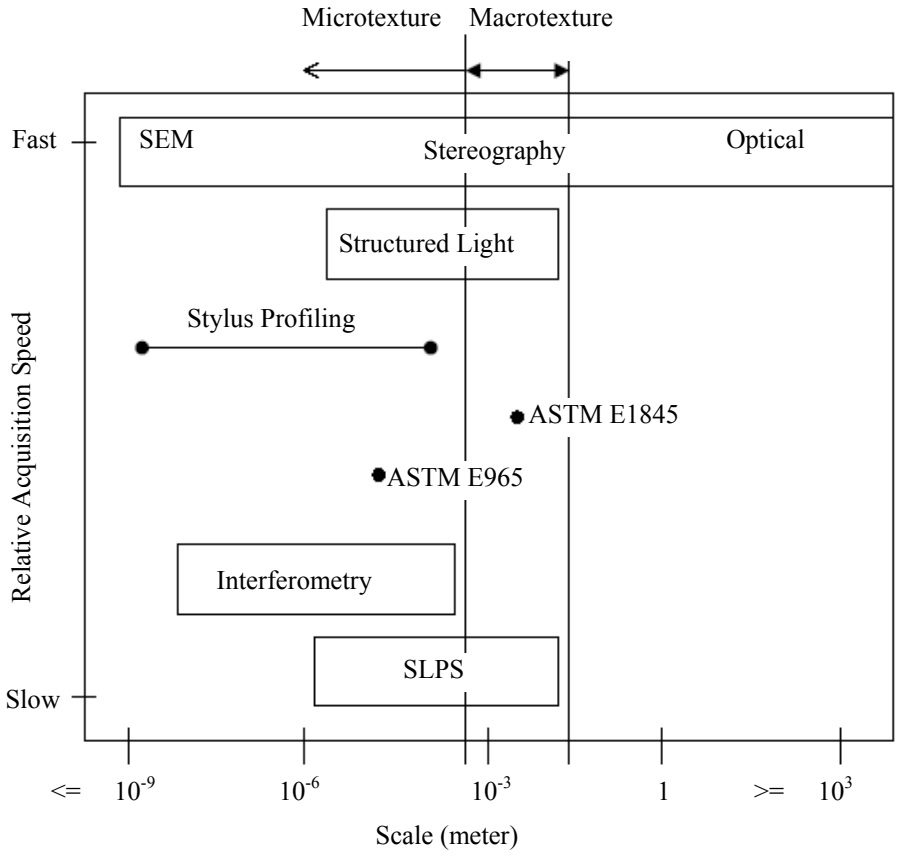

Figure 5. Different Data Acquisition Methods (Johnsen, 1997).

Interferometry and the stylus profiling techniques are two different methods for measuring topographic data at scales that cover a portion of the target scales for determining pavement texture (Johnsen, 1997).

Structured light and the SLPS are new methods of acquiring surface topography. These methods, however, proved to have limited functionality in measuring the surface asperities in the full range of different surfaces elevations. The SLPS was designed specifically for acquiring topographic data from pavement surfaces. This device is highly portable and can be easily utilized for in-situ measurement (Johnsen, 1997).

Stereo photography is a historical tool for visual inspection of surface features qualitatively (Schonfeld, 1974). Visual inspection requires special focusing tools and a pair of images (stereo pair), each taken at a specific angle perpendicular to the inspected surface. This technique can potentially be used to measure the topographic features of the surface, but the precision is obviously limited to the utilized equipment. Digital scanning

systems and computer algorithms have recently been developed to analyze the pictures taken and generating the surface texture (Johnsen, 1997). Table 1 shows a summary comparison between different measuring devices and the advantages and disadvantages of each method.

The AIMS introduced by Masad et al. (2005) is one of the most recent methods measuring the aggregate texture directly by use of a microscope and a digital image processing technique. This technique will be discussed in the next chapter (Masad et al., 2005).

Table 1. Comparison between Different Skid Resistance and Texture Measuring Techniques (McDaniel and Coree, 2003).

Device	About Device	Properties	Strengths	Weaknesses	Specs/used by
British Pendulum Tester	Pendulum arm swings over sample	Evaluates the amount of kinetic energy lost when a rubber slider attached to the pendulum arm is propelled over the test surface	Portable. Very simple. Widely used	Variable quality of results. Cumbersome and sometimes ineffective calibration. Pendulum only allows for a	ASTM E303
Michigan Laboratory Friction Tester	Rotating wheel	One wheel is brought to a speed of 40 mph and dropped onto the surface of the sample. Torque measurement is recorded before wheel stops	Good measure of the tire/surface interaction. Similar to towed friction trailer	Poor measurement of pavement macrotexture. History of use on aggregate only	MDOT
Dynamic Friction Tester	Rotating sliders	Measures the coefficient of friction	Laboratory or field measurements of microtexture	N/A	ASTM E1911
North Carolina Variable Speed Friction Tester	Pendulum type testing device	Pendulum with locked wheel smooth rubber tire at its lower end	Can simulate different vehicle speeds	Uneven pavement surfaces in the field may provide inaccurate results	ASTM E707
Pennsylvania Transportation Institute (PTI) Tester	Rubber slider	Rubber slider is propelled linearly along surface by falling weight	Tests in linear direction	Companion to Penn State reciprocating polisher. Fallen into disuse	Formerly by PTI
Sand Patch	Sand spread over circular area to fill surface voids	Measures mean texture depth over covered area	Simple	Cumbersome. Poor repeatability. Average depth only	ASTM E965
Grease Patch	Grease spread over surface	Measures mean texture depth over covered area	Simple	Cumbersome. Poor repeatability. Average depth only. Not widely used	NASA

Table 1. Comparison between Different Skid Resistance and Texture Measuring Techniques (McDaniel and Coree, 2003)(cont.)

Device	About Device	Properties	Strengths	Weaknesses	Specs/used by
Outflow Meter	Water flows from cylinder through surface voids	Estimates average texture	Simple. Quick	For non-porous surfaces only	FHWA
Dromometer	Stylus traces surface	Lowers a tracing pin that creates a profile of the specimen surface	Can measure both microtexture and macrotexture	Can only be used on small areas of pavement	----
Surtronix 3+ Profilometer	Stylus traces profiles	Horiz. Res = 1 micrometer Vert. Res = 0.001 micrometer Traverse Length = 25.4 mm	Can read microtexture and macrotexture	Can only be used on small areas of pavement	----
Circular Track Meter	Laser based	Laser mounted on an arm that rotates on a circumference of 142 mm and measures the texture	Used with DFT Fast. Portable. Repeatable	Measures small area. Relatively new	ASTM E2157

SKID RESISTANCE VARIATION

Pavement skid properties or friction decreases with time if no surface distresses occur (Lee et al., 2005). Traffic- and weather-related factors also affect the surface microtexture and macrotexture properties of in-service pavements, and thus the pavement friction (Flintsch et al., 2005). The following subsections describe the factors that influence the skid resistance.

Age of the Surface

Almost all new road surfaces have high texture and skid resistance. Aggregates used in road construction have to be resistant to crushing and abrasion to provide adequate skid resistance (Hogervorst, 1974). Pavement texture, however, reduces over time due to the abrasive effects of traffic. Traffic has a cumulative effect on pavement, and it wears the pavement surface and polishes the aggregate (Flintsch et al., 2005). The traffic wears and polishes the road pavement surface to a value that may be less than that determined by the standard Polished Stone Value (PSV) test in the laboratory (Perry et al., 2001). This polishing is due to the horizontal forces applied by the vehicle tires on the pavement surface. Under these forces, the protruding aggregates are worn off, polished, or abraded, thus reducing surface microtexture and macrotexture (Kennedy et al., 1990; Forster, 1990; Harald, 1990; Kulakowski and Meyer, 1990; Dewey et al., 2001). In addition, under the compacting effect of traffic, the protruding aggregates may be embedded in the pavement structure that leads to a reduction in the depth of macrotexture. Accordingly, an average 40 percent reduction in skid resistance due to pavement wear has been reported (Kokkalis et al., 2002). Polishing of aggregates also relates to traffic intensity and classification. Furthermore, commercial vehicles contribute to most of the polishing (Colony, 1986). The geometry of the road gradients, curves, pedestrian crossings, roundabouts, and stop and give-way controlled intersections attract high stresses and result in more polished surfaces. Polishing relates to traffic volumes where high volume areas require a better mixture design and construction (Chelliah et al., 2003).

Road surfaces will attain their peak skid resistance condition after a few weeks of traffic action due to wearing of the surface asphalt. After that, skid resistance declines at rapid rate at first as the exposed aggregate is worn and some of its microtexture and macrotexture properties are lost as traffic loads polish the HMA in the wheel paths. Then, it declines more slowly and reaches equilibrium state in which small deviations in skid resistance are experienced while traffic levels are constant and no structural deterioration is evident. This usually happens after 1 to 5 million passenger vehicle passes or two years (Lay and Judith, 1998; Davis et al., 2002; Saito et al., 1996; Burnett et al., 1968, Chelliah et al., 2003). Figure 6 shows the variation of pavement skid resistance versus pavement age.

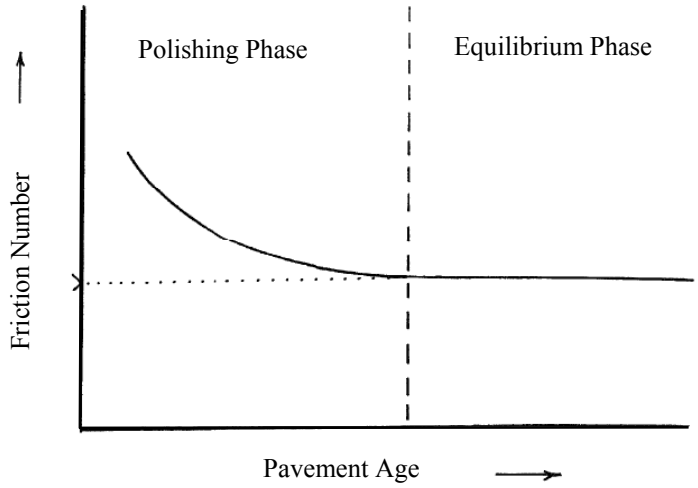

Figure 6. Decrease of Pavement Skid Resistance due to Polishing of Traffic (Skeritt, 1993).

Seasonal and Daily Variation

Weather-related factors (e.g., rainfall, air temperature, wind, etc.) are partially responsible for seasonal variations in the frictional properties of the tire-pavement interface (Flintsch et al., 2005). There are distinct seasonal patterns in skid resistance levels. Studies in the United Kingdom (Salt, 1977), U.S. (Hill and Henry, 1981; Jayawickrama and Thomas, 1998), and New Zealand (Cenek et al., 1997) showed a sinusoidal variation in skid resistance with seasonal change (Wilson and Dunn, 2005).

Generally, there is a decrease in pavement skid resistance from the seasonal changes of spring to fall (Transit New Zealand (TNZ), 2002). Summer months have the lowest levels of skid resistance. Dry weather in the summer allows the accumulation of

fine particles and debris that accelerate polishing of the pavement surface. West and Ross (1962) showed that the size of grit affects the polishing rate of aggregates. The combination of polishing and particle accumulation, together with the contamination from vehicles such as oil drippings and grease, results in a loss of microtexture and macrotexture during the summer months (Wilson and Dunn, 2005). A variation of approximately 30 percent of skid resistance has been observed between a minimum in summer to a peak during the winter (TNZ, 2002).

In winter, rainwater flushes out the finer particles responsible for polishing and reacts with the aggregate surface. This results in a higher microtexture and macrotexture and consequently, higher friction in the pavement surface (Wilson and Dunn, 2005). Some researchers also suggest that the water film covering the pavement for longer periods in winter acts as a lubricant and reduces the polishing effect of vehicles on the surface aggregate (Wilson and Dunn, 2005).

In summer, due to the accumulation of a higher amount of small particle and debris, the pavement surface polishes faster, and skid resistance decreases as a result.

Day-to-day fluctuation of pavement skid numbers of up to 15 skid numbers can occur because of extreme changes in weather conditions (Davis et al., 2002; Anderson et al., 1986). Figure 7 shows the generalized pavement-polishing model.

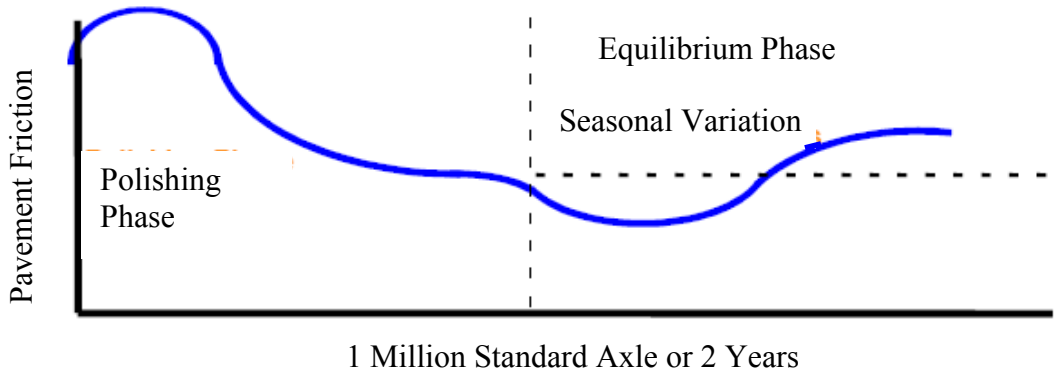

Figure 7. Generalized Pavement-Polishing Model (after Chelliah et al., 2003).

Flintsch et al. (2005) through statistical analysis showed that pavement temperature has a significant effect on the pavement frictional properties

(Flintsch et al., 2005). In their studies, they found that for the finer wearing surface mixes, pavement friction tends to decrease with an increase in the pavement temperature at low speeds. At high speeds, the effect is reversed, and pavement friction tends to increase with an increase in pavement temperatures. The temperature-dependent friction versus speed models appears to be mix-dependent (Flintsch et al., 2005). Subhi and Farhad (2005) in a different research study showed that both components of friction (hysteresis, adhesion) decrease with an increase in temperature (Subhi and Farhad, 2005).

AGGREGATE POLISHING CHARACTERISTICS

The ability of an aggregate to resist the polishing action of traffic has long been recognized as a highly important requirement for its use in pavement construction (Bloem, 1971; Whitchurst and Goodwin, 1955; Nichols et al., 1957; Gray and Renninger, 1965; Balmer and Colley, 1966; Csathy et al., 1968; Moore, 1969).

Coarse aggregate characteristics (e.g., angularity and resistance to wear) are believed to have a significant role in providing sufficient skid resistance in pavements. The desired texture is attained and retained by use of hard, irregularly shaped coarse aggregate. Hard, polish-resistant coarse aggregate is essential to avoid reducing skid resistance of asphalt surface (Bloem, 1971). The role of fine aggregate becomes significant only when used in relatively large quantities (Shupe, 1960). Sharp, hard sand particles are highly desirable for enhancing the adhesion component of pavement friction (Hogervorst, 1974).

Aggregates in the asphalt mixture are polished differently based upon their mineralogy. Aggregates have a different ability to maintain their microtexture against the polishing action of traffic, and therefore, aggregates polish or become smoother at different rates (McDaniel and Coree, 2003; Kowalski, 2007). It is a common practice to assume that aggregates with lower Los Angeles (LA) abrasion loss, lower sulfate soundness loss, lower freeze-thaw (F-T) loss, lower absorption, and higher specific gravity have better resistance to polishing. Many researchers, however, believe that the LA abrasion test and other physical tests (e.g., freeze and thaw test) may not yield good predictions of field friction, and reliability of predicting aggregate field polishing

resistance using a single laboratory test is poor (West et al., 2001; Kowalski, 2007; Prasanna et al., 1999).

The petrography examination is a valuable tool to understand the polishing process and to state recommendations for the use of aggregates, offering promise of quantitative evaluation (Do et al., 2002; Shupe 1960). Rocks containing igneous and metamorphic constituents are susceptible less to polishing than sedimentary rocks and could improve the overall frictional properties of pavement surface (West et al., 2001). Synthetic aggregates, e.g., slag or expanded lightweight aggregate (fabricated by heating natural clay), can also improve pavement frictional resistance (Roberts et al., 1996; Wasilewska and Gardziejczyk, 2005; Kowalski, 2007).

Limestone, the most common type of aggregate used in road construction, is the most susceptible aggregate type to polishing, produces the lowest skid resistance, and is the main cause of slipperiness on pavements (Csathy et al., 1968). Individual limestone based on its constituents differs considerably in its resistance to polishing. For some types of carbonate aggregates (e.g., dolomite), polishing susceptibility was found to decrease with an increase of clay content (West et al., 2001). Liang and Chyi (2000) found that as the calcite and dolomite contents increase, the polish susceptibility of aggregates decreases to a certain level. Further increases in the calcite and dolomite contents result in a loss of polish resistance. The difference between polishing susceptibility is also attributed to differences in their content of wear-resistant minerals, mainly silica (Bloem, 1971). The siliceous particle content is considered to be equal to the insoluble residue after treatment in hydrochloric acid under standardized conditions. The resistance of limestone to polishing decreased as its purity increased (Shupe and Lounsbury, 1958). Bloem (1971) stated that the siliceous particle content should be at least 25 percent to have satisfactory polish resistance. Furthermore, the size of the siliceous particle is also important and affects polishing tendencies. Bloem (1971) set the particle No. #50 as the limit for the particles to be discounted in setting the required amount of acid-insoluble material in aggregates. Sandstone is considered excellent in frictional properties and exhibits higher wet-friction values because differential wear and pulling out of individual particles under traffic contributes to the desired surface texture (Mills, 1969;

Stutzenberger, 1958). Sand and gravel are usually comprised of wear-resistant particles and have desirable frictional properties (Bloem, 1971).

The sandstone group is composed of hard quartz particle cemented together with brittle binder. The resistance of these particles against abrasion is very satisfactory (Bloem, 1971). These particles are exposed when the cement is worn away by traffic; therefore, this kind of aggregate has an excellent frictional performance, and its resistance to polishing is always high. The limestone and flint groups yield the lowest resistance. These types of aggregates have a simple fine cryptostalline structure and uniform hardness. Other groups, such as basalt, granite, and quartzite, have intermediate resistance against polishing. This intermediate resistance is due to the presence of altered feldspars and shattered grains of quartz and quartzite dislodging from a more resistant matrix. The basalt group, however, yields high resistance due to its softer mineral composition and the proportion and hardness of secondary minerals. In groups of indigenous rocks, the petrologic characteristics that affect resistance to polishing are variation in hardness between the minerals and the proportion of soft minerals. Finer-grained allotriomorphic igneous rocks have a tough, cohesive surface that will polish considerably. Rocks with cracks and fractured in the individual mineral grains have higher resistance since such grains are weak and dislodge from the matrix easily, whereas finer-grained rocks tend to polish more readily (Bloem, 1971; Knill, 1960; Chelliah et al., 2003).

Figure 8 shows four different methods by which aggregates provide texture to a pavement surface. The first aggregate is a very hard, angular aggregate composed of a single mineral type. This aggregate will resist polishing, but it will eventually become less textured and more rounded. Furthermore, rocks consisting of minerals with nearly the same hardness wore uniformly and tended to have a low resistance to polishing (Chelliah et al., 2003).

The second aggregate type will result in nearly the same type of wear pattern as the first, unless the crystals forming the particle are not well cemented together. The soft mineral mass wears away quickly, exposing the hard grains and providing a harsh surface. Before polishing the asperities of these hard grains, the aggregate matrix has been worn out to such extent that it can no longer hold the hard particles, allowing them

to be dislodged so that fresh unpolished grains could be exposed (Abdul-Malak et al., 1990; Skerritt, 1993). This continual renewal of the pavement surface is believed to maintain good skid resistance properties. The aggregates that have coarse, angular, and harder mineral grains uniformly distributed in a softer mineral matrix are believed to have higher skid resistance (Kokkalis and Panagouli, 1999).

The third and fourth aggregate types will both wear in similar fashion. Both of these aggregates are composed of a hard mineral and a weak mineral. For the fourth method, the air voids act as the weak mineral type. As the particles are weathered, the weak mineral will break down and release the worn hard minerals. This will expose fresh, unweathered surfaces that will retain their texture for extended periods of time and keep its frictional properties for a longer period (Luce, 2006).

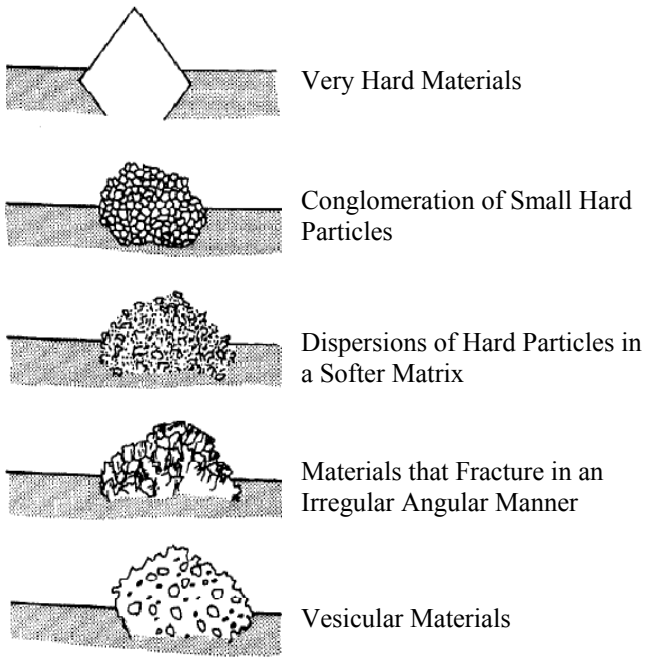

Figure 8. Aggregate Methods for Providing Pavement Texture (Dahir, 1979).

PRE-EVALUATING OF AGGREGATE FOR USE IN ASPHALT MIXTURE

The resistance of an aggregate type against polishing is the key factor in providing skid resistance. The use of polish-resistant coarse aggregates or other aggregates with good frictional performance has always been considered a useful way to

maintain friction above an acceptable level (Kokkalis and Panagouli, 1999). As mentioned earlier, microtexture mainly depends on aggregate property that can be controlled through the selection of aggregates with desirable polish-resistant characteristics. The evaluation of the aggregates with respect to their polishing behavior can be accomplished by using a laboratory test procedure (Noyce et al., 2005).

Several researchers tried to develop laboratory test methods to pre-evaluate the aggregates and relate the properties of aggregates to skid resistance; however, there is little agreement among researchers as to what engineering properties should be considered in an aggregate to provide adequate frictional resistance at various average daily traffic (ADT) levels.

Methods that are used for pre-evaluation of aggregates are mainly based upon using the British Polish Value (BPV). This test, however, is believed to measure only the microtexture of the pavement or the terminal polished value once the pavement reaches its equilibrium skid resistance (Henry and Dahir, 1979). Recent studies performed by Fwa et al. (2003) and Liu et al. (2004) showed the BPN value is a function of many factors (e.g., magnitude and number of gaps between the aggregates' coupon curvature, the arrangement of aggregate particles in a coupon for heterogeneous materials such as gravel, the length of the contact path, and slider load), and this test has a high variability (Won and Fu, 1996).

Crouch et al. (1996) believed that current methods of pre-evaluating the aggregates for asphalt surface courses such as the British Pendulum and British Polishing Wheel and chemical or mineralogical methods are only able to classify well-performing aggregates. They used a modified version of the American Association of State Highways and Transportation Officials (AASHTO) standard device (AASHTO TP33) to measure the uncompacted voids in coarse aggregates that were subjected to various times in the LA abrasion test. Measuring the change in aggregate weight in the LA abrasion test for various times is an indication of the aggregates, abrasion and breakage rate. By this method, they were able to measure the angularity change indirectly. Although this method does evaluate how the aggregates change over time, it is still considered an indirect method, and it uses the LA test, which primarily breaks aggregates rather than abrading them (Luce, 2006).

Do et al. (2000) used lasers to measure the surface profile of pavement sections to determine the microtexture and macrotexture of the pavement. These measurements were related to skid resistance (Luce, 2006). Gray and Renninger (1965) showed that the polish susceptibility decreases as the presence of insoluble constituents such as silica increases. Tourenq and Fourmaintraux (1971) proposed a formula to calculate the PSV values of stones from their mineral hardness.

Prowell et al. (2005) suggested Micro-Deval as a surrogate to determine an aggregate resistance to weathering and abrasion instead of a sulfate soundness test. It is also stated that the Micro-Deval abrasion loss is related to the change in macrotexture over time. Mahmoud (2005) recommended the use of Micro-Deval to polish aggregate and AIMS to measure loss of texture.

Polishing techniques are part of any aggregate classification system that evaluates the aggregate for use in the pavement surface. There are several types of polishing equipment used in the past for polishing asphalt mixes including:

- Penn State Reciprocating Polishing Machine (ASTM E1393),
- Circular Track Polishing Machine,
- Michigan wear track, and
- The North Carolina State University (NCSU) Wear and Polishing Machine (ASTM E660).

Among the polishing techniques mentioned above, only the Michigan wear track is still being used while the others were discontinued. There is another type of the Michigan wear track at Berlin Technical University called the Wehner/Schulze polishing machine. This machine polishes flat circular specimens, and the polishing action is simulated by three conical rubber rollers in the presence of water and grits (Dames 1990; Kowalski, 2007).

The National Center of Asphalt Technology (NCAT) has recently developed a new machine for polishing asphalt pavement slabs. In this machine, three rotating wheels move around a circle with the same diameter as the DFT and CTMeter devices, making it a suitable device for studying the effect of polishing with DFT and CTMeter. This machine will be discussed in detail in the next section (Vollor and Hanson, 2006). Table 2 shows comparisons between different polishing devices.

Table 2. Comparison between Different Polishing Techniques (McDaniel and Coree, 2003).

Device	About Device	Properties	Strengths	Weaknesses	Specs/used by
British Polishing Wheel	Wheel for polishing away macrotexture	Curved aggregate specimens polished by a rotating wheel	Accelerated polishing for lab testing. Bench sized	Coarse aggregate coupons only. Does not affect macrotexture or mix properties	ASTM D 3319
Michigan Indoor Wear Track	Large circular track	Wheels centered around pivot point, move in circle around track	Close to real world	Track is very large and cumbersome. Time-consuming sample preparation. Used for aggregates only	MDOT
NCSU Polishing Machine	Four wheels rotate around central pivot	Four pneumatic tires are adjusted for camber and toe-out to provide scrubbing action for polishing	No need for water or grinding compounds, can polish aggregate or mixes	Polishes a relatively small area or few number of samples	ASTM E 660
NCAT Polishing Machine	Three wheels rotate around central pivot	Three pneumatic tires are adjusted for camber and toe-out to provide scrubbing action for polishing	Sized to match DFT and CTMeter	New device developed by NCAT based on older devices	NCAT
Penn State Reciprocating Polishing Machine	Reciprocating pad	Reciprocates rubber pad under pressure against specimen surface while slurry of water and abrasive are fed to surface	Portable. Can be used to polish aggregate or mix in lab or field	Polishes a relatively small area. Oscillation obliterates directional polishing. Fallen into disuse	ASTM E 1393

PREDICTIVE MODELS FOR SKID RESISTANCE

Having a model to predict friction change during the lifetime of a pavement would aid in predicting pavement performance and identifying the appropriate time for any treatment and rehabilitation measures. Due to the complex interaction between many factors affecting pavement skid resistance, developing such a model is not easy. Many researchers tried to develop theoretical and empirical models to predict skid resistance. These models range from ones based on simple laboratory tests to complicated theoretical interaction between tire and pavement surface. These models are useful tools to predict pavement skid resistance over its life span.

Tire/pavement models are categorized into three different categories including (Kowalski, 2007):

- statistical-empirical that is mainly based on road-collected data with different characteristics and statistical analysis,
- fundamental that is based on physical modeling of pavement surface and tire, and
- hybrid that is a combination of statistical and fundamental models.

Stephens and Goetz (1960) used the fineness modulus as a key factor to predict the skid resistance of an asphalt pavement. Dahir et al. (1976) were the first to try relating aggregate characteristics to pavement skid resistance. In their research, they found some correlation between acid insoluble percent to field skid performance, but not enough to support a regression equation. They were the first to propose the use of the laboratory BP value as a surrogate for field terminal condition. They also considered the difference between the initial and terminal laboratory BPV as a measure of polishing characteristics of the aggregate (Luce, 2006). Henry and Dahir (1978) and Kamel and Musgrove (1981) then used the BPV of an aggregate sample as a parameter for the prediction of a pavement skid resistance. Henry and Dahir (1979) in other research found a relationship between BPV and microtexture. Moreover, they introduced the concept of

percent-normalized gradient[2], a function of macrotexture, to incorporate both aspects into the prediction of pavement skid resistance (Henry and Dahir, 1979).

Mullen et al. (1974) studied the mineralogy of aggregates in relation to skid resistance. An optimum percentage of hard minerals distributed within a softer matrix were discovered, which allows for the selection of materials that should perform well in the field (Figure 9).

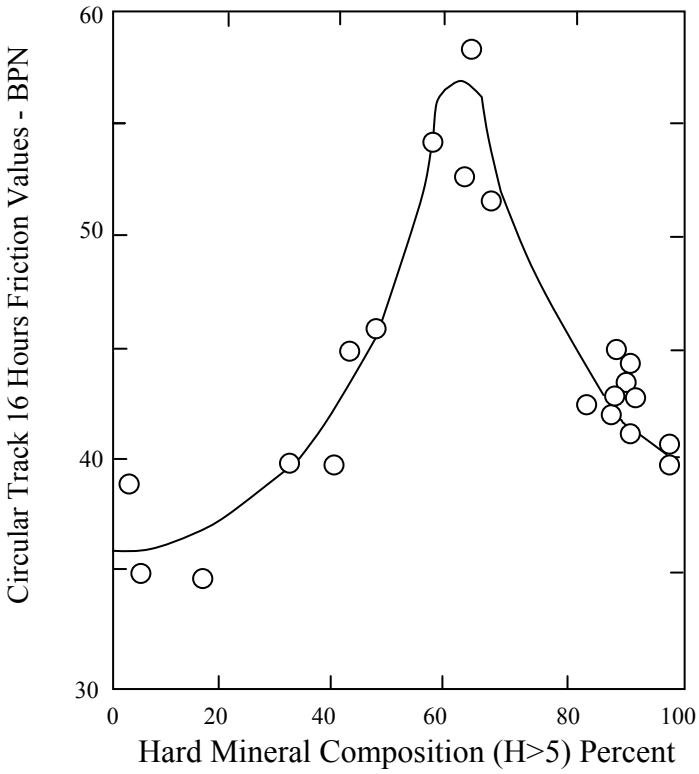

Figure 9. Mineral Composition Related to Skid Resistance (Mullen et al., 1974).

Emery (1982) developed a pavement friction prediction model relating skid resistance to pavement age, accumulated traffic level and mix properties including aggregate polish resistance, mixture volumetrics, and Marshall stability and flow. The field measurements showed a good agreement between measured and predicted values (Emery, 1982). Yandell et al. (1983) developed a complex physical model based on tire pavement interaction. In their model, they considered the pavement surface and tread

[2] Percent-normalized gradient is the gradient of friction values measured below and above 60 km/hr speed and shows how strongly friction depends on the relative sliding speed (Hall et al., 2006).

rubber properties as main factors affecting skid number. Field verification showed a good agreement between predicted and measured values (Yandell et al., 1983).
Ergun et al. (2005) tried to relate pavement skid resistance and texture measurements by use of image analysis. He also showed there is a good agreement between measured and predicted values (Ergun et al., 2005).

Stroup-Gardner et al. (2004) found a good correlation between MPD and skid number and developed a model to predict skid number. Ahammed and Tighe (2007) found a close relationship between vehicle speed, surface texturing type, cumulative traffic volume and concrete compressive strength, and concrete pavement skid resistance and developed a model that was able to predict skid numbers for concrete pavements.

Luce et al. (2006) investigated the relationship between pavement friction and polishing susceptibility, mix gradation, and aggregate type. Based on measuring changes in the aggregate texture due to abrasion in Micro-Deval, they proposed a method to relate pavement skid resistance to aggregate polishing resistance that was verified for nine different field test sections.

INTERNATIONAL FRICTION INDEX

There are several measurement techniques throughout the world to assess pavement skid resistance. There are many indices explaining the skid resistance of a road including coefficient of friction, British Pendulum Number, Skid Number, Friction Number, and International Friction Index (Henry, 2000; Kowalski, 2007). It has been a concern how to harmonize different measurements of the skid resistance and make a ground for comparing them. International Friction Index is a recent index that has been developed to harmonize friction and texture measurements by means of different test methods (Henry 1996; Henry et al. 2000; Wambold et al., 1986; Wambold et al., 1995; Yeaman, 2005; Kowalski, 2007). This index was developed through collecting a wide range of friction data measured by several test methods on different pavement surfaces mainly in Spain and Belgium during an international PIARC study. In this study, a model originated by Penn State researchers was used. In this model, two important factors affecting pavement skid resistance were considered. The original model has the form of (Wambold et al., 1995; Kowalski, 2007):

$$F_{\mu}(s) = F_0 . e^{\frac{-s}{S_P}} \quad \textbf{(1)}$$

where:

S is sleep speed,

F_{μ} is friction,

F_0 is a constant that relates to microtexture, and

S_P is a constant that relates to macrotexture.

During the international study done by PIARC, a curve relating slip-speed was established for each pavement section. This so-called golden curve shows the friction experienced by a driver during emergency breaking. Then, by using proper calibration factors, the equipment was able to predict the golden curve. It is worthwhile to know the friction reported for each test section was at a speed of 60 km/h. The IFI is composed of two numbers—F60 and S_p—that are calculated as follows (Wambold et al., 1995; Kowalski, 2007).

- Speed constant (S_p) parameter is calculated based on texture measurements:

$$S_p = a + b\ T_x \quad \textbf{(2)}$$

Where "a" and "b" are calibration factors and different for each measuring device and T_x is a measure of pavement texture.

- The friction measurement at a slip speed FR(S) is then converted to a measurement at 60 km/h FR(60);

$$FR(60) = FR(S) \times e^{\left(\frac{S-60}{S_P}\right)} \quad \textbf{(3)}$$

- Finally, the F(60) is recalculated by use of speed adjusted friction value FR(60) and the following equation:

$$F60 = A + B\ \ FR(60) + C\ T_x \quad \textbf{(4)}$$

Where; "A," "B," and "C" are calibration constants for a selected friction device. These values have been standardized for each measuring device in ASTM E1960.

Two parameters used in the IFI calibrated model—wet friction at 60 km/h (F60) and the speed constant of wet pavement friction (S_P)—are indications of the average wet coefficient of friction experienced by a driver during a locked-wheel slide at a speed of

60 km/h and dependence of the wet pavement friction on the sliding speed, respectively (Cenek et al., 1997; Kowalski, 2007).

Based on the ASTM E 1960, the calibration factors for the CTMeter are (a = 14.23 b = 89.72) and for DFT are (A = 0.081, B = 0.732). Based on these values, the F60 and S_p could be calculated as:

$$F60 = 0.081 + 0.732 DF_{20} e^{\frac{-40}{S_P}} \quad \textbf{(5)}$$

$$S_P = 14.2 + 89.7 MPD \quad \textbf{(6)}$$

where:

DF_{20} = wet friction number measured by DFT at the speed of 20 km/h,

MPD = MPD measured by CTMeter (mm).

These equations indicate that the effect of wet friction coefficient at 20 km/h is more pronounced than MPD. MPD is a parameter defined by ASTM E1845 (2005) as "the average of all of the mean segment depths of all of the segments of the profile," where mean segment depth is "the average value of the profile depth of the two halves of a segment having a given base length," and profile depth is "the difference between the amplitude measurements of pavement macrotexture and a horizontal line through the top of the highest peak within a given baseline." This value could be easily read from a CTMeter (ASTM, 2007; Kowalski, 2007).

The F60 value for the locked wheel friction trailer using a smooth tire (A = 0.04461, B = 0.92549, and C = 0.097589) and rib tire (A = -0.02283, B = 0.60682, and C = 0.097589) at desired speeds are (Kowalski, 2007):

$$F(60) = 0.045 + 0.925 \times 0.01 \times SN(64)S.e^{\frac{4}{S_P}} \quad For\ Smooth\ Tire \quad \textbf{(7)}$$

$$F(60) = -0.023 + 0.607 \times 0.01 \times SN(64)R.e^{\frac{4}{S_P}} + 0.098 \times MPD \quad For\ Rib\ Tire \quad \textbf{(8)}$$

where:

SN(64)S = skid number measured at test speed of 64 km/h using a smooth or rib tire divided by 100.

Since the value of the texture is not measured during the friction measurement by trailer, using the above equations for calculating the IFI requires two separate measurements by rib and smooth tire. Moreover, to determine the IFI, the two equations for rib and smooth tire should be set equal; using another equation relating MPD and S_p values, the total unknowns reduce to one. Then, the IFI can be easily calculated (Kowalski, 2007).

WET WEATHER ACCIDENT REDUCTION PROGRAM (WWARP)

In 1999, Texas Department of Transportation (TxDOT) implemented a statewide program to reduce skid-related accidents in the state of Texas. The objective of this program was to develop the most effective method to minimize wet weather skidding accidents at a reasonable cost. This program uses all available resources such as accident data and analytical expertise, friction test devices, and local knowledge of roadway friction conditions to identify and correct sections of the roadway with high skid accidents to ensure that the pavement has adequate and durable skid resistance throughout the design life of pavement (Ivey et al., 1992).

Based on this program, the minimum acceptable friction level on the road surface is identified. TxDOT required the friction level be classified into three categories—low, moderate, and high—based on roadway attributes. The amount of rainfall (inches/year), traffic (Average Daily Traffic), speed (mph), percent of trucks, vertical grade (percent), horizontal curve, driveway (per mile), cross slope (in/ft), surface design life, and intersecting roadways are road attributes that define the required friction level.

The WWARP includes material testing and evaluation, pavement design and construction, and pavement management and rehabilitation practices to ensure that pavement meets the acceptable friction level. Pavement design and construction, as part of this program, consist of evaluating the aggregate capability to provide adequate skid resistance properties. It also controls the mix design to provide sufficient stability, which ensures the durability of skid resistance (FHWA, 1980).

Selecting the polish-resistant aggregate is a key factor to ensure adequate and durable pavement skid resistance. The Surface Aggregate Classification (SAC) system is one of the WWARP's outcomes that has experienced several changes since the inception

of WWARP. The SAC system enables the mixture design engineer to select appropriate aggregates to be used in the pavement surface based on pavement frictional requirements.

The first SAC was developed in 1999. In this SAC, the aggregates are classified into four groups based on their PSV and magnesium sulfate soundness test results as shown in Figure 10. The chart was adopted from October 1, 1999, to February 28, 2006.

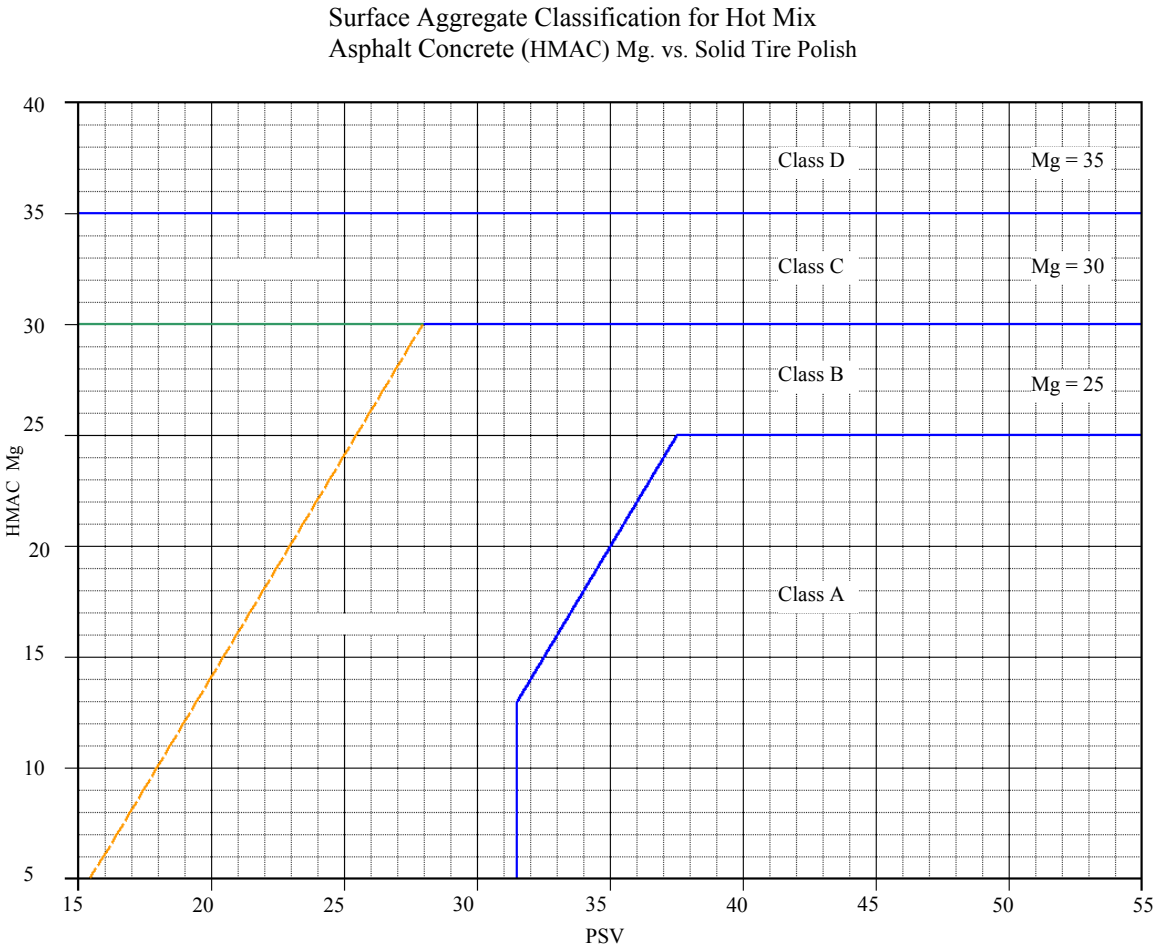

Figure 10. First Aggregate Classification Chart.

This chart changed after February 28, 2006, and the inclined line between class B and class C was removed.

Figure 11 shows the second version of the SAC chart that had been used from March 2006 to December 2007. Based on this system, researchers classified the aggregates by one of the two methods shown below.

- All bituminous coarse aggregates that have both an Acid Insoluble Residue of 70 percent or greater and magnesium sulfate soundness loss of 25 percent or less will be classified as class "A" sources.
- All aggregate sources that do not meet the criteria of a low carbonate source as defined above will be classified based on a combination of their Residual Solid Tire Polish Value and magnesium sulfate soundness weight loss. These materials are classified into groups (A, B, and C), as shown in Figure 11.

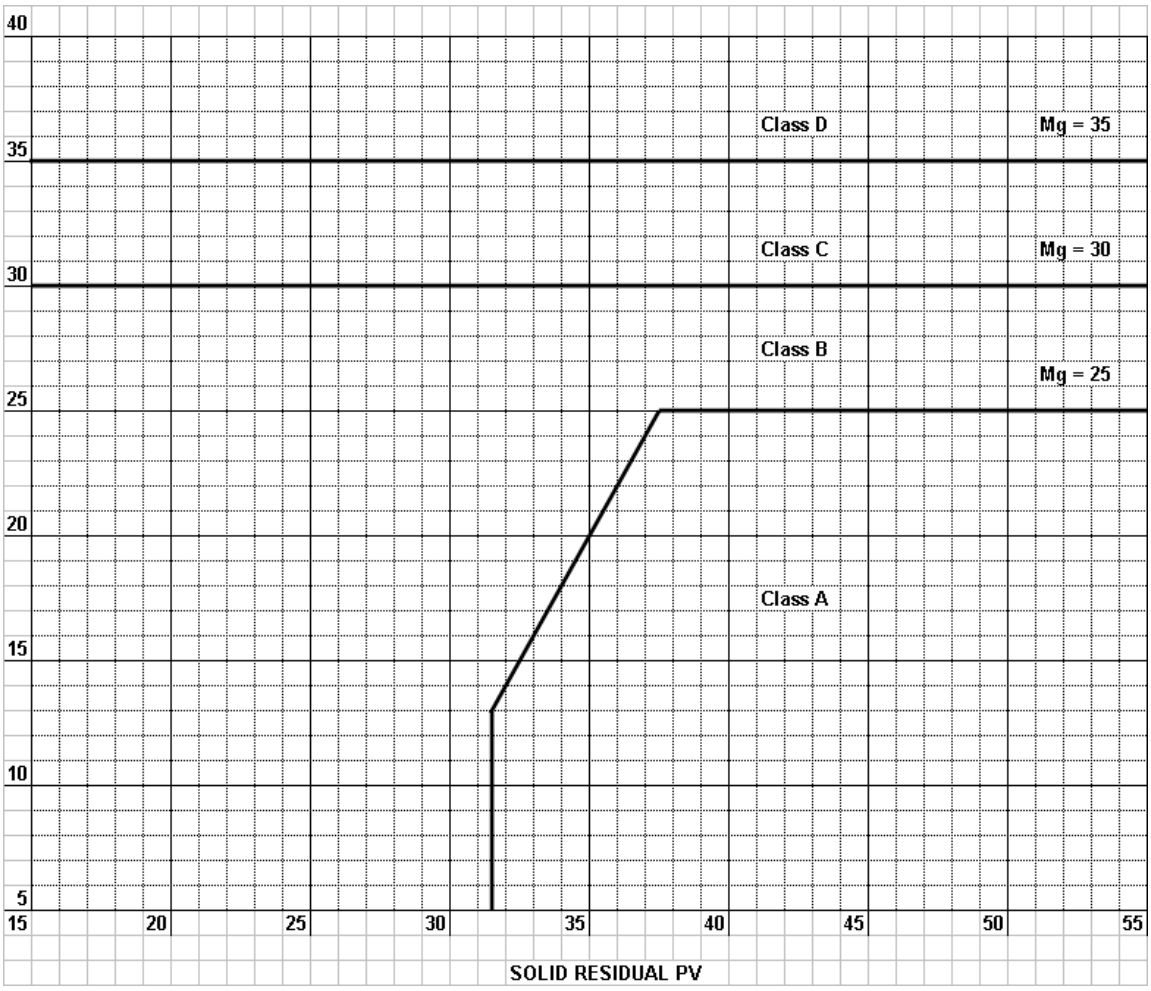

Figure 11. Modified Aggregate Classification Chart (Second Edition).

In 2006, TxDOT contracted with the Texas Transportation Institute to undertake a project to implement the AIMS in TxDOT operations. This research focused on measuring aggregate shape characteristics. Moreover, a new method was proposed in this research to better test aggregate resistance to polishing. This method is based on the magnesium sulfate soundness and texture results from AIMS. It proved to be more sensitive than the method that was being used by TxDOT. Furthermore, the new SAC system allows the aggregates to be spread more evenly in four different categories (Masad et al., 2006).

TxDOT began a program called Aggregate Quality Monitoring Program (AQMP) in 1995 to provide the requirements and procedures for the Construction Division, Materials and Pavements Section (CST/M&P) to accept aggregate products that have demonstrated continuing quality and uniformity. In this program, TxDOT has revised the SAC system and released the new aggregate classification system. This system has been effective since December 2007. Based on the new system, the aggregates are classified according to Table 3.

Table 3. Aggregate Classification Table.

Property	Test Method	SAC A	SAC B	SAC C
Acid Insoluble Residue, % min	Tex-612-J	55		
5-Cycle Mg, % max	Tex-411-A	25	30	35
Crushed Faces, 2 or more, % min	Tex-460-A	85	85	85

CHAPTER III – MATERIALS AND EXPERIMENTAL DESIGN

INTRODUCTION

The research undertaken in this study examines the relationship between aggregate properties such as angularity, texture, and pavement friction characteristics. The results will be used to recommend a method for the selection of aggregates used in asphalt pavement surface to ensure acceptable skid resistance. Since different aggregates are used in different parts of the state, researchers tried to select aggregates that have been used in projects in various locations in the state of Texas. To study the effect of mix type, three different mixture types were selected. The following section briefly explains the characteristics of the selected aggregates and mixture designs.

AGGREGATE SOURCES

As it was mentioned in the literature survey, aggregate type and geological sources have a significant effect on the skid resistance of the pavement. Five different types of aggregates were selected from:

- Beckman pit,
- Brownwood pit,
- McKelligon pit,
- Brownlee pit, and
- Fordyce pit.

It should be noted that since the frictional performance of the asphalt mixes is mainly governed by coarse aggregates, type of coarse aggregate was considered as the representation of that pit. For instance, in the Brownlee pit, coarse aggregate is comprised of sandstone, and fine part is limestone from a different pit (Georgetown pit). In the analysis, the properties of sandstone represented that of the Brownlee aggregate.

Because it is a common practice in Texas to blend soft limestone aggregates with a polish-resistant aggregate, another combination including 50 percent sandstone and 50 percent soft limestone was also tested. Figure 12 shows the geographical location of aggregate sources on a Texas map.

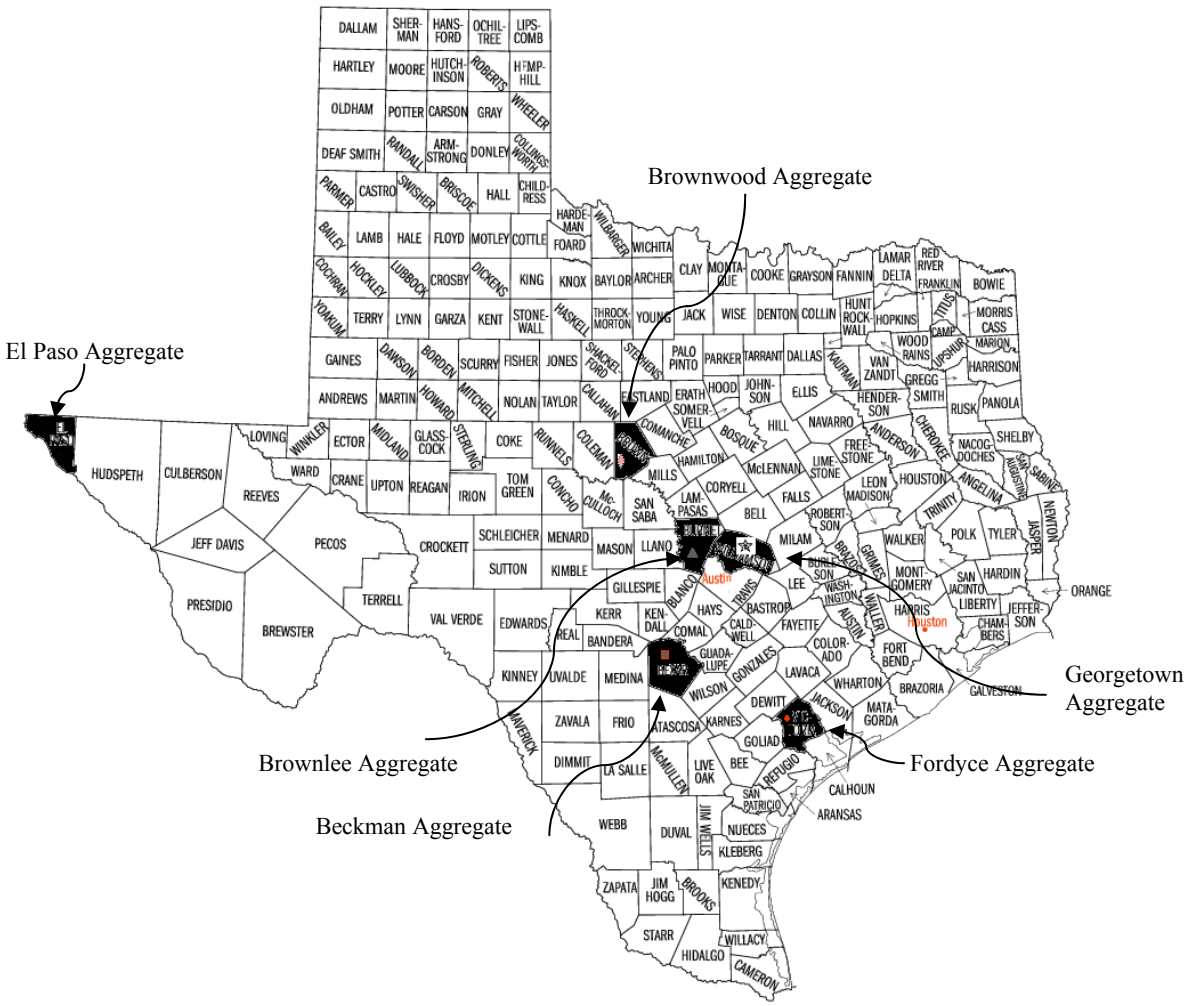

Figure 12. Map of Texas Showing Aggregate Quarries by County Location.

Figure 13 shows the aggregate classification based on the old classification systems used in Texas.

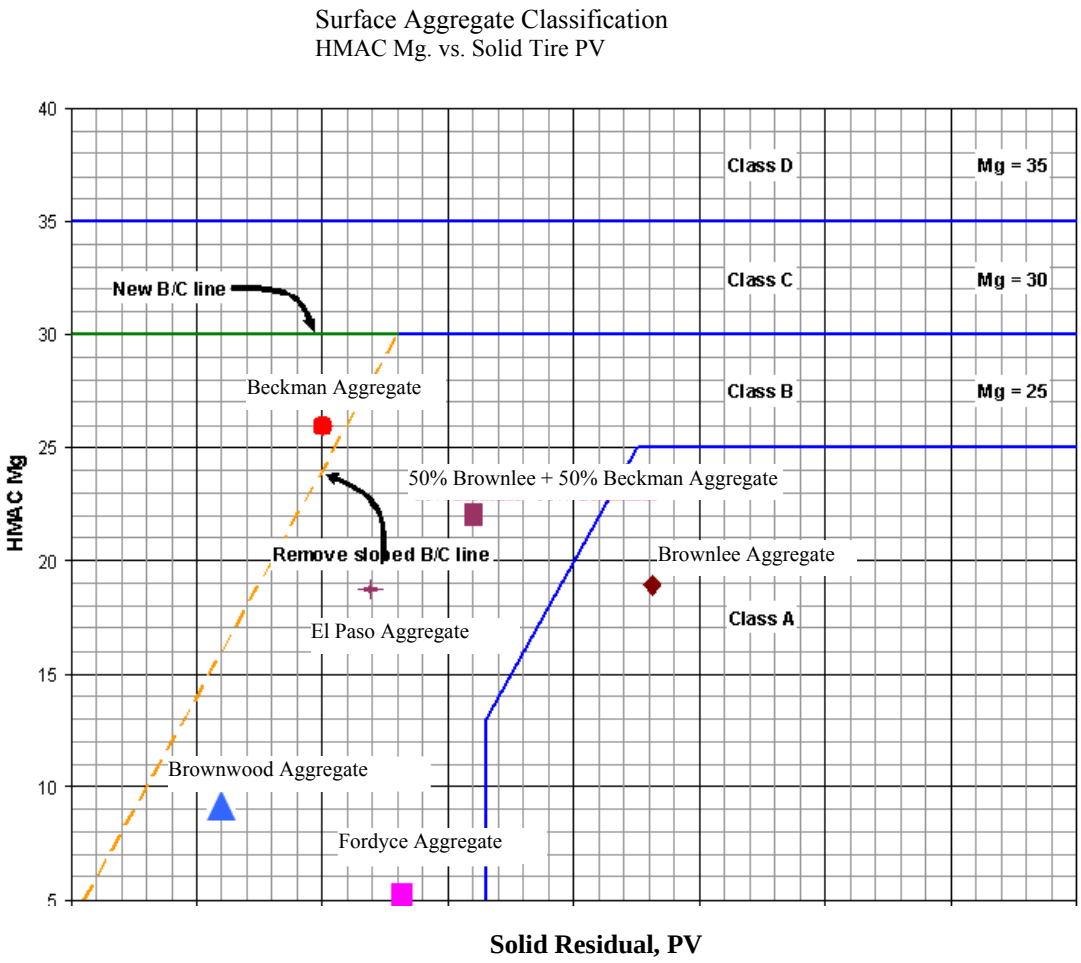

Figure 13. Aggregate Classification Based on Old Aggregate Classification System.

Based on the two older versions of TxDOT SAC (Figure 13), Brownlee aggregate falls in class A; Beckman aggregate is classified as class C, and the remaining aggregates are classified as class B.

The new classification system uses Table 3. Based on this table, aggregates are classified as shown in Table 4. Table 4 shows that Fordyce aggregate, which was classified as B in a previous version of the SAC system, were promoted to class A, and Beckman aggregate classifies as SAC B in the new system. Other aggregates remain the same in both systems.

Table 4. Aggregate Classification Based on New System.

Aggregate	Class
Brownlee	SAC A
El Paso	SAC B
Fordyce	SAC A
Brownwood	SAC B
Beckman	SAC B
50% Brownlee + 50% Beckman	SAC B

PETROGRAPHIC ANALYSIS OF AGGREGATES WITH RESPECT TO SKID RESISTANCE

To understand skid properties of aggregate used in this study, the researchers analyzed thin sections of selected aggregates from six different Texas aggregate sources (Table 5). The mineralogy and relative hardness (Mohs hardness scale) of each aggregate are listed as well. Different size fractions from each aggregate source were washed in distilled water to remove foreign matter and allow close inspection with a Meiji binocular microscope to select pieces of aggregate that were representative of the variations in each source. The aggregate pieces were selected for thin-section analysis based on color, angularity, density, and variations in surface texture.

Table 5. Aggregates Analyzed in Petrographic Study.

Aggregate Source	Mineralogy	Mohs Hardness
Beckman pit	Calcite	3
Brownlee pit	Quartz, Feldspar, Dolomite, Calcite, Glauconite	7, 6, 3.5-4, 3, 2
Brownwood pit	Zircon, Quartz, Rutile, Feldspar, Dolomite, Calcite	7.5, 7, 6-6.5, 6, 3.5-4, 3
Fordyce pit	Quartz, Feldspar, Dolomite Siderite, Calcite	7, 6, 3.5-4, 3.5-4, 3
McKelligon pit	Quartz, Feldspar, Dolomite Siderite	7, 6, 3.5-4, 3.5-4
Georgetown pit	Quartz, Dolomite, Calcite	7, 3.5-4, 3

The aggregate pieces were then shipped to Texas Petrographic Services, Inc., in Houston to make thin sections. Each thin section was impregnated with blue-dyed epoxy (for easy pore delineation), and one-half of the section was stained with Alizarin Red-S to distinguish calcite and aragonite from dolomite. The calcite and aragonite are stained a red color, and dolomite remains unstained (Scholle, 1978).

The thin sections were analyzed with a Zeiss Axioskop 40 petrographic microscope equipped with a rotating stage and a Pixelink digital camera. Photomicrographs were made of representative features for each aggregate fraction.

The following section will explain the results of the observations and petrographic analysis that have been done on each aggregate type.

Beckman Pit

This aggregate type is produced by Martin Marietta Corporation, and the quarry is located near San Antonio Texas. Samples from this site are characterized by a monomineralic composition (100 percent calcite). The texture varies from a low porosity fossiliferous grainstone to poorly cemented euhedral calcite with moldic porosity. Figure 14 is a micritic limestone composed of 100 percent calcite. The red stain shows that the sample is composed of pure calcite. The darker areas are calcite mud (micrite), and the light areas are fossil fragments made of calcite. The grainstone in Figure 15 is a low porosity limestone with abundant fossil fragments, which are composed entirely of calcite. This aggregate would have better skid resistance than the micrite above, but it is monomineralic, which would decrease the skid resistance.This, however, might not be true since sometimes the monomieralic aggregates have a different hardness between the fabric and the matrix of the rock depending on whether the matrix weathered more than the fabric. If the fabric is more durable than matrix, the texture is created. Moreover, characterizing this aggregate, however, can be studied by measurement of the skid resistance of prepared samples of mixes containing this type of aggregate.

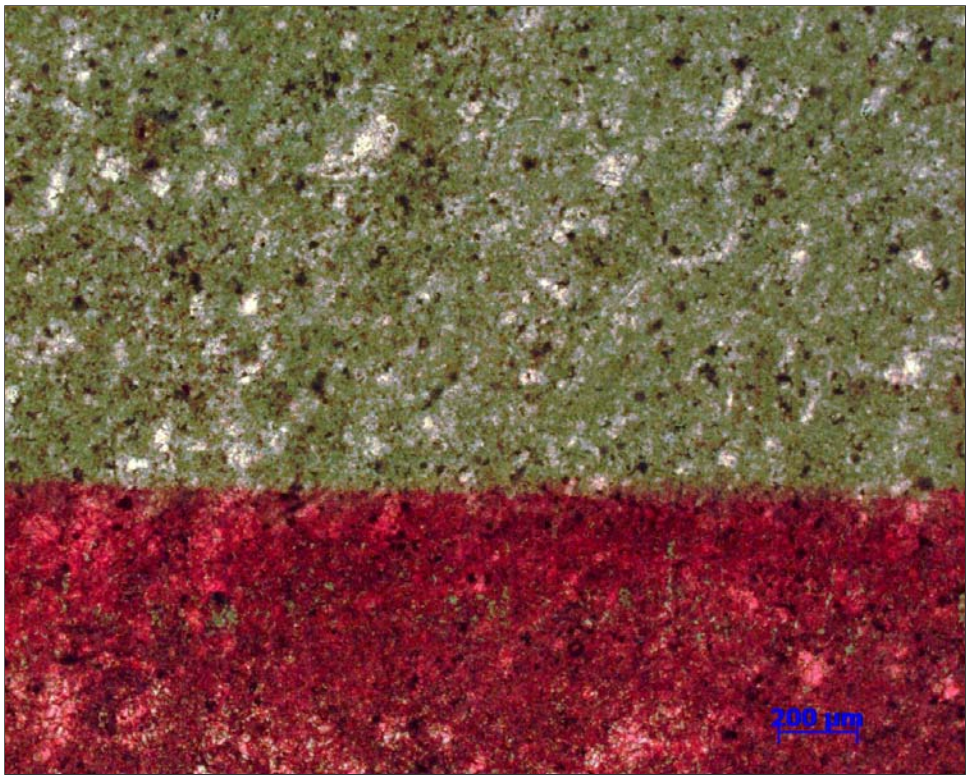

Figure 14. Micritic, Low Porosity Limestone from the Beckman Pit.

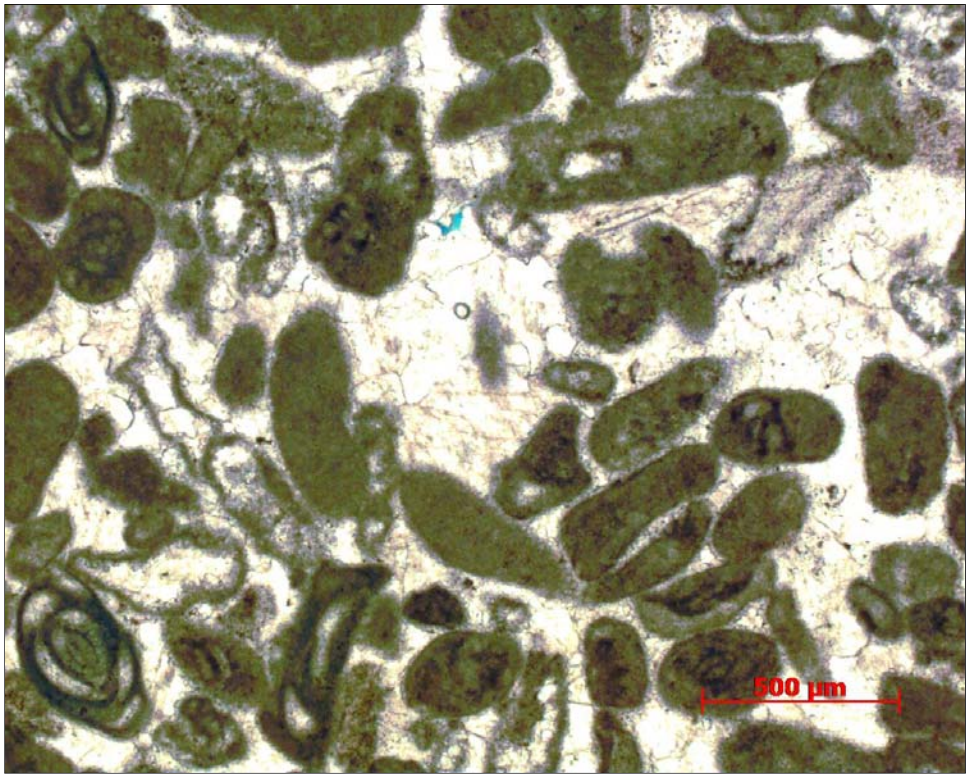

Figure 15. Grainstone with Coated Fossil Fragments from the Beckman Pit.

The limestone shown in Figure 16 has moldic (vuggy) porosity that increases its skid resistance. However, there is very little of this material in the aggregate sample collected. This aggregate would have a lower skid resistance due to being composed predominantly of only one mineral.

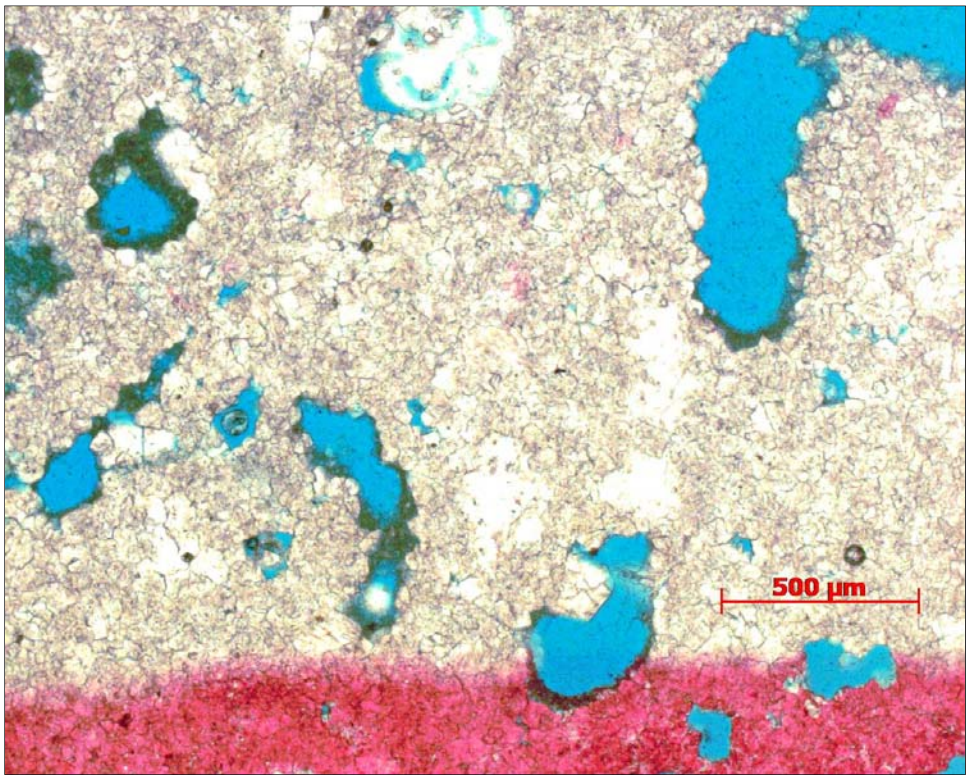

Figure 16. Coarsely Crystalline Limestone with Moldic Pores from the Beckman Pit.

Brownlee Pit

This aggregate is a blend of sandstone and partly limestone. The sandstone is produced by Capitol Aggregate Corporation near Marble Falls, Texas. There are numerous rock types in this aggregate that include chert, glauconitic sandstone, limestone, sandy limestone, dolomite, and glauconitic dolomite. Some of the aggregate pieces are heavily weathered, and other pieces are unaltered rock. Examples include an altered glauconitic sandstone, and fresh to highly altered dolomite. Figure 17 is an unaltered glauconitic dolomite. The unweathered glauconite grains are dark green, and

the dolomite crystals are white to gray. Figure 18 is a calcite and dolomite-cemented sandstone. This rock should have good skid properties because it has cements with different hardness, and there is very little porosity to weaken the rock. The sand grains are angular, which will contribute to improved skid properties.

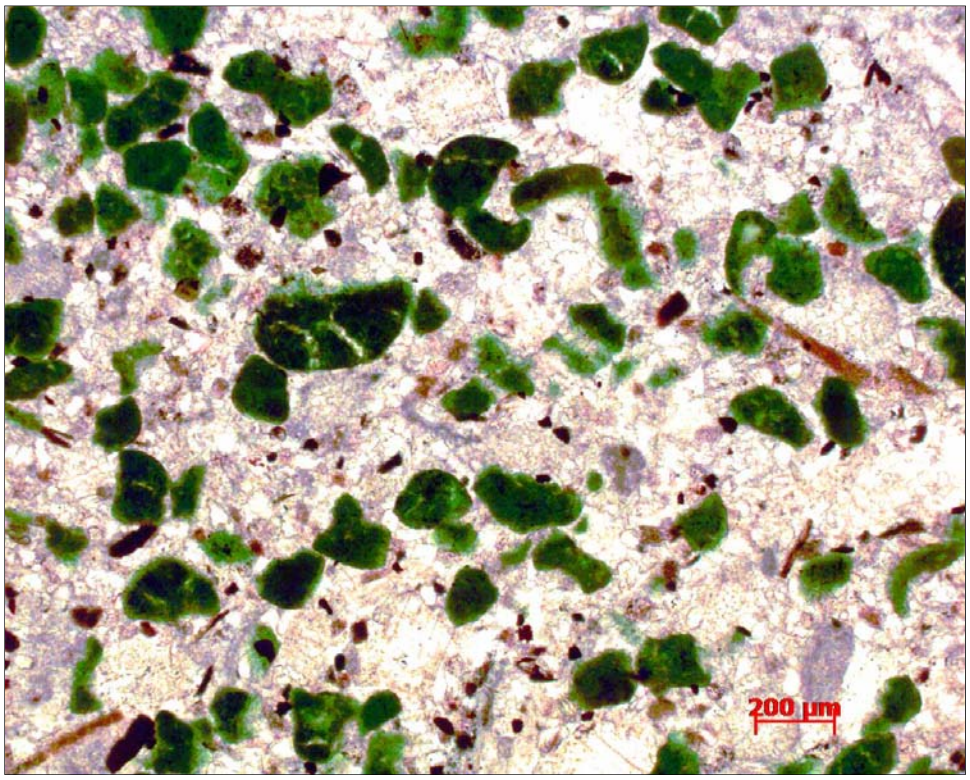

Figure 17. Glauconitic Dolomite from the Brownlee Pit.

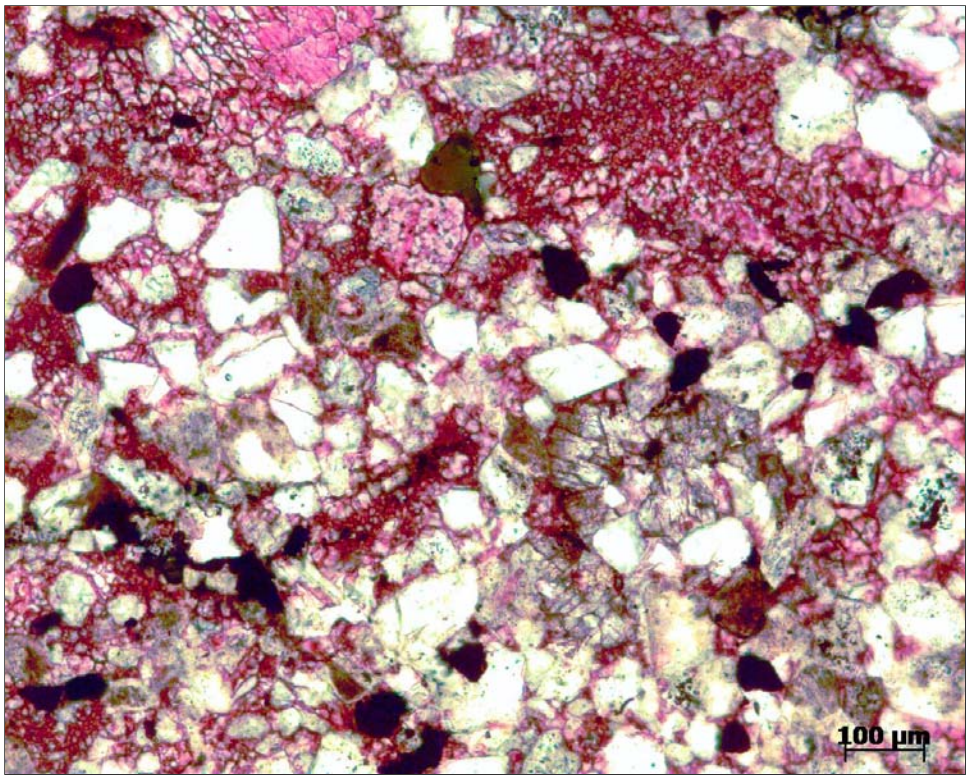

Figure 18. Calcite and Dolomite-Cemented Sandstone from the Brownlee Pit.

Figure 19 shows a heavily weathered dolomite. One can see abundant pore space (blue areas) between individual crystals in addition to many crystals being etched or partially dissolved. The mineralogy and texture of the Brownlee Pit is very diverse. The skid properties of this aggregate will be highly dependent on relative percentages of fresh and heavily altered rock. The microtextural properties of the Brownlee pit is higher in the altered rock due to continual rejuvenation of the aggregate surface due to sand being plucked during wear. Moreover, this fresh rock may have better wear resistance characteristics but may be less texture over time. Furthermore, a detailed laboratory study is needed to characterize the frictional properties of this rock.

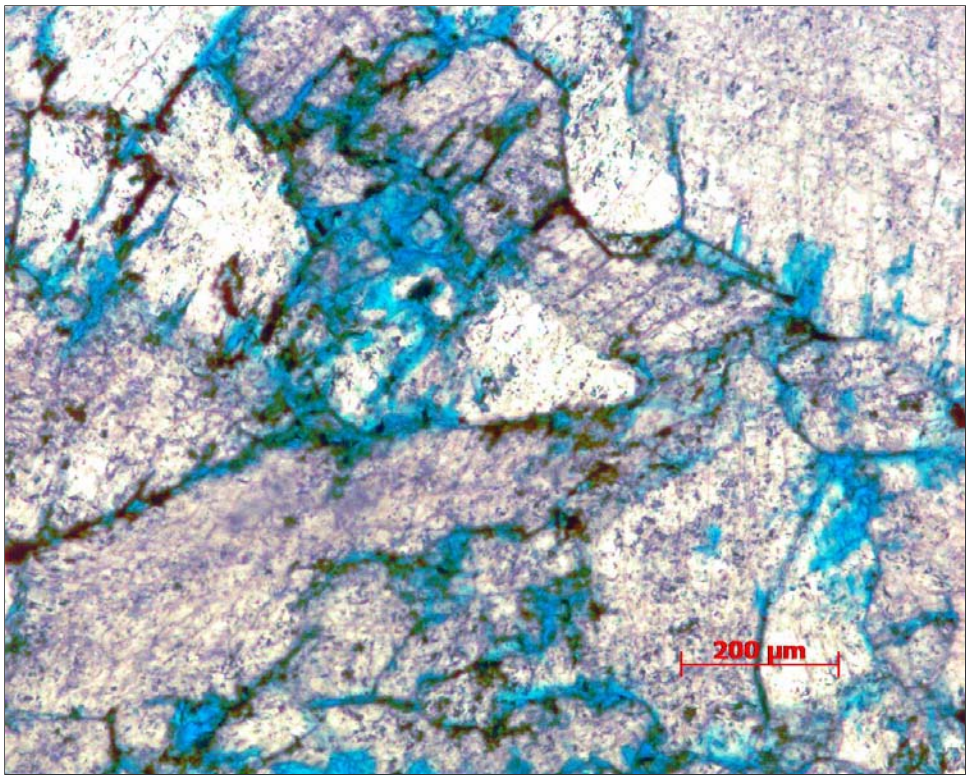

Figure 19. Heavily Weathered Dolomite from the Brownlee Pit.

Brownwood Pit

This aggregate is produced by Vulcan Materials Corporation, and the quarry is located near Brownwood, Texas. The aggregate from this location is predominantly limestone with variations in sand content. Most of the samples exhibit very little to no porosity and contain a variety of minerals. There was no evidence of heavily weathered aggregate in the Brownwood samples. Figure 20 is a limestone with abundant dolomite and quartz sand clasts. The dolomite may be primary, or it may be a replacement of original aragonite filling voids in fossil fragments. Quartz grains are subrounded to angular white grains dispersed throughout the image along with calcite fossil fragments; micrite fills the intergranular volume. Although the properties give an indication of good skid resistance, other characteristics such as skid insoluble material is needed to estimate the amount of skid resistance particles in this aggregate type. Moreover, relying only on the result of an aggregate geological test could be misleading.

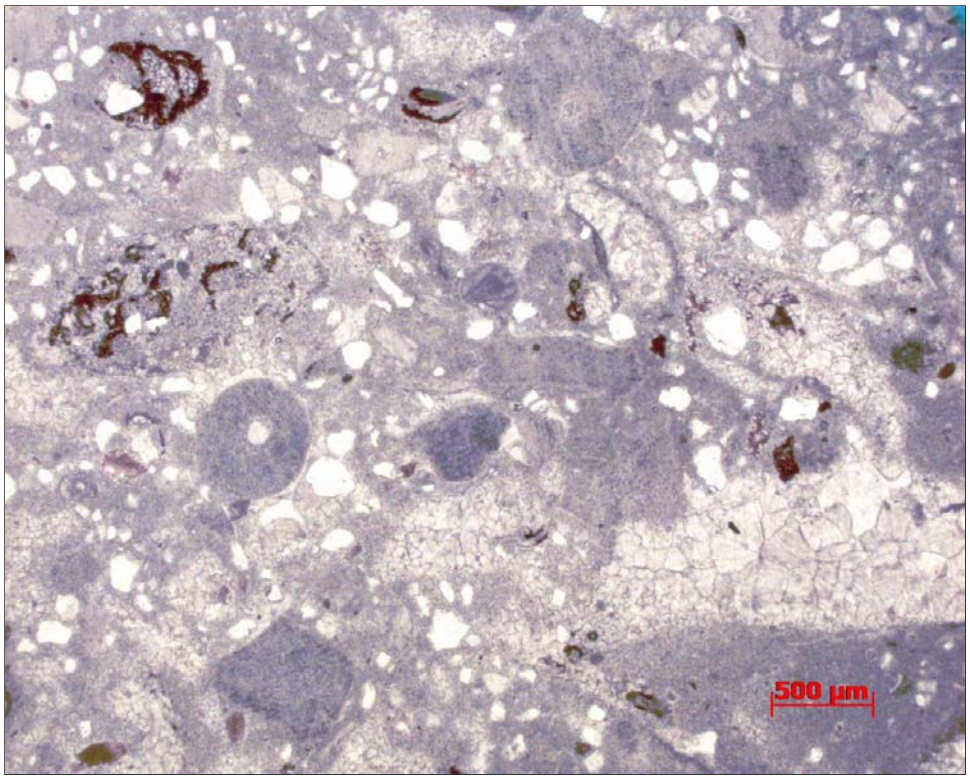

Figure 20. Sandy Dolomitic Limestone from the Brownwood Pit.

The image in Figure 21 is sandstone with quartz and feldspar as the dominant constituents cemented by calcite (red) and lesser amounts of dolomite. This sample has a heterogeneous distribution of intergranular pore space. The angularity of the detrital grains and the carbonate cement should give this aggregate good skid property. Heavy minerals (zircon, rutile) abound in the photomicrograph of carbonate-cemented sandstone in Figure 22. The heavy minerals appear opaque and are concentrated in the lower half of the figure. There is no porosity visible in this image.

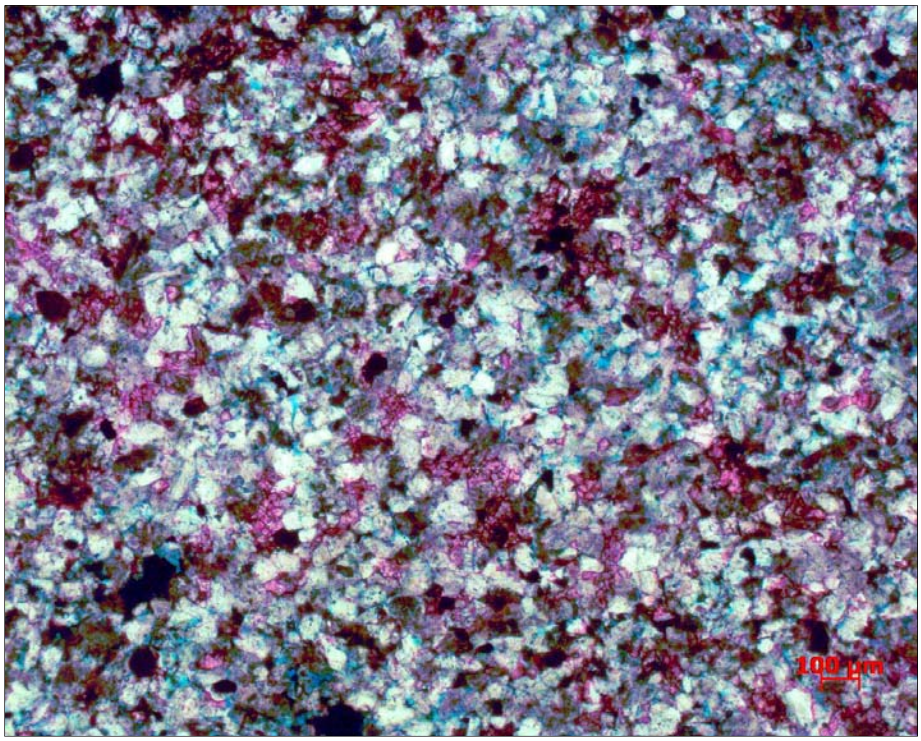

Figure 21. Calcite and Dolomite-Cemented Sandstone from the Brownwood Pit.

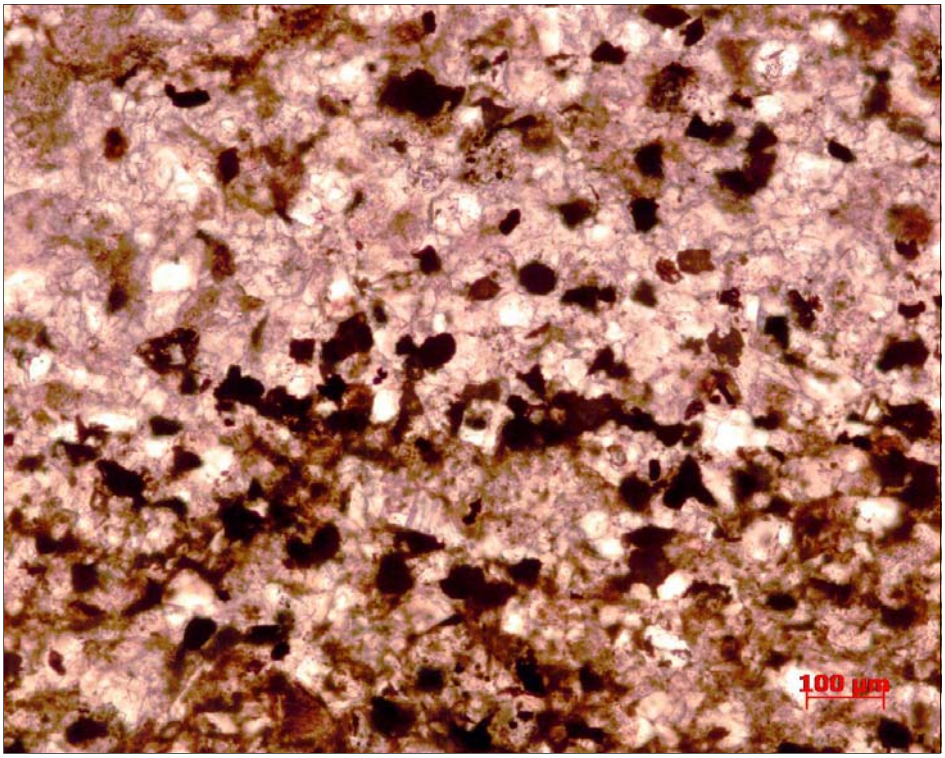

Figure 22. Carbonate-Cemented Sandstone with Abundant Heavy Minerals.

Fordyce Pit

This aggregate is produced by Fordyce Sand and Gravel Corporation, and the quarry is near Victoria, Texas. Aggregates selected from the Fordyce pit samples show a diverse origin. Rock types range from a metamorphosed sandstone to sedimentary chert, fossiliferous limestone, silica-cemented sandstones, and dolomite. Figure 23 shows chalcedony replacing a fossil fragment (cigar-shaped object) as well as moldic pores derived from the dissolution of dolomite or calcite (blue). Calcite, dolomite, and siderite are preserved in the heavily silica-cemented region in the right half of the image. This aggregate should have good skid properties.

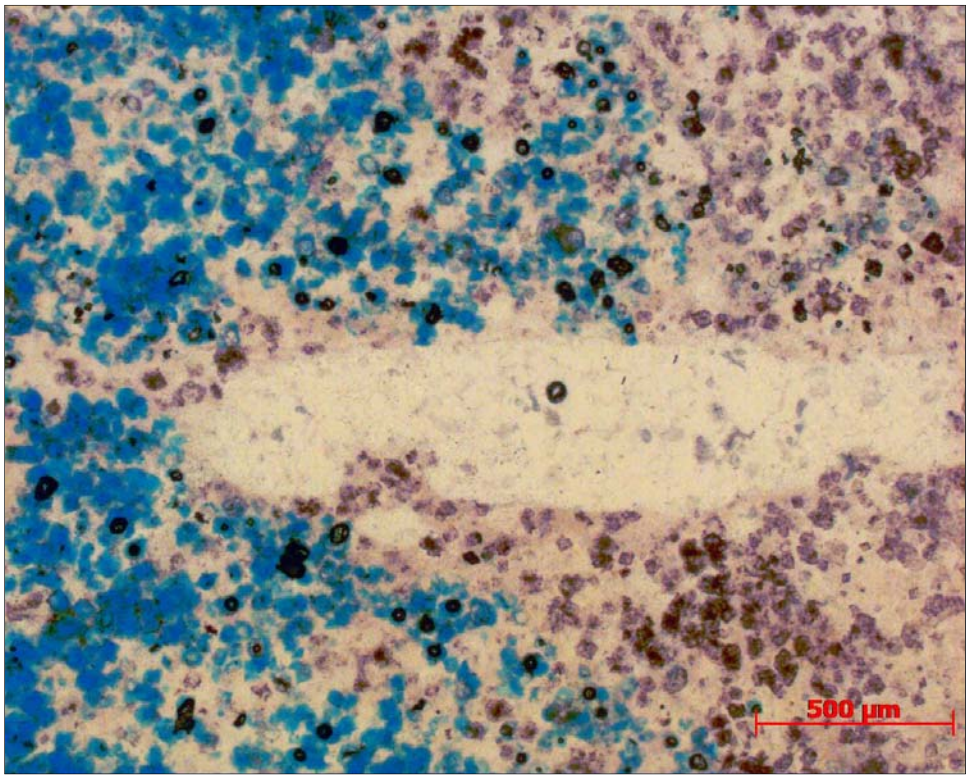

Figure 23. Chalcedony Replacement of Fossils and Moldic Porosity of Fordyce Pit.

The aggregate depicted in Figure 24 is composed predominantly of chalcedony (microcrystalline quartz) with some rhombohedral calcite, dolomite, and siderite crystals preserved. There are some rhombohedral pores developed from the dissolution of dolomite or calcite that may help make this aggregate have good skid properties if the

pores are large enough. Overall, the different aggregate types found in this pit should yield good skid resistance.

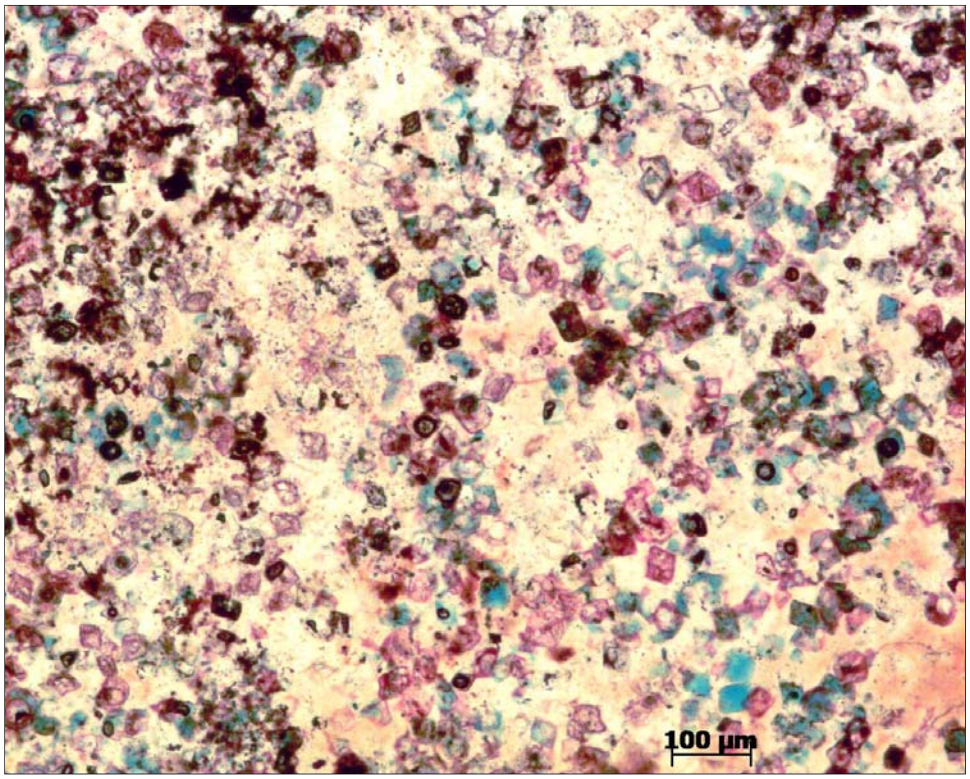

Figure 24. Chalcedony Matrix with Moldic Pores from the Fordyce Pit.

McKelligon Pit

This aggregate type is produced by Cemex Corporation, and the quarry is near El Paso, Texas. There is some highly weathered granite in the finer fractions (< 3/8 inch), but the aggregate is predominantly dolomite and sandy dolomite with minor fossiliferous limestone and sandstones with dolomite and siderite cement. This aggregate should have good skid properties provided the fine-grained limestone (Figure 26) be kept to a minimum.

The most dominant rock type in this pit is a sand-bearing dolomite, shown in Figure 25. The sand grains (white) are angular and composed of quartz, which will make a rough surface when the rock is polished, so this rock should give good skid properties. Figure 26 is a very fine-grained limestone, composed of small calcite crystals. This rock

would not have good skid properties because of the small crystals all composed of the same mineral that would generate a nice uniform polish.

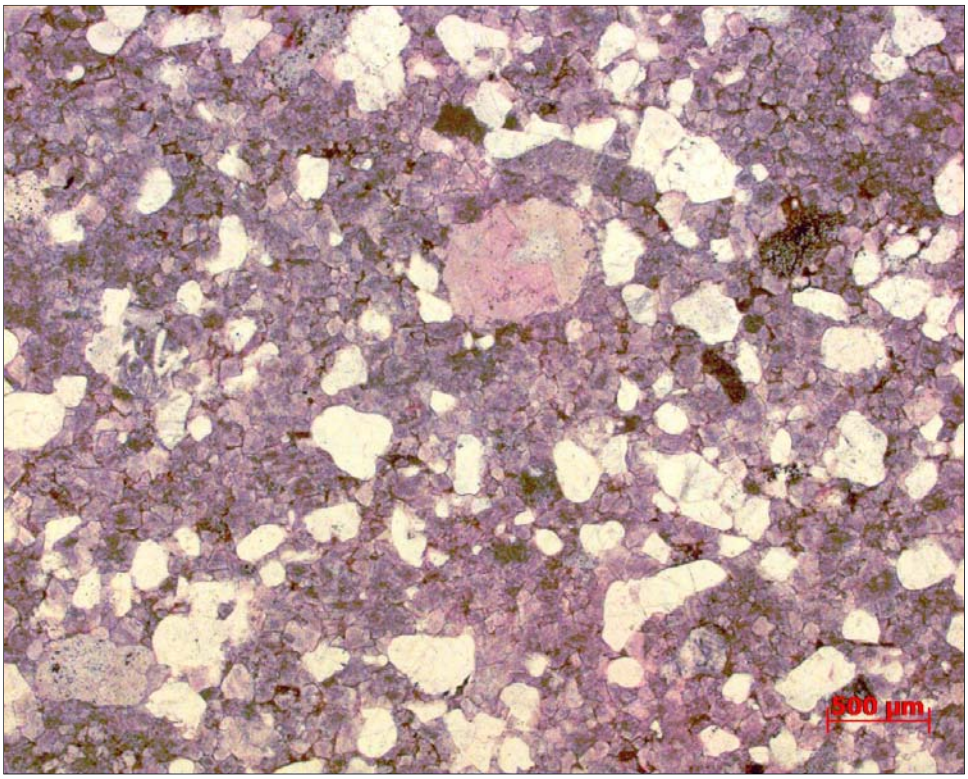

Figure 25. Sandy Dolomite from the El Paso, McKelligon Pit.

Figure 26. Fine-Grained Limestone from the El Paso, McKelligon Pit.

The sandstone shown in Figure 27 is composed of quartz and feldspar detrital grains with dolomite dominating the intergranular volume. There is minor siderite (opaque-looking rhombs) and pore space (blue). There is also some quartz overgrowth cement present that would greatly increase the durability of the sample. This aggregate should have good skid properties.

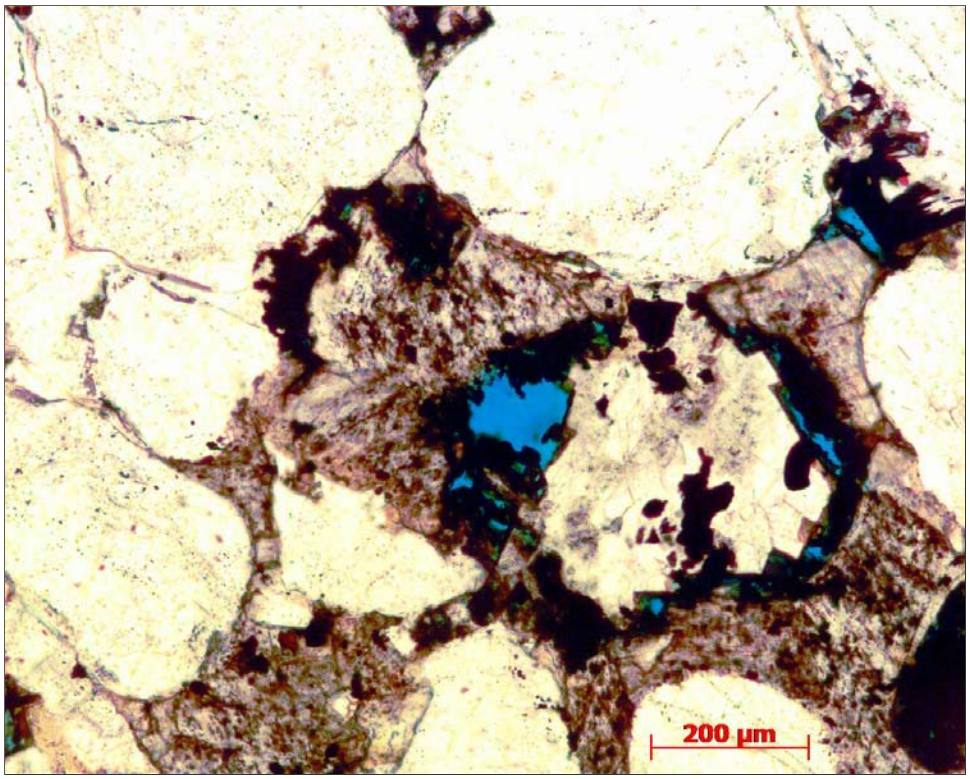

Figure 27. Dolomite and Siderite-Cemented Sandstone from the McKelligon Pit.

Figure 28 depicts one of only four granite samples. This piece is from a weathered rock because many of the grains are etched and are being chemically altered (mottled texture of feldspar grain in upper left corner of image). Due to the sharp contacts and large grain sizes, and alteration granite can be considered to have satisfactory skid resistance but a more comprehensive field and laboratory study is required to classify this aggregate as a good skid resistant aggregate.

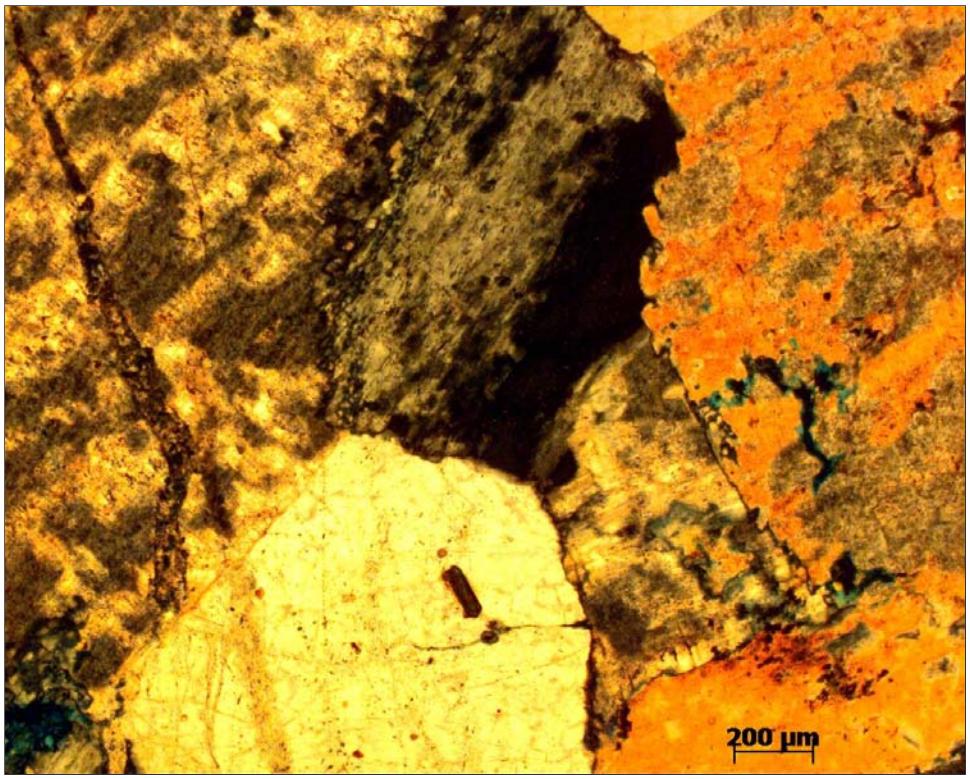

Figure 28. Cross-Polarized Light View of Altered Granite from McKelligon Pit.

Georgetown Pit

This aggregate constitutes part of aggregate called sandstone from Brownlee in this research. The aggregate samples from Georgetown are generally not very durable, but the poor durability can be an asset when it comes to skid performance. These aggregates will abrade rapidly and provide a continuously rough texture. Figure 29 is an image of a fine-grained limestone with chalcedony (microcrystalline quartz) in the lower right side of image. This image was taken under cross-polarized light to accentuate subtle differences in crystallography. There is a large percentage of chalcedony and chert in these samples that will aid in skid resistance. Moldic pores (vesicles) also provide good skid resistance in rocks with lower durability (Figure 30). One can see from this image that the aggregate is extremely porous and poorly cemented, which will result in low durability, but it will generally increase the skid resistance.

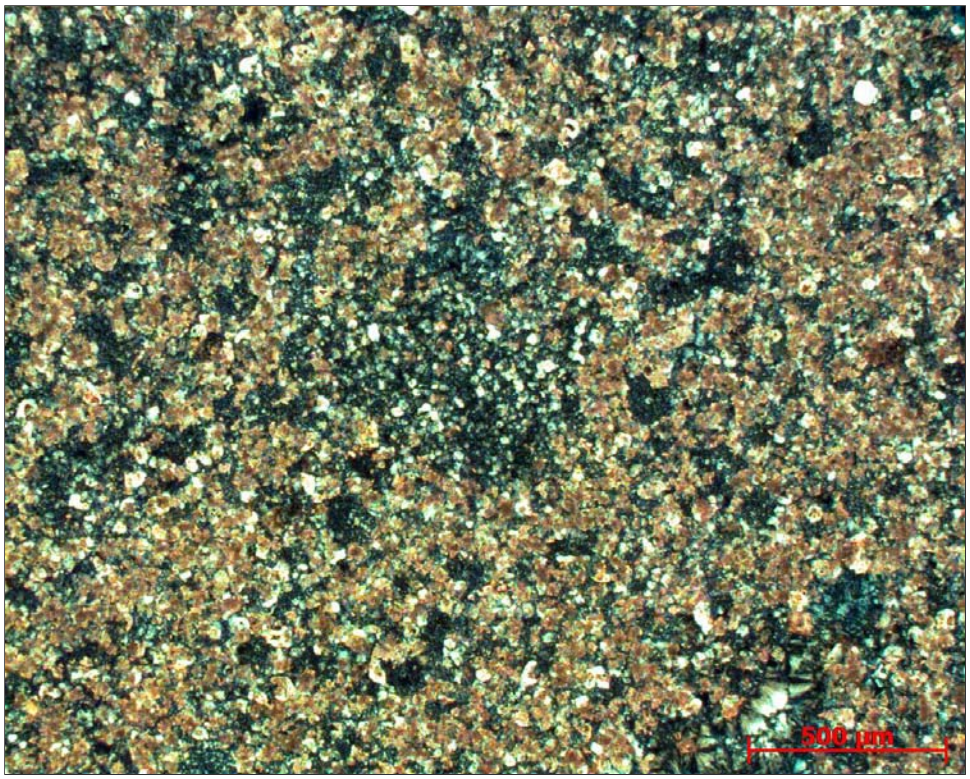

Figure 29. Fine-Grained Limestone with Chalcedony from the Georgetown Pit.

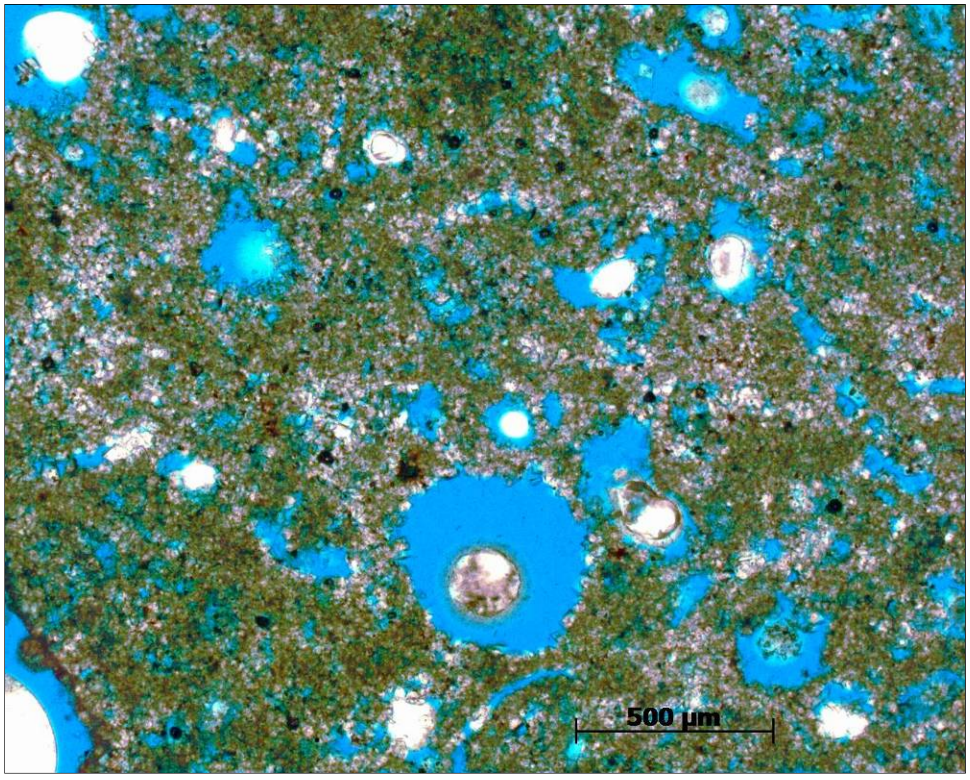

Figure 30. Moldic Pores in Limestone from the Georgetown Pit.

In summary, all sources but one (Beckman aggregate) contained multiple mineral types and textures, which have been shown to exhibit favorable skid properties. The quality will depend on the percentage of good to poor aggregate present in a sample. Aggregate durability does not necessary correlate with skid performance.

From a mineralogical point of view, El Paso, Brownwood, and Fordyce are predicted to have satisfactory skid properties. The combination of Georgetown and Brownlee, considered as Brownlee aggregate in this study, would have good skid properties.The worst aggregate would be the Beckman pit.

The Beckman pit contained 100 percent calcite, which would result in the poorest skid resistance. The Brownlee pit contained a fair amount of weathered aggregates that in one hand could significantly reduce skid resistance and on the other hand might be able to maintain its skid properties due to rejuvenation of the aggregate texture. The Georgetown pit has a lot of low durability aggregates, but the texture will help give it better skid properties as long as the rock does not disappear. The El Paso (McKelligon pit) aggregates contained a fair percentage of weathered rocks, but weathering is not as detrimental for the El Paso aggregates due to the coarse grain size and variable mineralogy.

Although the petrographic analysis could yield a good insight into mineral constituents, one should not rely only on the results of petrographic analysis. Other mechanical and physical tests, e.g., soundness and Micro-Deval, are necessary to evaluate aggregate polishing susceptibility.

TESTING OF AGGREGATE RESISTANCE TO POLISHING AND DEGRADATION

As discussed earlier, macrotexture and microtexture are two important factors providing skid resistance on the road surface. Macrotexture depends on the mixture characteristics and aggregate gradation, but microtexture depends mainly on the aggregate surface texture.

Microasperities on the surface of the aggregates provide surface microtexture, which plays a key role in providing skid resistance at lower speeds. The ability of an aggregate type to maintain its rough texture against traffic loading is an important factor

that has to be considered in a comprehensive aggregate classification system. There are several methods to evaluate the potential of an aggregate to resist polishing made by traffic loading. These methods are classified into two major groups—the methods that measure the aggregate abrasion (loss of angularity and some breakage) during traffic loading and the methods that measure aggregate polishing (loss of texture). Furthermore, in these methods, change in one aggregate characteristic, e.g., magnesium sulfate soundness weight loss or BPV, is measured after special load application, and the changes are attributed to the aggregate polish or breakage resistance ability. These changes in aggregate properties are related to aggregate potential to resist polishing. Recent studies reveal that aggregate shape change such as texture and angularity during loading are more relevant to aggregate skid properties; hence, the methods that are able to measure aggregate shape characteristics directly such as AIMS are more preferable (Luce, 2006). In this study, several methods were applied to evaluate the aggregate polishing, abrasion, and breakage characteristics. These methods are discussed herein.

Los Angeles Abrasion and Impact Test

This test is an indication of aggregate degradation during transport and handling. It has been standardized under ASTM C535, AASHTO T 96, and Tex-410-A. In this test, the portion of aggregate retaining on the sieve #12 is placed in a big rotating drum. This drum has some plates attached to its inner walls. A specified number of steel spheres are added to the drum, and it starts to rotate at 30 to 33 rpm for 500 revolutions. The material is then extracted and separated by use of a #12 sieve, and the proportion of the materials remained on the sieve is weighed. The difference between this new weight and the original weight is compared to the original weight and reported as LA value or percent loss. The LA abrasion and impact test is believed to assess an aggregate resistance to breakage rather than abrasion due to wear (Luce, 2006; Meininger, 2004).

Magnesium Sulfate Soundness

This test is an indication of the durability of aggregates and is standardized under AASHTO T104 or Tex-411-A. The test involves submerging an aggregate sample in a solution of magnesium for a specified number of cycles (often five) and measuring the

weight loss afterwards. According to the standard procedure for performing this test, the aggregate sample is dried and placed in the magnesium solution for 18 hours. Then, it is removed from the solution and dried again at oven temperature. This process is repeated five times; then, the loss of aggregate weight is reported.

British Pendulum Test

The British Polish Value is a measure of aggregate surface texture and shows how rough the aggregate surface is. This test has been standardized under ASTM E3033-93 and Tex-438-A. The test was discussed in detail in Chapter II.

Micro-Deval Test

This test is used to evaluate aggregate capability to resist abrasion in a wet environment. The test method originated in France in 1960 and was accepted as the European Union standard afterwards. The first use of this method was in Canada by the Ontario Ministry of Transportation and adopted by AASHTO under the AASHTO T 327-05 test method entitled "Standard Test Method for Resistance of Coarse Aggregate to Degradation by Abrasion in the Micro-Deval Apparatus" (Meininger, 2004). In this test, the durability and aggregate resistance to abrasion in the presence of water is evaluated. Moreover, this test evaluates how aggregates degrade when tumbled in a rotating steel container with steel balls in a wet environment (Cooley and James, 2003; Meininger, 2004). This test method has been adopted by TxDOT in the Tex-461-A standard procedure. In this test, a steel container is loaded with 5000 grams of steel balls and 1500 grams of an aggregate sample in the range of 4.75 mm to 16 mm and 2000 ml tap water. This material is subjected to 9600 to 12,000 revolutions, and the sample weight loss (weight of aggregate passed #16 sieve size) is calculated and reported. Figure 31 shows the Micro-Deval apparatus, and Figure 32 shows the schematic mechanism of aggregate degradation.

Figure 31. Micro-Deval Apparatus.

Figure 32. Mechanism of Aggregate and Steel Balls Interaction in Micro-Deval Apparatus.

This test addresses the aggregate resistance to abrasion better than other tests such as the LA abrasion test specifically in base and HMA materials where stone-to-stone interaction in a wet condition is more important. Moreover, the wet environment of the Micro-Deval is believed to simulate the field condition (Rogers, 1991). Furthermore, recent studies show that this method is more repeatable and reproducible than the other aggregate degradation tests such as the magnesium sulfate soundness test (Jayawickrama et al., 2006).

Aggregate Imaging System

The AIMS is an automated aggregate imaging system to characterize aggregate shape characteristics. This system determines the angularity, shape, and texture of coarse aggregate as well as the shape and angularity of fine aggregates based on a scanning system and digital image processing. Masad et al. (2005) showed that there is no operator bias associated with this test method, and operator training for using this equipment is not complicated. In this system, coarse aggregates are placed on a tray with 7×8 grid points, and fine aggregates are spread uniformly on the tray with 20×20 grid points. Then, a digital camera with a predefined zoom level takes digital pictures of the aggregates. This system is also equipped with back-lighting and top-lighting units that can provide enough light intensity to capture a clear image of the aggregates. Three measures of aggregate shape properties are calculated based on these 2-D images taken from aggregates.

Aggregate texture that shows the aggregate surface microasperities is measured by use of wavelet theory and presented as a texture index. Aggregate angularity described as a deviation from a perfect circle shows the irregularities on the aggregate surface on the macro level. Angularity is calculated by use of the gradient method and presented as an angularity index. Sphericity is another index that is extracted from digital images of aggregates. This index simply shows how close the aggregate is to a perfect sphere. The system is a result of a very comprehensive study being done in Texas A&M University, and all details and analysis procedures have been documented in Al-Rousan's Ph.D. dissertation (Al-Rousan, 2004). Figure 33 is a schematic view of the AIMS system.

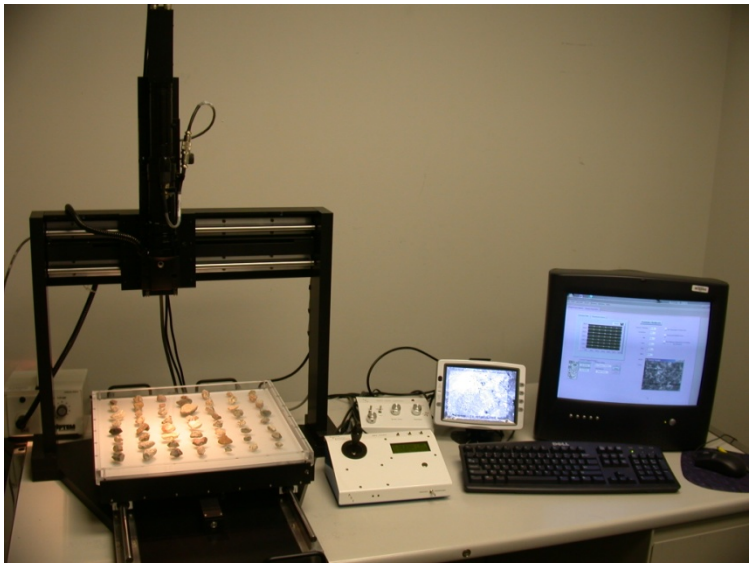

Figure 33. Schematic View of the AIMS System.

ASPHALT MIXTURE TYPES

During the laboratory part of the study, different asphalt mixture types with different aggregate types were fabricated and tested using slabs produced from these mixes. Three different mixture designs were selected. These three mix designs show different frictional field performance and are common mix types used by TxDOT. During the sample preparation stage, laboratory-produced mixes were compacted into special metal molds and polished in a laboratory polisher to obtain the frictional resistance curve. Friction and texture measurements were performed intermittently after sample compaction and during the polishing. The following section describes each mix design.

Type C Mix Design

Type C mix design is used as both an intermediate and a wearing course in TxDOT projects. This mix is usually utilized on the highways and major arterials. Type C mix design has a maximum aggregate size of 0.75 inch and consists of minimum 60 percent particles with two or more crushed faces. Moreover, this mix is used in asphalt layer thickness of 2 to 4 inches. This mix has a good performance against the permanent

deformation due to heavy loading and also has good skid properties. Type C mix design has become the most common mixture design in TxDOT projects (txhotmix, 2008).

Type D Mix Design

Type D mix design is exclusively used for surface application and has a 0.5 inch maximum aggregate size. Moreover, this mixture gives smooth riding characteristics to the road and has good frictional properties. This mix is also used in overlay projects (txhotmix, 2008).

Porous Friction Course

Porous Friction Course consists of an open-graded asphalt mixture containing a large proportion of one-sized coarse aggregates typically from 0.375 to 0.5 inch in size and a small percentage of fine aggregates. The large air content in the range of 20 ± 2 percent lets the water pass through and drain quickly; therefore, this mixture has high skid resistance and reduces the chance of hydroplaning. Utilizing this mixture also improves visibility and reduces water splash and spray. PFC is usually laid over a stronger dense-graded asphalt mixture. This mixture is susceptible to moisture damage such that in the new generation of PFCs, different kinds of additives are used (e.g., polymers, cellulose fibers, lime) to make it more durable (txhotmix, 2008). Table 6 includes a summary of the selected mixtures and aggregates.

Table 6. Abbreviation Selected for Aggregates and Mix Types in This Study.

Mixture Type / Aggregate Type	Type C	PFC	Type D
Fordyce Aggregate	CFY		
Beckman Aggregate	C-BK	P-BK	D-BK
Brownwood Aggregate	C-BW	P-BW	
El Paso Aggregate	C-EP	P-EP	
Brownlee Aggregate	C-BL	P-BL	D-BL
50% Beckman + 50% Brownlee	C-BKBL		D-BKBL

ASPHALT MIXTURE PREPARATION

To have a base for further comparisons, the mixture designs for each asphalt mixture were adopted based upon a mixture design that had been used in the field. In this regard, the mixture design for each mixture was collected by contacting TxDOT officials and consultant engineers who were responsible for the mixture design. Tables 37 to 48 in Appendix A show the mix design for each asphalt mixture. For two mixes—Type D with 50 percent Beckman aggregate + 50 percent Brownlee aggregate, and Brownlee—a separate mixture design based on 4 percent air void criteria, a TxDOT mixture design procedure for Type D mix was done. The optimum asphalt content was also estimated and used in preparation of test specimens.

Based on the mix designs, the required amount of each aggregate type was collected from the producer, and the gradation of each of the individual types of aggregate quarry was determined following the ASTM C 136 (2006) specification. The final gradation used in the production of the HMA mixes was obtained by blending individual fractions in proportions specified in the mix design. Researchers noticed during the blending of each bin that the final blend did not differ from the target gradation by more than ±5 percent for each sieve size. A modified PG 76-22s binder was

used to prepare the laboratory mixtures. Based on the pavement temperatures experienced in Texas, this binder grade is commonly used in the state.

Two methods of measuring friction characteristics were selected in this research to evaluate skid resistance variability with regard to polishing cycles. These methods were the Dynamic Friction Tester and Circular Texture Meter and will be described later in this report. In addition to DFT and CTMeter, two conventional skid resistance measuring methods (British Pendulum Test and Sand Patch method) were used in this study.

In this study, one slab from each mixture type was prepared and tested. Given that the minimum slab size required to measure the skid resistance by DFT and CTMeter is 17.75 inch by 17.75 inch, researchers decided to prepare a 60-inch by 26-inch slab from each mixture. This slab size would provide three locations for measuring the skid resistance of the asphalt mixture surface. Figure 34 shows a schematic layout of the locations of the DFT and CTMeter measurements on a slab. Measurements were not taken close to the slab edge because of the unevenness caused during compaction.

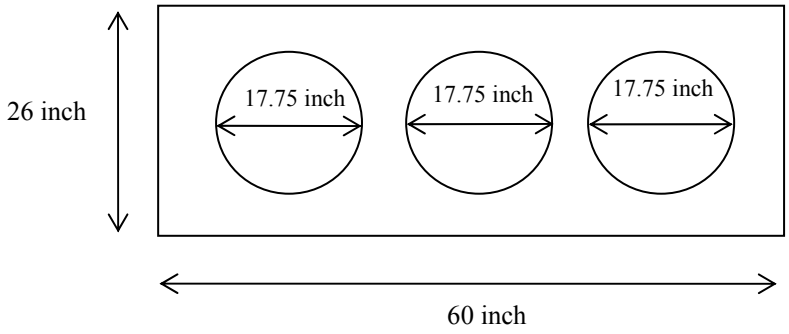

Figure 34. Schematic Layout of Each Slab.

The experimental design for this study deals with a large amount of materials. The amount of HMA batch used for each slab was about 125 kg, with a total of about 1900 kg for all mixtures. About 100 kg of binder was used in preparing all mixes.

Aggregates of each mix were blended and split into seven four-gallon buckets for heating. The HMA mix weight was calculated to produce a 2.5-inch thick slab given the

mold volume and bulk specific gravity (G_{mb}). The target percent air voids was 7 percent for Type C and Type D mixtures and 20 percent for the PFC mixture.

The four-gallon buckets containing aggregates were put into the oven one night before compaction at the mixing temperature. The asphalt binder was also split into small cans to achieve uniform heating. The small cans of desired asphalt type were also heated to their mixing temperature. The heated aggregate was weighed, and the optimum asphalt content was added to it and placed in the mixer for Type C and Type D mixtures. For the PFC mixtures, a 15-second dry-mixing time was applied to the aggregate and fiber blend prior to adding asphalt to have a consistent mix. The mixing was performed in a four-gallon "bucket type" laboratory mixer. In both cases, mixing continued to assure a consistent mix with a uniform asphalt film thickness around each particle. During the mixing time, a long spatula was used to aid the mixing process and scratch off any fines and asphalt from the side of the container. This process helped to obtain a uniform mix with minimum segregation and total number of uncoated aggregate (Vollor and Hanson, 2006). After mixing, the mix samples were placed into an oven in separate batches, and the mixes were conditioned for two hours at the compaction temperature (145°C or 293°F) according to the AASHTO R 30 (2002) specification.

A specially developed laboratory compaction procedure was adopted to prepare the specimens in this study. Since the large size of the slabs limits the use of conventional compaction methods (e.g., kneading compactor), researchers decided to use a walk-behind roller compactor. This equipment has been successfully utilized in the field and is fast. A metal mold was fabricated to confine the mix during the compaction. This mold consists of five metal pieces bolted together and forms a frame to confine the mixture. In this form, a 66 inch × 33 inch baseplate is underlying two 2.36 inch × 2.36 inch L-shape sections as the walls. Two ramp-shape metal pieces were also fabricated and mounted at both ends of the frame to facilitate moving of the walk-behind roller compactor up to the frame. Figure 35 shows the schematic of the mold used to confine the mixture during compaction.

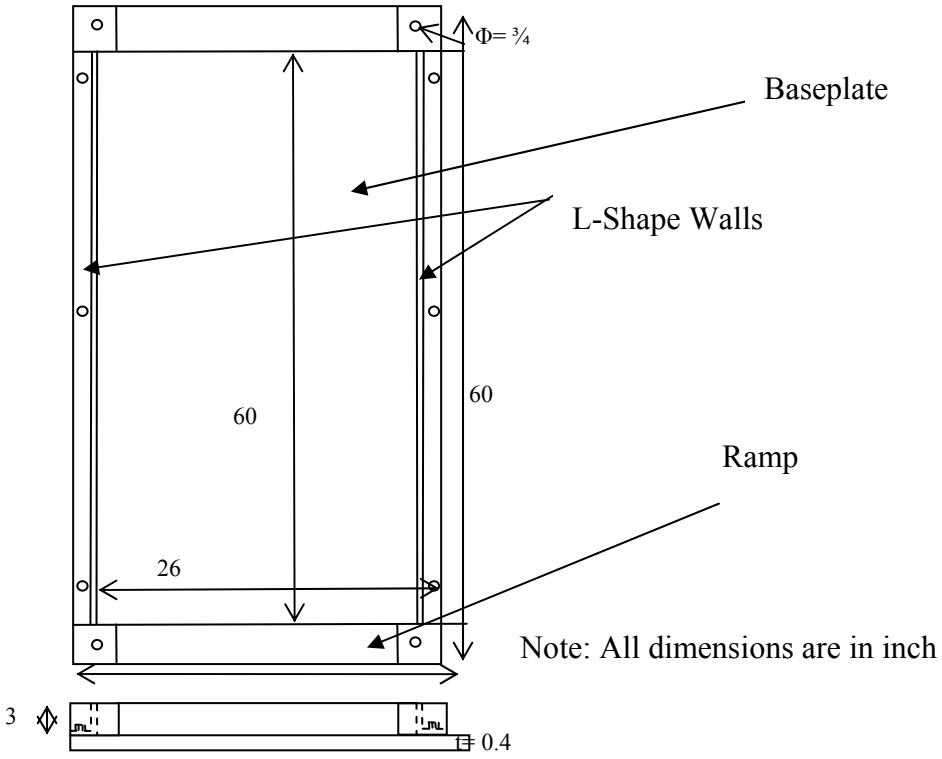

Figure 35. Schematic of the Mold Used in Slab Compaction.

It is difficult to measure the air void directly by nuclear gauge because the metallic baseplate interrupts any direct-measuring device and results in incorrect measurements. Therefore, a scale was built to control the thickness of the slab as an indirect measure of air void (Figure 36). Consequent measurements showed that this method was successful in controlling the compaction effort to obtain the desired air void.

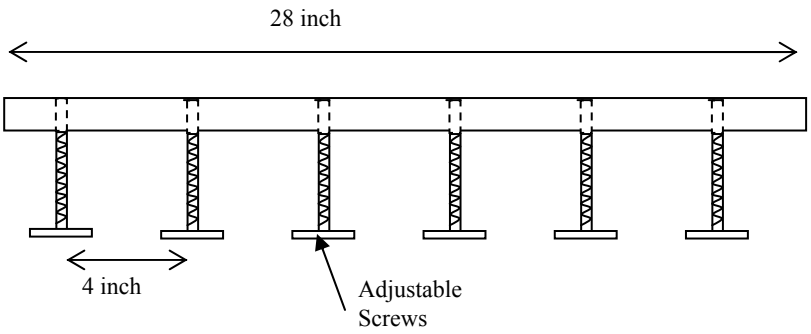

Figure 36. Slab Thickness Measuring Scale Used to Adjust Slab Thickness.

After mixing, the mixture was transported to the compacting area by a cart in the metal buckets and spread inside the frame, being uniformly distributed and smoothened by a 30-inch rake. This process was done fast and carefully to provide a smooth surface with minimum segregation and temperature loss (Vollor and Hanson, 2006). The mixture was then compacted by using the vibrator roller compactor (Ingersoll-Rand SX-170H). According to factory specifications, this compactor has a 595-lb operating weight, 60.4-inch length, and 22-inch width drum size. Based on the manufacturer's recommendation, this compactor could be used to compact the layers up to 9 inches in thickness. Figure 37 shows a picture of this compactor.

Figure 37. Walk-Behind Roller Compactor.

During compaction, the slab thickness was measured periodically to assure the correct slab thickness. Rolling was continued until a regular surface was obtained at the required thickness. The typical rolling process took about 20-25 minutes. The slab was then left for one day to cool down and become ready for polishing and further measurement.

As previously mentioned, the target air void of Type C, D, and PFC mixes was 7, 7, and 20 percent, respectively. To investigate the uniformity of compaction throughout

the slab, six cores with 6-inch diameters were taken from each slab after measuring terminal skid resistance. ASTM D 2726 (saturated surface-dry technique for dense-graded mixes) and D6752 (2004) (CoreLok apparatus for PFC mixes) test methods were used to determine the bulk specific gravity (G_{mb}). The air void content for each sample was calculated based on this G_{mb} and previously measured G_{mm}. Table 7 shows the results of the average air voids for each slab, with an average air void content of 7.9, 9.9, and 21 percent for Type C, Type D, and PFC, respectively.

Table 7. Average Air Content Measured for Each Slab.

Aggregate Type	Mix Type	Average Air Void Content (%)
Brownlee	Type C	8.9
Brownwood		7.7
Beckman		7.1
El Paso		7.8
Fordyce		7.8
50% Brownlee + 50% Beckman		8.0
Brownlee	PFC	23.0
Brownwood		18.8
Beckman		24.0
El Paso		18.0
Brownlee	Type D	9.0
Beckman		10.8
50% Brownlee + 50% Beckman		9.8

SLAB-POLISHING METHODS

Several polishing methods were investigated to select the one that:

- test aggregate susceptibility to polishing in a large-scale asphalt mixture specimen,
- has the ability to polish different mixture types on an area that is required by DFT and CTMeter,
- can adjust the number of polishing cycles, and
- adjusts the value of loading.

Two methods were investigated for polishing the slabs. The first approach was by using a one-third scale Model Mobile Load Simulator (MMLS3). MMLS3 is an accelerated pavement testing system. The load has been scaled down with the tire

pressure at the same level of real traffic loading. Load frequency, tire pressure, temperature, and speed can be adjusted in this equipment (UMass, 2008). The MMLS3 consists of four rotating axles equipped with a 300-mm (11.8 inch) diameter pneumatic tire. The load level on each tire could vary between 2.1 kN to 2.7 kN by adjusting the suspension system. The tire pressure could be raised up to 800 kPa. This equipment is able to apply up to 7200 loads per second (Smit et al., 2004). Figure 38 shows a picture of the MMLS3. Slabs were compacted and placed under the MMLS3 for polishing. After several attempts, the use of MMLS3 for polishing was discontinued due to the following problems observed during polishing:

- The rate of polishing was very slow, and even after 200,000 cycles, the surface was not polished significantly.
- In each turn, only one strip with a 3-inch width is polished, and to make a measurement with the DFT and CTMeter, at least six polished strips were needed side by side. Therefore, the polishing process was time-consuming.
- A significant amount of rutting was observed that was believed to adversely affect the friction measurements by DFT and CTMeter.

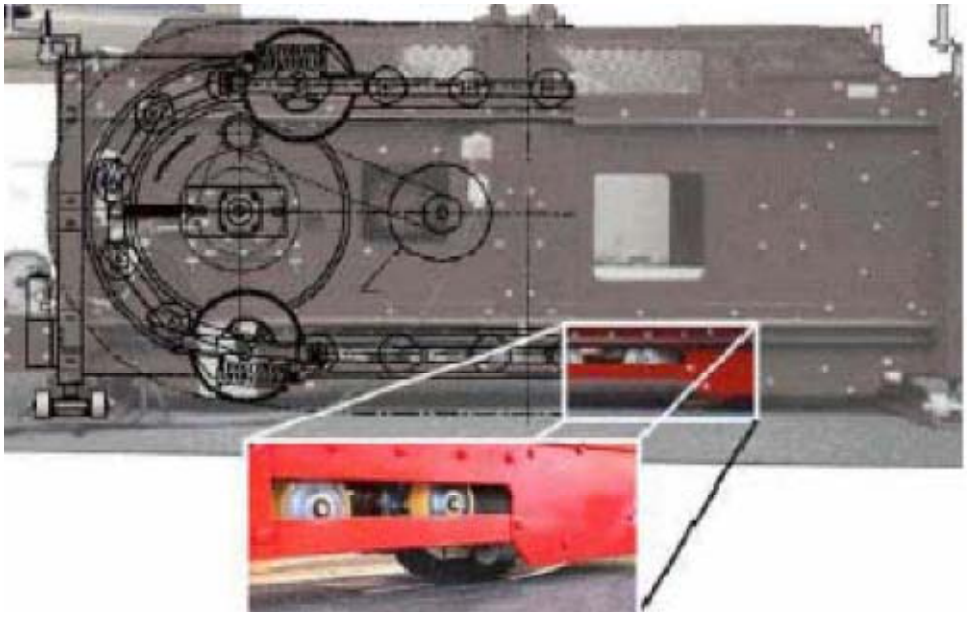

Figure 38. Schematic View of MMLS3 (after Hugo 2005).

In the second method, a polishing test machine already evaluated by NCAT was used. The results of the study by Vollor and Hanson (2006) showed that this machine has satisfactory performance and could simulate the field condition (Vollor and Hanson, 2006). This machine has three 8-inch × 3-inch caster wheels attached to a turntable. These three wheels spin on an 11.188 inch diameter path; therefore, it is possible to measure the polished area by DFT and CTMeter. It is believed that this configuration polishes the surface of the slabs similar to the way that traffic does on a pavement. To guide the wheels in an 11.188 inch circular track, the wheels are equipped with ball bearings that use a mounted fixture, maintaining the wheels on the track during the polishing time. The applied load on the wheels is variable and could be adjusted through adding and subtracting of circular iron plates on the turning table. The turntable is hinged to the motor shaft by use of a square shaft and can easily move up and down; hence, this system facilitates adjusting the applied load to the wheels. Figure 39 shows the polishing machine assembly. This system is turned by a 0.5 horsepower electrical motor through a gearbox. The motor is equipped with a Baldor motor speed controller that facilitates varying the rotation speed. There is also a counter system provided to control the number of revolutions by use of an Omega digital counter and laser light pick-up. Moreover, this system could turn off the motor by reaching a preset value for number of revolutions. The turntable was put in a cage for safety. There is also a water spray system included in this polisher. The spraying system consists of three 0.25 inch PVC pipes on each side of the cage that can wash away the abraded material from the surface and allow polishing of the slab. An electric cut-off valve attached to the water spray system is synchronized with the Omega counter that cuts off the water after reaching the desired revolutions (Vollor and Hanson, 2006). The original machine was designed with the slabs inserted into the protecting cage, but in this research, the square rod linking turntable and motor was modified so that it was possible to place the polisher on the slab and polish it.

Figure 39. Polishing Machine Assembly.

TESTING OF MIXTURE RESISTANCE TO POLISHING

There is no standard test procedure for measuring pavement friction during mix design; however, four different tests have been widely used to evaluate mixture skid properties such as macrotexture and microtexture. These tests include: British Pendulum skid tester (ASTM D3319-00 and E303-93 (re-approved 2003)), measuring pavement macrotexture depth using a volumetric technique—Sand Patch Test—(ASTM E965), measuring pavement surface frictional properties using the Dynamic Friction Tester (E1911-98), and measuring pavement macrotexture properties using the CTMeter (ASTM E2157-01). The following sections give a brief review of test methods (Vollor and Hanson, 2006).

British Pendulum Skid Tester

The British Pendulum skid tester is probably the most widespread equipment in the world to measure skid resistance. BPT was invented by Percy Sigler in the 1940s and

modified by UK Transport Laboratory in the 1960s (Britishpendulum, 2008). “The skid tester consists of a pendulum with tubular arm that rotates about a spindle attached to a vertical pillar. At the end of the tubular arm a head of constant mass is fitted with a rubber slider” (Britishpendulum, 2008). Moreover, this test is low-speed testing equipment measuring the frictional properties of the test material by swinging a pendulum with a specific normal load and standard rubber pad. The test results are reported as a number (British Pendulum Number) that is a measure of kinetic energy loss when the rubber slider is dragged on the surface, and that is an indirect measure of pavement microtexture. This equipment can be used to measure the change in material skid characteristics as described in ASTM D 3319-00. The rubber slider has two different sizes for testing aggregate samples and road surface. The small rubber slider has a 1.25 inch width used for measuring aggregate properties. The large rubber slider with 3 inch width is used for measuring road surface skid resistance. Figure 40 shows a picture of the British Pendulum (Britishpendulum, 2008).

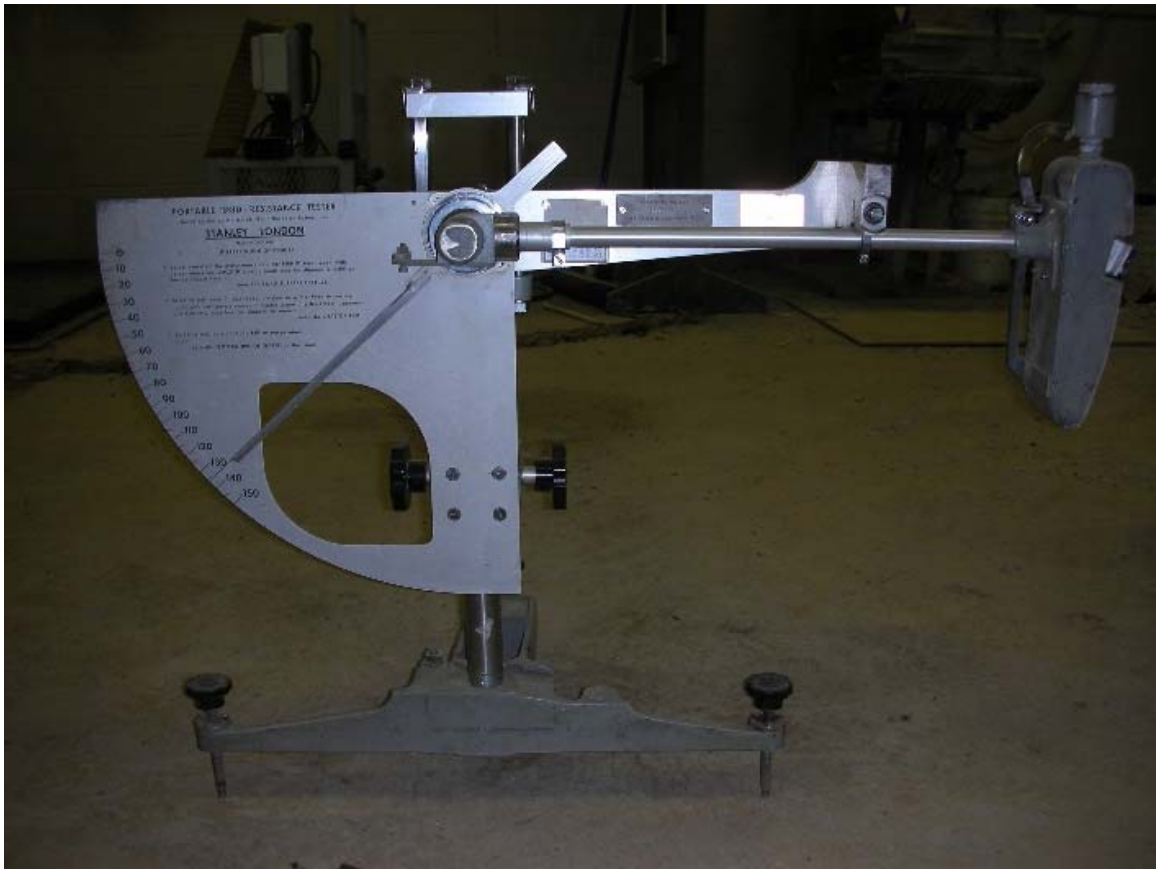

Figure 40. British Pendulum Device.

The Volumetric Method for Measuring Macrotexture – Sand Patch Method

This is a simple test to measure the pavement macrotexture. The test is undertaken on any dry surface with spreading a known quantity of sand or any particulate fine grain materials with uniform gradation, e.g., glass beads on the surface. The material is then evenly distributed over a circular area to bring it flush with the highest aggregate peaks. The diameter of this circle is measured in four different angles evenly spaced and averaged. By knowing the test material volume and diameter of the circle, the Mean Texture Depth could easily be calculated. Figure 41 shows the sand patch test being performed on an asphalt slab.

Figure 41. Schematic of Sand Patch Method.

Dynamic Friction Tester

The Dynamic Friction Tester as described by ASTM E 1911 consists of three rubber sliders and a motor that reaches to 100 km/h tangential speed. The rubber sliders

are attached to a 350 mm circular disk by spring-like supports that facilitate the bounce back of the rubber sliders from the pavement surface. The test is started while the rotating disk is suspended over the pavement and driven by a motor to a particular tangential speed. The disk is then lowered, and the motor is disengaged. In the meantime, water is sprayed on the rubber and pavement interface through surrounding pipes to simulate wet weather friction. By measuring the traction force in each rubber slider by use of transducers and considering the vertical pressure that is reasonably close to the contact pressure of vehicles, the coefficient of friction of the surface is determined. DFT could measure a continuous spectrum of dynamic coefficient of friction of pavement surface over the range of 0 to 80 km/h with good reproducibility (Vollor and Hanson, 2006; Nippou, 2008). In addition, the DFT measurement at 20 km/h is an indication of the microtexture and is being used as a replacement of BPN (Hall et al., 2006). Figure 42 shows a picture of the Dynamic Friction Tester.

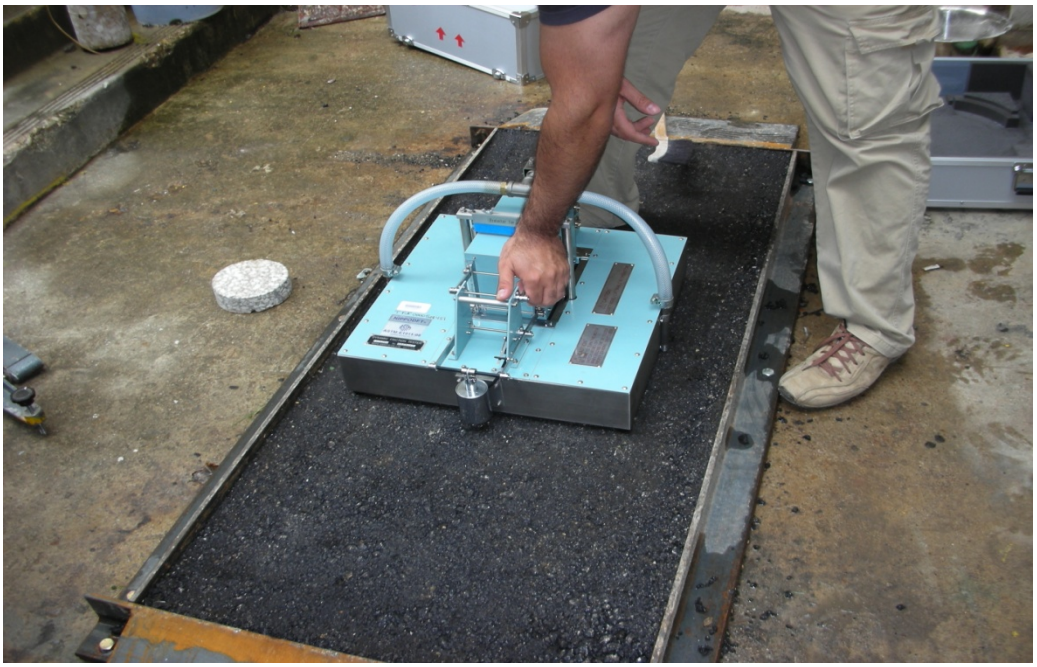

Figure 42. Schematic of Measuring Pavement Skid Resistance by DFT.

Circular Texture Meter

The most current technology in measuring pavement macrotexture is the Circular Texture Meter described in ASTM E2157. In this device, a Charged Couple Device (CCD) laser displacement sensor mounted on an arm 80 mm above the surface rotates around in a circle with a 142 mm radius. A motor at a tangential velocity of 6 mm/min drives the arm. The CCD laser takes 1024 samples of the pavement surface in one round with 0.87 mm spacing. The data are converted to digital format and stored in the memory of a laptop. To calculate the Mean Pavement Depth, the data are divided into eight equal 111.5 mm arcs. The calculated MPD for each segment is averaged and presented as MPD for the test surface. The individual MPD values for each segment are also available for further investigation (tics, 2008). Figure 43 shows a picture of a CTMeter.

Figure 43. CTMeter (Courtesy of Hanson and Prowell, 2004).

EXPERIMENTAL SETUP

Thirteen different slabs were prepared and polished by the polishing machine. The measurements were done after predefined polishing cycles. The polishing cycles

continued to 100,000 cycles for dense mixes and 200,000 cycles for PFC mixtures. Table 8 presents the different slabs and polishing cycles for designed mixtures.

Table 8. Experimental Setup

Mixture Type	Aggregate Type	Polishing Cycles
Type C	Beckman Brownwood Brownlee El Paso Fordyce 50% Beckman + 50% Brownlee	Before Polishing, 5000, 10,000, 20,000, 35,000, 50,000, 75,000, 100,000 cycles, Completely Polished
PFC	Beckman Brownwood Brownlee El Paso	Before Polishing, 5000, 10,000, 20,000, 35,000, 50,000, 75,000, 100,000, 150,000, 200,000 cycles, Completely Polished
Type D	Beckman Brownlee 50% Beckman + 50% Brownlee	Before Polishing, 5000, 10,000, 20,000, 35,000, 50,000, 75,000, 100,000 cycles, Completely Polished

According to Table 8, each slab was prepared and tested the day after compaction. The sand patch test, British pendulum test, DFT, and CTMeter were conducted on the slabs before the slab was subjected to any polishing. Then, the polisher was placed on top of the slab and the polishing started.

All Type D mixes degraded after 5000 polishing cycles and showed signs of raveling (Figure 44). Due to raveling occurring in these mixes, researchers decided to discontinue polishing these mixes, and they were dropped from the experimental design program.

Figure 44. Type D Mixes Degraded after 5000 Cycles.

After application of the specified number of wheel passes on Type C and PFC mixtures, the specimen was removed and tested for texture and friction according to ASTM E 1911 (2002) and ASTM E 2157 (2005), respectively. Each of these tests was conducted twice on the polished area. It should be noted that since the limited width of the polished area restricts performing the sand patch and British pendulum test, it was decided to continue performing British Pendulum test by 1.5-inch rubber slider rather than 3-inch rubber slider, and the sand patch test was removed from the experimental program. This test was just used to measure the macrotexture of slabs before polishing and after terminal condition. After testing, the polisher was properly positioned on top of the slab such that the polishing was performed in the same path and polishing continued to the next level.

To achieve an entirely polished surface, the slabs were polished by a floor polisher. This machine includes a rotating plate driven by a 175-rpm electrical motor. A #150 sandpaper mesh was used along with the floor polisher to polish the slabs to their terminal condition. Figure 45 shows a photo of the floor polisher used in this research to reach terminal condition.

Figure 45. Floor Polisher.

CHAPTER IV – RESULTS AND DATA ANALYSIS

INTRODUCTION

This chapter contains the results of the different measurements performed on the aggregates and mixes. The results of the DFT, CTMeter, British pendulum, and sand patch measurements are analyzed and discussed. It discusses the results of the texture and angularity measurements by AIMS. In addition, the aggregate characteristics measured by AIMS were analyzed along with DFT and CTMeter measurements to find the relationship between aggregate properties and skid resistance characteristics of different mixes. These analyses will help to develop a comprehensive aggregate classification system based on mixture skid characteristics.

AGGREGATE CHARACTERISTICS

As mentioned earlier, aggregate properties such as gradation, size of particle, texture, shape, porosity, toughness, abrasion resistance, mineralogy, and petrography affect the pavement skid resistance (Mahmoud, 2005). A complete set of measurements for evaluating different aggregate characteristics were performed, and the results are tabulated in Table 9.

Table 9. Aggregate Test Results.

Test Procedure	Brownlee	Brownwood	El Paso	Beckman	Fordyce	Beckman + Brownlee
LA % Wt. Loss	24	25	30	33	19	28.5
Mg Soundness	19	9	19	26	4	22.5
Polish Value	38	21	24	25	28	31.5
Micro-Deval % Wt. Loss	16.2	11.2	14	24	2.1	20.1
Coarse Aggregate Acid Insolubility	58	1	10	1	80	29.5

As mentioned earlier, it has been a common practice in Texas to mix the aggregate with inferior performance with better aggregate to obtain a better-performing blend of aggregate. In this study, the aggregates from the Beckman quarry showed

unsatisfactory field performance with respect to polishing combined with aggregates from the Brownlee quarry on a 50/50 proportion basis. The aggregate characteristic for this mix is believed to be the average of two values for Brownlee and Beckman. Figure 46 illustrates the different aggregate characteristics.

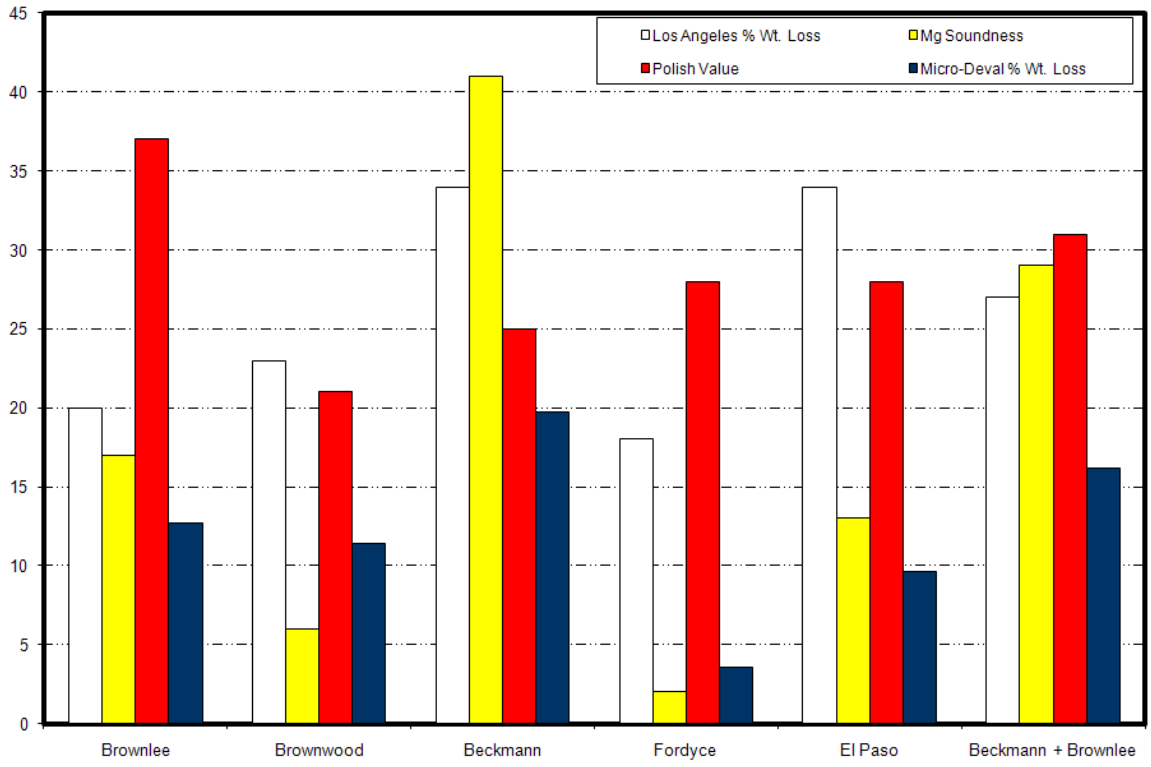

Figure 46. Aggregate Properties (after Alvarado et al., 2006; TxDOT BRSQ, 2008).

Figure 46 shows the Brownlee aggregate has the highest polished value. The Beckman aggregate has the highest weight loss in the Micro-Deval, magnesium sulfate soundness, and LA abrasion tests. Aggregate shape characteristics were also measured, and results are tabulated in Table 10.

Table 10. Result of Shape Measurements by AIMS.

Test Procedure	Brownlee	Brownwood	El Paso	Beckman	Fordyce	Beckman + Brownlee (average)
Texture before Micro-Deval	265	193	269.3	80	142	172.5
Texture after Micro-Deval	222	95	192.6	36	108	129
Angularity before Micro -Deval	2868	2323	2865.6	2195	3959	2531.5
Angularity after Micro -Deval	1883	1730	2126.5	1671	2787	1777

Figures 47 and 48 show the change in texture and angularity before and after Micro-Deval. Figures 91 to 98 in Appendix B show the texture distribution for each aggregate type measured by AIMS.

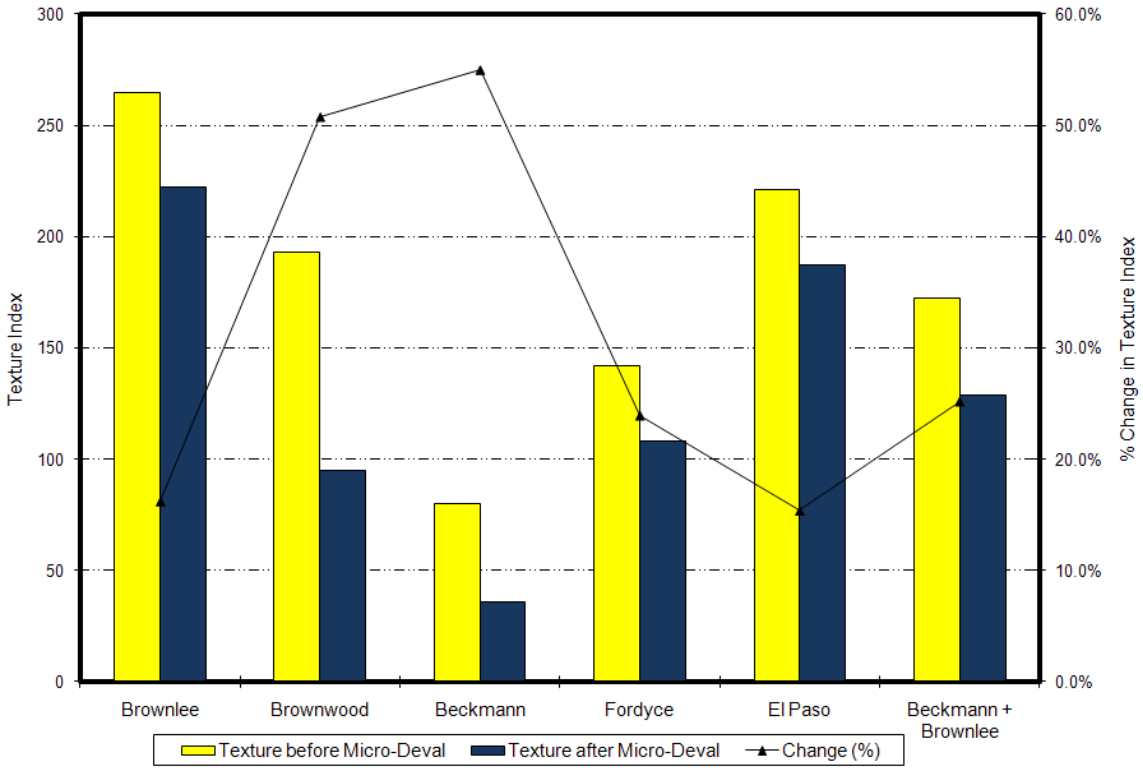

Figure 47. Aggregate Texture before and after Micro-Deval and Percent Change.

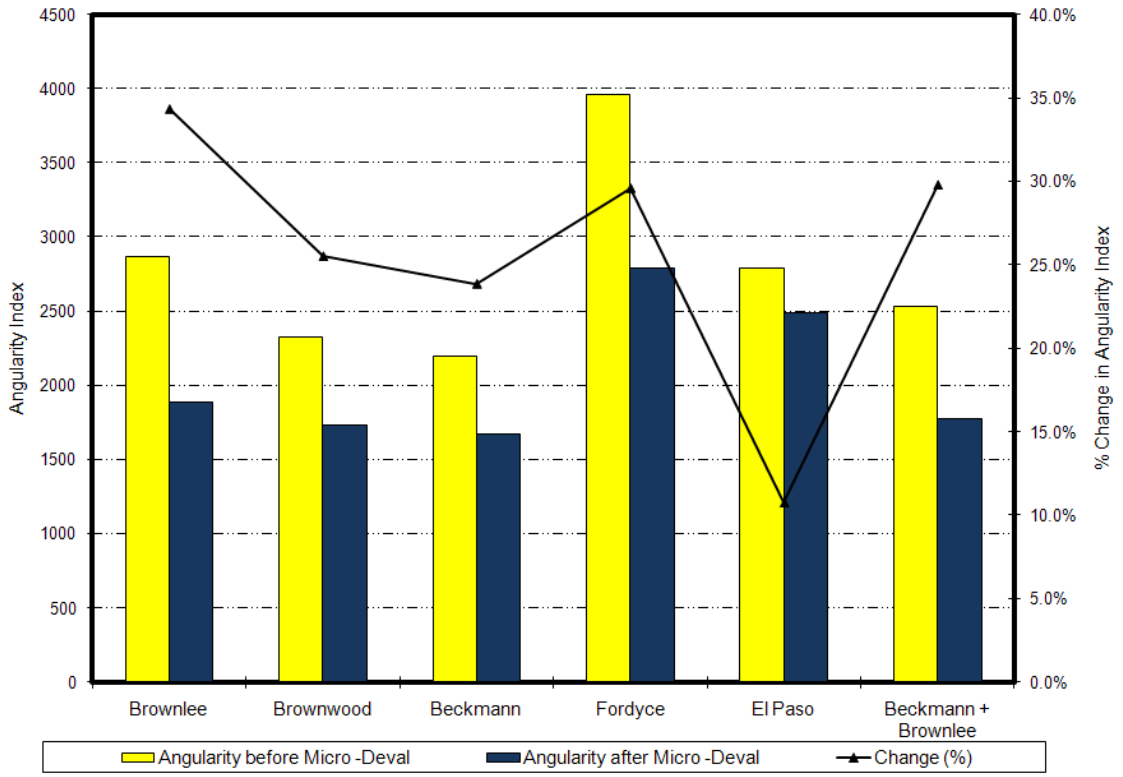

Figure 48. Aggregate Angularity before and after Micro-Deval and Percent Change.

Figures 47 and 48 show that the El Paso aggregate and Brownlee aggregate had the highest texture before and after Micro-Deval. Brownlee aggregate experienced the lowest drop in texture. Beckman aggregate had the lowest texture before and after Micro-Deval, and the highest change in texture occurred in this aggregate type.

Luce (2006) performed a more detailed study to model the texture change in different aggregate types (Luce, 2006). In his study, he evaluated the aggregates' resistance to abrasion and polishing using the method originally developed by Mahmoud (2005). In this method, the Micro-Deval test and the AIMS are used to estimate the aggregate polish resistance. Aggregates are subjected to 15, 30, 45, 60, 75, 90, 105, and 180 minutes abrasion time in the Micro-Deval machine according to Tex-461-A. Aggregates are scanned after polishing using AIMS to determine the change in aggregate shape properties over time and their terminal condition (Luce, 2006). Mahmoud (2005) proposed the following equation to describe texture as a function of polishing time:

$$AIMSTexture = a + b \cdot \exp(-c \cdot t) \quad \textbf{(9)}$$

In this equation, a, b, and c are regression constants while t is the time in the Micro-Deval (Luce, 2006). The regression constants can be determined using non-linear regression analysis. Table 11 shows the values of regression constants of the different aggregate types.

Table 11. Regression Coefficient of Texture Model (Luce, 2006).

Parameter	Sandstone	Hard Limestone	Soft Limestone	Gravel	Granite
A	167.90	83.531	39.125	99.813	178.689
B	70.56	119.931	37.463	14.288	39.021
C	0.00788	0.020	0.025	1.600	0.013

Luce (2006) showed that texture and angularity of the aggregates decrease as the time in the Micro-Deval increases. Furthermore, he found that sandstone aggregate can maintain its original texture, and the curve is almost flat for this type of aggregate (Luce, 2006). Figure 49 shows the texture change for different aggregate versus polishing time in Micro-Deval.

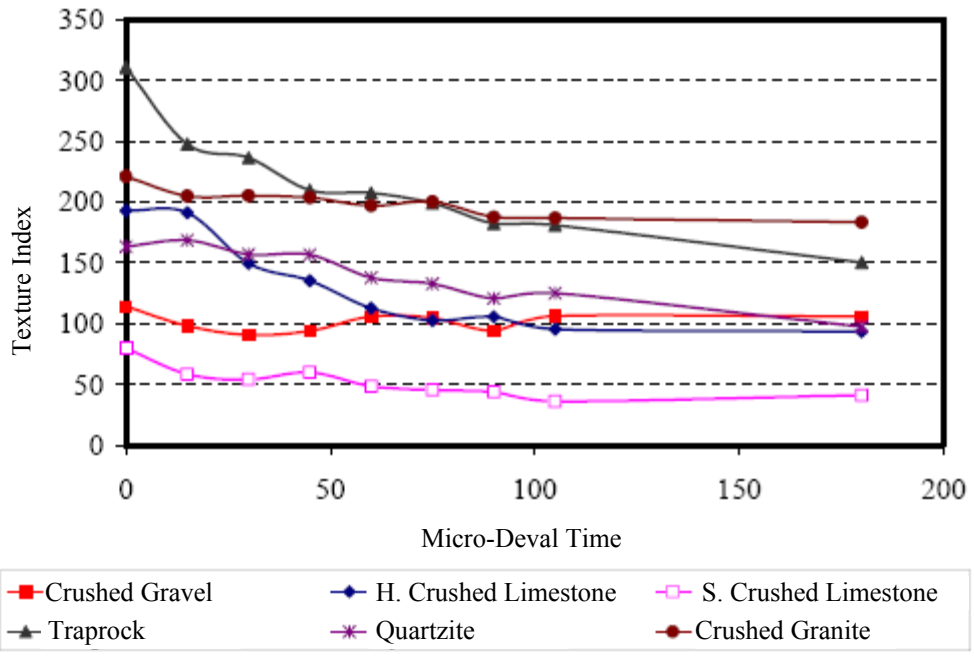

Figure 49. Aggregate Texture as Function of Micro-Deval Time (Masad et al., 2005).

Further analysis by Masad et al. (2006) revealed that the loss of texture curve could be obtained by using only three different polishing intervals in Micro-Deval polishing (0, 105, and 180 minutes) instead of nine different times. The regression constants fitted, using three time intervals, are shown in Table 12.

Table 12. Regression Constants Based on Three Measuring Times (Masad et al., 2006).

Parameter	Brownlee	Brownwood	Beckman	Fordyce	El Paso
A	166.7	93.6	39.13	105.67	189.1
B	99.43	99.15	37.46	36.33	72.704
C	0.00553	0.04087	0.02505	0.02617	0.023

MIXTURE-POLISHING CHARACTERISTICS

This section presents the results of the Sand Patch, British Pendulum, DFT, and CTMeter measurements. It is followed by analysis of the effect of each aggregate type on frictional properties of asphalt mixture.

Results of the Sand Patch Test

The sand patch test was done in six locations on the slabs before polishing and after final polishing (terminal condition). Figure 50 shows the MTD for different mixes before and after polishing. This test was not performed on the PFC slabs, because the glass beads used to measure the MTD penetrated into PFC voids.

Figure 50 and Table 13 show that the average MTD for Type C mixes was about 23 percent greater than Type D mixes. A smaller MTD value indicates a smoother surface. The smaller nominal aggregate size used in Type D provided a smoother pavement with less macrotexture. Except for Brownlee and Brownwood aggregates, all mixes lose their macrotexture due to the abrasion effect of the polishing machine. It could be seen that the macrotexture of mixes containing Brownwood aggregate slightly increased after polishing.

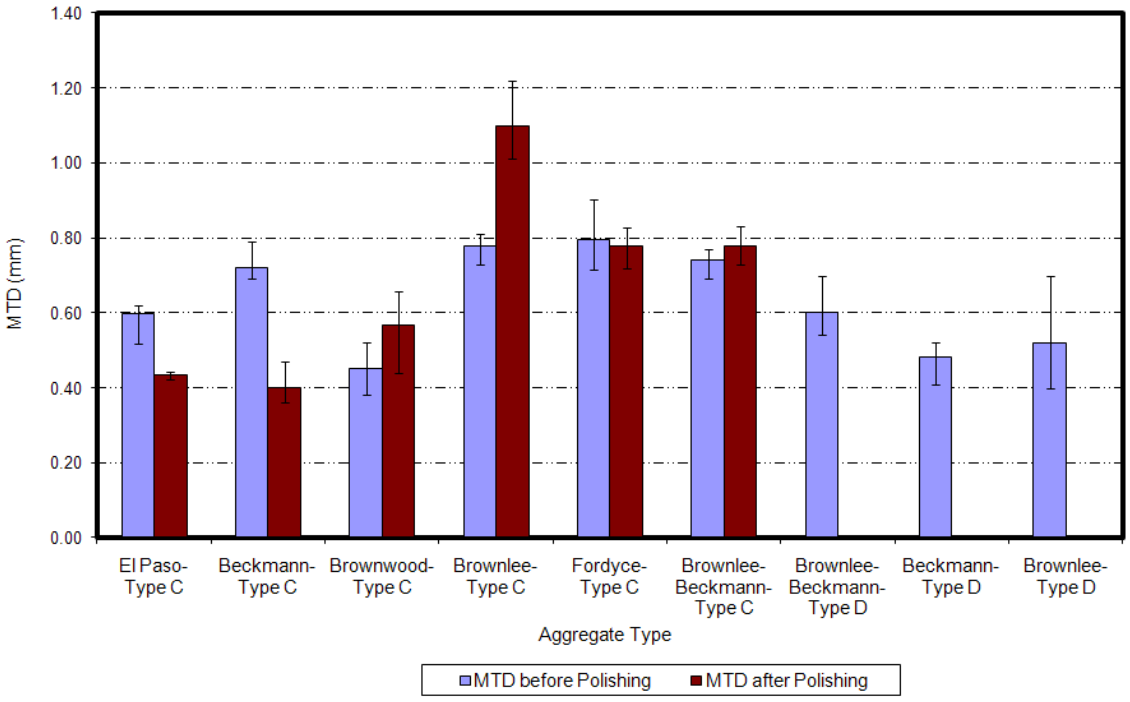

Figure 50. Measured MTD by Sand Patch Method for Different Aggregates before and after Polishing.

Table 13. Measured MTD by Use of Sand Patch Method for Different Mixes.

Aggregate Type	Mix Type	MTD	
		Before Polishing	After Polishing
El Paso	Type C	0.60	0.43
Beckman		0.72	0.40
Brownwood		0.45	0.57
Brownlee		0.78	1.10
Fordyce		0.79	0.78
Brownlee-Beckman		0.74	0.78
Brownlee-Beckman	Type D	0.60	
Beckman		0.48	
Brownlee		0.52	

To study the effect of aggregate type, mixture type, and polishing on the measured macrotexture of each slab using the sand patch method, one-way Analysis of Variance (ANOVA) analysis was performed.

The ANOVA is a powerful statistical procedure for handling data. The one-way ANOVA was used to test the equality of two population means for statistical significance. This analysis is done by partitioning the total variance into two components. One component is calculated based on random error, and the other one is determined based on the difference between two means. The second component is then tested for statistical significance. The F-distribution is used to investigate the significance of this component. The null hypothesis that there is no significant difference between different groups of data is rejected, and the alternative hypothesis that they are different is accepted, if the test indicates significance.

An important step analysis using ANOVA is verifying the validity of assumptions used in this analysis. One assumption of ANOVA analysis is that the variances of different groups are equivalent. The Levene test is a standard approach to test homogeneity of variances. The Levene statistic in Table 14 rejects the null hypothesis that the group variances are equal. ANOVA, however, is robust to this violation when the groups are of equal or near equal size and still could be used.

Table 14. Levene Statistic to Check the Homogeneity of Variances.

Levene Statistic	Df1	df2	Sig.
5.864	5	83	.000

Table 15 shows the results of the ANOVA analysis for the effect of aggregate type. The significance of the F-test in the ANOVA analysis is less than 0.001. Thus, the hypothesis that the average macrotexture values for different aggregates are equal is rejected. Therefore, mixtures with different aggregate types have different macrotexture.

Table 15. Results of the ANOVA Analysis for the Effect of Aggregate Type.

Sum of Squares		df	Mean Square	F	Sig.
Between Groups	1.774	5	.355	24.766	.000
Within Groups	1.189	83	.014		
Total	2.963	88			

The results of the ANOVA analysis are also tabulated in Table 16 in terms of mixture type.

Table 16. Results of the ANOVA Analysis for the Effect of Mix Type.

Sum of Squares		df	Mean Square	F	Sig.
Between Groups	.003	1	.003	.099	.753
Within Groups	2.960	87	.034		
Total	2.963	88			

The significance of F-test in ANOVA analysis is 0.753. This suggests that the null hypothesis that the macrotexture for Type C and Type D are equal, and it cannot be rejected. The results of this table show there is no significant difference between Type C and Type D mixes. The results of the F-test in Table 17 indicate the difference between macrotexture before and after polishing is not significant.

Table 17. Results of the ANOVA Analysis for the Effect of Polishing Cycles.

Sum of Squares		df	Mean Square	F	Sig.
Between Groups	.012	1	.012	.350	.555
Within Groups	2.951	87	.034		
Total	2.963	88			

The results of this analysis indicate that the sand patch does not detect the difference between macrotexture before and after polishing in this polishing technique.

The ANOVA analysis shows the equality or inequality of the means between different groups. To learn more about the structure of the differences, other statistical methods are required. A pairwise comparison has been performed in both Type C and Type D mixtures to find the source of the difference within each group. Tables 18 and 19 are the results for Type C and Type D, respectively. The numbers in the third column show the mean difference between measured values of macrotexture for two different aggregates. A small asterisk next to the number denotes the mean difference is significant at 0.05 level.

These tables show that in almost all cases, Brownlee aggregate had higher macrotexture. Beckman aggregates produced the lowest macrotexture.

Table 18. Significance Level for Different Aggregate Types in Type C Mix.

(I) Aggregate Type	(J) Aggregate Type	Mean Difference (I-J)	Std. Error	Sig.	95% Confidence Interval	
					Lower Bound	Upper Bound
Brownlee	Brownwood	.4189(*)	.06390	.000	.1963	.6415
	Beckman	.3343(*)	.07783	.006	.0740	.5945
	El Paso	.4114(*)	.06295	.000	.1902	.6326
	Fordyce	.1431	.05986	.407	-.0751	.3613
	Brownlee-Beckman	.2373(*)	.06395	.032	.0146	.4600
Brownwood	Brownlee	-.4189(*)	.06390	.000	-.6415	-.1963
	Beckman	-.0847	.05993	.949	-.2954	.1261
	El Paso	-.0075	.03870	1.000	-.1346	.1196
	Fordyce	-.2758(*)	.03342	.000	-.3882	-.1635
	Brownlee-Beckman	-.1817(*)	.04030	.003	-.3139	-.0495
Beckman	Brownlee	-.3343(*)	.07783	.006	-.5945	-.0740
	Brownwood	.0847	.05993	.949	-.1261	.2954
	El Paso	.0772	.05891	.972	-.1321	.2864
	Fordyce	-.1912	.05559	.080	-.3977	.0154
	Brownlee-Beckman	-.0970	.05998	.872	-.3078	.1138
El Paso	Brownlee	-.4114(*)	.06295	.000	-.6326	-.1902
	Brownwood	.0075	.03870	1.000	-.1196	.1346
	Beckman	-.0772	.05891	.972	-.2864	.1321
	Fordyce	-.2683(*)	.03157	.000	-.3737	-.1629
	Brownlee-Beckman	-.1742(*)	.03878	.003	-.3015	-.0468
Fordyce	Brownlee	-.1431	.05986	.407	-.3613	.0751
	Brownwood	.2758(*)	.03342	.000	.1635	.3882
	Beckman	.1912	.05559	.080	-.0154	.3977
	El Paso	.2683(*)	.03157	.000	.1629	.3737
	Brownlee-Beckman	.0942	.03352	.159	-.0185	.2069
Brownlee-Beckman	Brownlee	-.2373(*)	.06395	.032	-.4600	-.0146
	Brownwood	.1817(*)	.04030	.003	.0495	.3139
	Beckman	.0970	.05998	.872	-.1138	.3078
	El Paso	.1742(*)	.03878	.003	.0468	.3015
	Fordyce	-.0942	.03352	.159	-.2069	.0185

* The mean difference is significant at the .05 level.

Table 19. Significance Level for Different Aggregate Types in Type D Mix.

(I) Aggregate Type	(J) Aggregate Type	Mean Difference (I-J)	Std. Error	Sig.	95% Confidence Interval	
					Lower Bound	Upper Bound
Brownlee	Beckman	.2933(*)	.04685	.002	.1402	.4464
	Brownlee-Beckman	.0417	.05254	.833	-.1145	.1978
Beckman	Brownlee	-.2933(*)	.04685	.002	-.4464	-.1402
	Brownlee-Beckman	-.2517(*)	.03119	.000	-.3466	-.1567
Brownlee-Beckman	Brownlee	-.0417	.05254	.833	-.1978	.1145
	Beckman	.2517(*)	.03119	.000	.1567	.3466

* The mean difference is significant at the .05 level.

Results of the British Pendulum Test

The British pendulum test was performed three times in each of the three locations on the slabs. Figures 51 and 52 show the BP values for different mixes.

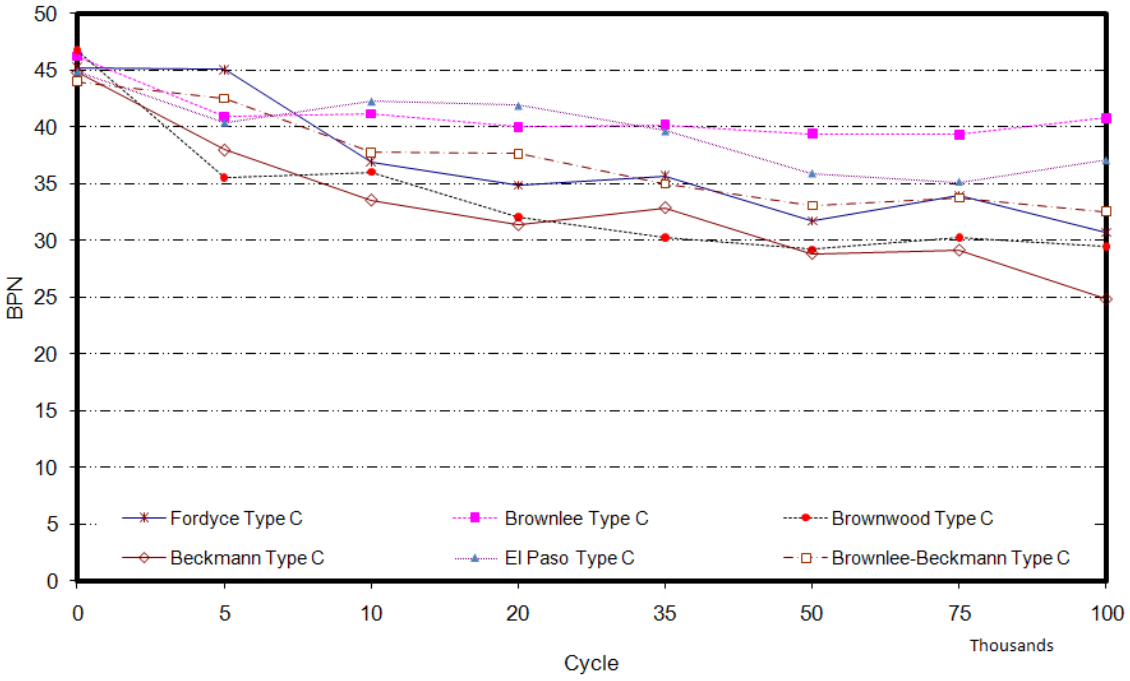

Figure 51. Results of British Pendulum Test for Type C Mixes.

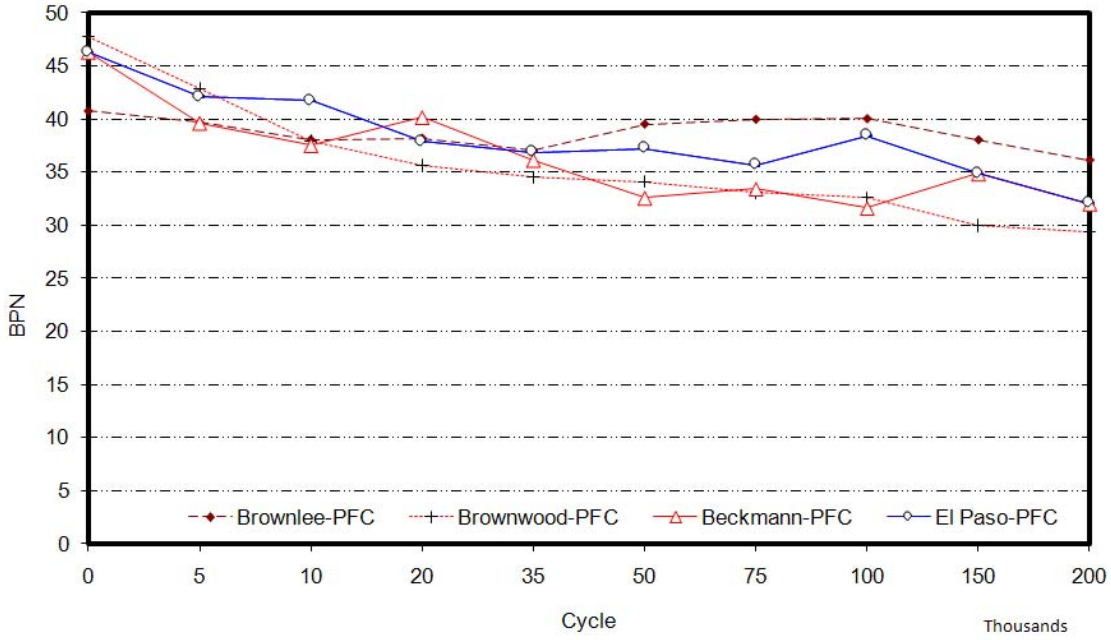

Figure 52. Results of the British Pendulum Test for PFC Mixes.

As a general trend, it is clear that the BP value decreases as the number of polishing cycles increase. The rate of decrease in the British Pendulum Value is dependent on the aggregate type. Table 20 summarizes the results of the ANOVA analysis at 95 percent confidence level for different aggregates. The results show that there is a significant difference between the mean BP values for each aggregate type in each polishing cycle. Moreover, it indicates the polisher has an effect in decreasing the surface skid resistance and obviously can polish the surface.

Table 21 shows the significance level of the equality of mean measured BP values at different numbers of polishing cycles. This table shows that in almost all cases—except sandstone—the significance is negligible, and this analysis supports the idea that there is significant difference between measured BP values in different aggregates at a 95 percent confidence level. Further study in this section, however, revealed that this difference is only due to Brownlee aggregate, and there is no significant difference between other aggregates.

Another ANOVA analysis was done to examine the effect of mixture type on frictional characteristics of asphalt pavement (Table 22). The results indicate that there is no statistical difference between the skid resistance of Type C and PFC mixes containing Brownlee aggregate. Furthermore, this aggregate has the same frictional performance in Type C and PFC mixes in both low and high numbers of polishing cycles. This is a result of continuous renewal of the aggregate surface exposed to a rubber slider. Moreover, Brownlee aggregate consists of hard particles in a softer matrix. Wearing the softer matrix off the aggregate allows the new hard particles to be exposed to traffic and will help this mix to maintain its frictional properties. The PFC and Type C mixes containing Brownwood aggregate statistically have equal BP values in low-polishing cycles; however, when the polishing cycles increase, the PFC could maintain its skid properties relatively better than Type C mixes, and the BP value is higher. The difference between the BP value of Type C and PFC mixes containing Beckman aggregate is always significant. Moreover, PFC mixes containing Beckman aggregate always have a higher BP value than Type C mixes. The difference between skid properties of the mixes containing El Paso aggregate does not follow a clear trend. The PFC mixes containing this kind of aggregate are likely to have higher BP value in low-polishing cycles, and the

results of the analysis do not show significant difference between PFC and Type C mixes in high-polishing cycles.

Table 20. Significance Level for the Effect of Different Polishing Cycles on Mixtures with Different Aggregates.

Aggregate Type	Mix Type	Polishing Cycle (thousands)									
		0	5	10	20	35	50	75	100	150	200
El Paso Beckman Brownwood Brownlee Fordyce Brownlee-Beckman	Type C	0.039	0.009	0.002	0	0	0	0	0	NA	NA
Brownlee El Paso Brownwood Beckman	PFC	0	0.001	0	0	0.054	0	0	0	0	0

Table 21. Significance Level for the Mean BP Values for Different Loading Cycles.

Aggregate Type	Mix Type	Sig.
El Paso	Type C	0.0001
Beckman		0
Brownwood		0
Brownlee		0.0581
Fordyce		0
Brownlee-Beckman		0
Brownlee	PFC	0
El Paso		0
Brownwood		0
Beckman		0

Table 22. Significance Level for the Mean BP Values for Different Mixture Type.

Aggregate Type	Mix Type	Cycle (thousands)							
		0	5	10	20	35	50	75	100
El Paso	Type C PFC	0.30*	0.027	0.630	0.015	0.105	0.346	0.354	0.448
Beckman	Type C PFC	0.000	0.005	0.024	0.00	0.003	0.000	0.002	0.006
Brownwood	Type C PFC	0.148	0.11	0.36	0.001	0.014	0.005	0.001	0.006
Brownlee	Type C PFC	0.001	0.281	0.067	0.168	0.107	0.964	0.796	0.715

* Highlighted numbers show the difference is not statistically significant.

To have a better understanding of the variation of the BP values for different mixes, the equation suggested by Mahmoud (2005) was fitted to the data substituting texture with British Pendulum value and time with polishing cycles in terms of 1000 cycles. This equation has the form of Equation 9.

Figures 53 to 62 show the data and the fitted lines for different mixes. The results show that this equation could fit the data very well.

Table 23 shows the values of the regression coefficients for different mixes after removing the outliers and fitting the function by the least square method.

Table 23. Regression Coefficients for Different Aggregate.

Aggregate type	Mix type	A	B	C
El Paso	Type C	35	9	0.026
Beckman		29	16	0.091
Brownwood		30	16	0.140
Brownlee		39	3	0.027
Fordyce		32	14	0.064
Brownlee-Beckman		33	11	0.053
Brownlee	PFC	37	3	0.052
El Paso		35	11	0.042
Brownwood		32	15	0.070
Beckman		33	11	0.050

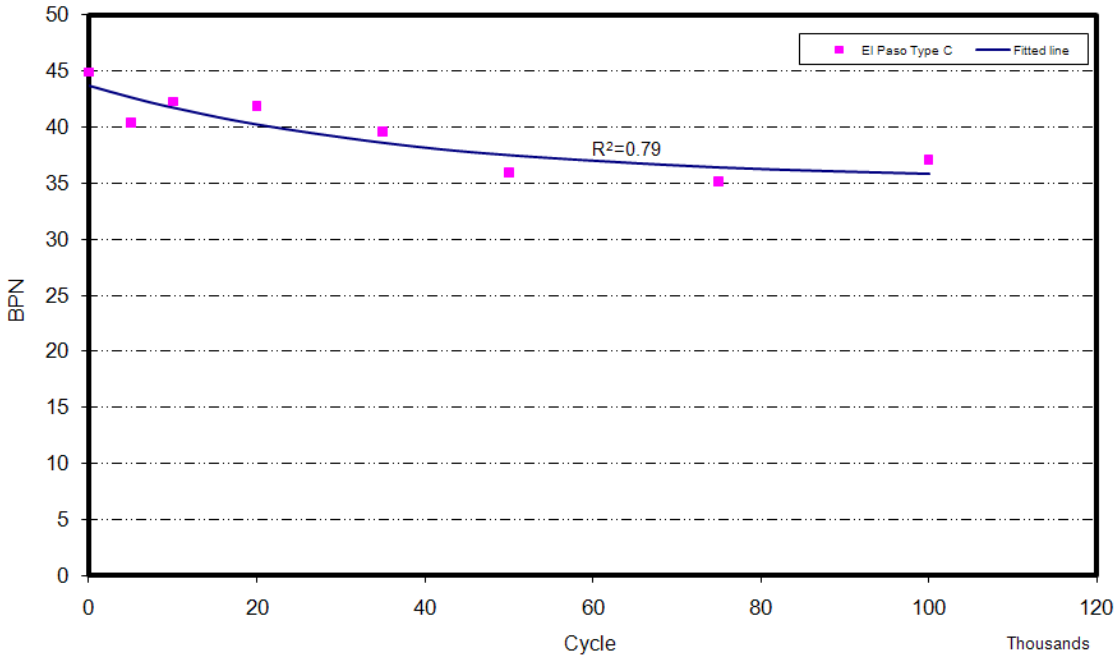

Figure 53. British Pendulum Values for El Paso Aggregate vs. Polishing Cycles.

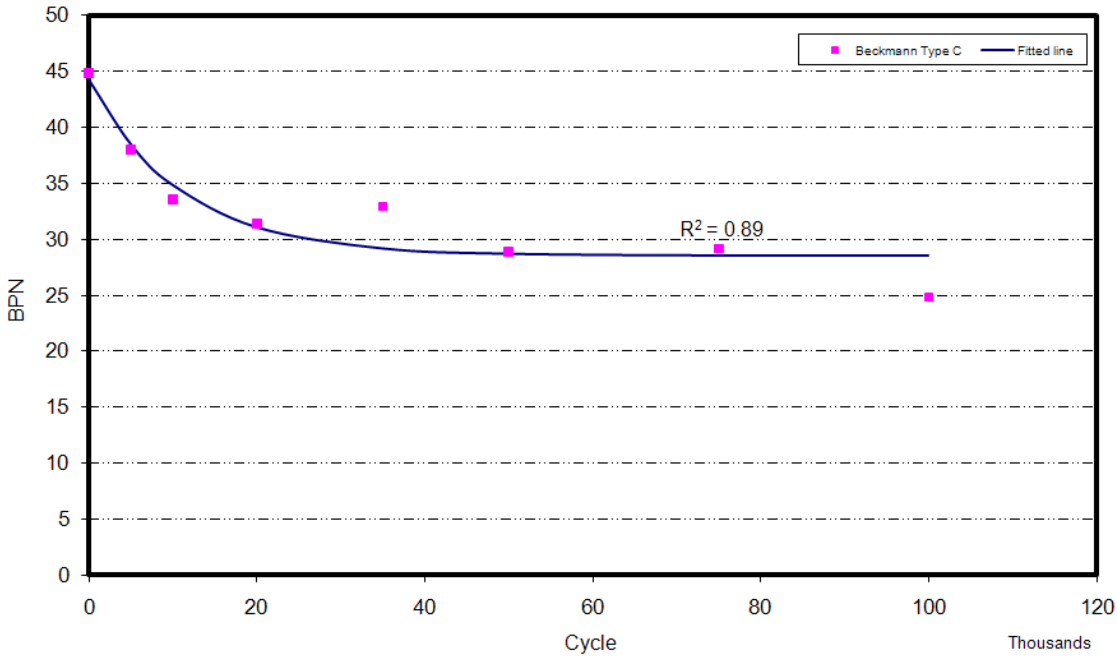

Figure 54. British Pendulum Values for Beckman Aggregate vs. Polishing Cycles.

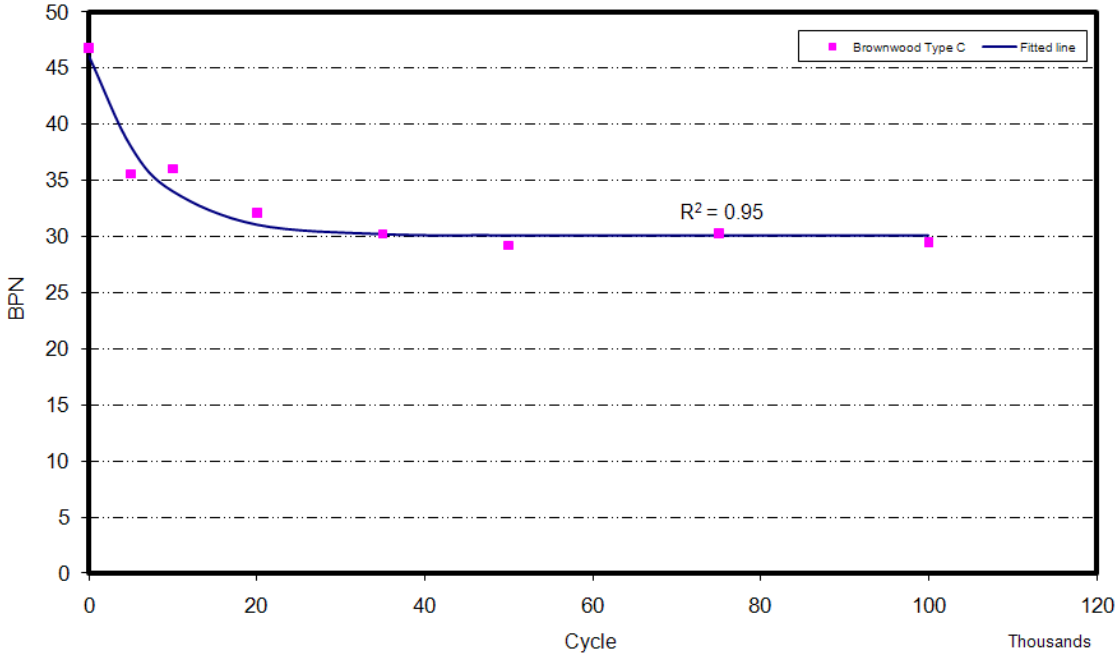

Figure 55. British Pendulum Values for Brownwood Aggregate vs. Polishing Cycles.

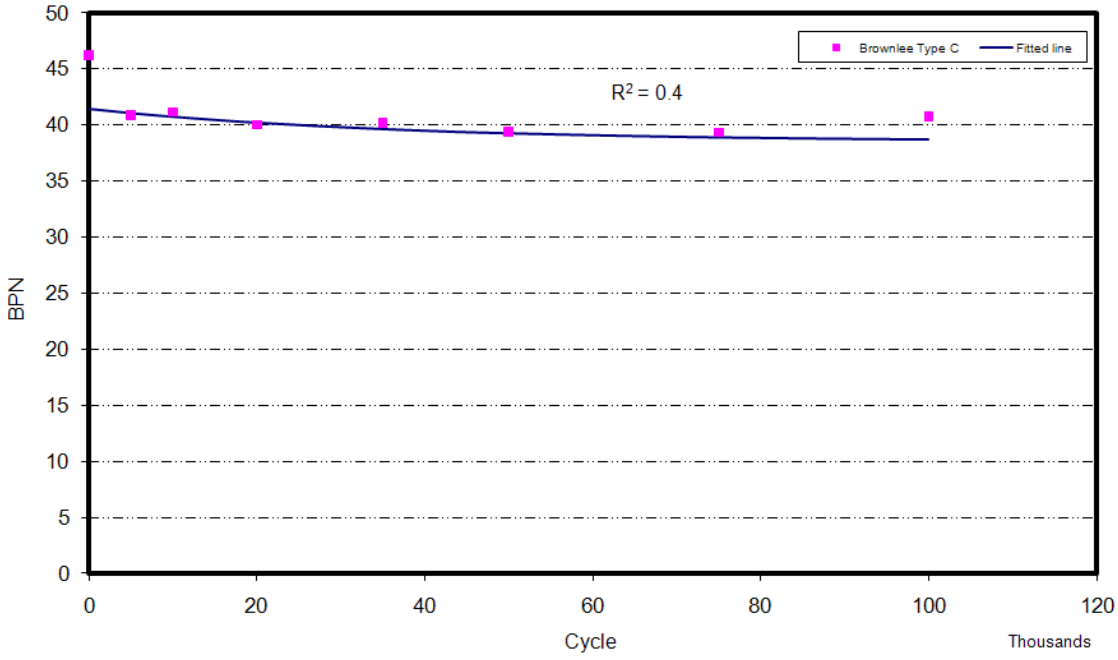

Figure 56. British Pendulum Values for Brownlee Aggregate vs. Polishing Cycles.

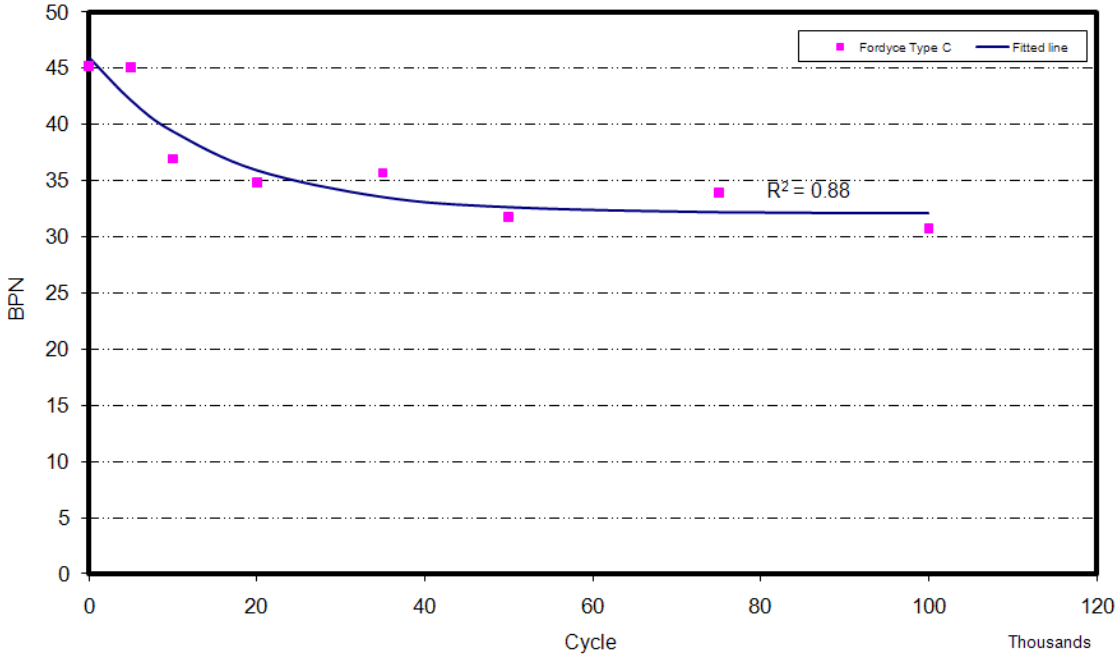

Figure 57. British Pendulum Values for Fordyce Aggregate vs. Polishing Cycles.

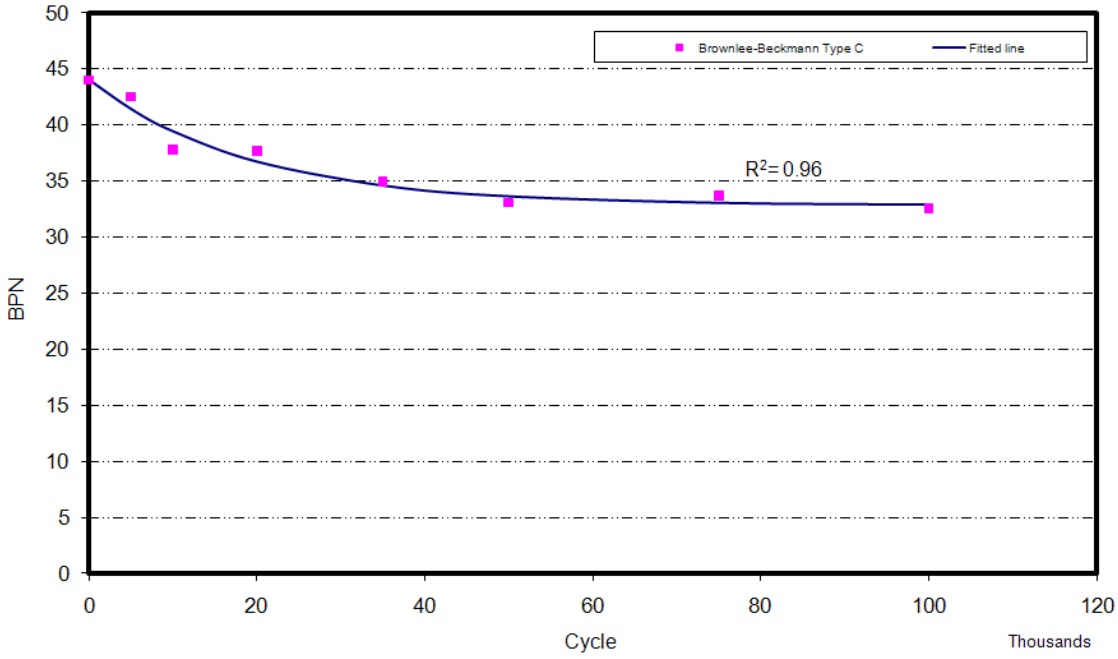

Figure 58. British Pendulum Values for the 50 Percent Beckman 50 Percent Brownlee vs. Polishing Cycles.

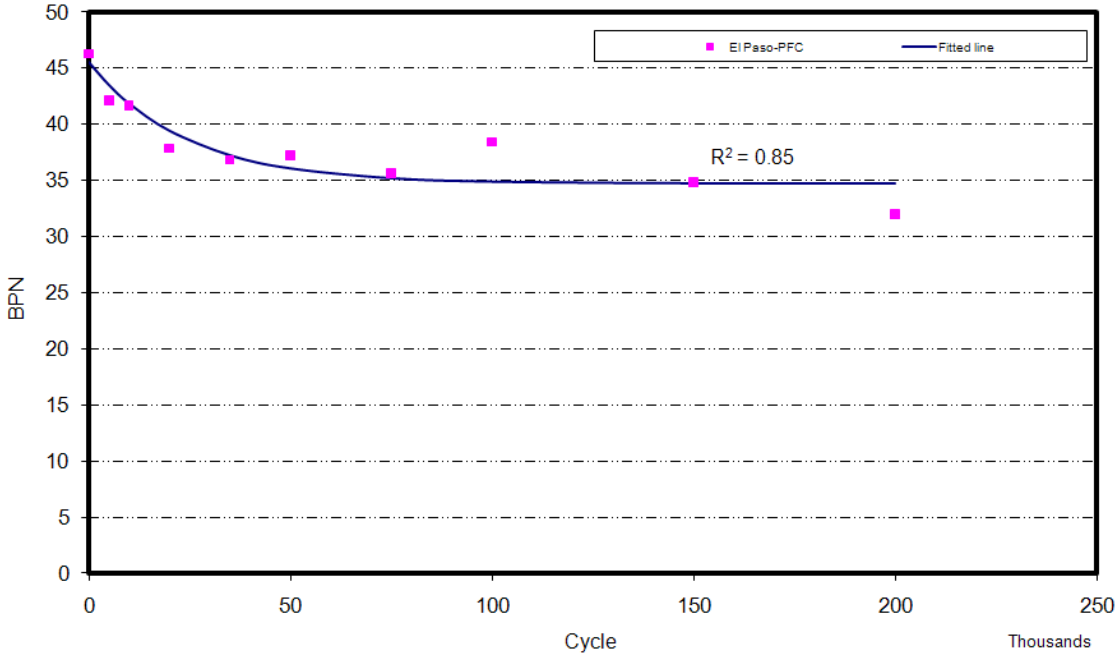

Figure 59. British Pendulum Values for El Paso Aggregate vs. Polishing Cycles in PFC Mix.

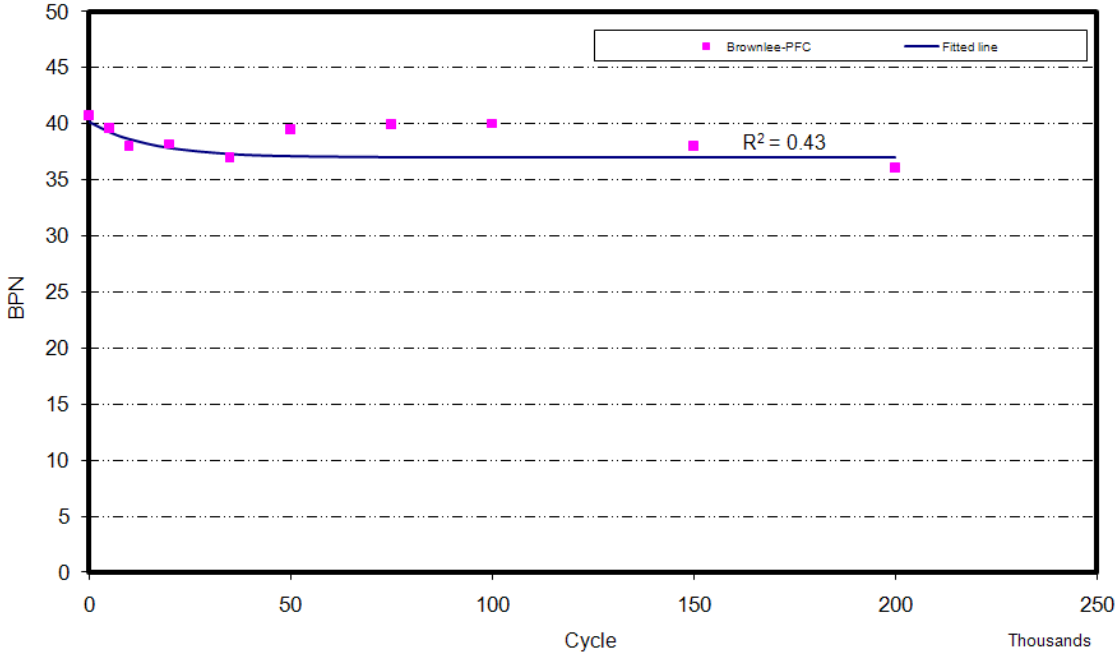

Figure 60. British Pendulum Values for Brownlee Aggregate vs. Polishing Cycles in PFC Mix.

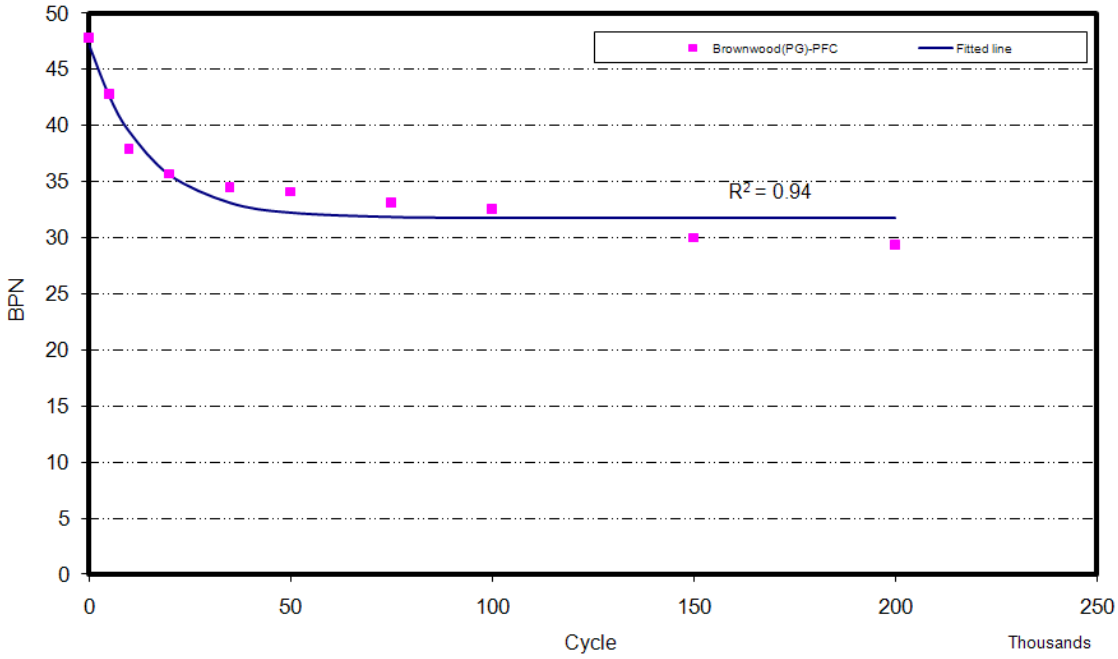

Figure 61. British Pendulum Values for Brownwood Aggregate vs. Polishing Cycles in PFC Mix.

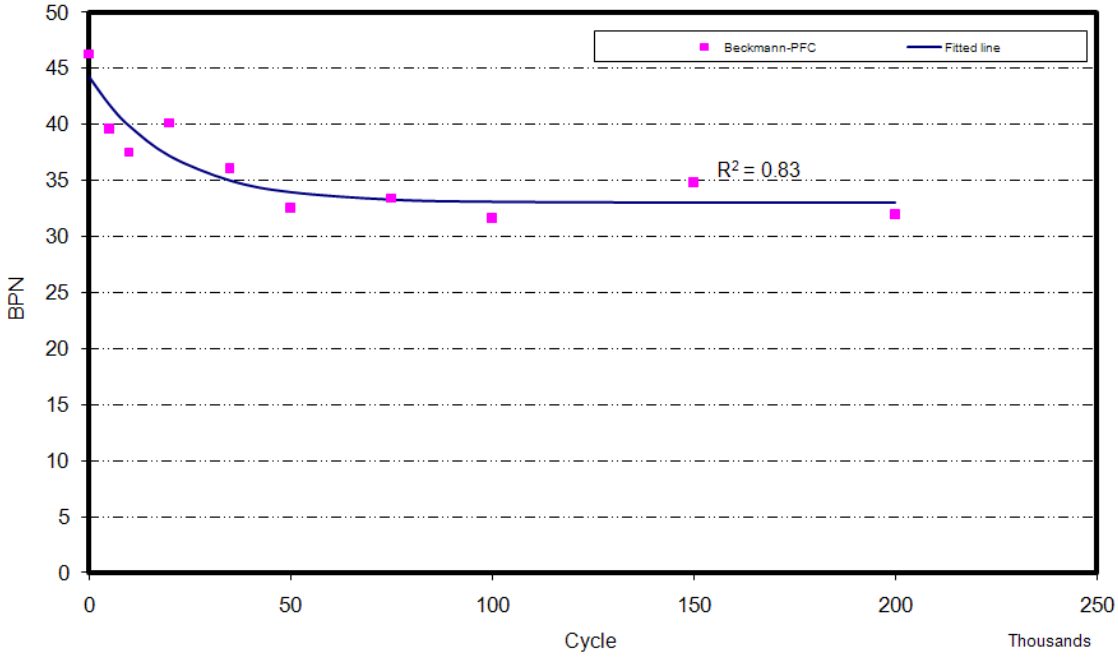

Figure 62. British Pendulum Values for Beckman Aggregate vs. Polishing Cycles in PFC Mix.

Figures 56 and 60 for Brownlee aggregate show that the change of BP values versus polishing cycle is very small. The same results were reported by Luce (2006). This aggregate has the lowest change with regard to the polishing cycles, highest terminal value compared to other aggregates. Moreover, this small change in BP value against polishing cycles in Brownlee aggregate texture contributes to its high-skid resistance. El Paso aggregate has the second-lowest rate of decrease in BP value against polishing cycles and is polish-resistant. Mixing Beckman aggregate with Brownlee aggregate shows promising results since this mixture has the third-lowest rate of change versus polishing cycle. Brownwood aggregate has the highest rate of BP value lost versus polishing cycle and does not have a high terminal BP value. BP values for Brownlee aggregate in the PFC mixture are almost constant, which is similar to Type C mixes.

The results of the ANOVA analysis tabulated in Table 24 show the comparison between measured BP values for each pair of aggregates. In this table, the numbers in the third column show the mean difference between BP values of corresponding aggregates. An asterisk next to a number shows the difference is significant at the 0.05 level. Table 24 does not show a statistical difference between each pair except for very high values (i.e., Brownlee aggregate) and other aggregates. This indicates the limitation of British Pendulum to detect the difference between frictional performances of aggregates with known differences in frictional characteristics.

Table 24. Pairwise Comparison between Different Aggregates in Type C Mix.

(I) Aggregate Type	(J) Aggregate Type	Mean Difference (I-J)	Std. Error	Sig.
El Paso	Beckman	6.70875(*)	1.42299	.000
	Brownwood	5.92500(*)	1.43491	.003
	Brownlee	-1.35375	.94971	.928
	Fordyce	2.86958	1.31902	.418
	Beckman-Brownlee	2.61208	1.12609	.315
Beckman	El Paso	-6.70875(*)	1.42299	.000
	Brownwood	-.78375	1.72790	1.000
	Brownlee	-8.06250(*)	1.35226	.000
	Fordyce	-3.83917	1.63294	.296
	Beckman-Brownlee	-4.09667	1.48147	.120
Brownwood	El Paso	-5.92500(*)	1.43491	.003
	Beckman	.78375	1.72790	1.000
	Brownlee	-7.27875(*)	1.36480	.000
	Fordyce	-3.05542	1.64334	.660
	Beckman-Brownlee	-3.31292	1.49293	.387
Brownlee	El Paso	1.35375	.94971	.928
	Beckman	8.06250(*)	1.35226	.000
	Brownwood	7.27875(*)	1.36480	.000
	Fordyce	4.22333(*)	1.24239	.025
	Beckman-Brownlee	3.96583(*)	1.03528	.006
Fordyce	El Paso	-2.86958	1.31902	.418
	Beckman	3.83917	1.63294	.296
	Brownwood	3.05542	1.64334	.660
	Brownlee	-4.22333(*)	1.24239	.025
	Beckman-Brownlee	-.25750	1.38191	1.000
Beckman-Brownlee	El Paso	-2.61208	1.12609	.315
	Beckman	4.09667	1.48147	.120
	Brownwood	3.31292	1.49293	.387
	Brownlee	-3.96583(*)	1.03528	.006
	Fordyce	.25750	1.38191	1.000

* The mean difference is significant at the .05 level.

Results of CTMeter and DFT

As previously stated, the frictional properties of each mix were measured by CTMeter and DFT periodically during polishing. Using Equations 5 and 6 presented in the previous chapter, IFI components were calculated. The measured friction at 20 km/h (DF_{20}) was also reported as a good representation of the microtexture change against polishing. Figures 63 through 65 show the results of the F60, DF_{20} , and MPD values.

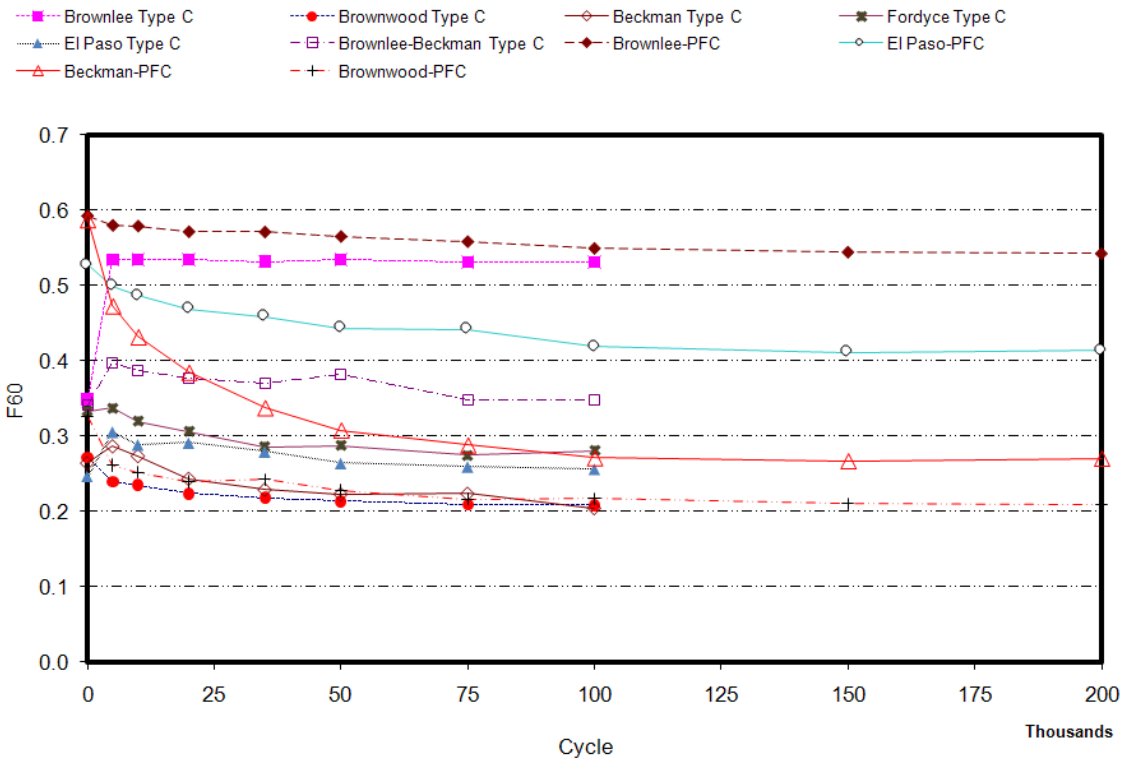

Figure 63. Calculated F60 for Different Aggregate vs. Polishing Cycle.

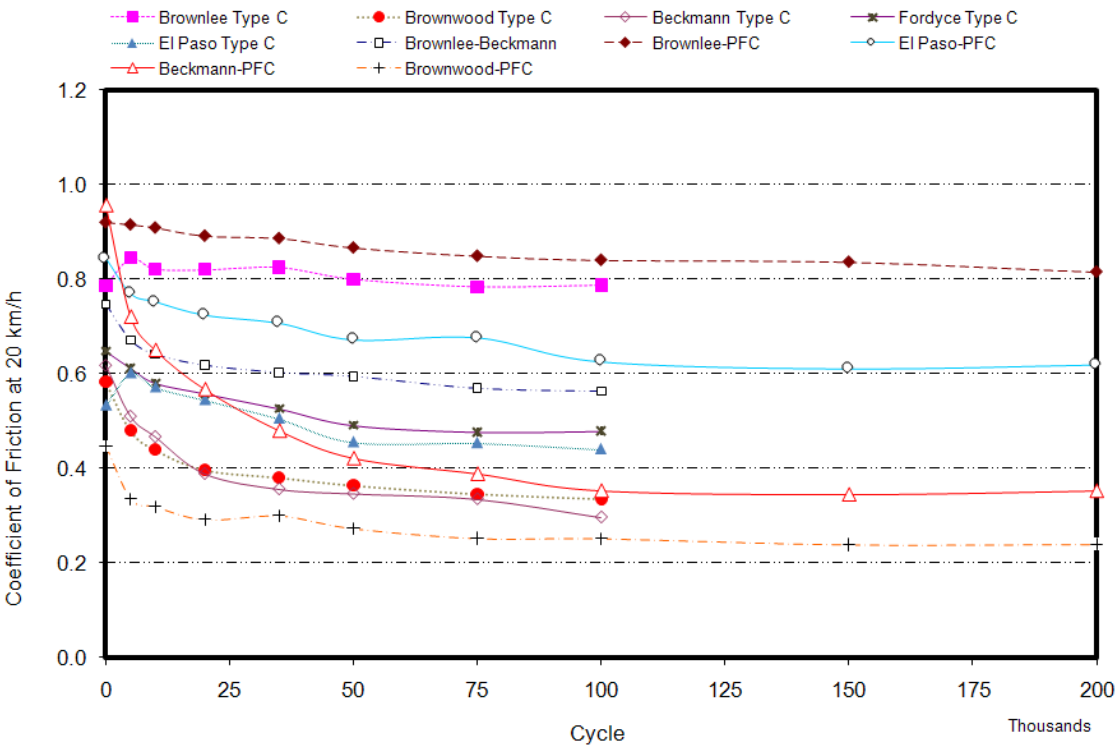

Figure 64. Coefficient of Friction for Different Aggregate vs. Polishing Cycle at 20 km/h.

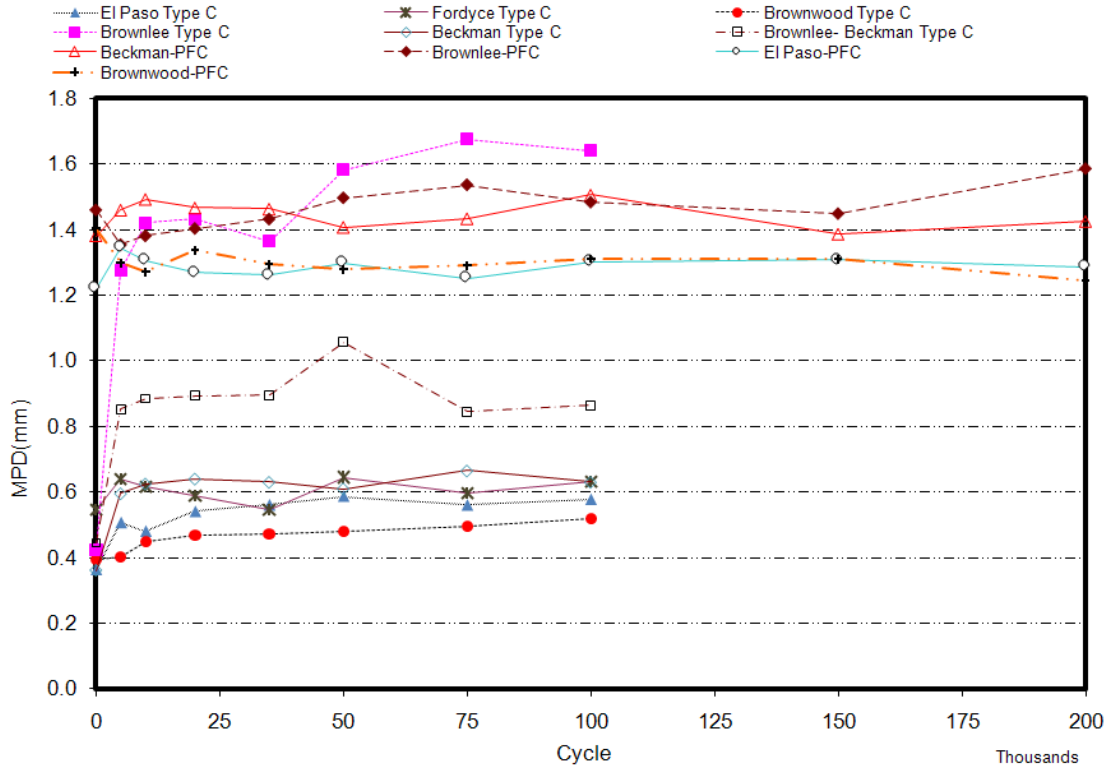

Figure 65. MPD for Different Aggregate vs. Polishing Cycle.

It is evident from Figure 64 that the coefficient of friction decreases when the polishing cycle increases. In addition, some aggregates such as Beckman aggregate show a rapid change in their measured coefficient of friction, and some of them such as Brownlee aggregate remain almost constant during the polishing. It is clear that after a particular number of polishing cycles, each mix reached a terminal condition in which no other changes occur afterwards. The rate of change and the terminal value of DF_{20} can be an indication of an aggregate susceptibility to polishing and will be investigated in this report.

The MPD values of different mixes in Figure 65 vary in terms of polishing cycles and do not show a clear trend. Moreover, small changes in MPD could be related to aggregate abrasion during polishing or experimental error. For some types of aggregate (Brownlee aggregate), aggregate raveling due to moisture susceptibility was also noticed.

Figure 63 shows the calculated F60 based on the Equations 5 and 6. The F60 decreases as the polishing cycles increase. Moreover, the variation of microtexture—DF_{20}—has a more important role on the variation of F60 than macrotexture does. Therefore, the variation of DF_{20} and F60 are consistent and following the same trend. ANOVA analysis was performed to study the effect of polishing cycles, speed, and aggregate type on measured values of DF_{20} for different mixes in different speed and polishing cycles. The results are tabulated in Tables 25 and 26.

Table 25. Significance Level (p-value) of the Mean DF_{20} Values for Different Aggregate Types in Type C Mix.

Mix Type	Aggregate	Speed	Polishing	Before Polish		5000		10,000		20,000	
				Speed Effect	Aggregate Type	Speed Effect	Aggregate Type	Speed Effect	Aggregate Type	Speed Effect	Aggregate Type
Type C	Brownlee-Beckman	20	0.00	0.00	0.00	0.00	0.00	0.00	0.00	0.00	0.00
		40	0.00		0.00		0.00		0.00		0.00
		60	0.00		0.00		0.00		0.00		0.00
		80	0.00		0.00		0.00		0.00		0.00
	El Paso	20	0.00	0.00	0.00	0.00	0.00	0.00	0.00	0.00	0.00
		40	0.00		0.00		0.00		0.00		0.00
		60	0.00		0.00		0.00		0.00		0.00
		80	0.00		0.00		0.00		0.00		0.00
	Fordyce	20	0.00	0.00	0.00	0.00	0.00	0.00	0.00	0.00	0.00
		40	0.00		0.00		0.00		0.00		0.00
		60	0.00		0.00		0.00		0.00		0.00
		80	0.00		0.00		0.00		0.00		0.00
	Brownwood	20	0.00	0.00	0.00	0.00	0.00	0.00	0.00	0.00	0.00
		40	0.00		0.00		0.00		0.00		0.00
		60	0.00		0.00		0.00		0.00		0.00
		80	0.00		0.00		0.00		0.00		0.00
	Brownlee	20	0.00	0.00	0.00	0.00	0.00	0.00	0.00	0.00	0.00
		40	0.00		0.00		0.00		0.00		0.00
		60	0.00		0.00		0.00		0.00		0.00
		80	0.00		0.00		0.00		0.00		0.00
	Beckman	20	0.00	0.00	0.00	0.00	0.00	0.00	0.00	0.00	0.00
		40	0.00		0.00		0.00		0.00		0.00
		60	0.00		0.00		0.00		0.00		0.00
		80	0.00		0.00		0.00		0.00		0.00

Table25. Significance Level of the Mean DF_{20} Values for Different Aggregate Types in Type C Mix (cont.).

Mix Type	Aggregate	35,000		50,000		75,000		100,000	
		Speed Effect	Aggregate Type	Speed Effect	Aggregate Type	Speed Effect	Aggregate Type	Speed Effect	Aggregate Type
Type C	Brownlee-Beckman	0.00	0.00	0.00	0.00	0.00	0.00	0.00	0.00
			0.00		0.00		0.00		0.00
			0.00		0.00		0.00		0.00
			0.00		0.00		0.00		0.00
	El Paso	0.00	0.00	0.00	0.00	0.00	0.00	0.00	0.00
			0.00		0.00		0.00		0.00
			0.00		0.00		0.00		0.00
			0.00		0.00		0.00		0.00
	Fordyce	0.00	0.00	0.00	0.00	0.00	0.00	0.00	0.00
			0.00		0.00		2.53		0.00
			0.00		0.00		0.00		0.00
			0.00		0.00		0.03		0.00
	Brownwood	0.00	0.00	0.00	0.00	0.00	0.02	0.00	0.00
			0.00		0.00		0.00		0.00
			0.00		0.00		0.00		0.00
			0.00		0.00		0.00		0.00
	Brownlee	0.00	0.00	0.00	0.00	0.00	0.00	0.07	0.00
			0.00		0.00		0.00		0.00
			0.00		0.00		0.00		0.00
			0.00		0.00		0.00		0.00
	Beckman	0.00	0.00	0.00	0.00	0.00	0.00	0.00	0.00
			0.00		0.00		0.00		0.00
			0.00		0.00		0.00		0.00
			0.00		0.00		0.00		0.00

Table 26. Significance Level of the Mean DF_{20} Values for Different Aggregate Types in PFC Mix.

Mix Type	Aggregate	Speed	Polishing	Before Polish		5000		10,000		20,000	
				Speed Effect	Aggregate Type	Speed Effect	Aggregate Type	Speed Effect	Aggregate Type	Speed Effect	Aggregate Type
PFC	El Paso	20	0.00	0.00	0.00	0.00	0.00	0.00	0.00	0.00	0.00
		40	0.00		0.00		0.00		0.00		0.00
		60	0.00		0.00		0.00		0.00		0.00
		80	0.00		0.00		0.00		0.00		0.00
	Brownwood	20	0.00	0.00	0.00	0.00	0.00	0.00	0.00	0.11	0.00
		40	0.00		0.00		0.00		0.00		0.00
		60	0.00		0.00		0.00		0.00		0.00
		80	0.00		0.00		0.00		0.00		0.00
	Brownlee	20	0.20*	0.00	0.00	0.03	0.00	0.00	0.00	0.09	0.00
		40	0.29		0.00		0.00		0.00		0.00
		60	0.29		0.00		0.00		0.00		0.00
		80	0.38		0.00		0.00		0.00		0.00
	Beckman	20	0.00	0.00	0.00	0.00	0.00	0.00	0.00	0.00	0.00
		40	0.00		0.00		0.00		0.00		0.00
		60	0.00		0.00		0.00		0.00		0.00
		80	0.00		0.00		0.00		0.00		0.00

* Highlighted numbers show the difference is not statistically significant.

Table 26. Significance Level of the Mean DF_{20} Values for Different Aggregate Types in PFC Mix (cont.).

Mix Type	Aggregate	35,000		50,000		75,000		100,000		150,000		200,000	
		Speed Effect	Aggregate Type	Speed Effect	Aggregate Type	Speed Effect	Aggregate Type	Speed Effect	Aggregate Type	Speed Effect	Aggregate Type	Speed Effect	Aggregate Type
PFC	El Paso	0.00	0.00	0.00	0.00	0.00	0.00	0.00	0.00	0.00	0.00	0.00	0.00
			0.00		0.00		0.00		0.00		0.00		0.00
			0.00		0.00		0.00		0.00		0.00		0.00
			0.00		0.00		0.00		0.00		0.00		0.00
	Brownwood	0.03	0.00	0.06*	0.00	0.01	0.00	0.53	0.00	0.27	0.00	0.58	0.00
			0.00		0.00		0.00		0.00		0.00		0.00
			0.00		0.00		0.00		0.00		0.00		0.00
			0.00		0.00		0.00		0.00		0.00		0.00
	Brownlee	0.02	0.00	0.00	0.00	0.00	0.00	0.06	0.00	0.00	0.00	0.00	0.00
			0.00		0.00		0.00		0.00		0.00		0.00
			0.00		0.00		0.00		0.00		0.00		0.00
			0.00		0.00		0.00		0.00		0.00		0.00
	Beckman	0.00	0.00	0.00	0.00	0.58	0.00	0.01	0.00	0.45	0.00	0.37	0.00
			0.00		0.00		0.00		0.00		0.00		0.00
			0.00		0.00		0.00		0.00		0.00		0.00
			0.00		0.00		0.00		0.00		0.00		0.00

* Highlighted numbers show the difference is not statistically significant.

The numbers in Tables 25 and 26 are the significance of the equality of means for each variable (e.g. aggregate type, speed, mix type) evaluated by ANOVA analysis. There is a significant statistical difference between the compared entities when significance is less than 0.05.

The results in Table 25 shows that the difference between the measured dynamic friction values for different aggregates in Type C mixes are significant at a 95 percent level of confidence. In this mix type, the measured values at different speeds for each polishing cycle are different significantly. The trends show that dynamic friction decreases as the speed increases in Type C mixes. The results also show that the difference between the measured values of friction in different polishing cycles is significant. These results confirm that the selected equipment is capable of polishing the surface that leads to a decrease in measured DF_{20} value as the polishing cycle increases.

Table 26 indicates that the equality of the average DF_{20} values for different aggregates in PFC mix is not significant, and the null hypothesis can be rejected. This indicates that aggregate type is a significant factor affecting frictional properties.

The results in Table 26 show the significance level of the equality of the measured values of DF_{20} for different speeds is significant in most cases except for El Paso aggregate. This means, in most cases, there is no evidence of changing the friction at different speeds. The results also show that for all cases except for Brownlee aggregate, the difference between measured frictions in different polishing cycles is significant. Moreover, there is not a significant difference between the measured values of the friction for Brownlee aggregate during polishing. Furthermore, continuous polishing of the sandstone aggregate does not change its frictional properties. This happens due to the petrographic nature of Brownlee aggregate.

Based on the measured values of dynamic friction in 20 km/h and MPD measured by CTMeter, the International Friction Index was calculated for each mix and plotted against polishing cycles.

The ANOVA analysis was performed by SPSS® software to study the effect of aggregate and mix type on the calculated F60. Results tabulated in Tables 27 and 28 support the hypothesis that there is a significant difference between calculated F60 in

Type C and PFC mixes. This result indicates that the PFC mixture has higher F60 value and consequently can provide better skid resistance.

Table 27. Results of Comparing Calculated Values F60 for Type C and PFC Mixes.

Mix Type	N	Mean	Std. Deviation	Std. Error Mean
Type C	132	.3190	.09861	.00858
PFC	105	.4058	.13285	.01296

Table 28. Results of the T-test for Comparing F60 Mean Values in Type C and PFC Mixes.

T-Value	df	Sig. (2-Tailed)	Mean Difference	Std. Error Difference	95% Confidence Interval of the Difference	
					Lower	Upper
-5.581	186.669	.000	-.0868	.01555	-.11745	-.05610

An equation with the same form as the one proposed by Mahmoud (2005) (Equation 9) was fitted to the data. Figures 66 through 69 show the measured DF_{20} and F60 values and the fitted curves for different mixes. The results show that this equation could fit the data substituting texture with F60 or DF_{20} values and time with polishing cycles in terms of 1000 cycles.

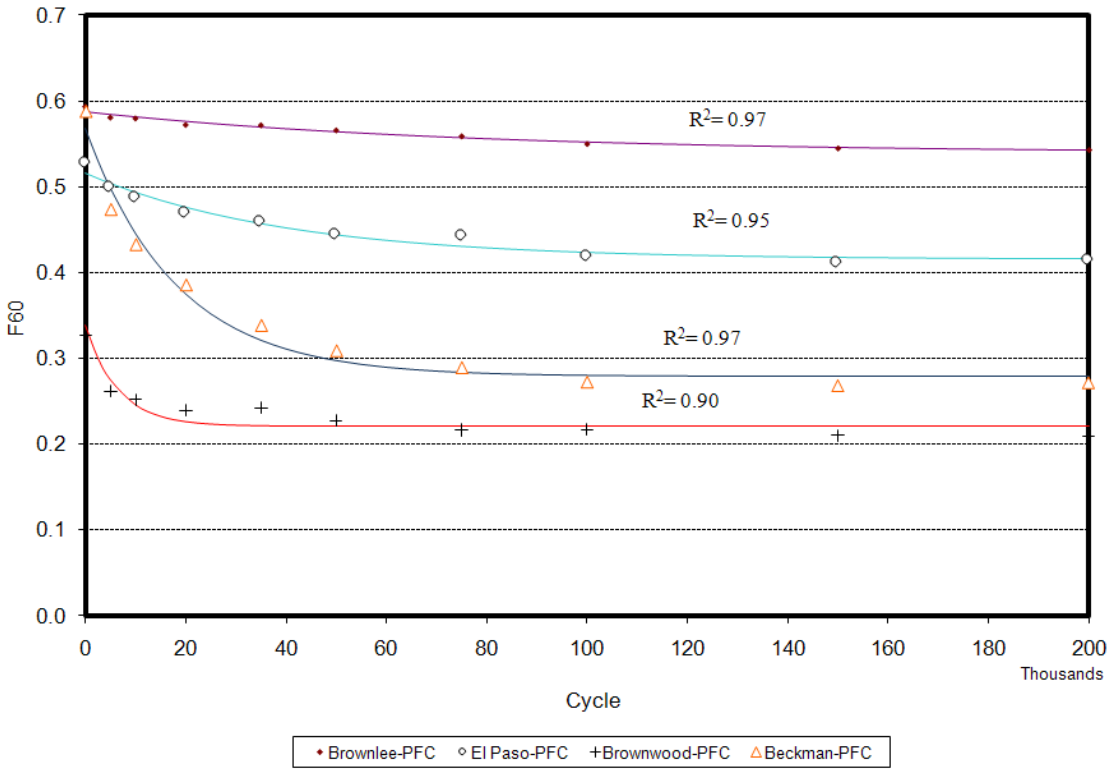

Figure 66. Calculated F60 Values vs. Polishing Cycle and Fitted Line for PFC Mixes.

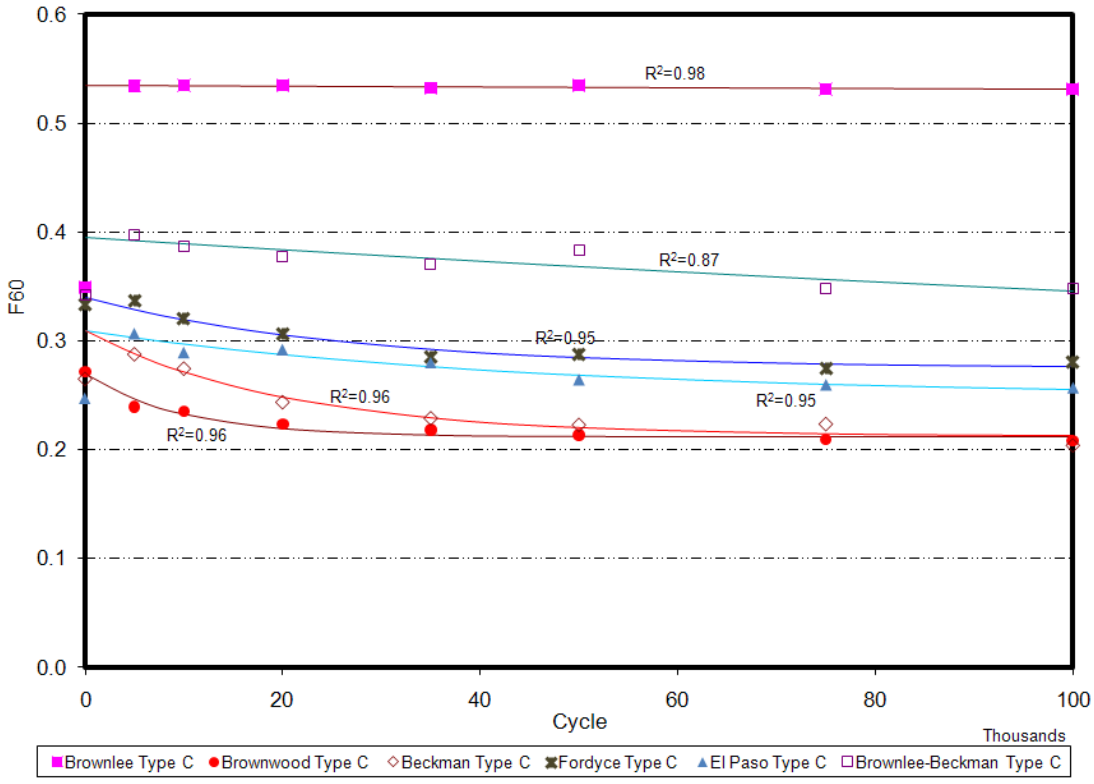

Figure 67. Calculated F60 Values vs. Polishing Cycle and Fitted Line for Type C Mixes.

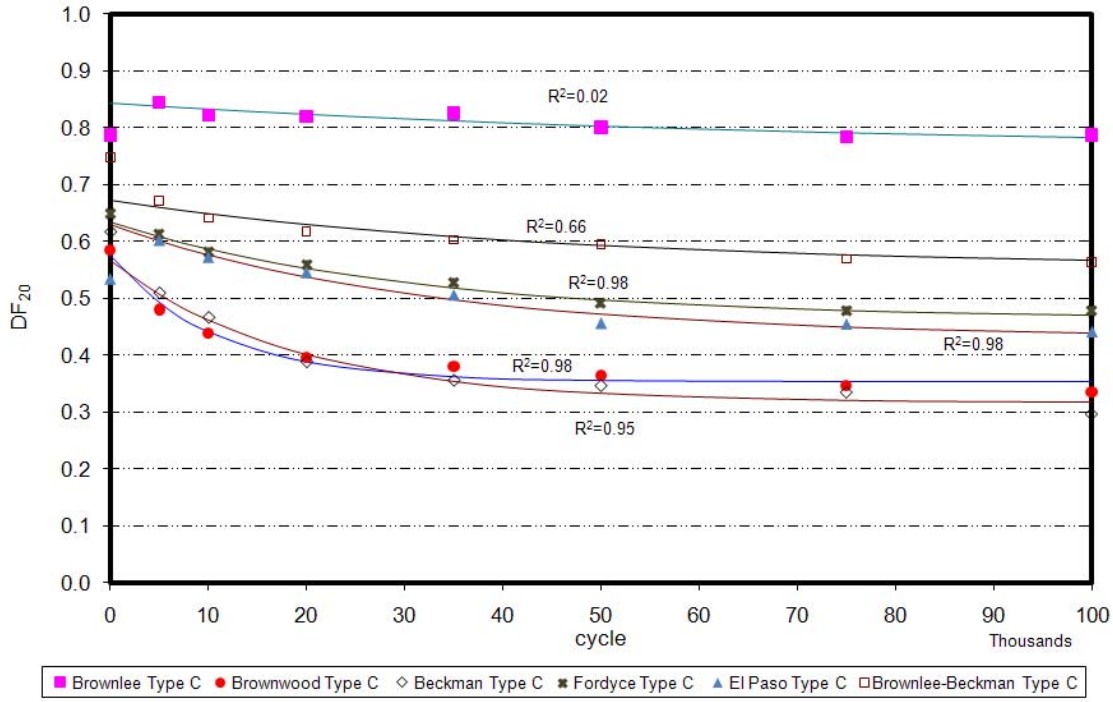

Figure 68. DF_{20} Values vs. Polishing Cycle and Fitted Line for Type C Mixes.

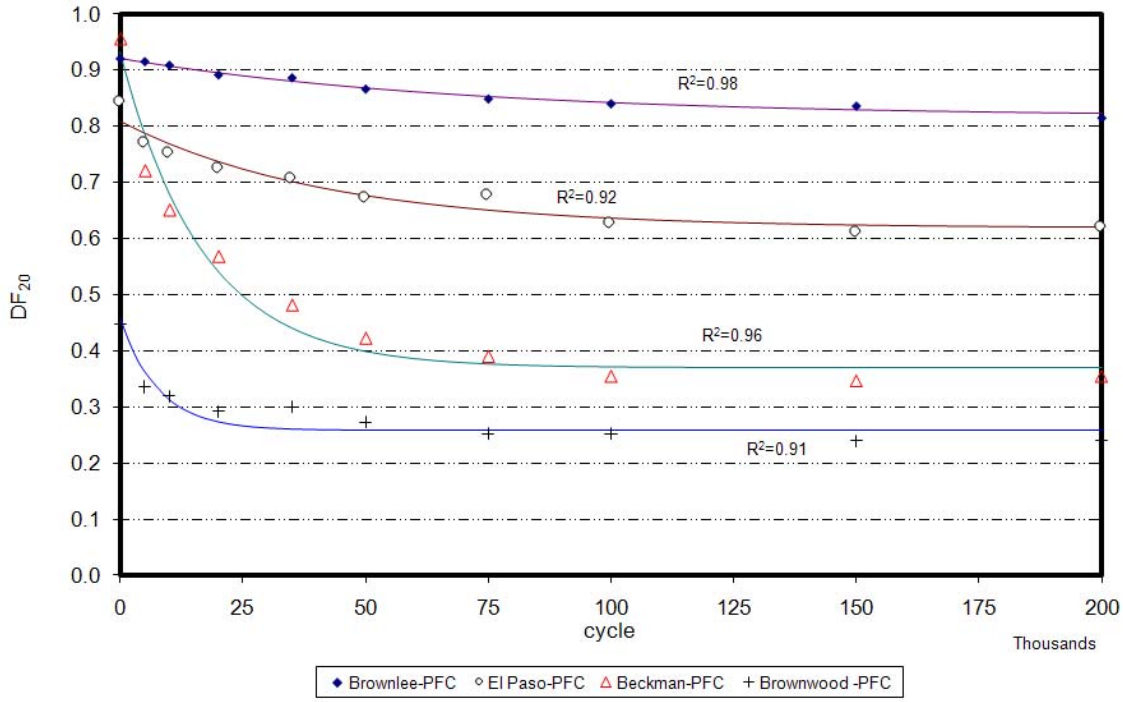

Figure 69. DF_{20} Values vs. Polishing Cycle and Fitted Line for PFC Mixes.

The model parameters were found by the least Sum of Square Errors (SSE) method. In this method, it is assumed that the minimum SSE would result in the model that best fits the measured data. Tables 29 and 30 show the magnitude of the regression coefficients for the DF_{20} and F60.

Table 29. Values of the Regression Parameters of Proposed Model for DF_{20}.

Mix Type	Aggregate Type	a	b	c
Type C	Brownlee	0.764	0.079	0.014
	Brownwood	0.354	0.223	0.093
	Beckman	0.317	0.251	0.054
	Fordyce	0.465	0.171	0.033
	El Paso	0.430	0.201	0.031
	Brownlee-Beckman	0.555	0.119	0.022
PFC	Brownlee	0.817	0.105	0.014
	El Paso	0.619	0.192	0.024
	Beckman	0.370	0.562	0.059
	Brownwood	0.258	0.201	0.129

Table 30. Values of the Regression Model Parameters for F60.

Mix Type	Aggregate Type	a	b	c
Type C	Brownlee	0.474	0.061	0.001
	Brownwood	0.212	0.058	0.102
	Beckman	0.213	0.097	0.050
	Fordyce	0.275	0.065	0.038
	El Paso	0.250	0.060	0.023
	Brownlee-Beckman	0.225	0.170	0.003
PFC	Brownlee	0.539	0.048	0.013
	El Paso	0.416	0.101	0.025
	Beckman	0.279	0.288	0.055
	Brownwood	0.221	0.117	0.155

The polishing rate (corresponding to the "c" parameter) is an important factor for the evaluation of pavement frictional properties. The lower the c value, the more resistant the specimen is to polishing. The other important parameter of the model is the "a" value, equivalent to the terminal friction value for either DF_{20} or F60. A high "a" value corresponds to high pavement terminal friction and indicates a pavement that could maintain its frictional properties to a higher degree.

Figures 70 through 75 depict the values shown in Tables 29 and 30. These figures indicate that the variation of both F60 and DF_{20} are consistent. In both cases, the Brownlee aggregate has the highest terminal and initial values, and Beckman and Brownwood aggregates have the lowest values. These figures also indicate that normally PFC mixes normally have higher F60 terminal and initial values than the Type C does. The rate of F60 change in Beckman and Brownwood aggregates is greater than other types of aggregates, which shows that limestone aggregates are not able to maintain their initial frictional properties against polishing action.

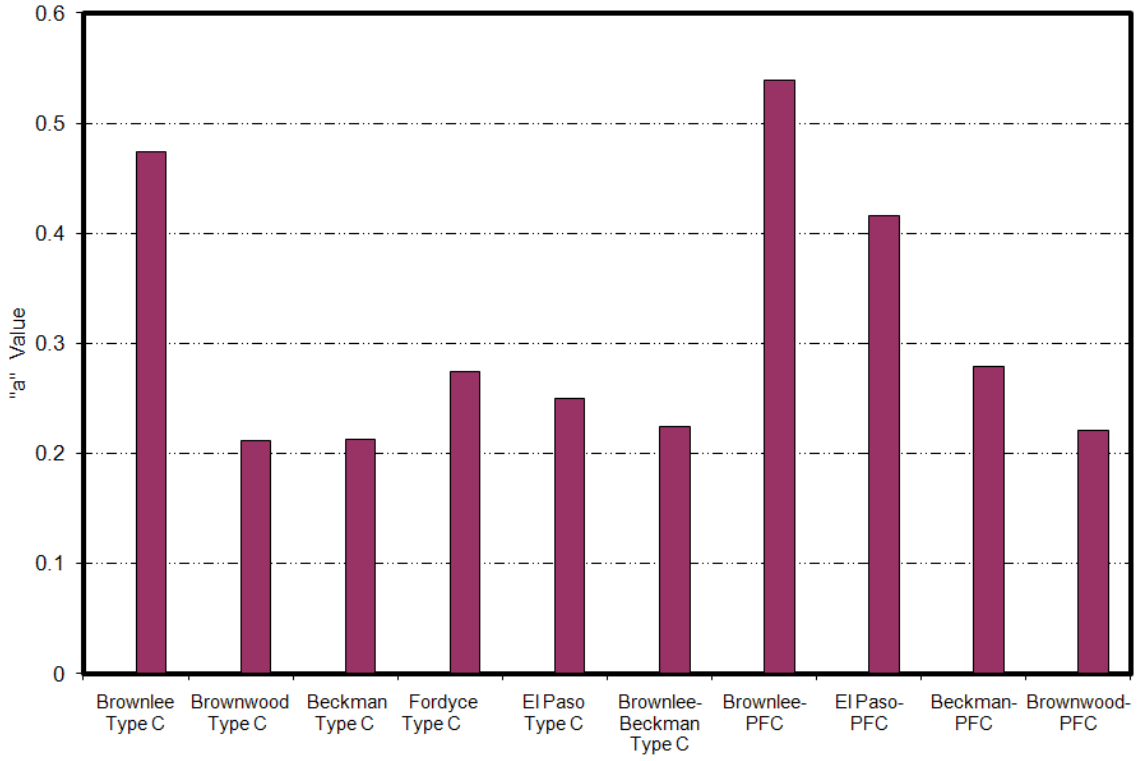

Figure 70. Terminal F60 Values for Different Aggregate Types.

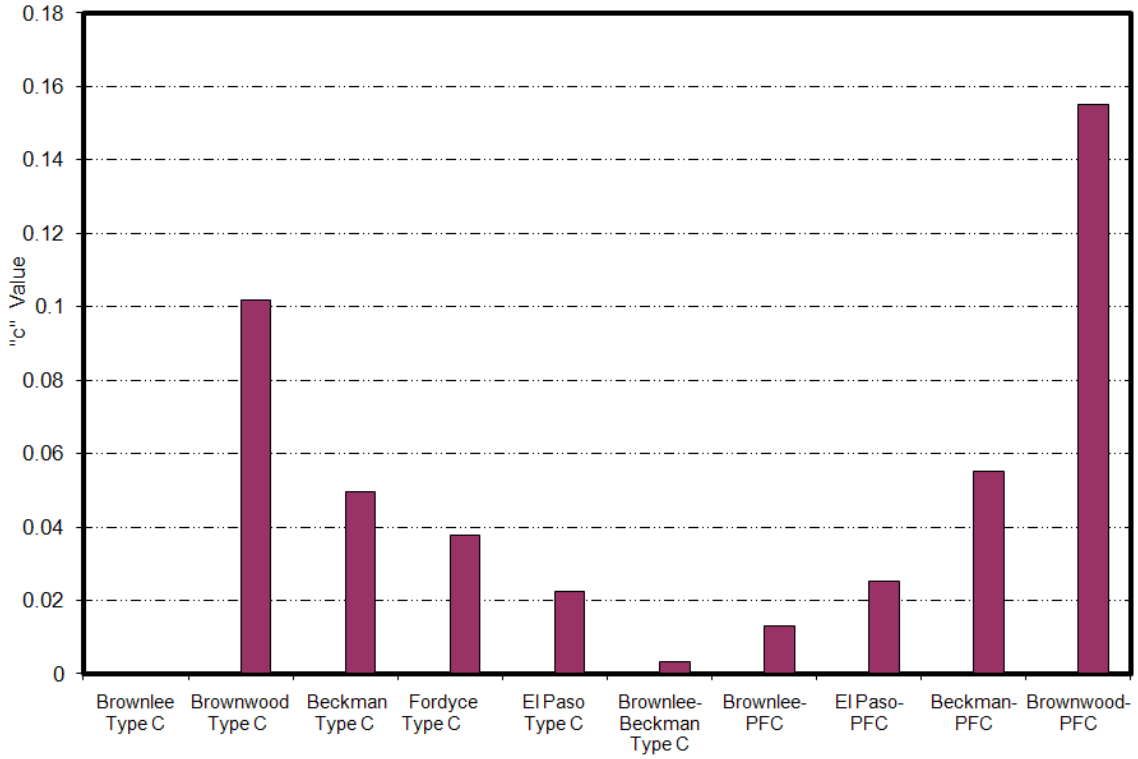

Figure 71. Rate of F60 Change for Different Aggregate Types.

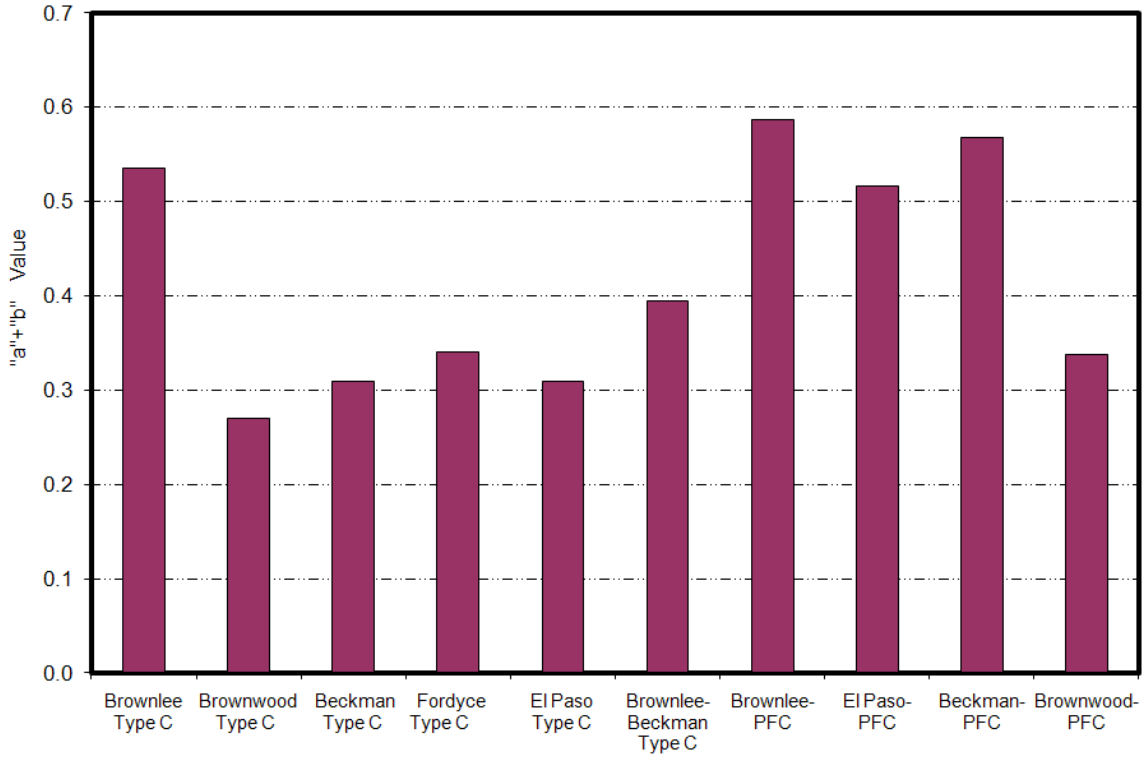

Figure 72. Initial F60 Values for Different Aggregate Types.

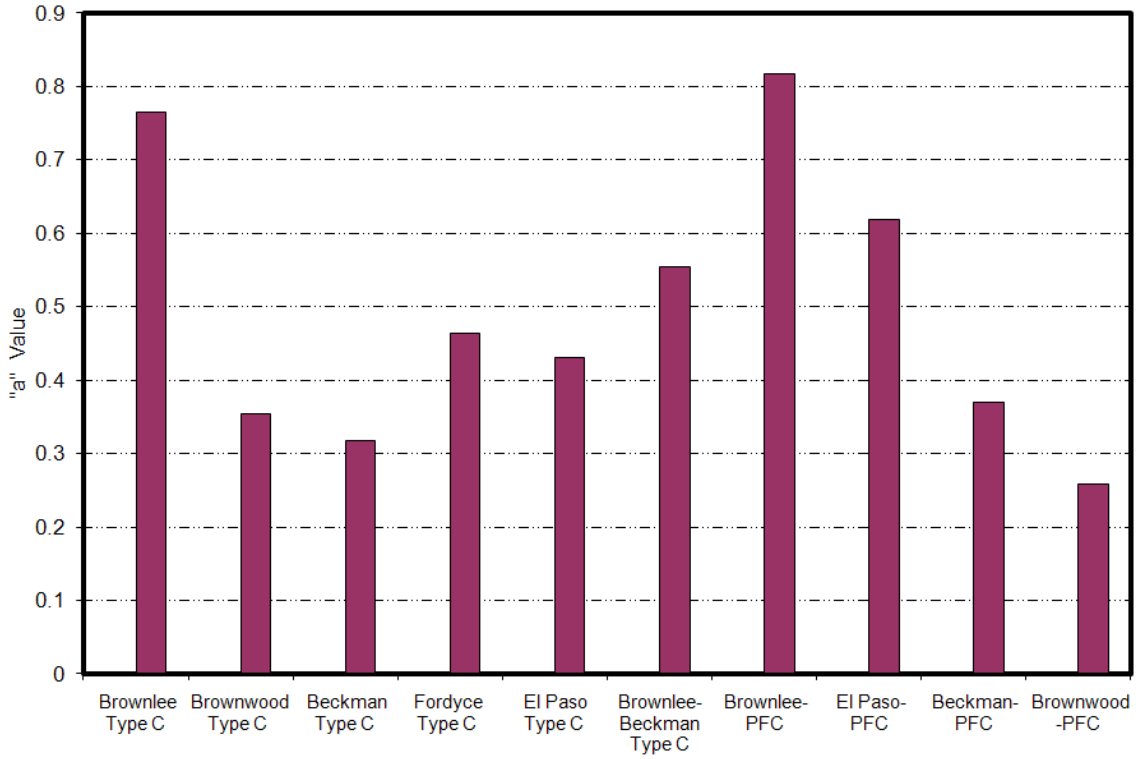

Figure 73. Terminal DF_{20} Values for Different Aggregate Types.

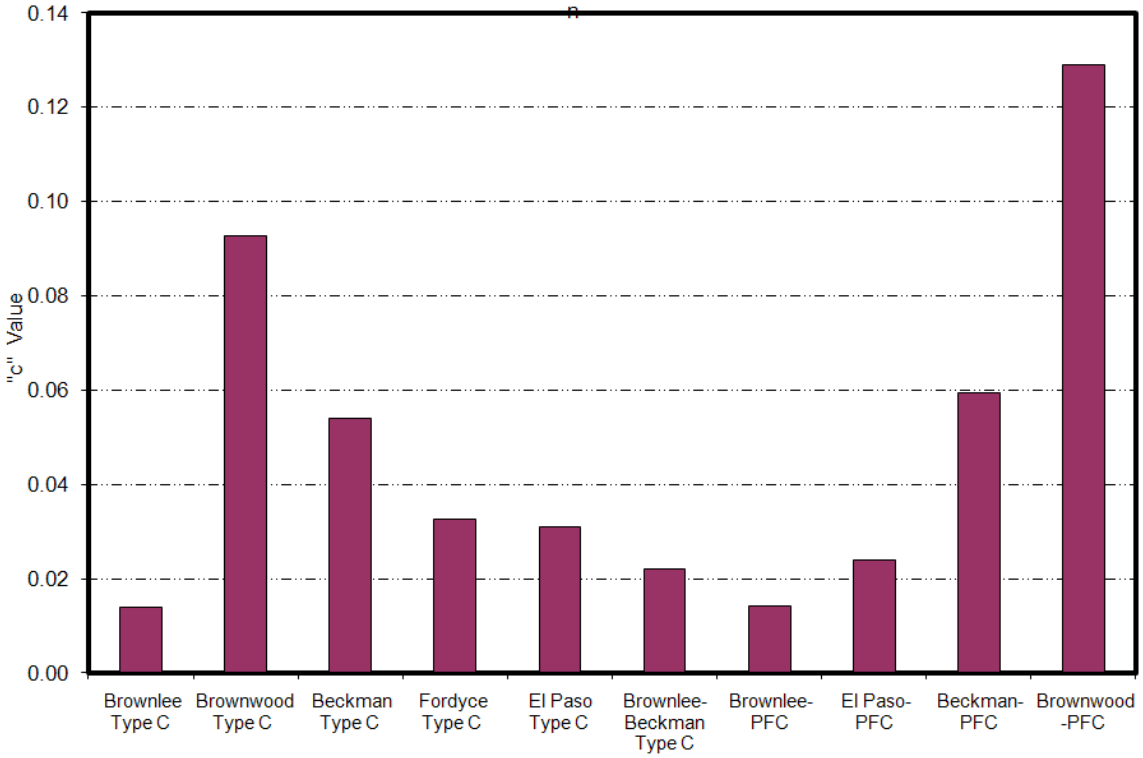

Figure 74. Rate of DF_{20} Change for Different Aggregate Types.

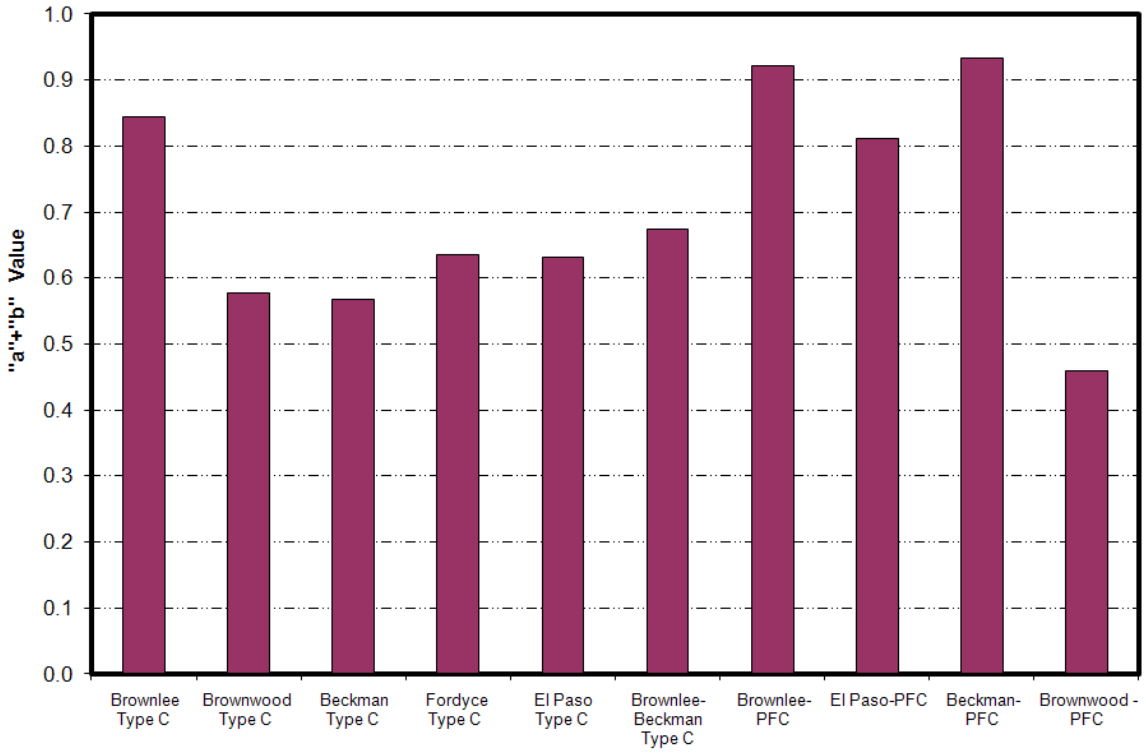

Figure 75. Initial DF_{20} Values for Different Aggregate Types.

In the subsequent sections, influence of different aggregate properties on the frictional properties of different mixes is discussed. Two parameters of the proposed model, the polishing rate ("c" value) and the terminal friction value F60 ("a" value) were selected as a measure of surface frictional properties. These two values were used to compare the influence of the aggregate properties on the skid resistance characteristics. A statistical correlation analysis was performed to evaluate the correlation between these two parameters and other aggregate properties.

In this analysis, two important statistical parameters were estimated, i.e., coefficient of correlation (R-value) and significance of correlation (p-value). The former is an indication of a linear relationship among variables, and the later is determined from the hypothesis testing that the chosen independent variable is significant. A low p-value below significance level—a significance level of α=0.05 was used in this study—indicates the chosen variable is important in explaining the behavior of the dependent

variable. Furthermore, this parameter shows if there is any significant statistical correlation between parameters.

Hence, different aggregate characteristics discussed in previous chapters were considered as the main aggregate characteristics affecting the frictional characteristics. To explain the effect of each aggregate's properties, a linear regression analysis was done, and the significance of the regression coefficients was studied. Figures 99 to 134 in Appendix C show the variation of F60 and DF_{20} terminal and change values against different aggregate properties for Type C and PFC mixes.

Tables 31 and 32 summarize the regression coefficients and the results of the statistical test on significance of the regression parameters for Type C and PFC mixes.

Table 31. Results of Regression Analysis on Type C Mix.

Mixture Frictional Characteristics	Aggregate Properties									
	LA % Wt Loss		Mg. Soundness		Polish Stone Value		MD % Wt. Loss		Acid Insolubility	
	R^2	p-value	R^2	p-value	R^2	p-value	R^2	p-value	R^2	p-value
DF_{20} Change	0.01	0.45	0.09	0.28	0.67	0.02	0.01	0.45	0.43	0.08
DF_{20} Terminal	0.14	0.23	0.01	0.43	0.90	0.00	0.00	0.50	0.38	0.09
F60 Change	0.00	0.45	0.09	0.28	0.68	0.02	0.05	0.33	0.27	0.14
F60 Terminal	0.16	0.22	0.01	0.43	0.70	0.02	0.01	0.44	0.35	0.11

Mixture Frictional Characteristics	Aggregate Properties							
	Texture Change BMD* and AMD		Angularity Change BMD and AMD		Texture AMD		Angularity AMD	
	R^2	p-value	R^2	p-value	R^2	p-value	R^2	p-value
DF_{20} Change	0.73	0.01	0.35	0.11	0.38	0.10	0.10	0.27
DF_{20} Terminal	0.69	0.02	0.84	0.01	0.62	0.03	0.00	0.46
F60 Change	0.64	0.03	0.32	0.12	0.37	0.10	0.02	0.39
F60 Terminal	0.44	0.08	0.64	0.03	0.53	0.05	0.01	0.43

* Before Micro-Deval

* After Micro-Deval

Table 32. Results of Regression Analysis on PFC Mix.

Mixture Frictional Characteristics	Aggregate Properties									
	LA % Wt Loss		Mg. Soundness		Polish Stone Value		MD % Wt. Loss		Acid Insolubility	
	R^2	p-value	R^2	p-value	R^2	p-value	R^2	p-value	R^2	p-value
DF_{20} Change	0.05	0.39	0.43	0.17	0.55	0.13	0.07	0.32	0.63	0.10
DF_{20} Terminal	0.05	0.39	0.09	0.35	0.81	0.05	0.00	0.48	0.96	0.01
F60 Change	0.09	0.35	0.53	0.13	0.51	0.14	0.13	0.32	0.54	0.13
F60 Terminal	0.09	0.35	0.08	0.36	0.83	0.04	0.00	0.48	0.97	0.01

Mixture Frictional Characteristics	Aggregate Properties							
	Texture Change BMD and AMD		Angularity Change BMD and AMD		Texture AMD		Angularity AMD	
	R^2	p-value	R^2	p-value	R^2	p-value	R^2	p-value
DF_{20} Change	0.61	0.11	0.10	0.34	0.42	0.18	0.35	0.20
DF_{20} Terminal	0.91	0.02	0.39	0.19	0.77	0.06	0.32	0.22
F60 Change	0.50	0.15	0.08	0.36	0.32	0.22	0.28	0.24
F60 Terminal	0.91	0.02	0.42	0.18	0.77	0.06	0.30	0.23

Tables 31 and 32 show a variety of aggregate properties assumed to have some effects on the measured friction of different surfaces. These properties include:

- LA abrasion weight loss,
- Magnesium soundness test value,
- Polish Stone Value,
- Micro-Deval weight loss,
- coarse aggregate acid insolubility,
- terminal texture measured by AIMS after Micro-Deval,
- terminal angularity measured by AIMS after Micro-Deval,
- change in texture before and after micro-Deval measured by AIMS, and
- change in angularity before and after micro-Deval measured by AIMS.

These tables show that the LA abrasion value could explain less than 20 percent variation in DF_{20} and F60 change, and the coefficient of regression is not significant at 95 percent confidence level. Therefore, the LA abrasion weight loss does not seem to be a significant factor in pavement skid resistance. The same result could be concluded for

magnesium sulfate soundness value, Micro-Deval weight loss, and terminal angularity after Micro-Deval. Moreover, R-squared values in both Type C and PFC mixes are very low, and the p-value is higher than 0.05. The coarse aggregate acid insolubility value is likely to be an important factor in both F60 and DF_{20} terminal values and rate of change, although the R-squared values are not high in Type C mixes. The low R-squared value might be due to data outliers. Further analysis was performed to investigate the effect of coarse aggregate insolubility value without considering outliers. The results will be discussed later in this chapter.

The results of analysis show that British Pendulum is a significant factor at 95 percent confidence level. The R-square values are about 0.6 for rate of change in both Type C and PFC mixes and 0.8 for terminal values. This indicates BP value is more important on terminal F60 and DF_{20} values. Moreover, the results of the analysis show that the F60 and DF_{20} terminal values increase and F60 and DF_{20} rate of change decrease when the British pendulum value increases.

Change in texture before and after Micro-Deval and the texture after Micro-Deval are significant factors in terminal DF_{20} and F60 values and rate of change. Moreover, change in texture before and after Micro-Deval accounts for 73 and 64 percent change in DF_{20} and F60 variation, respectively, and is significant in Type C mixes. Texture change before and after Micro-Deval accounts for a 91 percent change in DF_{20} and F60 terminal value and is significant in PFC mixes. It is evident that the texture change has more influence on DF_{20} than F60. This, in part, can be justified by the contribution of macrotexture on calculating the F60 value that makes the F60 change less dependent on microtexture than DF_{20}. Measured texture after Micro-Deval defines 62 and 53 percent change in DF_{20} and F60 terminal values and statistically is significant in Type C mixes. In PFC mixes, the terminal texture value after the Micro-Deval test is responsible for 77 percent change in Df_{20} and F60 terminal values and is significant. As a general trend, an increase in terminal texture will result in an increase in DF_{20} and F60 terminal values and a decrease in DF_{20} and F60 rate of change. The same effect could be seen in texture change before and after Micro-Deval. Increase in texture change before and after Micro-Deval decreases the terminal value of DF_{20} and F60 and increases their rate of change.

Change in angularity before and after Micro-Deval affects the terminal DF_{20} and F60 values. When the angularity change before and after Micro-Deval increases, the terminal F60 and DF_{20} values increase.

Since Brownlee aggregate had very high microtexture that might affect the results of the analysis, the mixes containing Brownlee aggregate were removed from the database and another analysis was performed. Figures 135 through 140 in Appendix C show the results of the analysis conducted without sandstone. Table 33 summarizes the estimated R-squared values and significance level of considered parameter in the analysis.

Table 33. R-squared Values and Significant Level for Type C Mix.

Mixture Frictional Characteristics	Aggregate properties					
	LA % Wt Loss		Mg. Soundness		MD % Wt. Loss	
	R^2	p-value	R^2	p-value	R^2	p-value
F60 Change	0.05	0.36	0.19	0.23	0.04	0.37
F60 Terminal	0.36	0.14	0.31	0.16	0.59	0.06

Mixture Frictional Characteristics	Aggregate properties					
	Acid Insolubility		Texture Change BMD and AMD		Angularity AMD	
	R^2	p-value	R^2	p-value	R^2	p-value
F60 Change	0.17	0.24	0.55	0.08	0.06	0.34
F60 Terminal	0.83	0.02	0.59	0.06	0.97	0.00

This analysis revealed that LA weight loss and magnesium soundness values are not statistically significant in predicting the DF_{20} and F60 terminal values and rate of change. However, this analysis showed that the coarse aggregate insolubility value is a significant factor on the terminal F60 value and could explain the 83 percent change in F60. This analysis also showed that angularity after Micro-Deval is also a statistically significant factor on explaining the F60 terminal values. Moreover, the terminal F60 value increases when angularity after Micro-Deval increases. Similarly, an increase in coarse aggregate acid insoluble value increases terminal F60 value.

AGGREGATE RANKING BASED ON LAB RESULTS

Selection of an aggregate type based on its frictional properties is an important step toward constructing a safe pavement with adequate skid resistance. A ranking system according to frictional properties will assist the selection of the most appropriate aggregate. The frictional properties of each aggregate type could be assessed by using friction-polish cycle curve. ANOVA analysis was done to study the effect of mix type and aggregate on the measured F60. It was demonstrated that the difference between the measured F60 values of Type C and PFC mixes is significant. Moreover, any aggregate classification system that tends to classify aggregates should consider the mix type as an important factor.

Figure 76 shows the terminal F60 values of different aggregate for different mixes. This figure shows the Brownlee aggregate had superior frictional performance in both Type C and PFC mixes. The results of the ANOVA analysis in the previous section showed that there is a significant difference between measured F60 values of Brownlee aggregate and other aggregates. This result is in agreement with the result of TxDOT aggregate classification that considers Brownlee aggregate in class A. The next aggregate in the list is El Paso aggregate that has been used in PFC mixes. This aggregate, however, does not have high terminal friction in Type C. The El Paso aggregate in the PFC mixture also had significant differences with all other aggregates and was the third in the list.

Mixing 50 percent Brownlee aggregate with 50 percent Beckman aggregate gives the blend superior frictional properties. Although the blend is classified B based on the current classification system, the frictional properties of the blend are significantly better than Fordyce aggregate and El Paso in Type C mixture.

Beckman aggregate shows relatively good frictional properties in PFC mixes. Beckman aggregate has a high amount of carbonate material that is abraded quickly from the surface of the aggregate, fills the pores of PFC mixture in the lab experiment, and improves the skid resistance of the mix. This effect, however, could lead to a decrease in permeability.

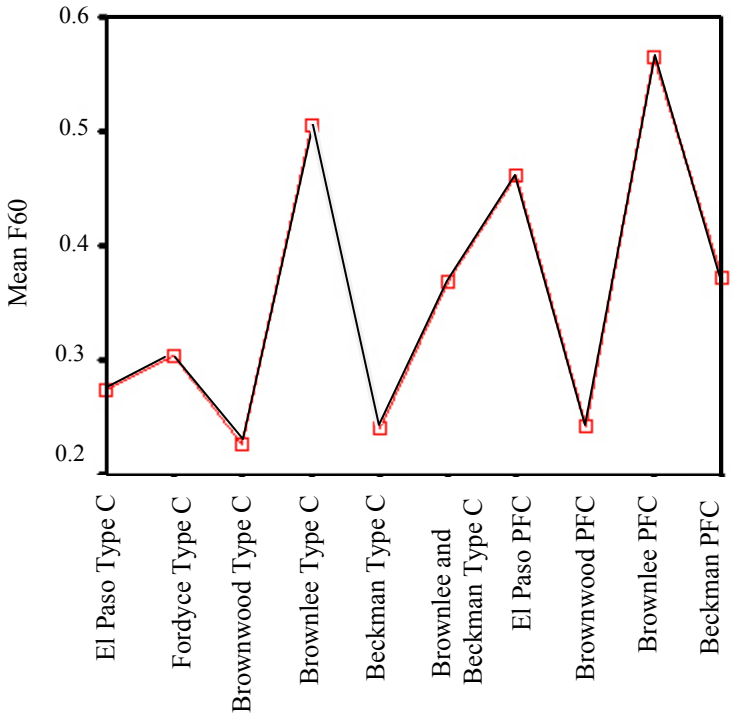

Figure 76. Mean F60 Values for Different Aggregate Types.

Although Fordyce aggregate is the next in the group and has slightly better frictional properties than El Paso aggregate, the difference is not significant. El Paso aggregate showed better frictional characteristics than Beckman and Brownwood aggregates.

Using Brownwood aggregate in the PFC mixture gives the mix slightly better frictional performance than Type C. No significant differences were observed in frictional properties of Beckman and Brownwood aggregate.

CHAPTER V – MIX FRICTION MODEL BASED ON AGGREGATE PROPERTIES

INTRODUCTION

This chapter presents a new model that expresses F60 values as a function of aggregate resistance to polishing and gradation. This model will assist in predicting the frictional performance of a road and select corrective measures to improve it. Figure 77 shows an overview of the friction model.

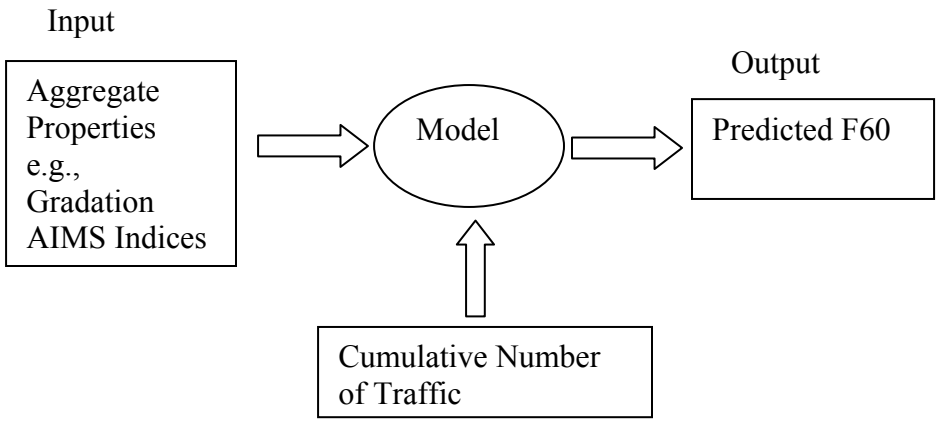

Figure 77. Overview of the Friction Model.

The friction model shown in Figure 77 consists of a set of equations that can predict F60 value at any given polishing level. Moreover, this model should predict three important parameters—initial F60 level ("a" + "b"), rate of F60 change "c," and terminal F60 value "a."

MODELING APPROACH

The previous chapter showed the mixture type; namely aggregate gradation has a significant effect on F60 parameters. To consider the aggregate gradation as a parameter in the friction model, a cumulative two-parameter Weibull distribution was used to fit the standard aggregate size distribution data (cumulative percent passing size). The cumulative two-parameter Weibull distribution has the form of:

$$F(x;k,\lambda)=1-e^{-\left(x/\lambda\right)^{k}} \quad \textbf{(10)}$$

where x is the variable (aggregate size in millimeter), and k and λ are model parameters known as shape and scale parameters, respectively. Figures 78 through 87 show the aggregate gradation and fitted line for different mixes.

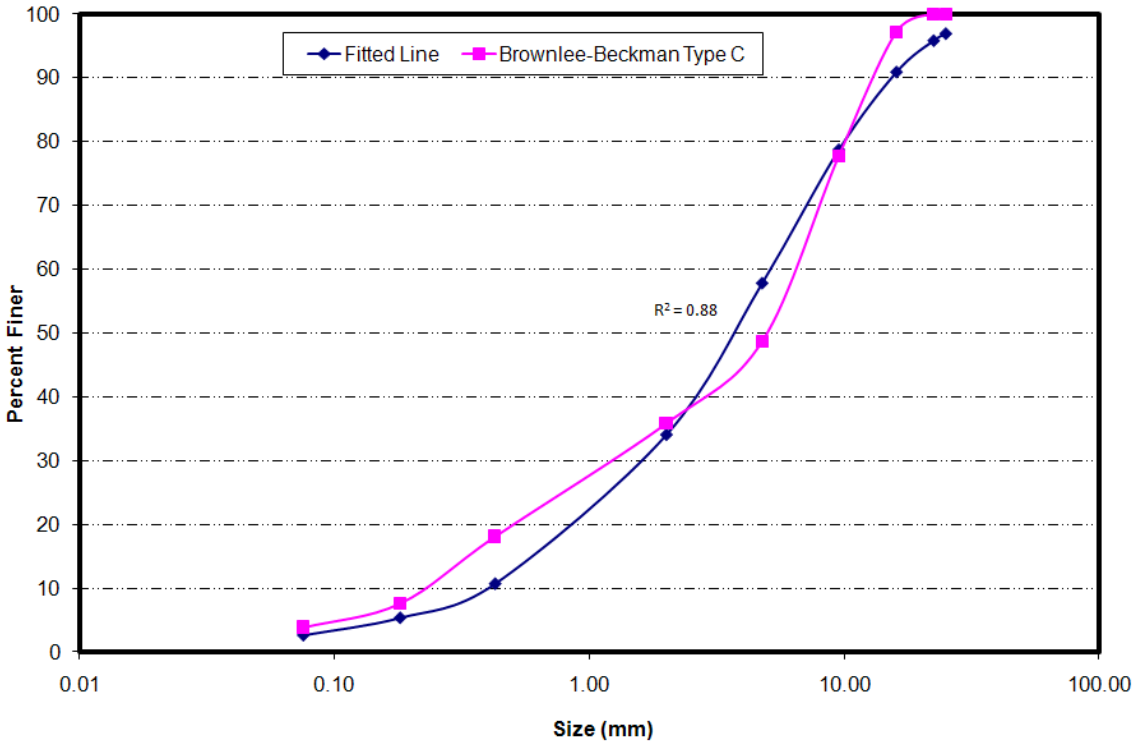

Figure 78. Aggregate Gradation and Fitted Line for Brownlee-Beckman Type C Mix.

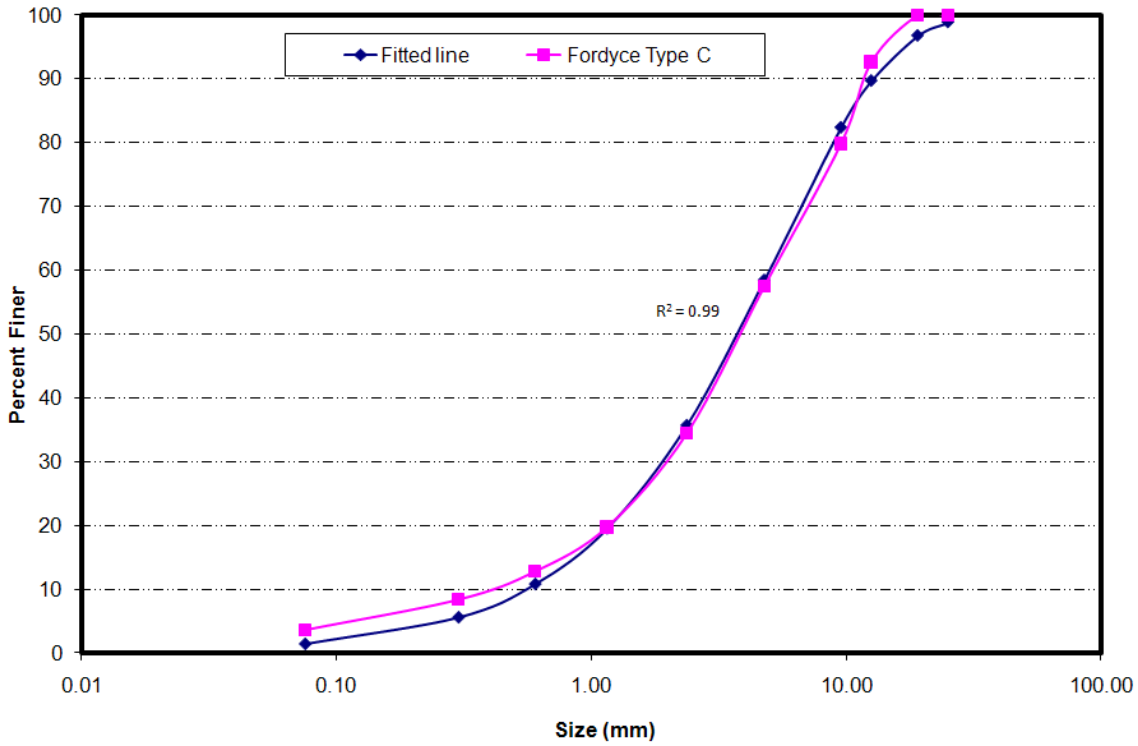

Figure 79. Aggregate Gradation and Fitted Line for Fordyce Aggregate Type C Mix.

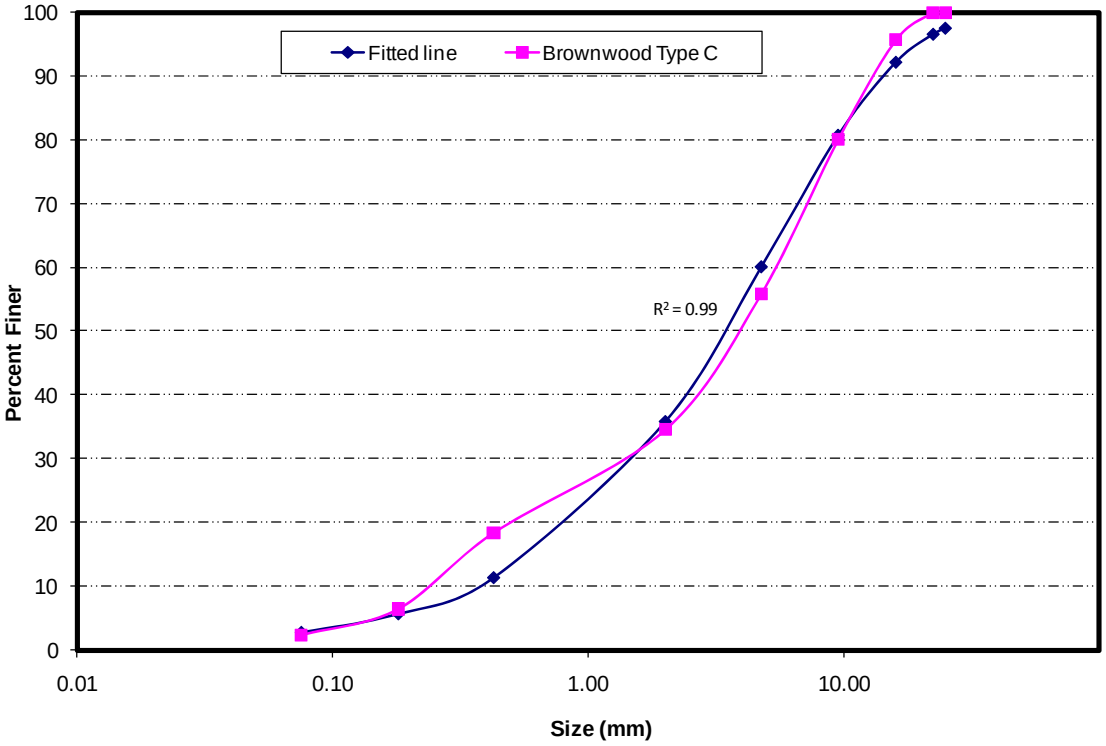

Figure 80. Aggregate Gradation and Fitted Line for Brownwood Aggregate Type C Mix.

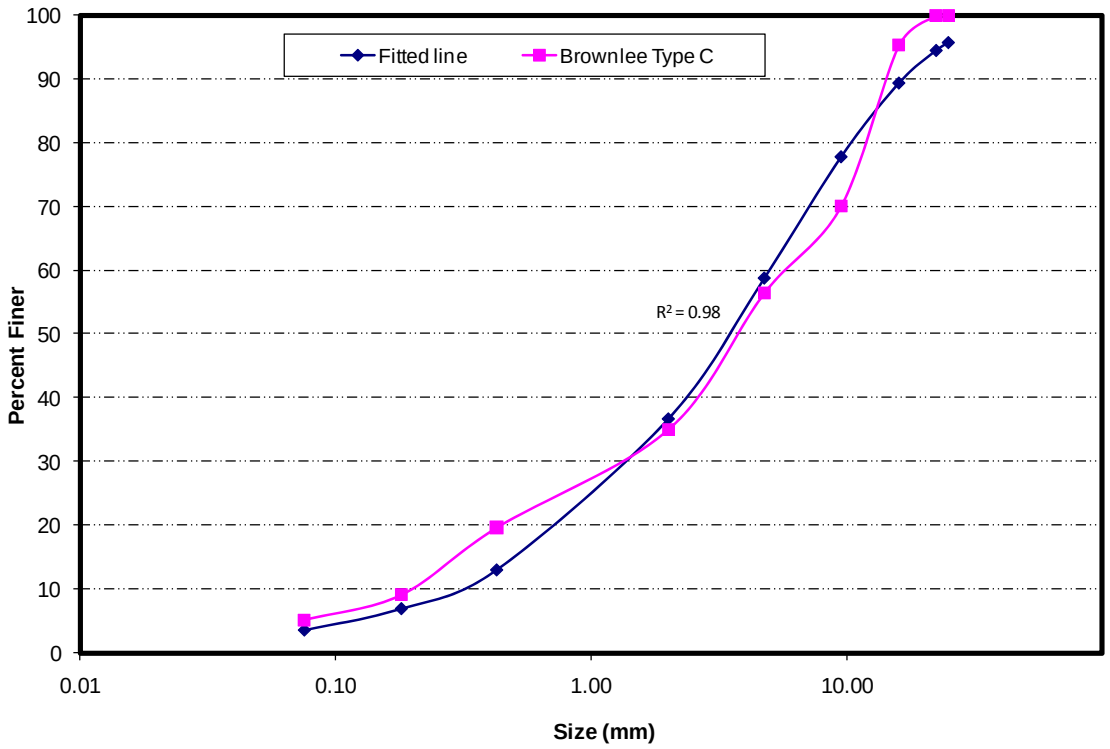

Figure 81. Aggregate Gradation and Fitted Line for Brownlee Aggregate Type C Mix.

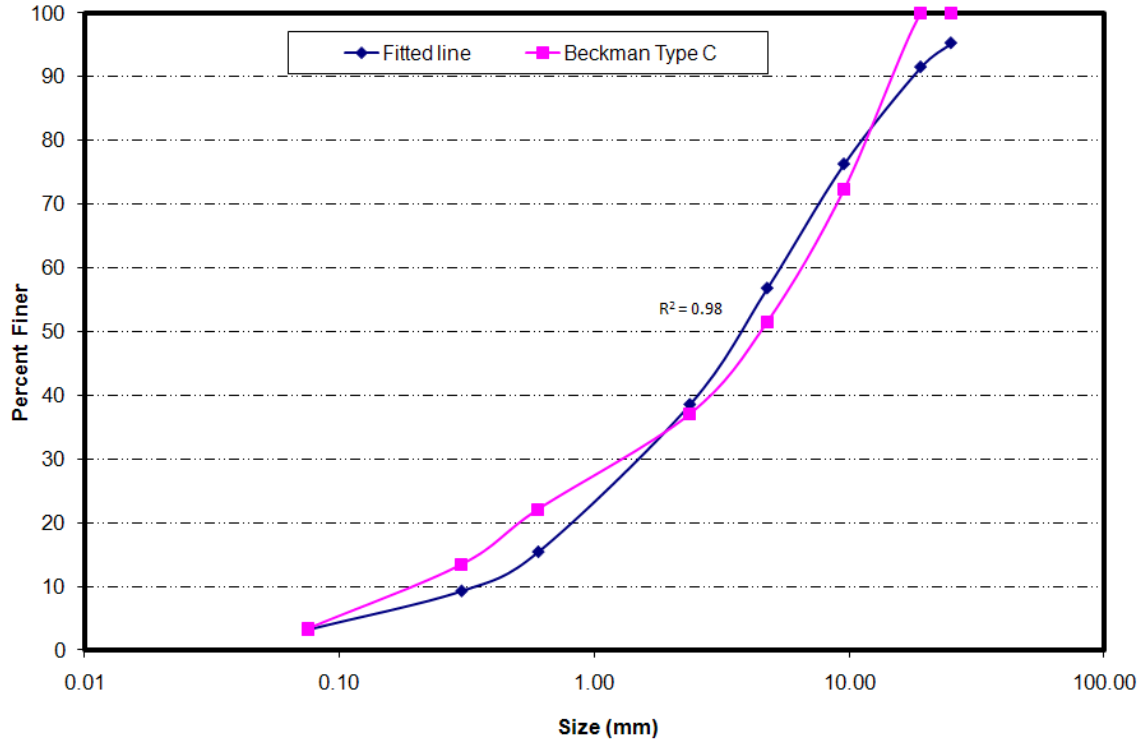

Figure 82. Aggregate Gradation and Fitted Line for Beckman Aggregate Type C Mix.

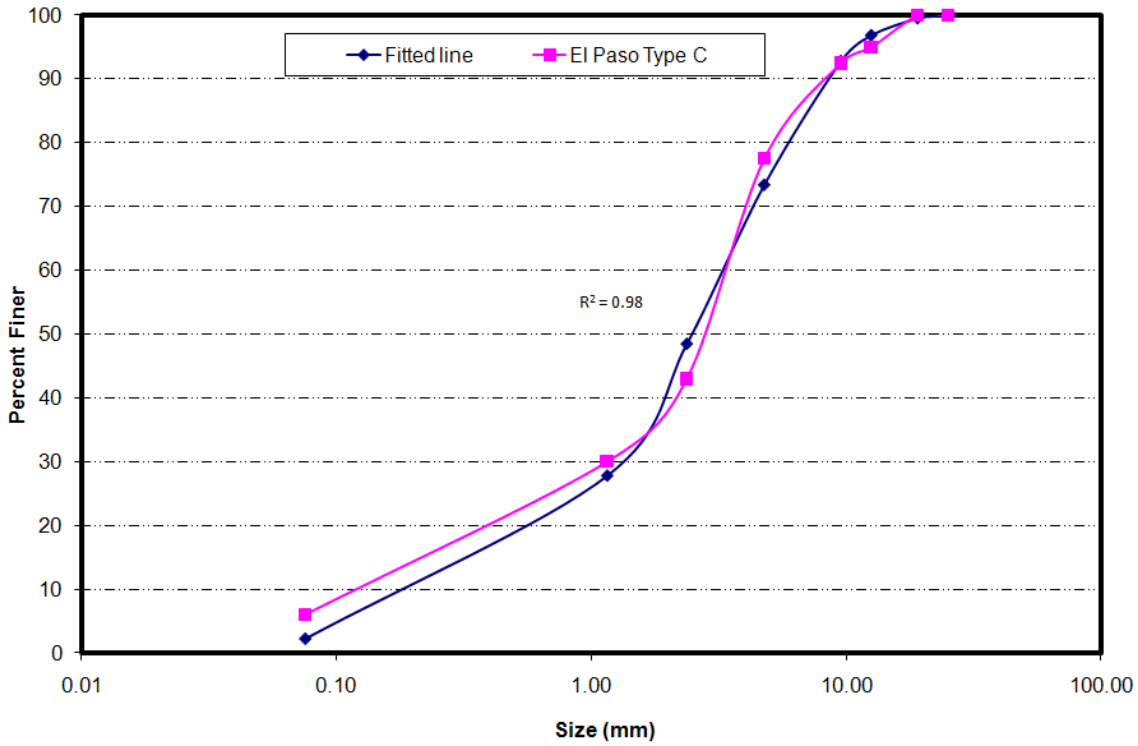

Figure 83. Aggregate Gradation and Fitted Line for El Paso Aggregate Type C Mix.

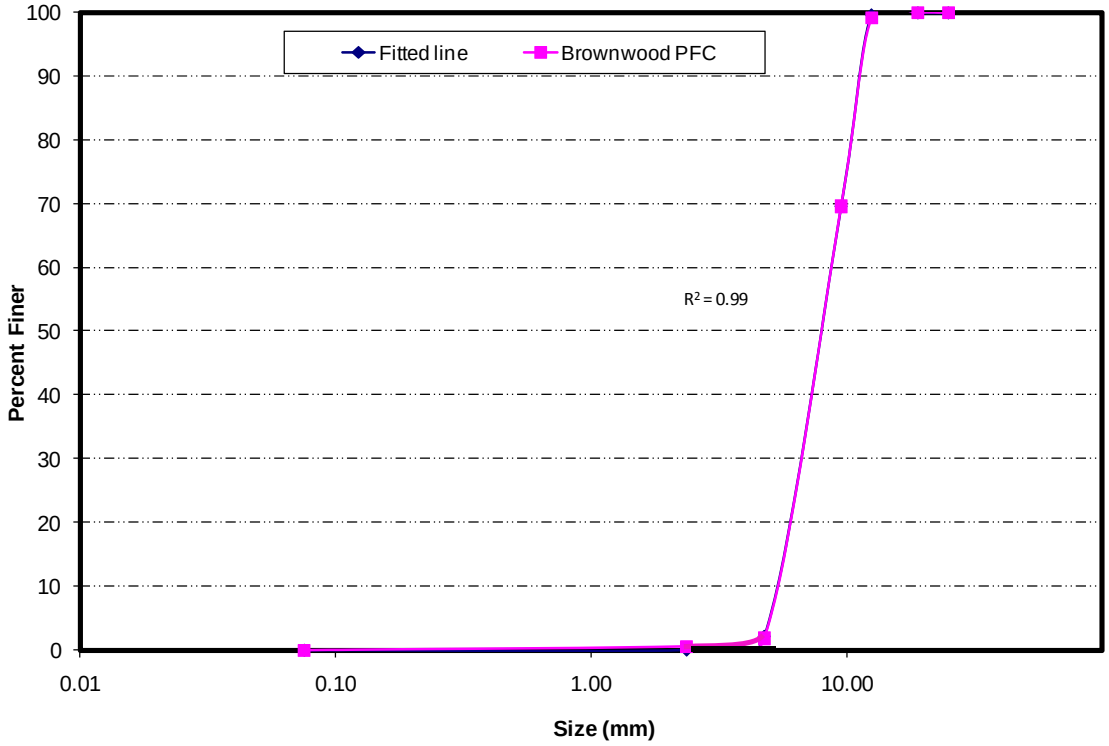

Figure 84. Aggregate Gradation and Fitted Line for Brownwood Aggregate PFC Mix.

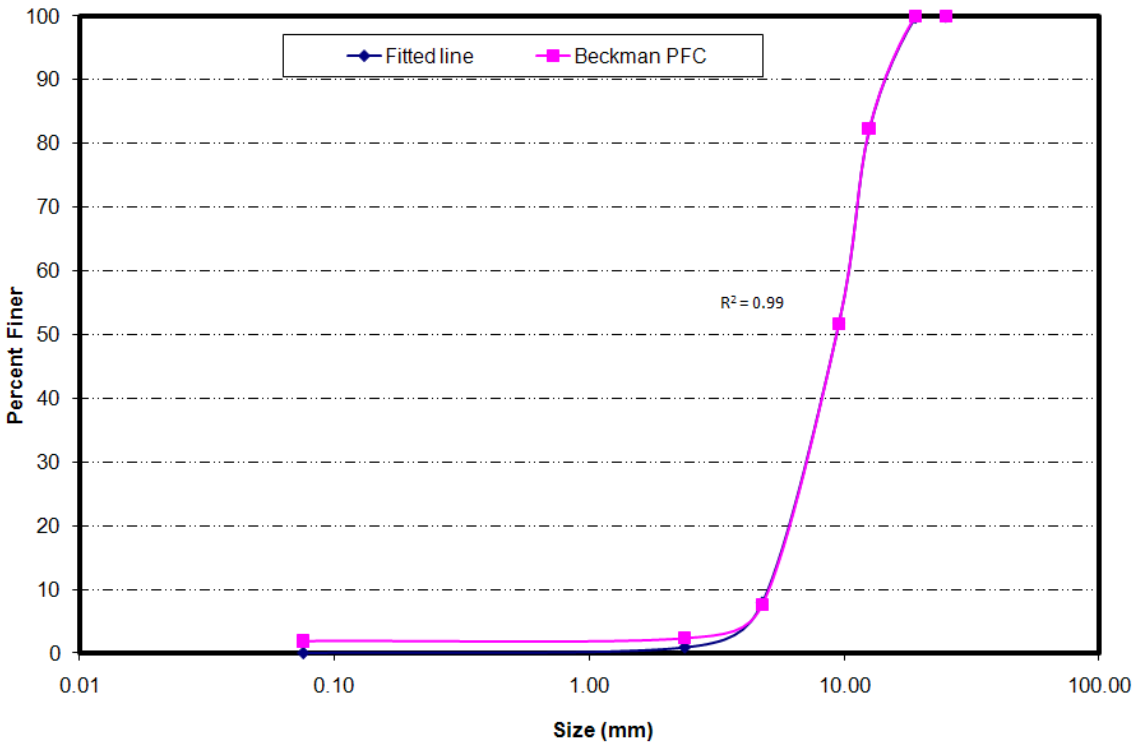

Figure 85. Aggregate Gradation and Fitted Line for Beckman Aggregate PFC Mix.

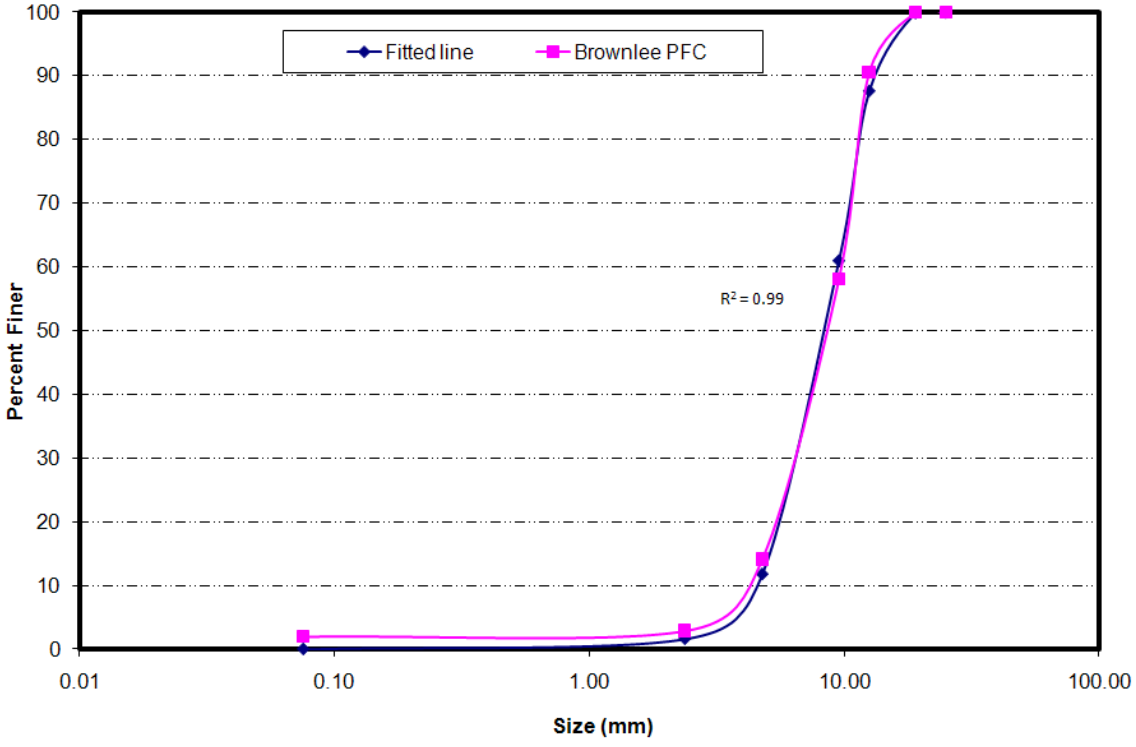

Figure 86. Aggregate Gradation and Fitted Line for Brownlee Aggregate PFC Mix.

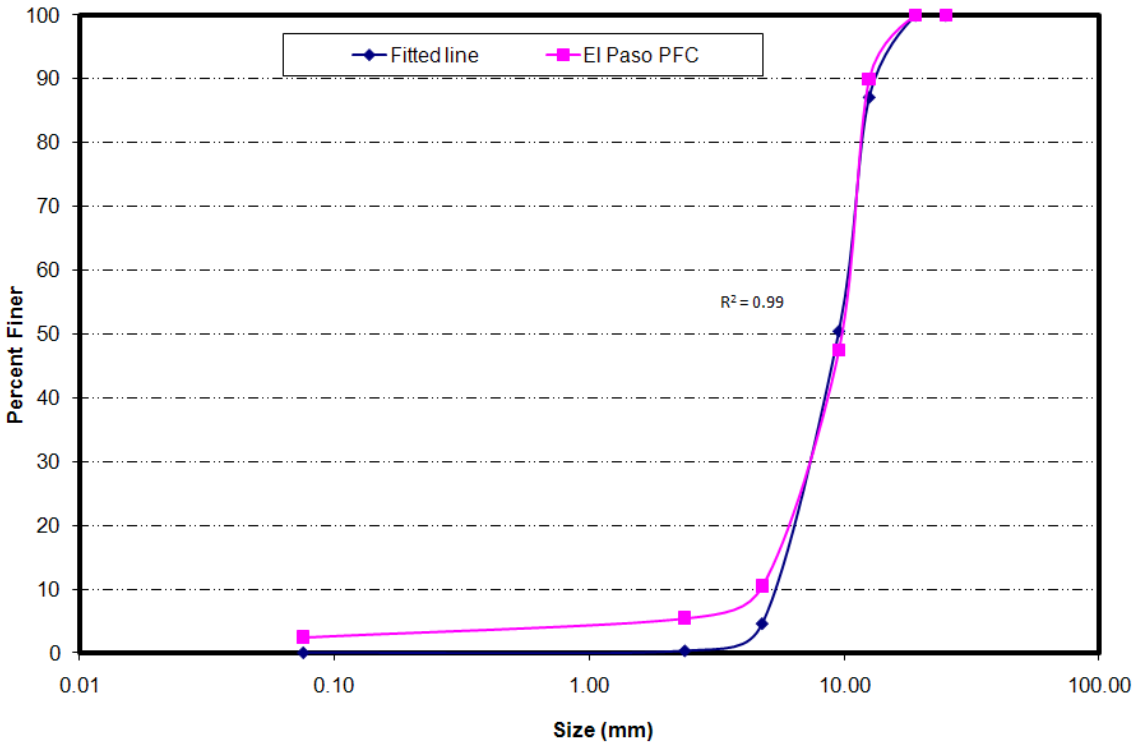

Figure 87. Aggregate Gradation and Fitted Line for El Paso PFC Mix.

Table 34 summarizes the calculated k and λ value for each mix. These parameters have been calculated by using the SSE method.

Table 34. Calculated Weibull Parameters for Different Mixes.

Aggregate Type	Mix Type	λ	κ
Brownlee-Beckman	Type C	5.653	0.843
Fordyce		5.419	0.983
Brownwood		5.245	0.842
Brownlee		5.554	0.764
Beckman		5.942	0.777
El Paso		3.495	0.863
Brownwood	PFC	9.213	5.755
Beckman		10.503	3.150
Brownlee		9.698	2.909
El Paso		10.399	3.908

The results of the previous chapter showed the AIMS texture indices have a high correlation with rate of change and terminal values of F60, and this value could be potentially used in any model explaining the F60. Selecting other aggregate properties that can be used in the model should be based on a statistical analysis. This analysis will show the minimum number of independent variables that can be used in the model. Any correlation between the independent variables will decrease the reliability of the model. Table 35 shows the cross correlation between different parameters considered to be significant in the model. This table shows that the "a" (terminal value), "c" (rate of change), and "a" + "b" (initial value)—parameters of aggregate texture model—have high correlation with polish value, texture after Micro-Deval, texture change before and after Micro-Deval, and coarse aggregate acid insolubility. This analysis shows that developing a model that includes parameters of the aggregate texture model proposed by Mahmoud (2005) along with aggregate gradation parameters could satisfactorily explain the variation of F60 for different mixtures without any redundancy and cross correlation.

Table 35. Correlation Coefficients for Different Aggregate Properties.

Parameter	(1)	(2)	(3)	(4)	(5)	(6)	(7)	(8)	(9)	(10)	(11)	(12)
(1)		85.5%	-27.2%	82.4%	-77.4%	-77.4%	-62.5%	-19.2%	-63.7%	-16.0%	-27.4%	-4.3%
(2)	85.5%		24.4%	95.4%	-48.0%	12.6%	-14.3%	1.1%	-68.1%	-7.4%	-14.7%	-47.9%
(3)	-27.2%	24.4%		14.9%	62.3%	62.3%	90.0%	61.4%	2.8%	42.6%	44.3%	-91.0%
(4)	82.4%	95.4%	14.9%		-62.2%	32.8%	-15.9%	-16.5%	-84.6%	-27.5%	-22.9%	-29.9%
(5)	-77.4%	-48.0%	62.3%	-62.2%		-80.7%	72.9%	44.4%	77.9%	39.9%	27.7%	-48.6%
(6)	-77.4%	12.6%	62.3%	32.8%	-80.7%		-72.6%	-82.1%	-49.4%	-77.8%	-61.6%	73.9%
(7)	-62.5%	-14.3%	90.0%	-15.9%	72.9%	-72.6%		52.5%	15.3%	34.3%	47.0%	-65.1%
(8)	-19.2%	1.1%	61.4%	-16.5%	44.4%	-82.1%	52.5%		16.6%	96.8%	92.3%	-67.3%
(9)	-63.7%	-68.1%	2.8%	-84.6%	77.9%	-49.4%	15.3%	16.6%		27.6%	2.1%	-1.2%
(10)	-16.0%	-7.4%	42.6%	-27.5%	39.9%	-77.8%	34.3%	96.8%	27.6%		88.9%	-53.2%
(11)	-27.4%	-14.7%	44.3%	-22.9%	27.7%	-61.6%	47.0%	92.3%	2.1%	88.9%		-42.1%
(12)	-4.3%	-47.9%	-91.0%	-29.9%	-48.6%	73.9%	-65.1%	-67.3%	-1.2%	-53.2%	-42.1%	

where:

(1) LA weight loss (percent),
(2) Mg. weight loss (percent),
(3) Polish Stone Value,
(4) Micro-Deval weight loss (percent),
(5) coarse aggregate acid insolubility,
(6) change in texture before and after Micro-Deval,
(7) change in angularity before and after Micro-Deval,
(8) texture after Micro-Deval,
(9) angularity after Micro-Deval,
(10) terminal texture for aggregates ("a_{agg}" value),
(11) initial texture for aggregates ("a_{agg}" + "b_{agg}"), and
(12) rate of texture change for aggregates ("c_{agg}" value).

A nonlinear regression analysis was performed to determine the coefficients for model parameters. Table 36 shows parameter estimates for the model.

Table 36. Different Parameter of the Friction Model Estimated by Regression Analysis.

Parameter	Model	R^2
Terminal F60 (a_{mix})	$\frac{18.422+\lambda}{118.936-0.0013\times(AMD)^2}$	0.96
Initial F60 (a_{mix} + b_{mix})	$0.4984\ln\left(5.656\times10^{-4}\left(a_{agg}+b_{agg}\right)+5.846\times10^{-2}\lambda-4.985\times10^{-2}k\right)+0.8$	0.82
F60 Rate of Change (c_{mix})	$0.765\cdot e^{\left(-7.297\cdot10^{-2}/c_{agg}\right)}$	0.90

where:

AMD: Aggregate texture after Micro-Deval,

"a_{agg}" + "b_{agg}": Aggregate initial texture using texture model,

c_{agg} : Aggregate texture rate of change using texture model,

k-value: Weibull distribution shape factor, and

λ-value: Weibull distribution scale factor.

The developed model for the terminal F60 value is significant at 95 percent confidence level. This model consists of the aggregate terminal texture value measured after Micro-Deval and λ-value related to mix gradation. Researchers noted that this model has a high R-square and can account for 96 percent of the variation in terminal F60.

Figure 88 shows the predicted terminal F60 values versus measured terminal F60 values. Based on this model, a higher texture after Micro-Deval will result in a higher terminal value for F60. Likewise, the mixes with high λ-values—primarily PFC mixes—have higher terminal F60 values.

Table 36 also shows the initial F60 value is depending on the aggregate initial texture value ("a_{agg}" + "b_{agg}"), which is calculated by fitting a model to a texture and corresponding gradation parameters k-value and λ-value. The model is significant overall and has a high R-square of 0.82. Figure 89 depicts the measured and predicted initial F60 values.

The rate of F60 change in Table 36 is only depending on the rate of texture change in corresponding aggregate. The model is significant, and the R-square is 0.91. Figure 90 shows the predicted and measured rate of F60 change ("c" value).

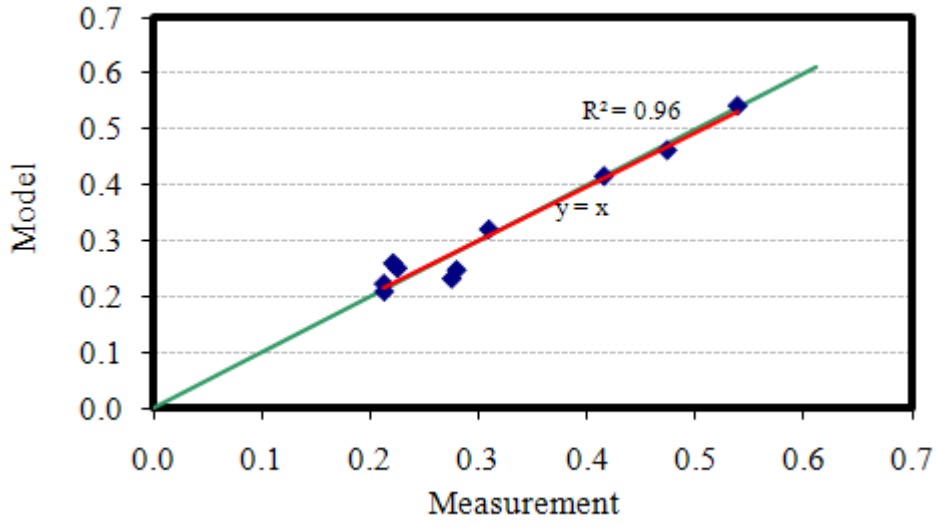

Figure 88. Predicted vs. Measured Terminal F60 Values.

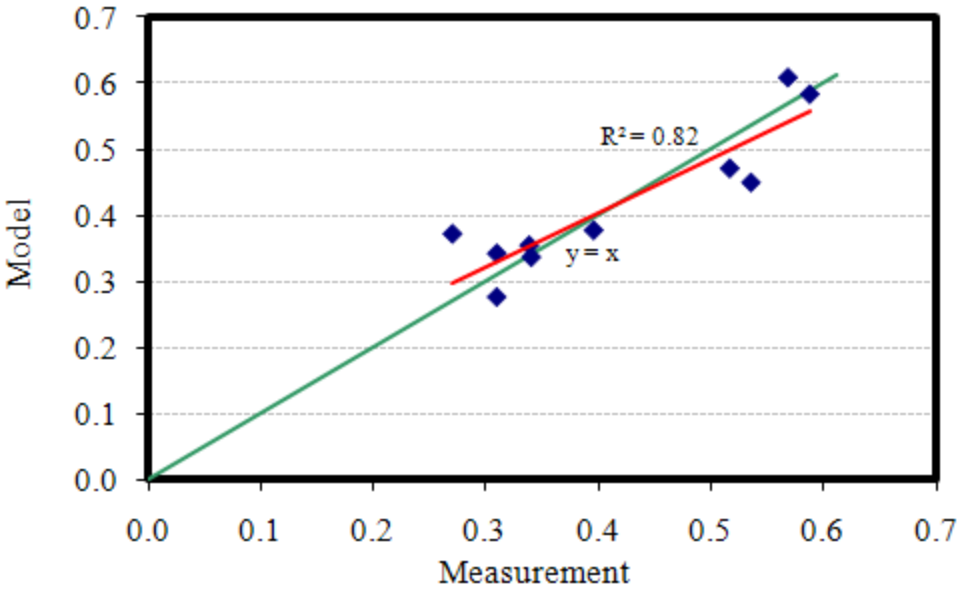

Figure 89. Predicted vs. Measured Initial F60 Values.

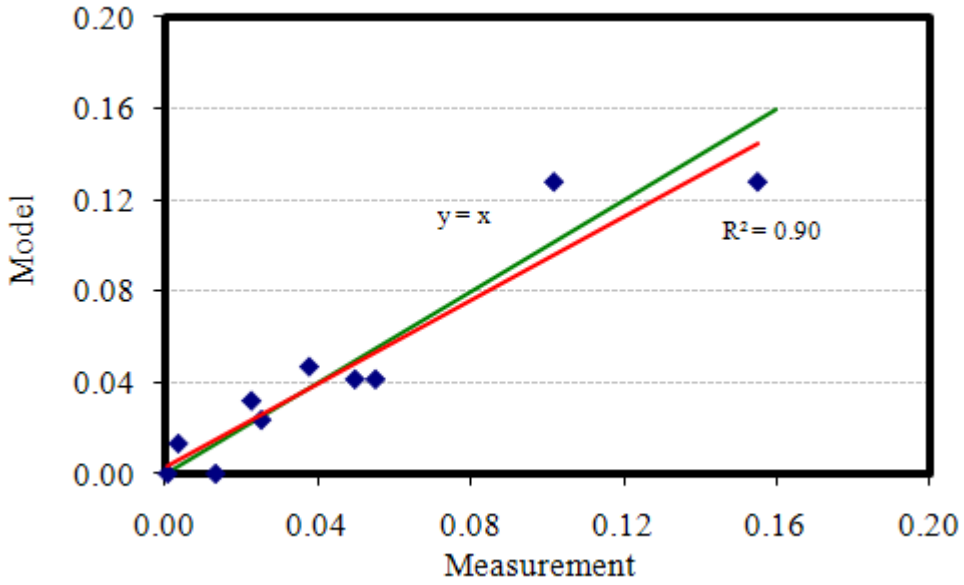

Figure 90. Predicted vs. Measured F60 Rate of Change.

The R-square value for each parameter is reasonably high and could be used in the F60 model (Equation 9). Equation 9 could also be rewritten as Equation 11 to include all three parameters discussed above:

$$F60 = (a_{mix} + b_{mix}) \cdot e^{-c_{mix} \cdot n} - a_{mix} \cdot e^{-c_{mix} \cdot n} + a_{mix} \quad \textbf{(11)}$$

where, n = polishing cycle in 1000 of repetitions.

This model is able to:

- predict mix friction (F60) based on mix gradation and aggregate resistance to polishing. These predictions can be used to do corrective measures when the skid resistance of a road drops below an acceptable level.
- select aggregate given the mix in which this aggregate will be used and desired mixture friction. The adequate level of skid resistance is different for each road category. Using this model will aid in the selection of the appropriate mix and aggregate type to provide the required friction level.
- predict reduction in mix friction as a function of polishing cycles. This reduction can be predicted from the rate of change in aggregate texture in Micro-Deval. The developed model is currently expanded to relate the polishing cycle in the lab to traffic loading.

CHAPTER VI – RESULTS AND CONCLUSIONS

INTRODUCTION

During the course of this study, the frictional behavior of different aggregates and mixture types were measured and analyzed. Several asphalt mix slabs were prepared and compacted in the lab, and their frictional properties were measured using the sand patch method, British Pendulum Test, Dynamic Friction Test, and Circular Texture Meter. The results of each test are summarized in this chapter.

SAND PATCH TEST

This test was performed on Type C and Type D mixes only. Comparing the mean MTD values of these two mixes before polishing showed that the average MTD values of Type C mixes were greater than those for Type D mixes. This is due to the larger maximum aggregate size in the Type C mix, which can result in a higher macrotexture before polishing.

Although it seemed as if the MTD values of almost all mixes (except for sandstone) after polishing were less than the MTD values before polishing, statistical analysis did not show any significant differences between MTD values before and after polishing. Hence, researchers concluded that the sand patch test was not able to detect changes in macrotexture due to polishing with the selected polishing device. The results showed that mixes with different aggregates had different MTD values. Thus, a pairwise comparison analysis was performed between the aggregates to find the differences between MTD values of different aggregate types. The results showed that Brownlee aggregate had the highest MTD values among all aggregates, and both Beckman and Brownwood aggregates produced the lowest MTD values.

BRITISH PENDULUM TEST

This test was performed on three different locations on each slab, and three measurements were conducted on each location. The TxDOT test requires using a 3-inch slider in the BP. However, it was not feasible to use this size because of the limited

polished area resulting from the polished machine used in this study. As a result, a 1.5-inch wide rubber slider was used in all BP measurements.

The results indicated that BP values decreased with an increase in polishing cycles for all aggregates except mixtures containing Brownlee aggregate. For Brownlee aggregate, the BP values remained almost constant

The BP values of PFC mixes were generally higher than those for Type C mixes. In addition, the frictional characteristics of some aggregates varied depending on the mix in which the aggregate was used. It is interesting to note that, for example, the PFC and Type C mixes with Brownwood aggregate had similar BP values at a low number of polishing cycles. However, the PFC with Brownwood aggregate had higher BP values than Type C at a high number of polishing cycles.

An analysis was performed to compare the results of measured BP values for each aggregate type. The results of the comparison between two aggregate types did not reveal any significant differences. Consequently, the British Pendulum test was not able to detect the difference between frictional performances of aggregates with a known difference in frictional characteristics.

CTMETER AND DFT TESTS

These two tests were performed at three different locations on each slab. The DFT was performed twice in each location while the CTMeter was conducted six times at each location. No particular trend was observed for MPD values from CTMeter of different mixes in terms of polishing cycles.

The result of dynamic friction testing at 20 km/h (DF_{20}) is an indication of microtexture (Hall et al., 2006). Therefore, this measure is a good indication of aggregate contribution to pavement skid properties. A plot of measured dynamic friction in terms of polishing cycles showed that DF_{20} decreased as polishing cycles increased. The DF_{20} curves leveled off and reached a terminal value after a certain number of polishing cycles.

Statistical analysis was performed to evaluate the effect of several variables (i.e., aggregate type, mix type, polishing cycles, and speed) on the measured dynamic friction. The results showed aggregate type affected the magnitude of dynamic friction in both

Type C and PFC mixes. The results also showed that there was a significant difference in the measured friction at different numbers of polishing cycles for Type C mixes. On the contrary, the magnitude of dynamic friction in PFC mixes did not have a significant difference between polishing cycles. The results also revealed that the PFC mix has a higher friction value than Type C mix.

The equation proposed by Mahmoud (2005) was fitted to the calculated F60 values. The rate of change and terminal value of friction were estimated from this equation. Comparing the rate of change and terminal values for different aggregates revealed that in all cases the Brownlee aggregate had the highest terminal values and lowest rate of change in both Type C and PFC mixes. On the contrary, mixes containing Beckman and Brownwood aggregates had the lowest terminal values and highest rate of change. This indicated that Beckman and Brownwood aggregates failed to preserve their frictional performance during load application. A combination of Brownlee and Beckman aggregates, however, performed satisfactorily and had a high terminal value and low rate of change compared to the Beckman aggregate. Fordyce and El Paso aggregates were almost the same and had fair frictional properties.

The dependency of terminal value and rate of change of DF_{20} and F60 on different aggregate characteristics was analyzed. The aggregate characteristics included in the analysis were LA impact and abrasion percent weight loss, magnesium soundness percent weight loss, British Pendulum value, Micro-Deval percent weight loss, coarse aggregate acid insolubility, texture measurements after Micro-Deval by AIMS, angularity measurements after Micro-Deval by AIMS, change in texture before and after Micro-Deval, and change in angularity before and after Micro-Deval. The coefficient of determination (R-square) and the statistical significance were evaluated to study if the considered variable is important and at what percent it could define the variability of DF_{20} and F60.

The results indicated that the LA impact and abrasion percent weight loss, magnesium soundness percent weight loss, Micro-Deval percent weight loss, angularity measurements after Micro-Deval by AIMS, and change in angularity before and after Micro-Deval were not significant factors in determining DF_{20} and F60 rate and terminal values.

British Pendulum value, texture after Micro-Deval by AIMS, and change in texture before and after Micro-Deval were proved to be significant factors in explaining the rate and terminal values of DF_{20} and F60. Furthermore, the rate of DF_{20} and F60 decreased as the stone BP value and texture after Micro-Deval increased. In addition, the terminal value of DF_{20} and F60 increased as the BP value and texture after Micro-Deval increased. The rate of change in texture before and after Micro-Deval affected the rate and terminal values of DF_{20} and F60. The results show the rate of change in DF_{20} and F60 decreases and the terminal value increases as she rate of change in texture before and after Micro-Deval decreases. The coarse aggregate acid insolubility test showed a significant effect on rate and terminal values of DF_{20} and F60 only when Brownlee aggregate was removed from the comparison. In such a case, the terminal DF_{20} and F60 increased as the acid insolubility test value increased. Change in angularity before and after Micro-Deval affects the terminal DF_{20} and F60 values. When the angularity change before and after Micro-Deval increased, the terminal F60 and DF_{20} values increased.

SUMMARY

In summary, the results of the research indicated that it is possible to control and predict frictional properties of the pavement by selecting the aggregate type and HMA mix type. A new laboratory testing methodology to evaluate the key parameters in frictional characteristics of a flexible pavement was developed. These two key parameters were defined to be the rate of decrease in friction and terminal value for friction. These two values could be used as a basis for further comparisons between frictional performances of different aggregate types.

During this study, a complete set of experiments was performed to evaluate the aggregate properties by all current testing methods. The results of this research confirmed the findings of the previous research about the superior performance of the Brownlee aggregate. The results also showed the polishing susceptibility of Beckman and Brownwood aggregates.

The influence of the aggregate type on asphalt concrete skid properties was investigated through preparing and testing laboratory slabs. The results of the analysis confirmed the strong relationship between mix frictional properties and aggregate

properties. The main aggregate properties affecting the mix skid resistance were recognized to be British Pendulum value, texture change before and after Micro-Deval measured by AIMS, terminal texture after Micro-Deval measured by AIMS, and coarse aggregate acid insolubility value. Based on the findings, a model that is able to predict initial F60, terminal F60, and rate of polishing was developed using the parameters in the texture model developed by Mahmoud (2005). This model confirmed the benefits of texture measurements by AIMS. This model will help to predict mix friction based on gradation and aggregate resistance to polishing. This model also facilitates selecting the appropriate aggregate type for the desired mixture friction. This model could also be used to classify aggregates based on their frictional properties.

REFERENCES

Abdul-Malak, M.A.U., Meyer, A.H., and Fowler, D.W. 1990. Research Program for Predicting the Frictional Characteristics of Seal-Coat Pavement Surface. *Transportation Research Record 1217*, Transportation Research Board, TRB, National Research Council, Washington, D.C.

Abe, H., Henry, J.J., Tamai, A., and Wambold, J. 2000. Measurement of Pavement Macrotexture Using the CTMeter. *Transportation Research Record 1764,* Transportation Research Board, TRB, National Research Council, Washington, D.C.

Agrawal S.K. and Henry, J.J. 1979. Technique for Evaluating Hydroplaning Potential of Pavements. *Transportation Research Record 633*, Transportation Research Board, TRB, National Research Council, Washington, D.C.

Ahammed A.M. and Tighe S.L. 2007. Evaluation of Concrete Pavement's Surface Friction Using LTPP Data: Preliminary Analysis and Texture Performance Models. *Proceedings of the 86th Transportation Research Board Annual Meeting* (CD), Washington, D.C., January.

Al-Rousan, T.M. 2004. Characterization of Aggregate Shape Properties Using a Computer Automated System. *Ph.D. Dissertation*, College Station, TX.

Alvarado, C., Mahmoud, E., Abdullah, I., Masad, E., Nazarian, S., Tandon, J., and Button, J. 2006. Feasibility of Quantifying the Role of Coarse Aggregate Strength on Resistance to Load in HMA. Center for Transportation Infrastructure Systems, University of Texas at El Paso, *Research Report 0-5268-2*, October.

Anderson, D.A., Meyer, W.E., and Rosenberger, J.L. 1986. Development of a Procedure for Correcting Skid-Resistance Measurements to a Standard End-of-Season Value. *Transportation Research Record, No. 1084*. Transportation Research Board, TRB, National Research Council, Washington, D.C.

ASTM. 2007. Annual *Book of ASTM Standards*, Vol. 04.03, American Society for Testing and Materials, West Conshohocken, PA.

Balmer, G.G. and Colley, B.E. 1966. Laboratory Studies of the Skid Resistance of Concrete. American Society for Testing and Materials, *Journal of Materials, Vol. 1-No. 3.*

Balmer, G.G. 1978. Pavement Texture: Its Significance and Development. *Transportation Research Record 666*. Transportation Research Board, TRB, National Research Council, Washington, D.C.

Bituminous Rated Sources Quality Catalogue (BRSQC). 2008. Texas Department of Transportation, ftp://ftp.dot.state.tx.us/pub/txdot-info/cmd/mpl/brsqc.pdf. Access date: 6/29/08.

Bloem, D.L. 1971. Skid-Resistance: The Role of Aggregates and Other Factors. *National Sand and Gravel Association Circular 109*, Silver Spring, MD.

Bond, R., Katekhda, I.E.D., Lees, G., and Williams, A.R. 1976. Tire/Road Surface Interaction. *Journal of the Institution of Highway Engineers*, November.

Bray, J. 2002. The Role of Crash Surveillance and Program Evaluation: NYSDOT's Skid Accident Reduction Program (SKARP). *Presented at 28th International Forum on Traffic Records and Highway Information System*, Orlando, FL.

Britishpendulum. 2008. http://www.Britishpendulum.co.uk/. Access date: 2/23/08.

Burnett, W.C., Gibson, J.L., and Kearney, E.J. 1968. Skid Resistance of Bituminous Surfaces. *Highway Research Record, No. 236*, Highway Research Board, National Research Council, Washington, D.C.

Cairney, P. 1997. Skid Resistance and Crashes – A Review of the Literature. *Research Report No. 311*, ARRB Transport Research Ltd., Vermont South Victoria, Australia.

Cenek, P.D., Davies, R.B., McLarin, M.W., and Griffith-Jones, N.J. 1997. Road Environment and Traffic Crashes. *Transfund Research Report No. 79*, Transfund New Zealand, Wellington, New Zealand.

Chelliah, T., Stephanos P., Shah, M.G., and Smith, T. 2003. Developing a Design Policy to Improve Pavement Surface Characteristics. *Presented in Transportation Research Board 82nd Annual Meeting*, Washington, D.C.

Choubane, B., Holzschuher, C.R., and Gokhale, S. 2004. Precision of Locked-Wheel Testers for Measurement of Roadway Surface Friction Characteristics. *Transportation Research Record 1869,* Transportation Research Board, TRB, National Research Council, Washington, D.C.

Colony, D.C. 1986. Overview of Skid Resistance on Ohio Pavements. *Journal of Transportation Engineering,* American Society of Civil Engineers, ASCE, September.

Cooley, L., Jr. and James, R. 2003. Micro-Deval Testing of Aggregates in the Southeast. *Transportation Research Record 1837*, Transportation Research Board, TRB, National Research Council, Washington, D.C.

Crouch, L.K., Shirley, G., Head, G., and Goodwin, W.A. 1996. Aggregate Polishing Resistance Pre-Evaluation. *Transportation Research Record 1530*, Transportation Research Board, TRB, National Research Council, Washington, D.C.

Csathy, T.I., Burnett, W.C., and Armstrong, M.D. 1968. State-of-the-Art of Skid Resistance Research. *Highway Research Board Special Report 95*, Highway Research Board, National Research Council, Washington, D.C.

Dahir, S.H., Meyer, W.E., and Hegmon, R.R. 1976. Laboratory and Field Investigation of Bituminous Pavement and Aggregate Polishing. *Transportation Research Record 584,* Transportation Research Board, TRB, National Research Council, Washington, D.C.

Dahir, S. 1979. A Review of Aggregate Selection Criteria for Improved Wear Resistance and Skid Resistance of Bituminous Surfaces. *Journal of Testing and Evaluation, Vol. 7*.

Dames, J. 1990. The Influence of Polishing Resistance of Sand on Skid Resistance of Asphalt Concrete. *Surface Characteristics of Roadways: International Research and Technologies*, ASTM STP 1031, W.E. Meyer, and J. Reichert, Eds., American Society for Testing and Materials, Philadelphia, PA.

Davis, R.M., Flintsch, G.W., Al-Qadi, I.L.K., and McGhee, K. 2002. Effect of Wearing Surface Characteristics on Measured Pavement Skid Resistance and Texture. *Presented at 81st Transportation Research Board Annual Meeting,* Washington, D.C.

Dewey, G.R., Robords, A.C., Armour, B.T., and Muethel, R. 2001. Aggregate Wear and Pavement Friction. *Presented at 80th Transportation Research Board Annual Meeting,* Washington, D.C.

Do, M.T. Zahouani, H., and Vargiolu, R. 2000. Angular Parameter for Characterizing Road Surface Microtexture. *Transportation Research Record 1723*, Transportation Research Board, TRB, National Research Council, Washington, D.C.

Do, M.T. and Marsac, P. 2002. Assessment of the Polishing of the Aggregate Microtexture by Means of Geometric Parameters. *Presented at 81st Transportation Research Board Annual Meeting*, Washington, D.C.

Emery, J.J. 1982. Slag Utilization in Pavement Construction. *Extending Aggregate Resources*. ASTM Special Technical Publication 774, American Society for Testing and Materials (ASTM).

Ergun, M., Iyinam, S., and Iyinam, A.F. 2005. Prediction of Road Surface Friction Coefficient Using Only Macrotexture and Microtexture Measurements. *Journal of Transportation Engineering, Vol. 131, No. 4.*

FHWA. 1980. Skid Accident Reduction Program. *Technical Advisory T5040.17*, Federal Highway Administration, U.S. Department of Transportation.

FHWA. 1990. Nationwide Personal Transportation Survey. NPTS Databook, *FHWA-Report FHWA-PL-94-010*, Federal Highway Administration, U.S. Department of Transportation.

Flintsch, G.W., Luo, Y., and Al-Qadi, I.L. 2005. Analysis of the Effect of Pavement Temperature on the Frictional Properties of Flexible Pavement Surfaces. *Presented at 84th Transportation Research Board Annual Meeting*, Washington, D.C.

Forde, M.C., Birse, R.M., and Fraser, D.M. 1976. An Assessment of British Pendulum Based Methods of Skid Resistance Evaluation Using Schonfield's Photo-Interpretation Method. *Proceedings of 8th ARRB Conference, 8(4), Session 17*.

Forster, S.W. 1981. Aggregate Microtexture: Profile Measurement and Related Frictional Levels. *Report FHWA/RD-81/107*, Federal Highway Administration, U.S. Department of Transportation.

Forster, S.W. 1989. Pavement Microtexture and its Relation to Skid Resistance. *Transportation Research Record 1215*, Transportation Research Board, TRB, National Research Council, Washington D.C.

Fulop, I.A., Bogardi, I., Gulyas, A., and Csicsely-Tarpay, M. 2000. Use of Friction and Texture in Pavement Performance Modeling. *ASCE Journal of Transportation Engineering*, Vol. 126, No. 3.

Fwa, T.F., Choo, Y.S., and Liu, Y.R. 2003. Effect of Aggregate Spacing on Skid Resistance of Asphalt Pavement. *Journal of Transportation Engineering, Vol. 129, No. 4,* American Society of Civil Engineering, ASCE.

Gallaway, B.M., Rose, J.G., and Schiller, R. E. 1972. The Relative Effect of Several Factors Affecting Rainwater Depths on Pavement Surface. *Transportation Research Record 396,* Transportation Research Board, TRB, National Research Council, Washington, D.C.

Gandhi, P.M., Colucci, B., and Gandhi, S.P. 1991. Polishing of Aggregates and Wet Weather Accident Rate for Flexible Pavements. *Transportation Research Record 1300*, Transportation Research Board, TRB, National Research Council, Washington, D.C.

Gardiner, S., Studdard, J., and Wagner, C. 2004. Evaluation of Hot Mix Asphalt Macrotexture and Microtexture. *Journal of Testing and Evaluation, January 2004, Vol. 32, No.1*.

Giles, C.G., Sabey, B.E. and Cardew, K.H.F. 1962. Development and Performance of the Portable Skid Resistance Tester. *ASTM Special Technical Publication No.326*, American Society of Testing and Materials (ASTM), Philadelphia, PA.

Giles, C.G., Sabey, B.E., and Cardew, K.H.F. 1964. Development and Performance of the Portable Skid Resistance Tester. *Road Research Technical Paper 66*, Road Research Laboratory, Department of Scientific and Industrial Research, HMSO, London, United Kingdom.

Goodman, S.N., Hassan, Y., and Abd El Halim, A.O. 2006. Preliminary Estimation of Asphalt Pavement Frictional Properties from Superpave Gyratory Specimen and Mix Parameters. *Transportation Research Record* 1949, Transportation Research Board, TRB, National Research Council, Washington, D.C.

Gothie, M. 1996. Relationship between Surface Characteristics and Accidents. *Proceedings of 3rd International Symposium on Pavement Surface Characteristics*, Christchurch, New Zealand.

Gray, J.E. and Renninger, F.A. 1965. The Skid Resistant Properties of Carbonate Aggregates. *Highway Research Record 120*, Highway Research Board, National Research Council, Washington, D.C.

Hall, J.W., Glover, L.T., Smith, K.L., Evans, L.D., Wambold, J.C., Yager, T.J., and Rado, Z. 2006. Guide for Pavement Friction. *Project No. 1-43*, Final Guide, National Cooperative Highway Research Program, Transportation Research Board, National Research Council, Washington, D.C.

Hanson, D.I. and Prowell, B.D. 2004. Evaluation of Circular Texture Meter for Measuring Surface Texture of Pavements. *NCAT Report 04-05*, National Center for Asphalt Technology, Auburn, AL.

Harald, A. 1990. Skid Resistance and Road Surface Texture. *Symposium: Surface Characteristics of Roadways*, American Society of Testing and Materials (ASTM), Philadelphia, PA.

Henry, J.J. and Hegmon, R.R. 1975. Pavement Texture Measurement and Evaluation. *ASTM Special Technical Publication 583*, American Society for Testing and Materials, Philadelphia, PA.

Henry, J.J. and Liu, M.C. 1978. Prediction of Skid Resistance as a Function of Speed from Pavement Texture. *Transportation Research Record 666*, Transportation Research Board, TRB, National Research Council, Washington, D.C.

Henry, J.J. and Dahir, S. 1979. Effects of Textures and the Aggregates that Produce them on the Performance of Bituminous Surfaces. *Transportation Research Record 712*, Transportation Research Board, National Research Council, Washington, D.C.

Henry J.J. 1996. Overview of the International PIARC Experiment to Compare and Harmonize Texture and Skid Resistance Measurements: The International Friction Index. *Proceedings of the 3rd International Symposium on Pavement Surface Characteristics,* Christchurch, New Zealand, September.

Henry, J.J. 2000. Evaluation of Pavement Friction Characteristics. *NCHRP Synthesis: Topic 30-11*, National Cooperative Highway Research Program, Washington, D.C.

Henry, J.J., Abe, H., Kameyama, S., Tamai, A., Kasahara, A., and Saito, K. 2000. Determination of the International Friction Index Using the Circular Track Meter and

the Dynamic Friction Tester. *Proceedings of SURF 2000*, the World Road Association. Paris, France.

Her, I., Henry, J.J., and Wambold, J.C. 1984. Development of a Data Acquisition Method for Non-contact Pavement Macrotexture Measurement. *Transportation Research Record 1000*, Transportation Research Board, TRB, National Research Council, Washington, D.C.

Hill, B.J. and Henry, J.J. 1981. Short-Term Weather Related Skid Resistance Variations. *Transportation Research Record 836*, Transportation Research Board, TRB, National Research Council, Washington, D.C.

Hogervorst, D. 1974. Some Properties of Crushed Stone for Road Surfaces. *Bulletin of the International Association of Engineering Geology*, *Vol. 10, No.1,* Springer.

Horne, W.B. 1977. Status of Runway Slipperiness Research. *Transportation Research Record 624*, Transportation Research Board, TRB, National Research Council, Washington, D.C.

Horne, W.B. and Buhlmann, F. 1983. A Method for Rating the Skid Resistance and Micro/Macrotexture Characteristics of Wet Pavements. *Frictional Interaction of Tire and Pavement,* ASTM Special Technical Publication 793, American Society of Testing and Materials (ASTM), Philadelphia, PA.

Hugo, F. 2005. *MMLS3* An APT Tool for Pavement Performance Prediction and Material Evaluation. *APT Meeting*, Accelerated Pavement Testing, http://www.gautrans-hvs.co.za/popup/APT%20Steering%20Committee%20Documents/15May07/fred_Hugo.pdf. Access date: 9/5/2008.

Ivey, D.L., Griffin, L.I., Lock, J.R., and Bullard, D.L. 1992. Texas Skid Initiated Accident Reduction Program. Texas Transportation Institute, *Research Report 910-1F*, College Station, TX.

Jayawickrama, P.W., Prasanna, R., and Senadheera, S.P. 1996. Survey of State Practices to Control Skid Resistance on Hot-Mix Asphalt Concrete Pavements. *Transportation Research Record 1536*, Transportation Research Board, TRB, National Research Council, Washington, D.C.

Jayawickrama P.W. and Thomas, B. 1998. Correction of Field Skid Measurements for Seasonal Variations in Texas. *Transportation Research Record 1639*, Transportation Research Board, TRB, National Research Council, Washington, D.C.

Jayawickrama, P.W., Hossain, S., and Phillips, F. 2006. Evaluation of Aggregate Durability Using Micro-Deval Test. *Presented in Transportation Research Board 85th Annual Meeting*, Washington, D.C.

Johnsen, W.A. 1997. Advances in the Design of Pavement Surfaces. *Ph.D. Dissertation*, Worcester Polytechnic Institute.

Kamel, N. and Gartshore, T. 1982. Ontario's Wet Pavement Accident Reduction Program. *ASTM Special Technical Publication 763*, American Society of Testing and Materials (ASTM), Philadelphia, PA.

Kamel, N., and G. R. Musgrove. 1981. Design and Performance of Bituminous Mixes in Ontario. *RTAC Forum, Vol. 5, Issue 3*.

Kennedy, C.K., Young, A.E., and Buttler, I.C. 1990. Measurement of Skidding Resistance and Surface Texture and the Use of Results in the United Kingdom. *Symposium: Surface Characteristics of Roadways*. American Society of Testing and Materials (ASTM), Philadelphia, PA.

Knill, D.C. 1960. Petrographical Aspects of the Polishing of Natural Roadstone. *Journal of Applied Chemistry, Vol. 10*: pp 28-35.

Kokkalis, A.G. and Panagouli, O.K. 1999. Fractal Evaluation of Pavement Skid Resistance Variations Surface Wear. *Chaos, Solutions and Fractals, Vol. 9, No. 11*.

Kokkalis, A.G., Tsohos, G.H., and Panagouli, O.K. 2002. Consideration of Fractals in Pavement Skid Resistance Evaluation. *Journal of Transportation Engineering, Vol. 128, No. 6*, American Society of Civil Engineering: pp 591-595.

Kokot, D. 2005. Evaluating Skidding Resistance in Slovenia. Slovenian National Building and Civil Engineering Institute, www.ectri.org/liens/yrs05/Session%205bis/Kokot.pdf. Access date: 11/27/2006.

Kowalski, K.J. 2007. Influence of Mixture Composition on the Noise and Frictional Characteristics of Flexible Pavements. *Ph.D. Dissertation*, Purdue University, West Lafayette, IN.

Kuemmel, D.A., Sontag, R.C., Crovetti, J., Becker, A.Y., Jaeckel, J.R. and Satanovsky, A. 2000. Noise and Texture on PCC Pavements. Final report multi state study. *Report Number WI/SPR-08-99*, Wisconsin Department of Transportation, Kinsman Blvd., Madison, WI.

Kulakowski, B.T. and Meyer, W.E. 1990. Skid Resistance of Adjacent Tangent and Nontangent Sections of the Roads. *Transportation Research Record 1215*, Transportation Research Board, TRB, National Research Council, Washington, D.C.

Kulakowski, B.T., Henry, J.J., and Lin, C., 1990. A Closed Loop Calibration Procedure for a British Pendulum Tester. Surface Characteristics of Roadways: International Research and Technologies, *ASTM Special Technical Publication 1031*, W.E. Mayer, and J. Reichert, Eds., American Society for Testing and Materials.

Kummer, H.W. and Meyer, W.E. 1963. Penn State Road Surface Friction Tester as Adapted to Routine Measurement of Pavement Skid Resistance. *Road Surface Properties, 42nd Annual Meeting*, January.

Kummer, H.W. 1966. *Unified Theory of Rubber and Tire Friction*. PA State University College of Engineering, University Park, PA.

Larson, R.M. 1999. Consideration of Tire/Pavement Friction/Texture Effects on Pavement Structural Design and Material Mix Design. Federal Highway Administration (FHWA), Office of Pavement Technology, Washington, D.C.

Lay, C. and Judith, B. 1998. Friction and Surface Texture Characterization of 14 Pavement Test Sections in Greenville, North Carolina. *Transportation Research Record 1639*, Transportation Research Board, TRB, National Research Council, Washington, D.C.

Lee, S.W., Cho, Y.H., Lee, H.J., Kim, N.C., and Chun, S.J. 2005. Rate of Skid Resistance Loss for Tinned Concrete Pavements. *Presented in Transportation Research Board 84th Annual Meeting*, Washington, D.C.

Lee, Y.P.K., Fwa, T.F., and Choo, Y.S. 2005. Effect of Pavement Surface Texture on British Pendulum Test. *Journal of the Eastern Asia Society for Transportation Studies, Vol. 6.*

Leland, T.J.W., Yager, T.J., and Joyner, U.T. 1968. Effects of Pavement Texture on Wet-Runway Braking Performance. *NASA Technical Note TN D-432*, National Aeronautics and Space Administration.

Leu, M.C. and Henry, J.J. 1978. Prediction of Skid Resistance as a Function of Speed from Pavement Texture. *Transportation Research Record 666*, Transportation Research Board, TRB, National Research Council, Washington D.C.

Li, S., Zhu, K., Noureldin, S., and Harris, D. 2005. Identifying Friction Variations with the Standard Smooth Tire for Network Pavement Inventory Friction Testing. *Presented in Transportation Research Board 84th Annual Meeting*, Washington D.C.

Liang, R.Y. and Chyi L.L. 2000. Polishing and Friction Characteristics of Aggregates Produced in Ohio. *FHWA Report FHWA/OH-2000/001*, Federal Highway Administration, Columbus, OH.

Linder, M., Kröger, M., Popp, K., and Blume, H. 2004. Experimental and Analytical Investigation of Rubber Friction. *XXI International Congress of Theoretical and Applied Mechanics*, Warsaw, Poland.

Liu, Y., Fwa, T.F., and Choo, Y.S. 2003. Finite Element Modeling of Skid Resistance Test. *Journal of Transportation Engineering, Vol. 129, No. 3,* American Society of Civil Engineering, ASCE.

Liu, Y., Fwa, T.F., and Choo, Y.S. 2004. Effect of Surface Macrotexture on Skid Resistance Measurements by the British Pendulum Test. *Journal of Testing and Evaluation, Vol. 32, No. 4,* American Society of Civil Engineering, ASCE.

Luce, A.D. 2006. Analysis of Aggregate Imaging System (AIMS) Measurements and Their Relationship to Asphalt Pavement Skid Resistance. *M.S.C.E Thesis*, Texas A&M University, College Station, TX.

Mahmoud, E.M. 2005. Development of Experimental Method for the Evaluation of Aggregate Resistance to Polish, Abrasion, and Breakage. *M.S.C.E Thesis*, Texas A&M University, College Station, TX.

Masad, E., Al-Rousan, T., Button, J., Little, D., and Tutumluer, E. 2005. Test Methods for Characterizing Aggregate Shape, Texture, and Angularity. *NCHRP Project 4-30A Final Report*, National Cooperative Highway Research Program, Washington, D.C.

Masad, E., Luce, A., and Mahmoud, E. 2006. Implementation of AIMS in Measuring Aggregate Resistance to Polishing Abrasion and Breakage. Texas Transportation Institute, *Research Report 5-1707-03-1*, Texas A&M University, College Station, TX.

McCullough, B.V. and Hankins, K.D. 1966. Skid Resistance Guidelines for Surface Improvements on Texas Highways. *Transportation Research Record 131*, Transportation Research Board, TRB, National Research Council, Washington, D.C.

McDaniel, R.S. and Coree B.J. 2003. Identification of Laboratory Techniques to Optimize Superpave HMA Surface Friction Characterization. *Phase I: Final Report SQDH 2003–6,* North Central Superpave Center, Purdue University, West Lafayette, IN.

McLean, J. 1995. The Relationship between Pavement Condition and Road Safety. *Paper Presented at the Load-Pavement Interaction Workshop,* Newcastle, United Kingdom.

Meininger, R. 2004. Micro-Deval vs. LA Abrasion. http://Rockproducts.com/mag/rock_microdeval_abrasion/. Access date: 22/2/2008.

Miller, M.M. and Johnson, H.D. 1973. Effects of Resistance to Skidding on Accidents: Surface Dressing on an Elevated Section of the M4 Motorway, *Report No. LR 542*, Transport and Road Research Laboratory, Berkshire, United Kingdom.

Mills, J.A. 1969. Control of Pavement Slipperiness: A Skid Resistance Study in Four Western States. *Highway Research Board Special Report 101*, Highway Research Board, National Research Council, Washington, D.C.

Moore, D.F. 1969. Recommendations for an International Minimum Skid-Resistance Standard for Pavements. *Highway Research Board Special Report 101*, Highway Research Board, National Research Council, Washington, D.C.

Moore, D.F. 1966. Prediction of Skid Resistance Gradient and Drainage Characteristics for Pavements. *Highway Research Record 131*, Highway Research Board, National Research Council, Washington, D.C.

Moore, D.F. 1972. *The Friction and Lubrication of Elastomers*. Pergamon Press LTD., Oxford, Great Britain.

Moore, D.F. 1975. *The Friction of Pneumatic Tires*. Elsevier Scientific Publishing Company, Amsterdam, Netherland.

Mullen, W.G., Dahir, S.H.M., and El Madani, N.F. 1974. Laboratory Evaluation of Aggregates, Aggregate Blends, and Bituminous Mixes for Polish Resistance. *Transportation Research Record 523*, Transportation Research Board, TRB, National Research Council, Washington, D.C.

NAPA. 1996. Hot Mix Asphalt Materials, Mixture Design, and Construction. National Asphalt Pavement Association, NAPA Education Foundation, Lanham, MD.

Nichols, F.P., Jr., Dillard, J.H., and Orwood, R.L. 1957. Skid Resistant Pavement in Virginia. Virginia Council of Highway Investigation and Research. *Reprint No. 18*.

Nippou. 2008. http://www.nippou.com/en/products/dft.html. Access date: 02/23/08.

Noyce D.A., Bahia, H.U., Yambó, J.M., and Kim, G. 2005. Incorporating Road Safety into Pavement Management: Maximizing Asphalt Pavement Surface Friction for Road Safety Improvements. Midwest Regional University Transportation Center Traffic Operations and Safety (TOPS) Laboratory.

Ong, G.P., Fwa, T.F., and Guo, J. 2005. Modeling Hydroplaning and Effects of Pavement Microtexture. *Presented at Transportation Research Board 84th Annual Meeting*, Washington, D.C.

Organization for Economic Cooperation and Development (OECD). 1984. Road Surface Characteristics – Their Interaction and Their Optimization. OECD Scientific Expert Group, Road Transport Research, Paris, France.

Pelloli, R. 1972. Road Surface Characteristics and Hydroplaning. *Transportation Research Record 624*, Transportation Research Board, TRB, National Research Council, Washington, D.C.

Perry, M., Woodside, R., and Woodward, W. 2001. Observations on Aspects of Skid Resistance of Greywacke Aggregate. *Quarterly Journal of Engineering Geology and Hydrology 24.*

Person, B.N.J. 1998. *Sliding Friction: Physical Principles and Applications*. Springer, Berlin, Germany.

PIARC Technical Committee on Surface Characteristics (C1) 1995. International PIARC Experiment to Compare and Harmonize Texture and Skid Resistance Measurements, Paris, France.

Prasanna R., Nageswaran B., and Jayawickrama P.W. 1999. Use of Relation Database Management Systems Principles in Reliable Prediction of Pavement Skid Resistance. *Transportation Research Record 1655*, Transportation Research Board, TRB, National Research Council, Washington D.C.

Prowell, B.D., Zhang, J., and Brown, E.R. 2005. Aggregate Properties and the Performance of Superpave-Designed Hot Mix Asphalt. National Cooperative Highway Research Program, *NCHRP Report 539*, Transportation Research Board, National Research Council, Washington, D.C.

Purushothaman, N., Heaton, B.S., and Moore, I.D. 1988. Experimental Verification of a Finite Element Contact Analysis. *Journal of Testing and Evaluation, Vol. 16, No. 6.*

Report of the Committee on Surface Characteristics. 1987. World Road Association (PIARC), 18th World Road Congress, Brussels, Belgium.

Rhode, S.M. 1976. On the Effect of Pavement Microtexture and Thin Film. *Traction, International Journal of Mechanic Sciences, Vol. 18*: pp 95-101.

Rizenbergs, R.L., Burchett, J.L., and Napier, C.T. 1972. Skid Resistance of Pavements. *Report No.KYHPR-64-24, Part II*, Kentucky Department of Highways, Lexington, KY.

Roberts, A.D. 1988. Rubber Adhesion at High Rolling Speeds. *Journal of Natural Rubber Research, Vol. 3, No. 4.*

Roberts, F.L., Kandhal, P.S., Brown, E.R., Lee, D.Y., and Kennedy, T.W. 1996. *HMA Materials, Mixture Design, and Construction*. Second Edition, NAPA, Research and Education Foundation.

Roe, P.G., Webster, D.C., and West, G. 1991. The Relation between Surface Texture of Roads and Accidents. *Transport and Road Research Laboratory, Research Report 296*, TRRL, Berkshire, United Kingdom.

Roe, P.G., Parry, A.R., and Viner, H.E. 1998. High and Low Speed Skidding Resistance: The Influence of Texture Depth. *Transport and Road Research Laboratory Report 367*, TRRL, Berkshire, U.K

Rogers, C. 1991. Laboratory Tests for Predicting Coarse Aggregate Performance in Ontario. *Advances in Aggregate and Armourstone Evaluation 13*.

Rose, J.G. and Gallaway, B.M. 1970. Macrotexture Measurement and Related Skid Resistance at Speeds from 20 to 60 Miles per Hour. *Transportation Research Record 341*, Transportation Research Board, TRB, National Research Council, Washington, D.C.

Saito, K., Horiguchi, T., Kasahara, A., Abe, H., and Henry, J.J. 1996. Development of Portable Tester for Measuring Skid Resistance and Its Speed Dependency on Pavement Surfaces. *Transportation Research Record 1536*, Transportation Research Board, TRB, National Research Council, Washington D.C.

Salt, G.F. 1977. Research on Skid Resistance at the Transport and Road Research Laboratory (1927-1977). *Transportation Research Record 622*, Transportation Research Board, TRB, National Research Council, Washington, D.C.

Samuels, S.E. 1986. The Feasibility of Measuring Road Surface Microtexture by Means of Laser Techniques. *Research Report No. TF 52-03*, Road User and Vehicle Division, VTI, Linköping, Sweden.

Savkoor, A.R. 1990. Tribology of Tire Traction on Dry and Wet Roads. *Proceedings of the 17th Leeds-Lyon Symposium on Tribology*, September 4-7.

Scholle, P.A. 1978. Carbonate Rock Constituents, Texture, Cements, and Porosities. *American Association of Petroleum Geologists Memoir 27*, Tulsa, OK.

Schonfeld, R. 1974. Photo-Interpretation of Pavement Skid Resistance in Practice. *Transportation Research Record 523*, Transportation Research Board, TRB, National Research Council, Washington, D.C.

Schulze, K.H., Gerbaldi, A., and Chavet, J. 1976. Skidding Accidents, Friction Numbers, and the Legal Aspects Involved. *Transportation Research Record 623*, Transportation Research Board, TRB, National Research Council, Washington, D.C.

Shupe, J.W. and Lounsbury, R.W. 1958. Polishing Characteristics of Mineral Aggregates. *Proceedings First International Skid Prevention Conference*, University of Virginia, Charlottesville, VA.

Shupe, J.W. 1960. Pavement Slipperiness. *Section 20 of the Highway Engineering Handbook by K.B. Woods*, McGraw-Hill Book Co., Inc., New York, NY.

Skerritt, W.H. 1993. Aggregate Type and Traffic Volume as Controlling Factors in Bituminous Pavement Friction. *Transportation Research Record 1418*, Transportation Research Board, TRB, National Research Council, Washington, D.C.

Smith, H. 1976. Pavement Contributions to Wet-Weather Skidding Accident Reduction. *Transportation Research Record 622*, Transportation Research Board, TRB, National Research Council, Washington, D.C.

Smit, A. de F., Hugo, F., and Yeldirim, Y. 2004. A Discussion of MMLS3 Performance Testing of Laboratory Prepared HMA Slabs and Briquettes Compared with Hamburg and APA Wheel Tracking Tests. CD-Rom, *Proceedings Second International APT Conference*, Seattle, WA, U.S.

Stephens, J.E. and Goetz, W.H. 1960. Designing Fine Bituminous Mixtures for High Skid Resistance. *Highway Research Board Proceedings, Vol. 39*, Highway Research Board, National Research Council, Washington, D.C.

Stroup-Gardiner, M., Studdard, J., and Wagner, C. 2004. Evaluation of Hot Mix Asphalt Macrotexture and Microtexture. *Journal of Testing and* Evaluation, Vol. 32, *No.1.*

Stutzenberger, W.J. 1958. A Study of the Polishing Characteristics of Limestone and Sandstone Aggregates in Regard to Pavement Slipperiness. *Highway Research Board Bulletin 186*, Highway Research Board, National Research Council, Washington, D.C.

Subhi, M.B. and Farhad R. 2005. Changes in Asphalt Pavement Friction Components and Adjustment of Skid Number for Temperature. *Journal of Transportation Engineering, Vol. 131, No. 6.*

Taneerananon, P. and Yandell, W.O. 1981. Microtexture Roughness Effect on Predicted Road/Tire Friction in Wet Conditions. *Wear, Vol. 69.*

Tics. 2008. http://www.tics.hu/CTMeter.htm. Access date: 02/23/08.

Tourenq, C. and Fourmaintraux, D. 1971. Road Surface Roughness and the Properties of Aggregates (in French). *Bulletin de Liaison des Laboratoires des Ponts et Chaussées, No. 51.*

Traffic Safety Facts. 2006. A Compilation of Motor Vehicle Crash Data from the Fatality Analysis Reporting System and the General Estimates System. National Highway

Traffic Safety Administration (NHTSA). http://www-nrd.nhtsa.dot.gov. Access date: 10 /29/2006.

Transit New Zealand. 2002. Specification for Skid Resistance Deficiency Investigation and Treatment Selection. *TNZ T/10* Transit New Zealand, Wellington, New Zealand.

Txhotmix. 2008. http://www.txhotmix.org. Access date: 02/18/08.

UMass, 2008. Hot Mix Asphalt Property and Performance Testing Equipment. http://www.umassd.edu/engineering/cen/materials/equipment/performance_testing.cfm. Access date: 2/22/08.

Vollor, T.W. and Hanson, D.I. 2006. Development of Laboratory Procedure for Measuring Friction of HMA Mixtures-Phase 1. *NCAT Report 06-06*, National Center of Asphalt Technology, Auburn University, AL.

Walker, R.S. and Payne, L.D. Use of Selcom Laser for Pavement Texture and Skid Resistance Measurement. *Technical Memorandum, Research Project 1290*. Transportation Instrumentation Laboratory, University of Texas, Arlington, TX, undated.

Wallman, C.G. and Astron, H. 2001. Friction Measurement Methods and the Correlation between Road Friction and Traffic Safety. Swedish National Road and Transport Research Institute, *VTI Meddelande 911A*, Linköping, Sweden.

Wambold, J.C., Henry, J.J., and Hegmon, R.R. 1986. Skid Resistance of Wet-Weather Accident Sites. *ASTM Special Technical Publication 929*, American Society of Testing and Materials (ASTM), Philadelphia, PA.

Wambold, J.C., Antle, C.E., Henry J.J., and Rado, Z. 1995. PIARC (Permanent International Association of Road Congress) Report. International PIARC Experiment to Compare and Harmonize Texture and Skid Resistance Measurement, C-1 PIARC Technical Committee on Surface Characteristics, France.

Wasilewska, M. and Gardziejczyk, W. 2005. Polishing Resistance of Road Aggregates Applied in Wearing Course. *Proceedings of the 3rd International Conference of Modern Technologies in Highway Engineering*, Poznan, Poland, September 8-9.

West, T.R., Choi, J.C., Bruner, D.W., Park, H.J., and Cho, K.H. 2001. Evaluation of Dolomite and Related Aggregates Used in Bituminous Overlays for Indiana

Pavements. *Transportation Research Record 1757*, Transportation Research Board, TRB, National Research Council, Washington, D.C.

West, N.W. and Ross, T.F. 1962. Polishing of the Road Surfaces in New South Wales. *Proceedings of the Australian Road Research Board, Vol. 1.*

Whitehurst, E.A. and Goodwin, W.A. 1955. Pavement Slipperiness in Tennessee. *Proceedings Highway Research Board, Vol. 34*, Highway Research Board, National Research Council, Washington, D.C.

Whitehurst, E.A. and Goodwin, W.A. 1958. A Device for Determining Relative Potential Slipperiness of Pavement Mixtures. *Highway Research Board Bulletin 186*, Highway Research Board, National Research Council, Washington, D.C.

Williams, A.R. and Lees, G. 1970. Topographical and Petrographical Variation of Road Aggregates and the Wet Skidding Resistance of Tires. *Journal of Engineering Geology, Vol. 2.*

Wilson, D.J. and Dunn, R.C.M. 2005. Analyzing Road Pavement Skid Resistance. Institute of Transportation Engineers ITE, *Proceedings of 2005 Annual Meeting*, Australia.

Won, M.C. and Fu, C.N. 1996. Evaluation of Laboratory Procedures for Aggregate Polish Test. *Transportation Research Record 1547*, Transportation Research Board, TRB, National Research Council, Washington, D.C.

Yandell, W.O. 1971. A New Theory of Hysteretic Sliding Friction. *Wear, Vol. 17*.

Yandell, W.O., Taneerananon, P., and Zankin, V. 1983. Prediction of Tire-Road Friction from Surface Texture and Tread Rubber Properties. *Frictional Interaction of Tire and Pavement*, ASTM Special Technical Publication 793, W.E Meyer and J.D. Walter, Ed., American Society of Civil Engineering, Washington, D.C.

Yandell, W.O. and Sawyer, S. 1994. Prediction of Tire-Road Friction from Texture Measurements. *Transportation Research Record 1435*, Transportation Research Board, TRB, National Research Council, Washington, D.C.

Yeaman, J. 2005. Are We Afraid on the IFI? *Proceedings of the International Conference on Surface Friction*, Christchurch, New Zealand, May 1-4.

Zimmer, R.A., Choubane, B., and Holzschuher, C.R. 2003. Friction Testing Method for Open-Grated Steel Bridge Decks. *Transportation Research Record 1860*, Transportation Research Board, TRB, National Research Council, Washington, D.C.

APPENDIX A- MIXTURE DESIGN

Table 37. Mix Design for Brownwood Aggregate and Type C Mixture.

Agg. Source	Vulcan								Total Cumulative Pass %	TxDOT Specs.	
	Brownwood		Brownwood		Brownwood		Brownwood				
	C rock		DF		M-Sand		Field Sand				
Sieve Size	Bin #1	Total	Bin #2	Total	Bin #3	Total	Bin #4	Total			
	26.0	%	32.0	%	32.0	%	10.0	%			
1"	100.0	26.0	100.0	32.0	100.0	32.0	100.0	10.0	100.0		
7/8"	100.0	26.0	100.0	32.0	100.0	32.0	100.0	10.0	100.0	98	100
5/8"	95.0	24.7	100.0	32.0	100.0	32.0	100.0	10.0	98.7	95	100
3/8"	15.5	4.0	98.5	31.5	100.0	32.0	100.0	10.0	77.5	70	85
#4	0.8	0.2	40.0	12.8	99.0	31.7	100.0	10.0	54.7	43	63
#10	0.4	0.1	5.0	1.6	79.5	25.4	100.0	10.0	37.1	30	40
#40	0.3	0.1	0.8	0.3	23.2	7.4	96.0	9.6	17.4	10	25
#80	0.3	0.1	0.4	0.1	6.6	2.1	35.0	3.5	5.8	3	13
#200	0.1	0.0	0.3	0.1	1.8	0.6	8.8	0.9	1.6	1	6
Pan											
Optimum Asphalt Content			5.20%								
Asphalt Source & Grade:			Koch Pav Solutions 76 - 22								

Table 38. Mix Design for Beckman Aggregate and Type C Mixture.

Agg. Source	Beckmann												Total Cumulative Pass %	TxDOT Specs.	
	3/4"-5/8"		5/8"-1/2"		3/8"-1/4"		Grade 10		Mfg Sand		W. Poteet Sand				
	Bin #1	Total	Bin #2	Total	Bin #3	Total	Bin #4	Total	Bin #5	Total	Bin #6	Total			
Sieve Size	20.0	%	19.0	%	13.0	%	10.0	%	28.0	%	10.0	%	100.0%		
1"	100.0	20.0	100.0	19.0	100.0	13.0	100.0	10.0	100.0	28.0	100.0	10.0	100.0	100	100
3/4"	94.6	18.9	100.0	19.0	100.0	13.0	100.0	10.0	100.0	28.0	100.0	10.0	98.9	95	100
3/8"	3.8	0.8	58.1	11.0	100.0	13.0	100.0	10.0	100.0	28.0	100.0	10.0	72.8	70	85
No. 4	1.1	0.2	3.6	0.7	26.0	3.4	84.0	8.4	99.9	28.0	100.0	10.0	50.7	43	63
No. 8	1.1	0.2	2.8	0.5	14.7	1.9	2.0	0.2	85.6	24.0	99.8	10.0	36.8	32	44
No. 30	1.0	0.2	1.7	0.3	2.8	0.4	2.0	0.2	32.9	9.2	88.0	8.8	19.1	14	28
No. 50	1.0	0.2	1.5	0.3	2.0	0.3	1.7	0.2	18.6	5.2	52.2	5.2	11.3	7	21
No. 200	0.7	0.1	1.3	0.2	1.6	0.2	1.5	0.2	8.6	2.4	1.6	0.2	3.3	1	6
Pan		0.0		0.0		0.0		0.0		0.0		0.0	0.0		
Optimum Asphalt Content			4.5%												
Asphalt Source & Grade:			Valero PG 76-22												

Table 39. Mix Design for 50 Percent Brownlee + 50 Percent Beckman Aggregate and Type C Mixture.

Agg. Source	Delta Materials				Beckmann								Total Cumulative Pass %	TxDOT Specs.	
	Type C		Type D		3/4"-5/8"		3/8"-1/4"		Mfg Sand		Washed Poteet Sand				
Sieve Size	Bin #1	Total	Bin #2	Total	Bin #3	Total	Bin #4	Total	Bin #5	Total	Bin #6	Total			
	9.0	%	19.0	%	8.0	%	22.0	%	27.0	%	15.0	%	100.0%		
7/8"	100.0	9.0	100.0	19.0	100.0	8.0	100.0	22.0	100.0	27.0	100.0	15.0	100.0	98	100
5/8"	96.6	8.7	100.0	19.0	89.2	7.1	100.0	22.0	100.0	27.0	100.0	15.0	98.8	95	100
3/8"	3.8	0.3	70.9	13.5	3.8	0.3	100.0	22.0	100.0	27.0	100.0	15.0	78.1	70	85
No. 4	1.5	0.1	16.3	3.1	1.1	0.1	26.0	5.7	99.9	27.0	100.0	15.0	51.0	43	63
No. 10	1.0	0.1	4.0	0.8	1.0	0.1	3.4	0.7	70.9	19.1	99.6	14.9	35.7	30	40
No. 40	0.7	0.1	2.3	0.4	1.0	0.1	2.1	0.5	25.0	6.8	69.2	10.4	18.3	10	25
No. 80	0.6	0.1	1.8	0.3	0.9	0.1	1.9	0.4	13.1	3.5	14.4	2.2	6.6	3	13
No. 200	0.4	0.0	1.1	0.2	0.7	0.1	1.6	0.4	8.6	2.3	1.6	0.2	3.2	1	6
Pan		0.0		0.0		0.0		0.0		0.0		0.0	0.0		
Optimum Asphalt Content			4.7%												
Asphalt Source & Grade:			Valero PG 76-22												

Table 40. Mix Design for Brownlee Aggregate and Type C Mixture.

Agg. Source	Delta Materials				Capitol-GT		RTI-N				TXI		Total Cumulative Pass %	TxDOT Specs.	
	Delta C		D-Rock		F-Rock		Dry Screenings		Washed Screening		Field Sand				
Sieve Size	Bin #1	Total	Bin #2	Total	Bin #3	Total	Bin #4	Total	Bin #5	Total	Bin #6	Total			
	24.0	%	27.0	%	5.0	%	9.0	%	23.0	%	12.0	%	100.0%		
7/8"	100.0	24.0	100.0	27.0	100.0	5.0	100.0	9.0	100.0	23.0	100.0	12.0	100.0	98	100
5/8"	95.6	22.9	100.0	27.0	100.0	5.0	100.0	9.0	100.0	23.0	100.0	12.0	98.9	95	100
3/8"	3.8	0.9	88.4	23.9	100.0	5.0	100.0	9.0	100.0	23.0	100.0	12.0	73.8	70	85
#4	3.7	0.9	37.6	10.2	73.2	3.7	99.8	9.0	98.7	22.7	100.0	12.0	58.4	43	63
#10	3.6	0.9	4.4	1.2	10.2	0.5	80.7	7.3	46.6	10.7	100.0	12.0	32.5	30	40
#40	3.5	0.8	0.7	0.2	2.2	0.1	49.6	4.5	17.4	4.0	87.2	10.5	20.1	10	25
#80	3.4	0.8	0.6	0.2	1.7	0.1	36.4	3.3	11.0	2.5	28.7	3.4	10.3	3	13
#200	3.3	0.8	0.4	0.1	1.1	0.1	27.6	2.5	4.7	1.1	6.0	0.7	5.2	1	6
Pan		0.0		0.0		0.0		0.0		0.0		0.0	0.0		
Optimum Asphalt Content			4.50%												
Asphalt Source & Grade:			Fina or Valero PG 76-22												

Table 41. Mix Design for Fordyce Aggregate and Type C Mixture.

Agg. Source	Fordyce C		Fordyce D/F		Fordyce Man Sand		Cl Mt Limestone Screening		Austin White		Total Cumulative Pass %	TxDOT Specs.	
	1323505		1323505		1323505		1504605		Lime				
Sieve Size	Bin #1	Total	Bin #2	Total	Bin #3	Total	Bin #4	Total	Bin #5	Total			
	18.0	%	57.0	%	10.0	%	14.0	%	1.0	%			
1"	100.0	18.0	100.0	57.0	100.0	10.0	100.0	14.0	100.0	1.0	100.0		
3/4"	100.0	18.0	100.0	57.0	100.0	10.0	100.0	14.0	100.0	1.0	100.0	98	100
1/2"	70.0	12.6	100.0	57.0	100.0	10.0	100.0	14.0	100.0	1.0	94.6	90	100
3/8"	10.0	1.8	95.0	54.2	100.0	10.0	100.0	14.0	100.0	1.0	81.0	70	95
No. 4	5.0	0.9	50.0	28.5	100.0	10.0	100.0	14.0	100.0	1.0	54.4	43	63
No. 8	3.0	0.5	15.0	8.6	99.0	9.9	92.0	12.9	100.0	1.0	32.9	32	44
No. 30	2.0	0.4	4.0	2.3	49.0	4.9	54.0	7.6	100.0	1.0	16.2	14	28
No. 50	1.5	0.3	3.0	1.7	23.0	2.3	41.0	5.7	100.0	1.0	11.0	7	21
No. 200	0.5	0.1	1.0	0.6	3.0	0.3	25.0	3.5	100.0	1.0	5.5	1	6
Pan													
Optimum Asphalt Content			4.50%										
Asphalt Source &Grade:			Eagle PG 76-22										

Table 42. Mix Design for El Paso Aggregate Type C and PFC Mixtures.

Property		Mixture Type	
		Superpave-C	PFC
Binder Grade		PG 76-22	
Binder Content,%		4.8	6.6
Sieve Size, inch	(Sieve No.)		
1	1"	100	100
0.75	3/4"	99	100
0.492	1/2"	95	90
0.375	3/8"	92.5	47.5
0.187	No. 4	77.5	10.5
0.0929	No. 8	43	5.5
0.0469	No. 16	30	5
0.0234	No. 30	-	4.5
0.0117	No. 50	-	3.5
0.0029	No. 200	6	2.5

Table 43. Mix Design for Brownlee Aggregate and PFC Mixture.

Agg. Source	Delta				Capitol		Austin White		Total Cumulative Pass %	TxDOT	
	C-Rock		GR. 4		F-Rock		Lime				
Sieve	Bin #1	Total	Bin #2	Total	Bin #3	Total	Bin #4	Total			
Size	21.0	%	68.0	%	10.0	%	1.0	%	100%		
3/4"	100.0	21.0	100.0	68.0	100.0	10.0	100.0	1.0	100.0		100
1/2"	58.2	12.2	98.7	67.1	100.0	10.0	100.0	1.0	90.3	90	100
3/8"	19.1	4.0	65.4	44.5	100.0	10.0	100.0	1.0	59.5	35	60
4	2.0	0.4	2.2	1.5	84.5	8.5	100.0	1.0	11.4	10	25
8	1.5	0.3	1.8	1.2	29.1	2.9	100.0	1.0	5.4	5	10
200	0.5	0.1	1.3	0.9	2.3	0.2	100.0	1.0	2.2	1	4
Pan											
Optimum Asphalt content			6.0%								
Asphalt Source & Grade:			Marlin PG 76-22S								

Table 44. Mix Design for Beckman Aggregate and PFC Mixture.

Agg. Source	Beckmann				Austin White		Hi-tech Fibers		Total Cumulative Pass %	TxDOT Specs.	
	C ROCK		D ROCK		LIME						
Sieve	Bin #1	Total	Bin #2	Total	Bin #3	Total	Bin #4	Total			
Size	32.7	%	66.0	%	1.0	%	0.3	%	100.0%		
3/4"	100.0	32.7	100.0	66.0	100.0	1.0	100.0	0.3	100.0	100	100
1/2"	54.1	17.7	99.3	65.5	100.0	1.0	100.0	0.3	84.5	80	100
3/8"	4.0	1.3	76.0	50.2	100.0	1.0	100.0	0.3	52.8	35	60
No. 4	1.1	0.4	7.5	5.0	100.0	1.0	100.0	0.3	6.6	1	20
No. 8	1.0	0.3	3.9	2.6	100.0	1.0	100.0	0.3	4.2	1	10
No. 200	0.4	0.1	1.4	0.9	100.0	1.0	100.0	0.3	2.4	1	4
Pan		0.0		0.0		0.0		0.0	0.0		
Optimum Asphalt Content			6.0%								
Asphalt Source & Grade:			Marlin PG 76-22S								

Table 45. Mix Design for Brownwood Aggregate and PFC Mixture.

Agg. Source	Vulcan BWD Grade 4		Total Cumulative Pass %	TxDOT Specs.	
Sieve	Bin#1	Total			
Size	100.0	Percent	100.0%		
3/4"	100.0	100.0	100.0	100	100
1/2"	99.2	99.2	99.2	95	100
3/8"	69.7	69.7	69.7	50	80
No. 4	2.0	2.0	2.0	0	8
No. 8	0.7	0.7	0.7	0	4
No. 200	0.1	0.1	0.1	0	4
Optimum Asphalt Content			6.40%		
Asphalt Source & Grade:			Valero 76-22		

Table 46. Mix Design for Beckman Aggregate and Type D Mixture.

Agg. Source	Beckmann										Total Cumulative Pass %	TxDOT Specs.	
	1/2" - 3/8"		3/8" - 1/4"		Grade 10		Mfg Sand/LSF		W. Poteet Sand				
Sieve Size	Bin #1	Total	Bin #2	Total	Bin #3	Total	Bin #4	Total	Bin #5	Total			
	9	%	34	%	20	%	22	%	15	%	100%		
3/4"	100	9	100	34	100	20	100	22	100	15	100	100	100
1/2"	100	9	100	34	100	20	100	22	100	15	100	98	100
3/8"	66	5.94	100	34	100	20	100	22	100	15	96.94	85	100
No. 4	4.7	0.423	26	8.84	84	16.8	99.9	21.978	100	15	63.041	50	70
No. 8	3.8	0.342	14.7	4.998	2	0.4	85.6	18.832	99.8	14.97	39.542	35	46
No. 30	2.7	0.243	2.8	0.952	2	0.4	32.9	7.238	88	13.2	22.033	15	29
No. 50	2.4	0.216	2	0.68	1.7	0.34	18.6	4.092	52.2	7.83	13.158	7	20
No. 200	2.1	0.189	1.6	0.544	1.5	0.3	8.6	1.892	1.6	0.24	3.165	2	7
Pan		0		0		0		0		0	0		
Optimum Asphalt Content			4.7										
Asphalt Source & Grade:			Valero PG 64-22										

Table 47. Mix Design for Brownlee Aggregate and Type D Mixture.

Agg. Source	Delta		Capitol-GT		Brownlee		RTI-N				TXI		Total Cumulative Pass %	TxDOT Specs.	
	D-Rock		F-Rock		Grade #4		Dry Screenings		Washed Screening		Field Sand				
Sieve Size	Bin #1	Total	Bin #2	Total	Bin #3	Total	Bin #4	Total	Bin #5	Total	Bin #6	Total			
	50.0	%	10.0	%	7.0	%	0.0	%	21.0	%	12.0	%	100.0		
7/8"	100.0	50.0	100.0	10.0	100.0	7.0	100.0	0.0	100.0	21.0	100.0	12.0	100.0	100	100
5/8"	100.0	50.0	100.0	10.0	100.0	7.0	100.0	0.0	100.0	21.0	100.0	12.0	100.0	98	100
3/8"	79.9	40.0	100.0	10.0	60.0	4.2	100.0	0.0	100.0	21.0	100.0	12.0	87.2	85	100
No. 4	40.3	20.1	77.9	7.8	10.4	0.7	97.5	0.0	99.6	20.9	100.0	12.0	61.6	50	70
No. 10	14.7	7.3	10.2	1.0	0.7	0.1	74.5	0.0	84.0	17.6	99.3	11.9	38.0	35	46
No. 40	9.4	4.7	2.7	0.3	0.6	0.0	41.9	0.0	32.0	6.7	84.4	10.1	21.8	15	29
No. 80	8.5	4.2	2.0	0.2	0.5	0.0	34.6	0.0	11.4	2.4	15.9	1.9	8.8	7	20
No. 200	6.9	3.4	1.5	0.2	0.5	0.0	26.7	0.0	3.1	0.7	0.7	0.1	4.4	2	7
Optimum Asphalt Content			5.3%												
Asphalt Source & Grade:			Valero PG 76-22												

Table 48. Mix Design for 50 Percent Beckman and 50 Percent Brownlee and Type D Mixture.

Agg. Source	Delta Materials		Beckmann				Beckmann				Total Cumulative Pass %	TxDOT Specs.	
	Brownlee Type D		3/8"-1/4"		Mfg Sand		W. Poteet Sand		Sieved Mfg Sand				
Sieve Size	Bin #1	Total	Bin #2	Total	Bin #3	Total	Bin #4	Total	Bin #5	Total			
	20.0	%	31.0	%	31.0	%	11.0	%	7.0	%	100%		
7/8"	100.0	20.0	100.0	31.0	100.0	31.0	100.0	11.0	100.0	7.0	100.0	100	100
5/8"	100.0	20.0	100.0	31.0	100.0	31.0	100.0	11.0	100.0	7.0	100.0	98	100
3/8"	70.9	14.2	100.0	31.0	100.0	31.0	100.0	11.0	100.0	7.0	94.2	85	100
No. 4	16.3	3.3	26.0	8.1	99.9	31.0	100.0	11.0	100.0	7.0	60.3	50	70
No. 10	4.0	0.8	3.4	1.1	70.9	22.0	99.6	11.0	100.0	7.0	41.8	35	46
No. 40	2.3	0.5	2.1	0.7	25.0	7.8	69.2	7.6	100.0	7.0	23.5	15	29
No. 80	1.8	0.4	1.9	0.6	13.1	4.1	14.4	1.6	100.0	7.0	13.6	7	20
No. 200	1.1	0.2	1.6	0.5	8.6	2.7	1.6	0.2	0.0	0.0	3.6	2	7
Optimum Asphalt Content			5.3%										
Asphalt Source & Grade:			Valero PG 76-22										

APPENDIX B – TEXTURE AND ANGULARITY MEASUREMENTS BY AIMS FOR DIFFERENT AGGREGATES

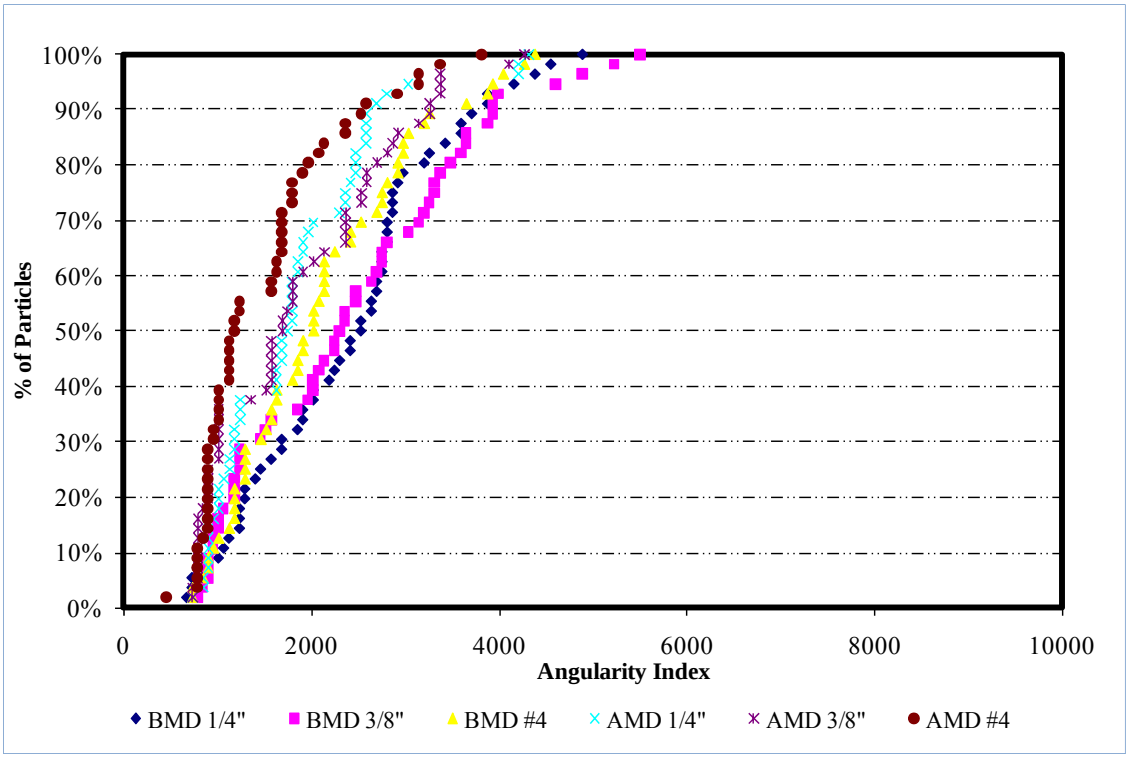

Figure 91. Results of Angularity Measurements by AIMS for Brownwood Aggregate.

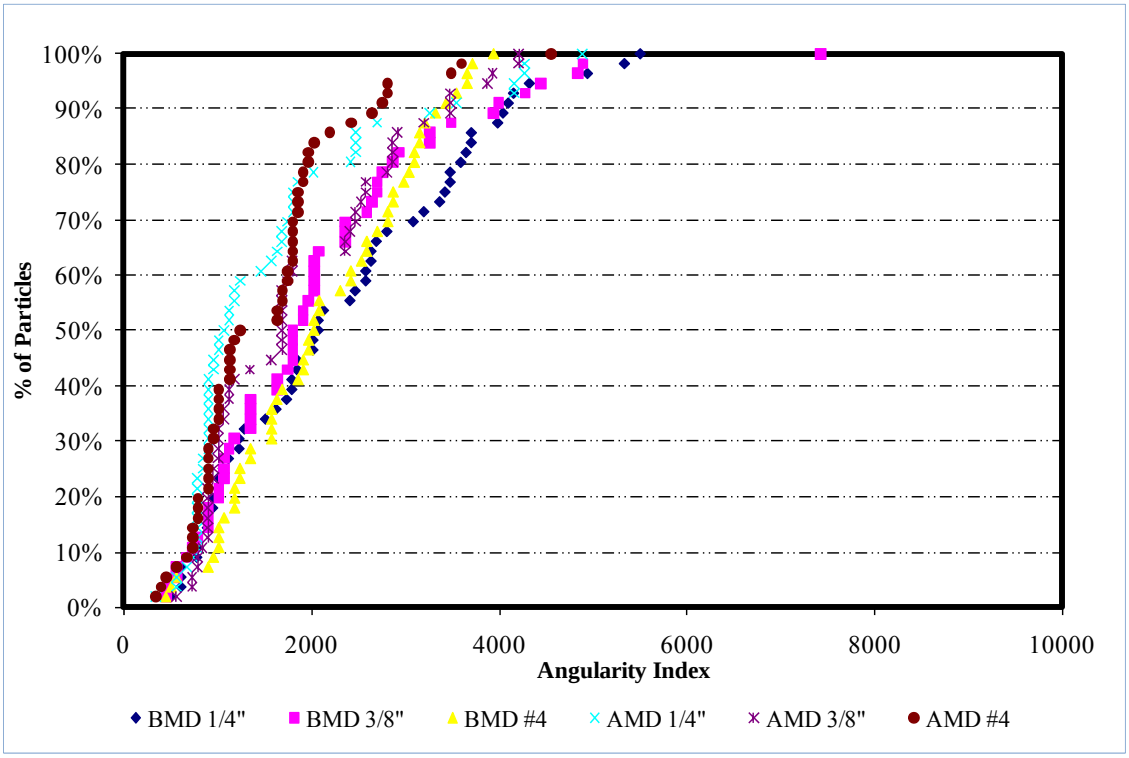

Figure 92. Results of Angularity Measurements by AIMS for Beckman Aggregate.

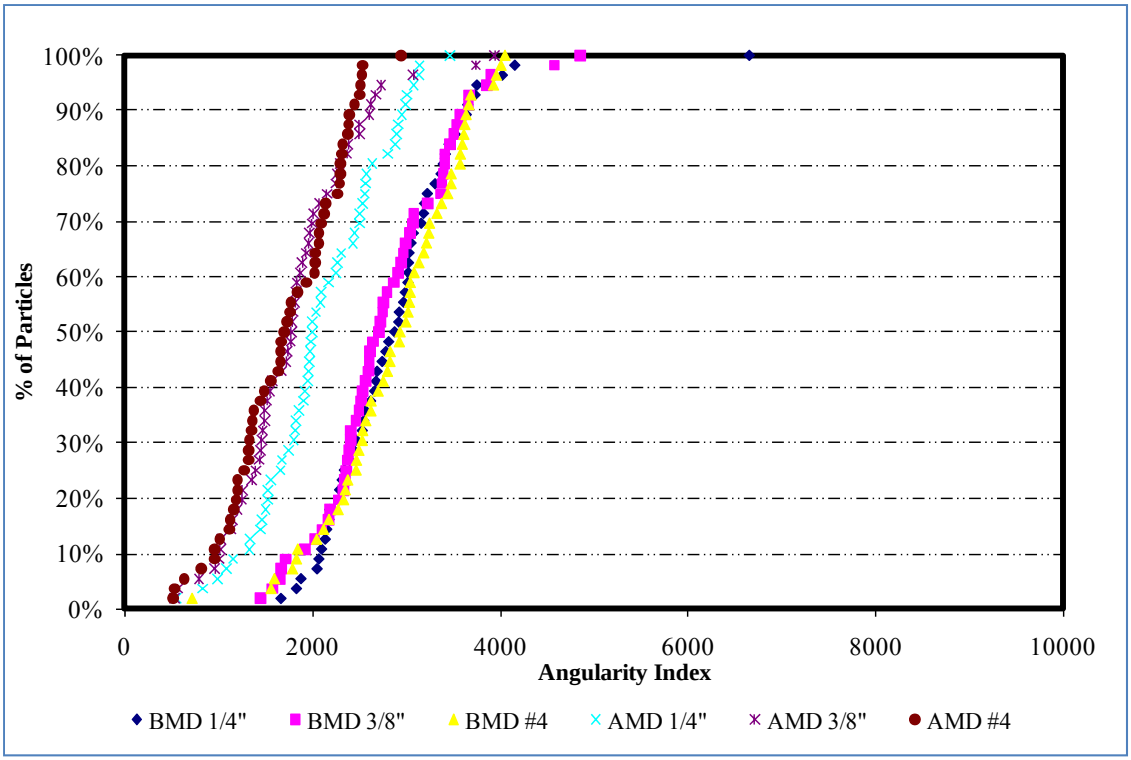

Figure 93. Results of Angularity Measurements by AIMS for Brownlee Aggregate.

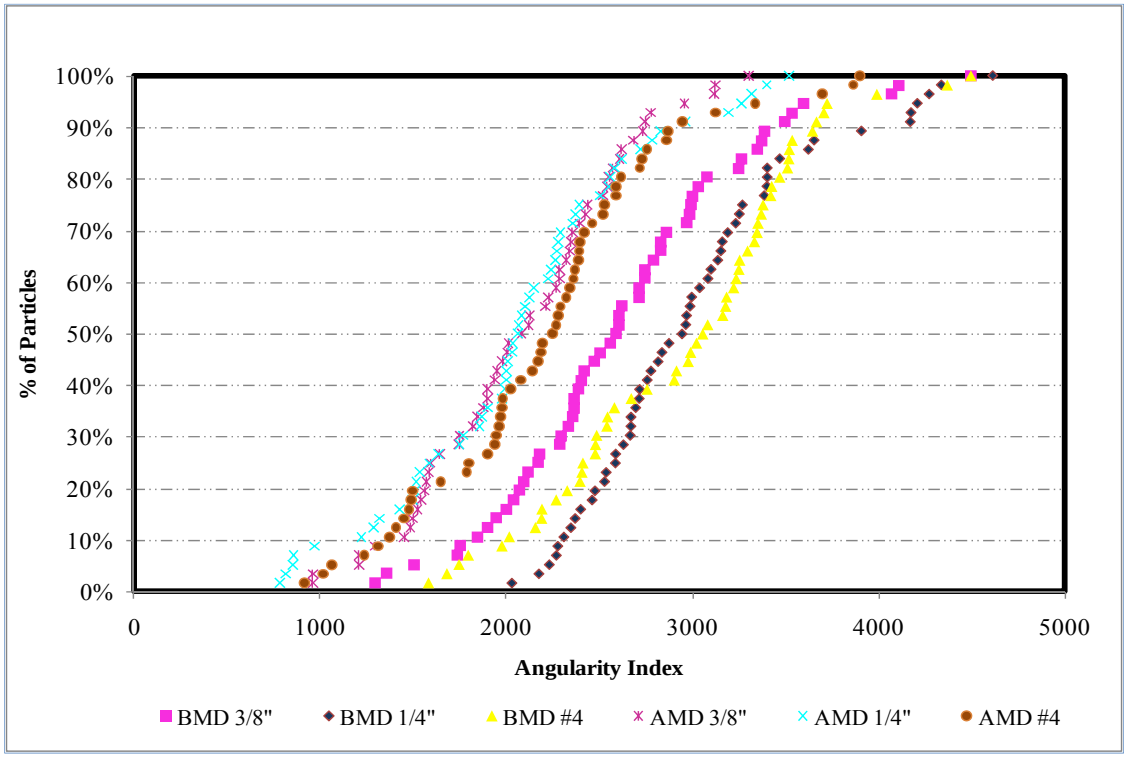

Figure 94. Results of Angularity Measurements by AIMS for El Paso Aggregate.

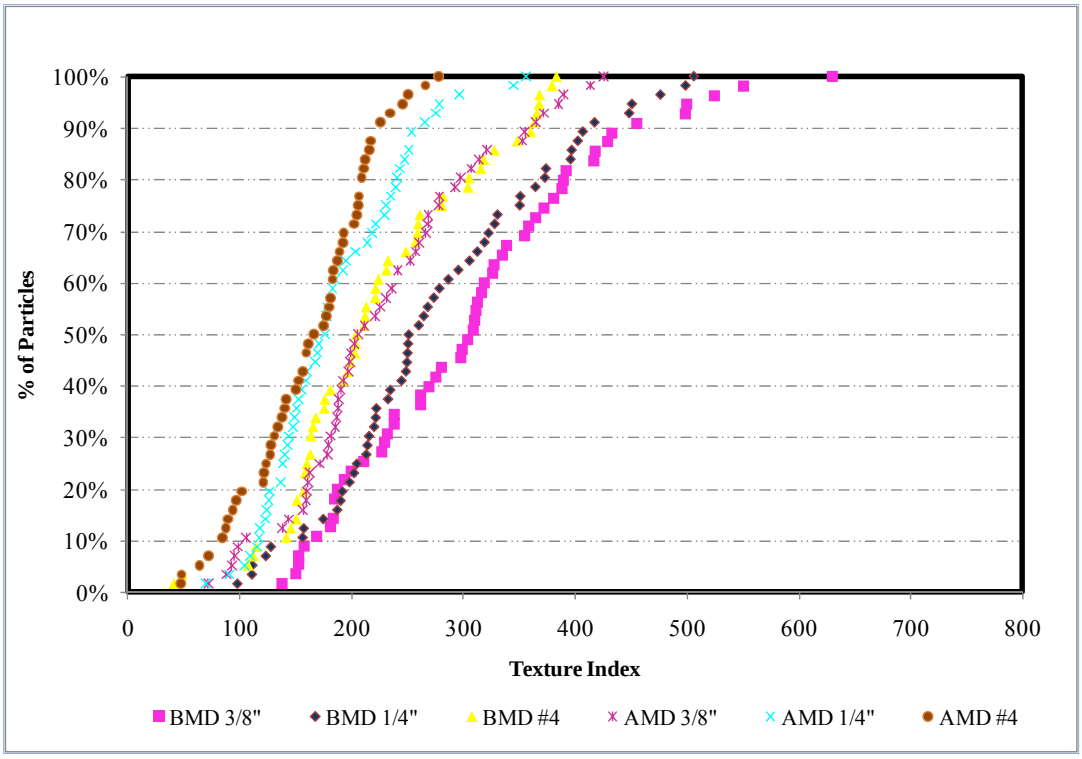

Figure 95. Results of Texture Measurements by AIMS for El Paso Aggregate.

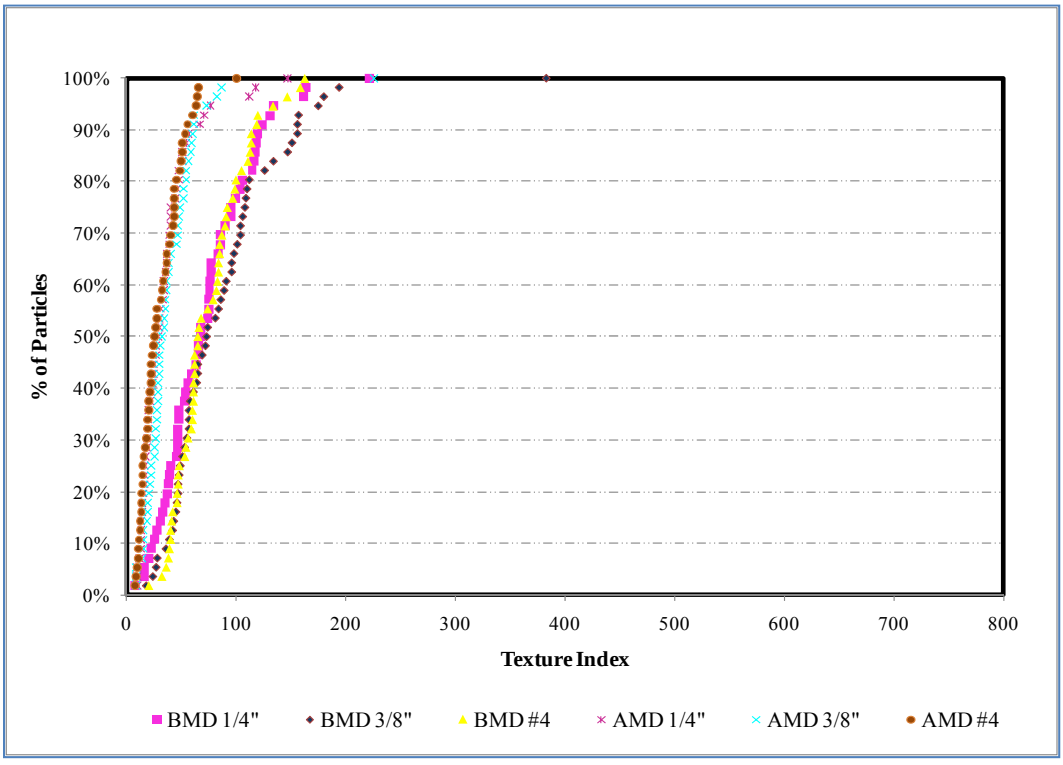

Figure 96. Results of Texture Measurements by AIMS for Beckman Aggregate.

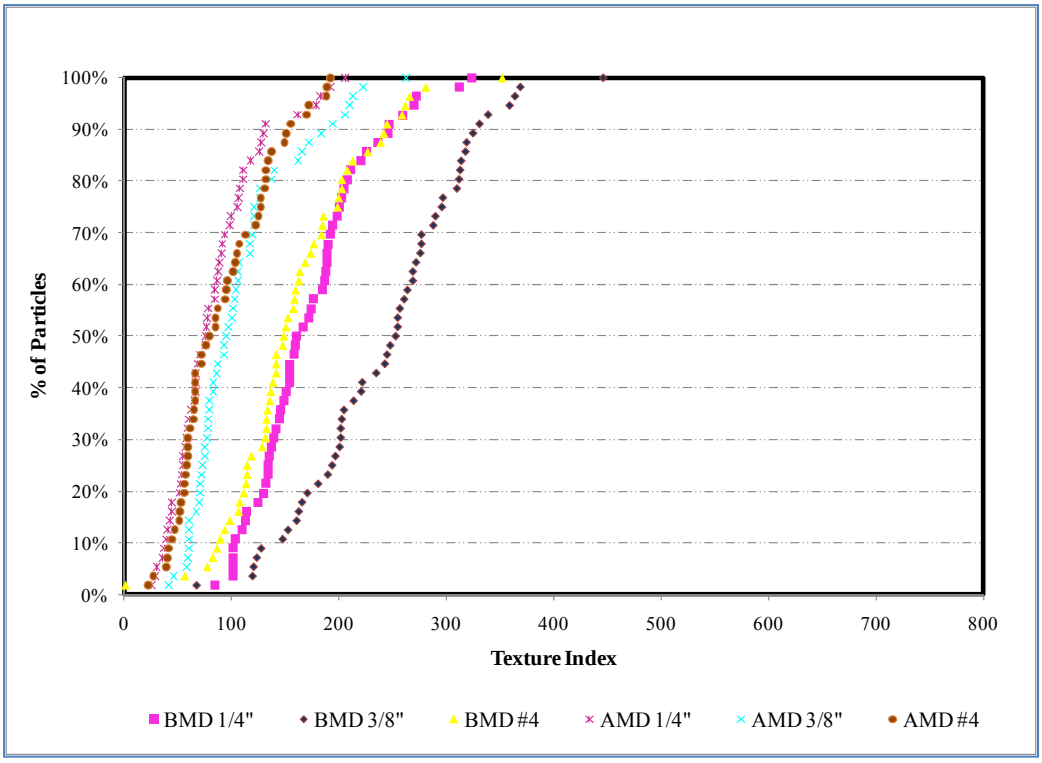

Figure 97. Results of Texture Measurements by AIMS for Brownwood Aggregate.

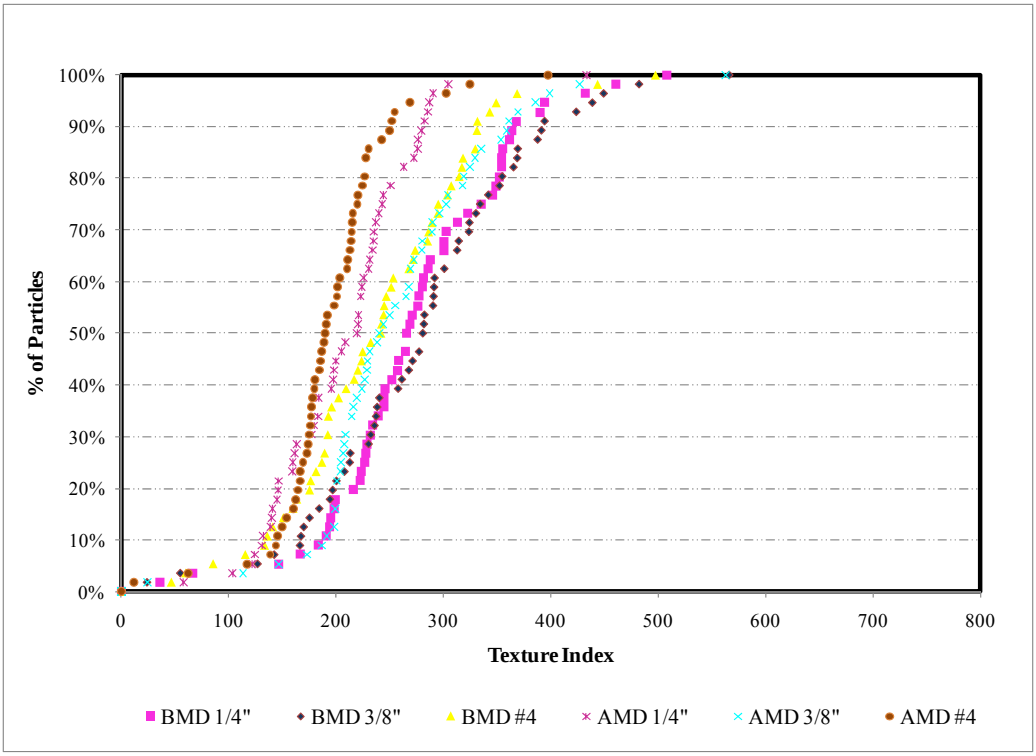

Figure 98. Results of Texture Measurements by AIMS for Brownlee Aggregate.

APPENDIX C – PLOTS OF TERMINAL AND RATE OF CHANGE VALUES FOR F60 AND DF_{20} FOR DIFFERENT AGGREGATE AND MIXES

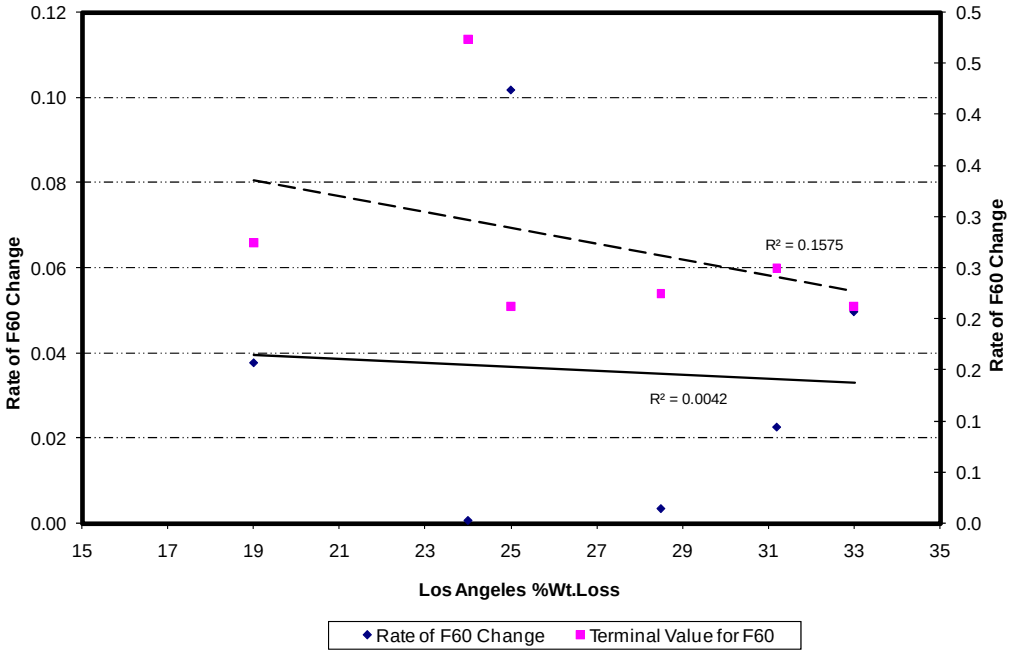

Figure 99. Rate of F60 Change and Terminal Value vs. Los Angeles Percent Weight Loss for Type C Mix.

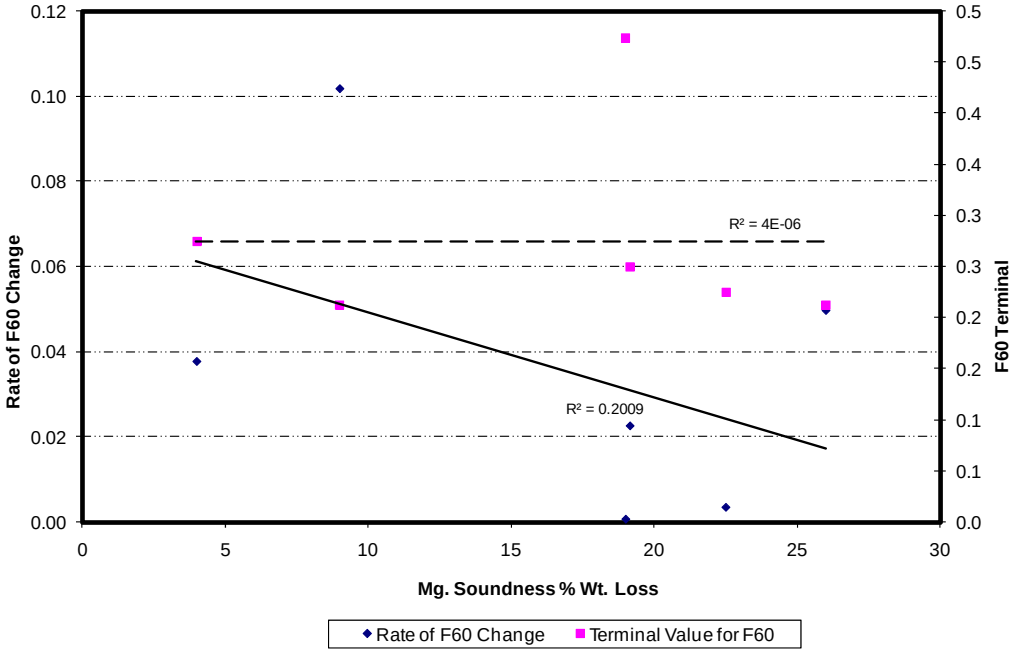

Figure 100. Rate of F60 Change and Terminal Value vs. Mg. Soundness for Type C Mix.

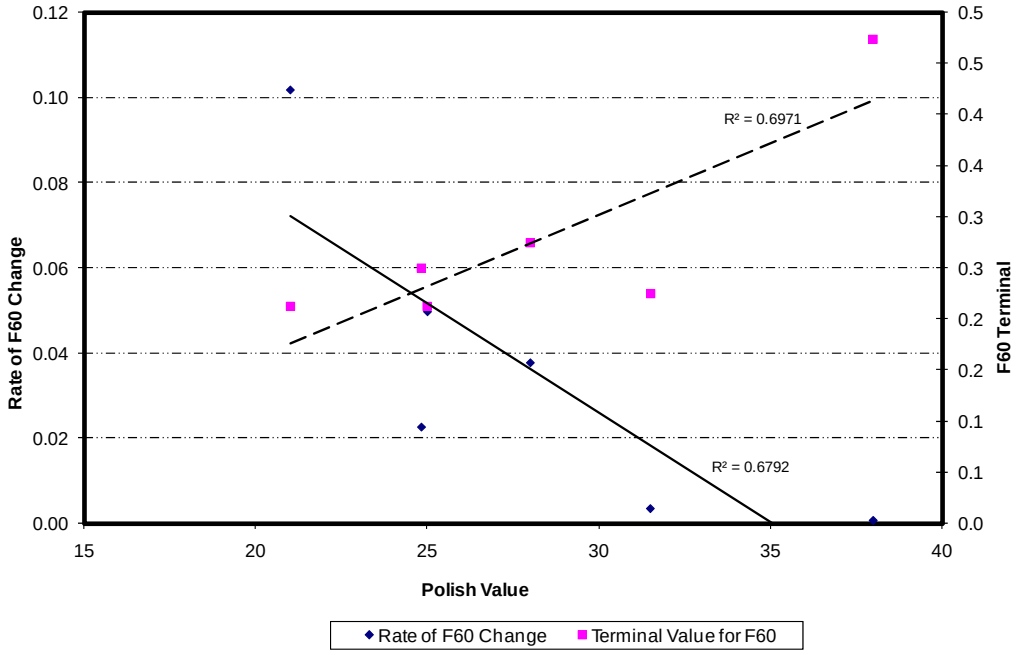

Figure 101. Rate of F60 Change and Terminal Value vs. Polish Value for Type C Mix.

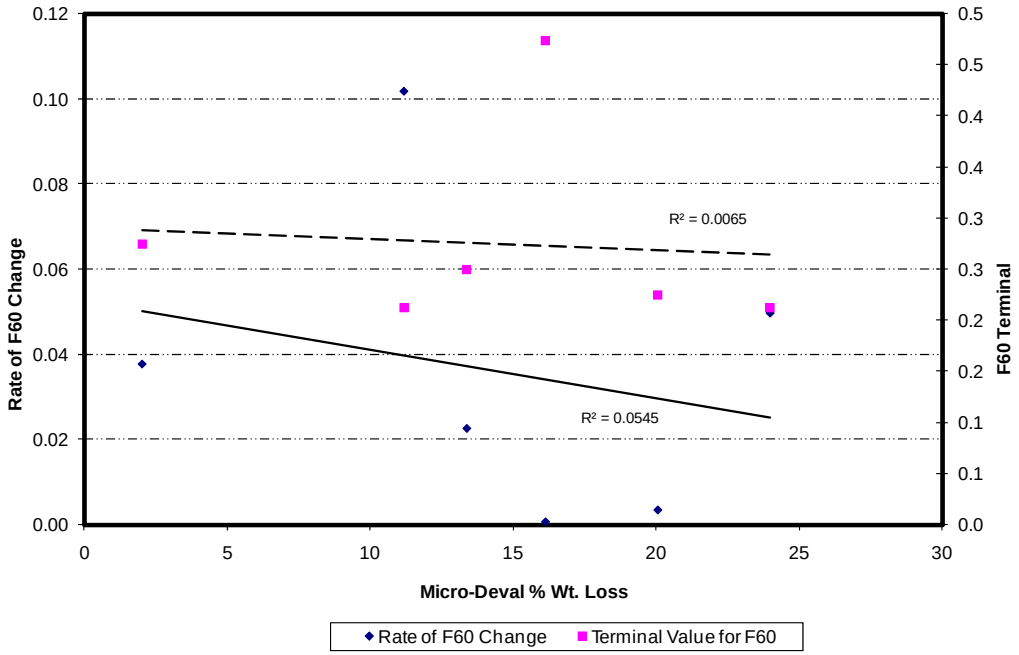

Figure 102. Rate of F60 Change and Terminal Value vs. Micro-Deval Percent Weight Loss for Type C Mix.

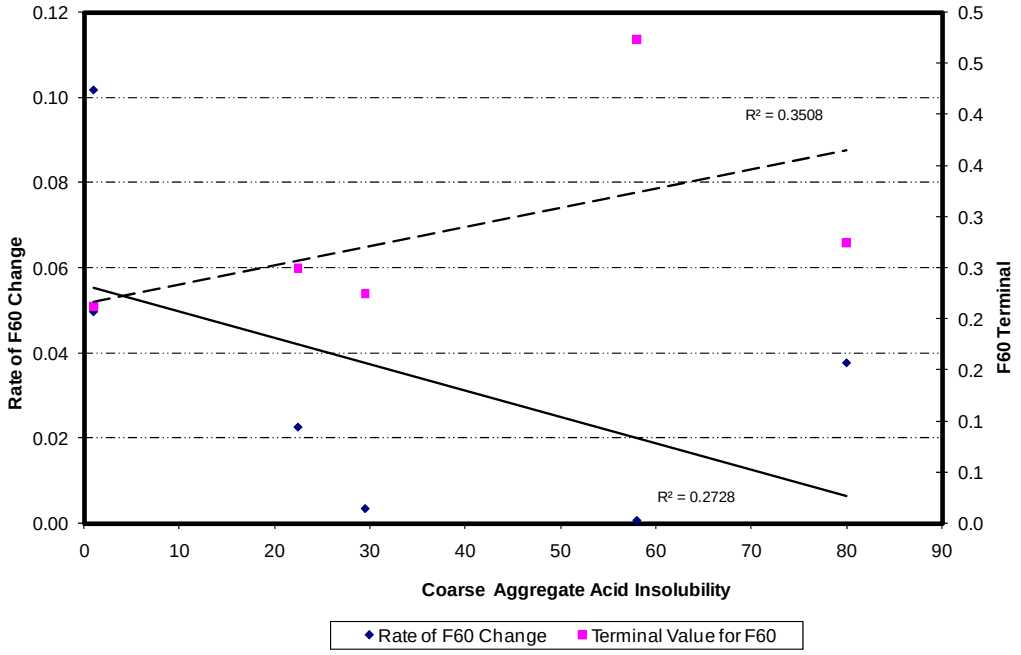

Figure 103. Rate of F60 Change and Terminal Value vs. Coarse Aggregate Acid Insolubility for Type C Mix.

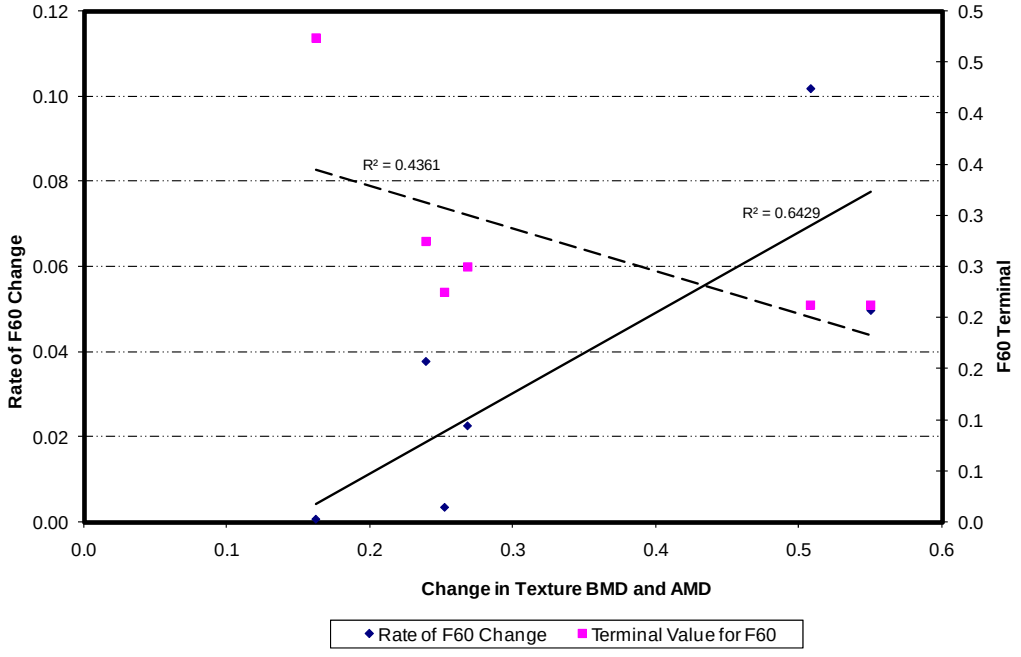

Figure 104. Rate of F60 Change and Terminal Value vs. Change in Texture BMD and AMD for Type C Mix.

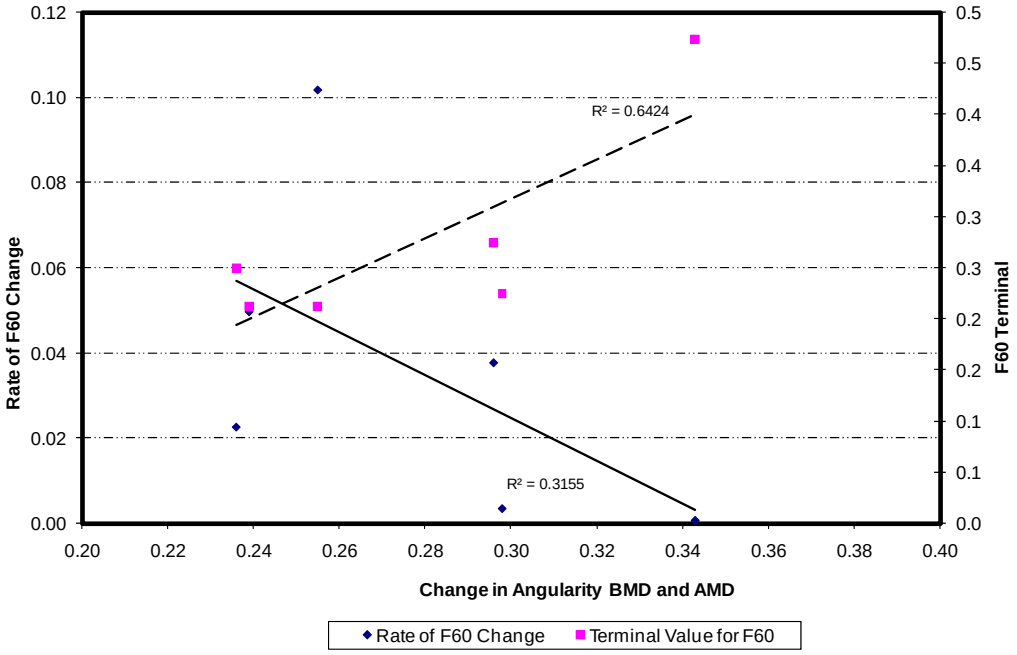

Figure 105. Rate of F60 Change and Terminal Value vs. Change in Angularity BMD and AMD for Type C Mix.

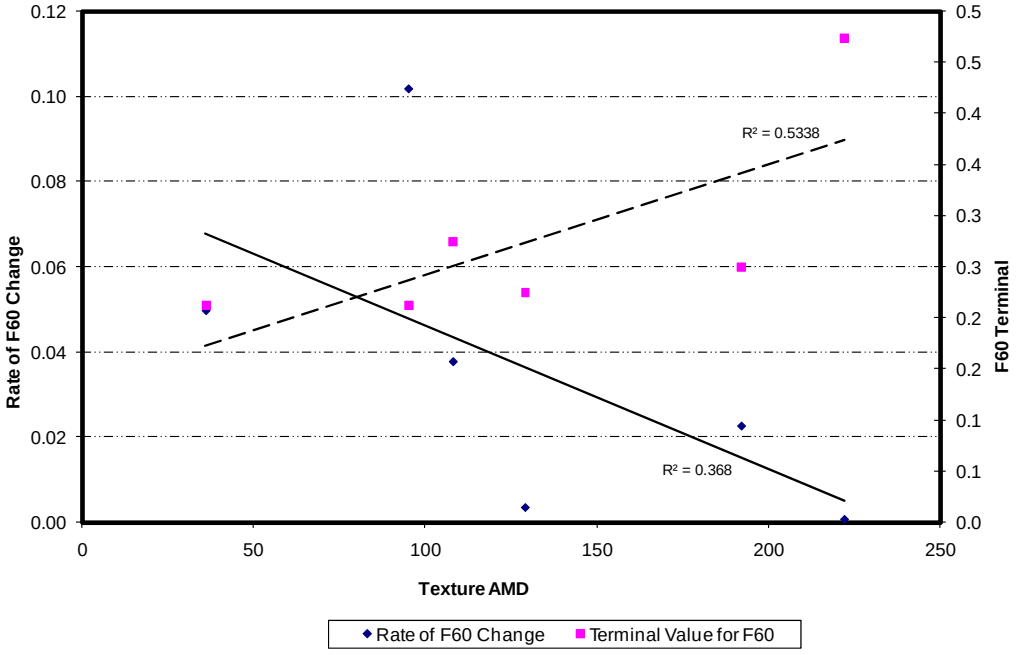

Figure 106. Rate of F60 Change and Terminal Value vs. Texture AMD for Type C Mix.

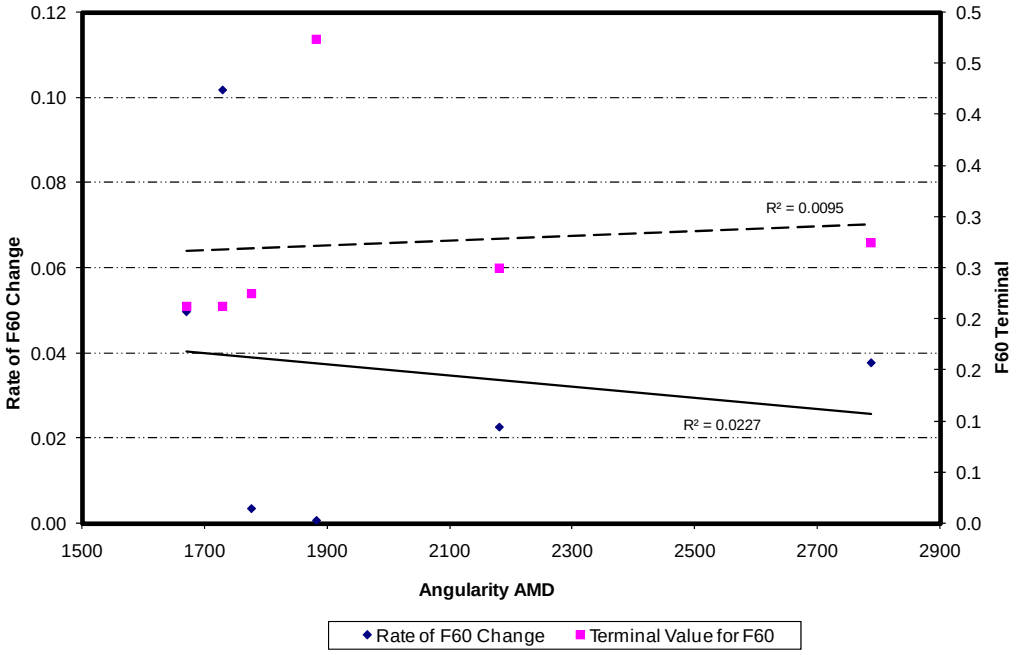

Figure 107. Rate of F60 Change and Terminal Value vs. Angularity AMD for Type C Mix.

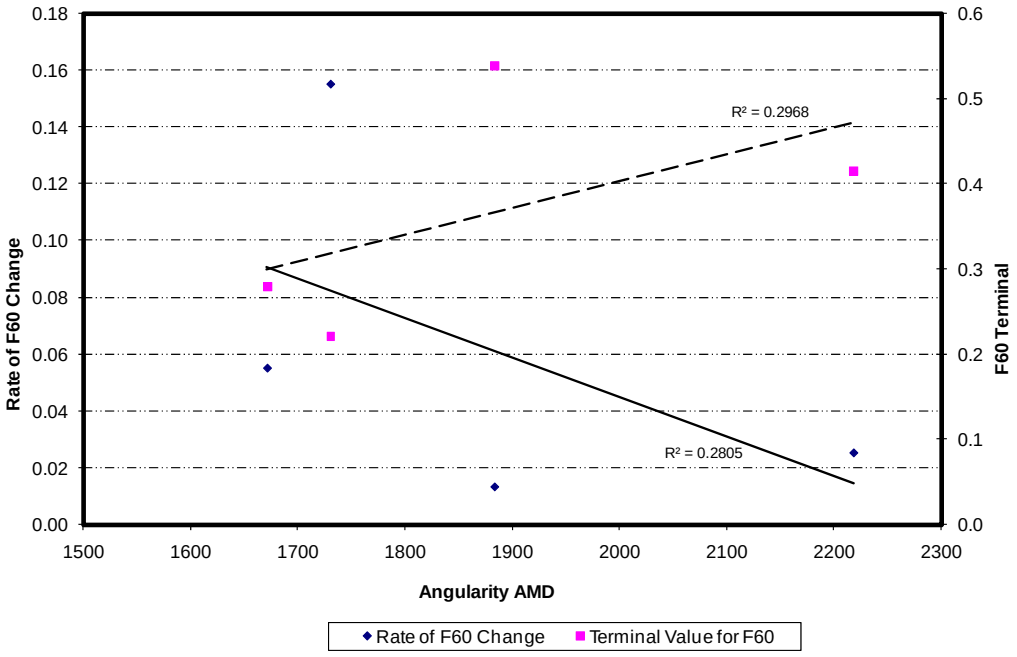

Figure 108. Rate of F60 Change and Terminal Value vs. Angularity AMD for PFC Mix.

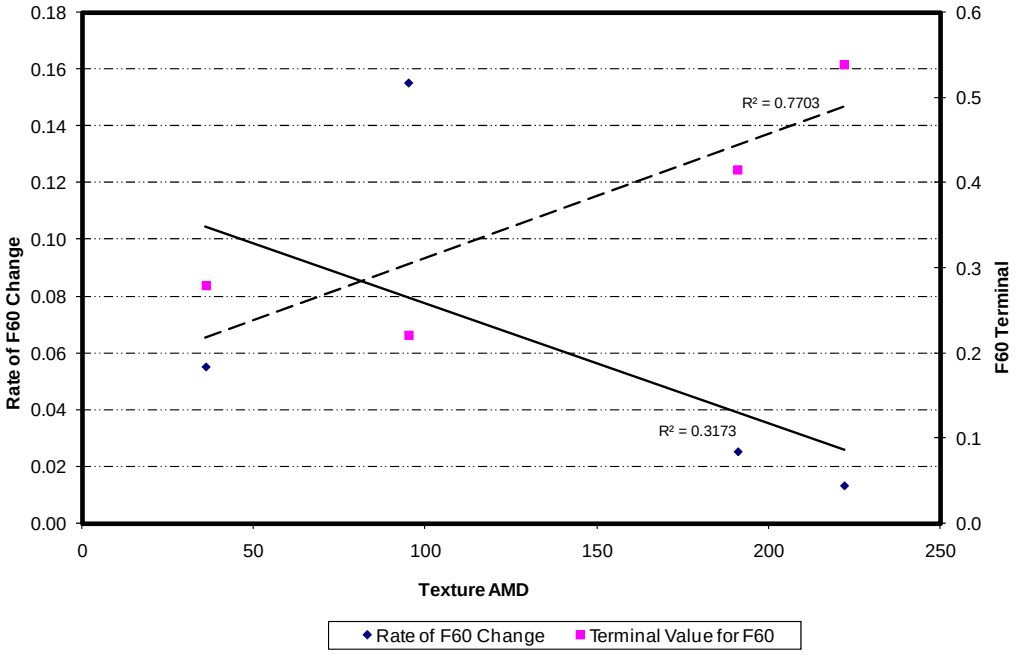

Figure 109. Rate of F60 Change and Terminal Value vs. Texture AMD for PFC Mix.

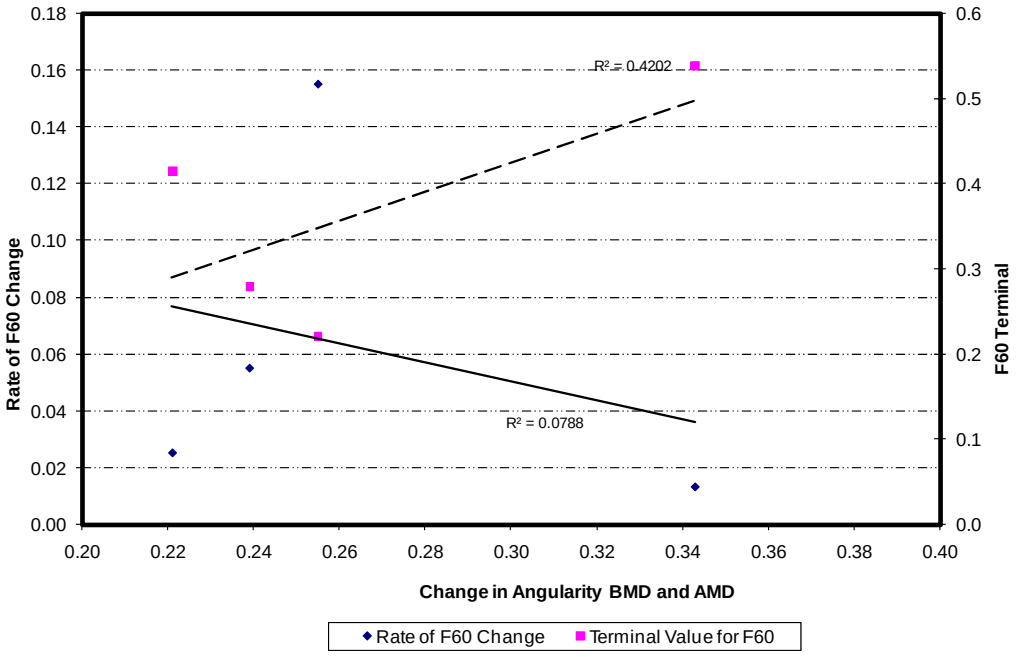

Figure 110. Rate of F60 Change and Terminal Value vs. Change in Angularity BMD and AMD for PFC Mix.

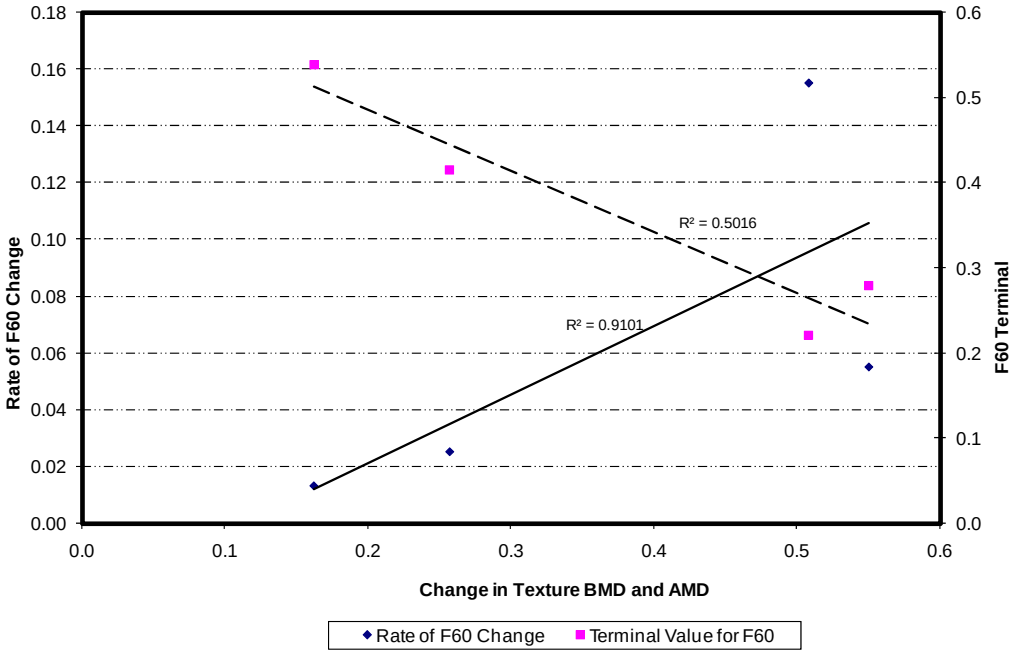

Figure 111. Rate of F60 Change and Terminal Value vs. Change in Texture BMD and AMD for PFC Mix.

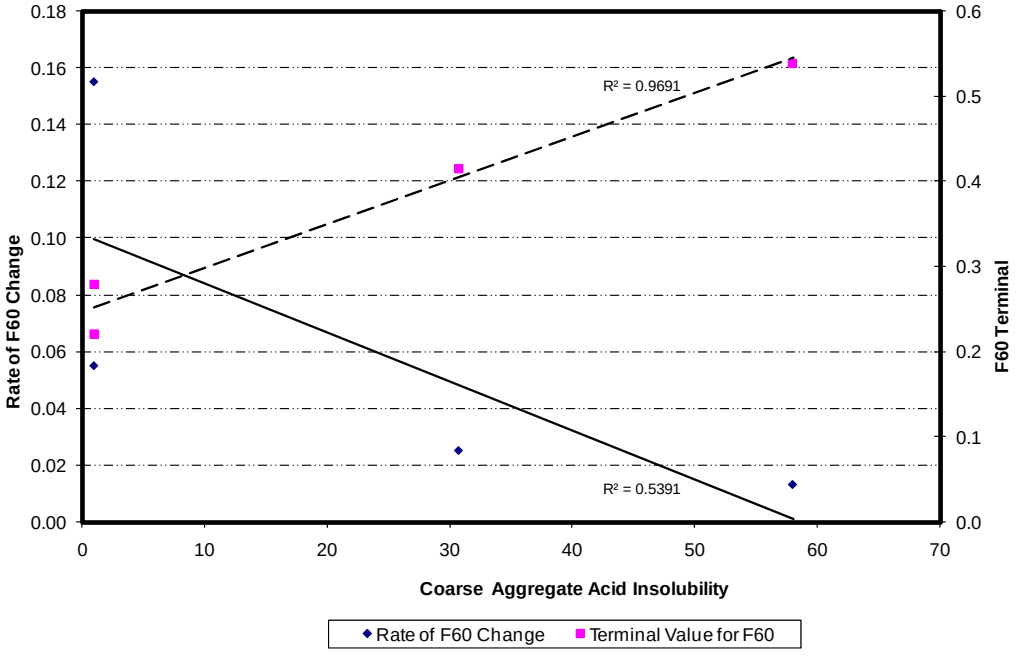

Figure 112. Rate of F60 Change and Terminal Value vs. Coarse Aggregate Acid Insolubility for PFC Mix.

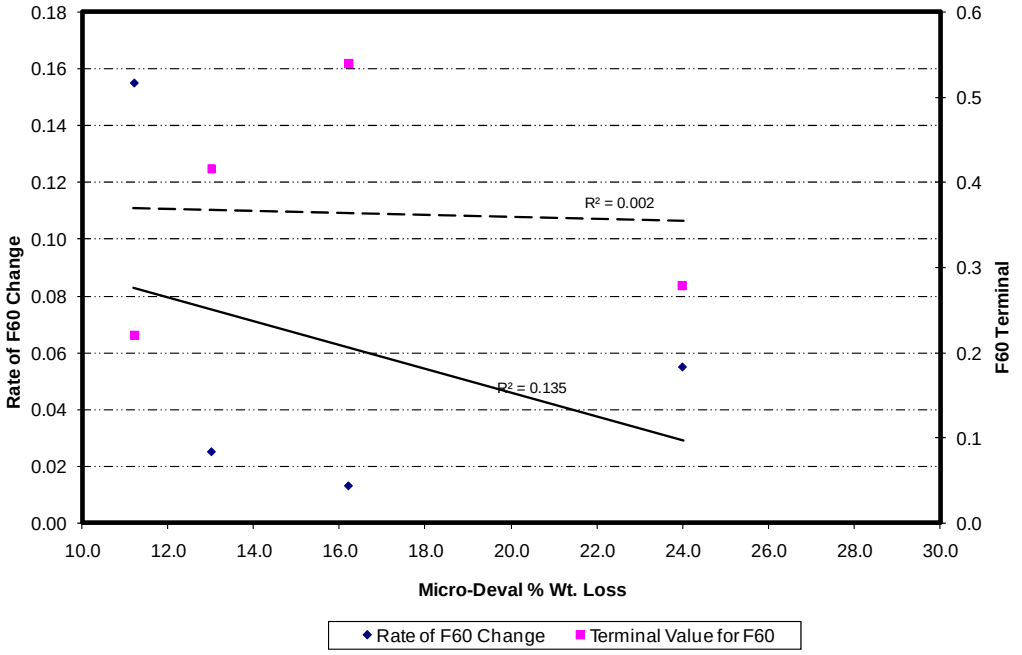

Figure 113. Rate of F60 Change and Terminal Value vs. Micro-Deval Percent Weight Loss for PFC Mix.

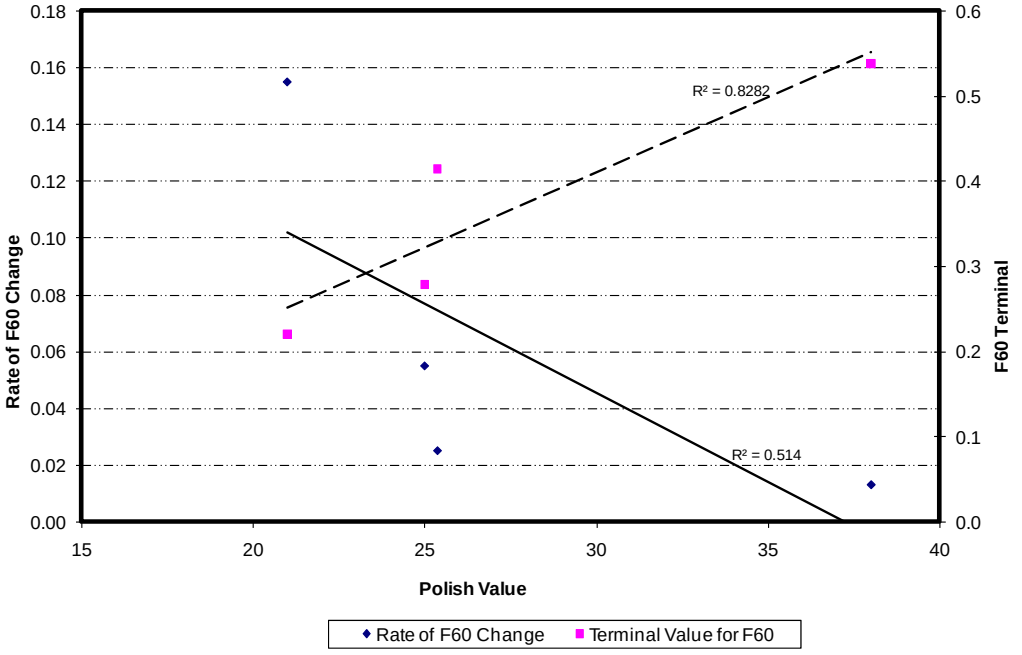

Figure 114. Rate of F60 Change and Terminal Value vs. Polish Value for PFC Mix.

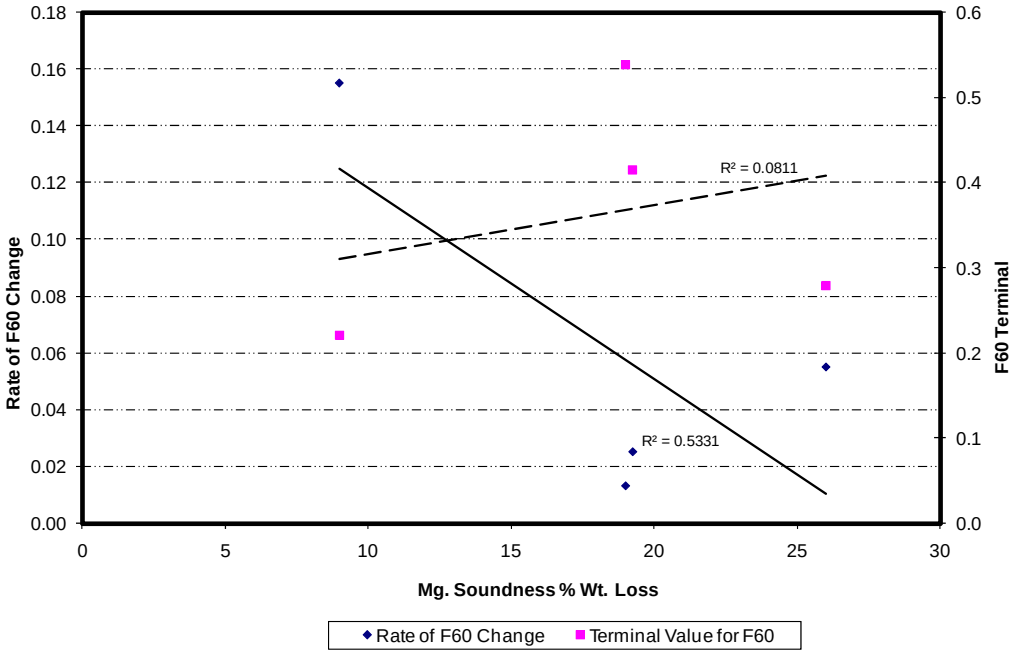

Figure 115. Rate of F60 Change and Terminal Value vs. Mg. Soundness for PFC Mix.

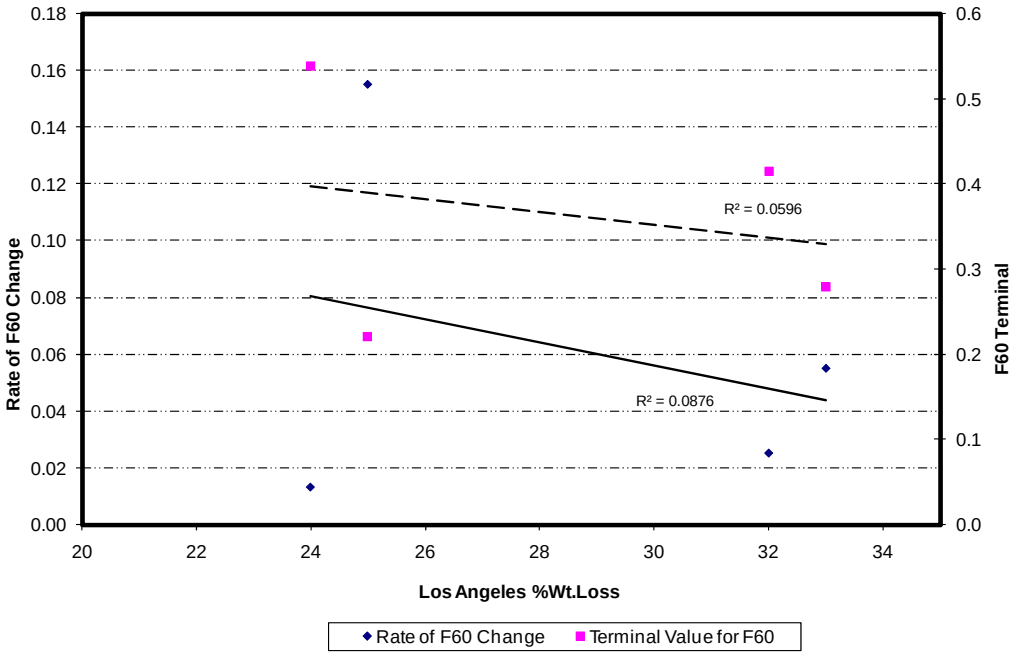

Figure 116. Rate of F60 Change and Terminal Value vs. Los Angeles Percent Weight Loss PFC Mix.

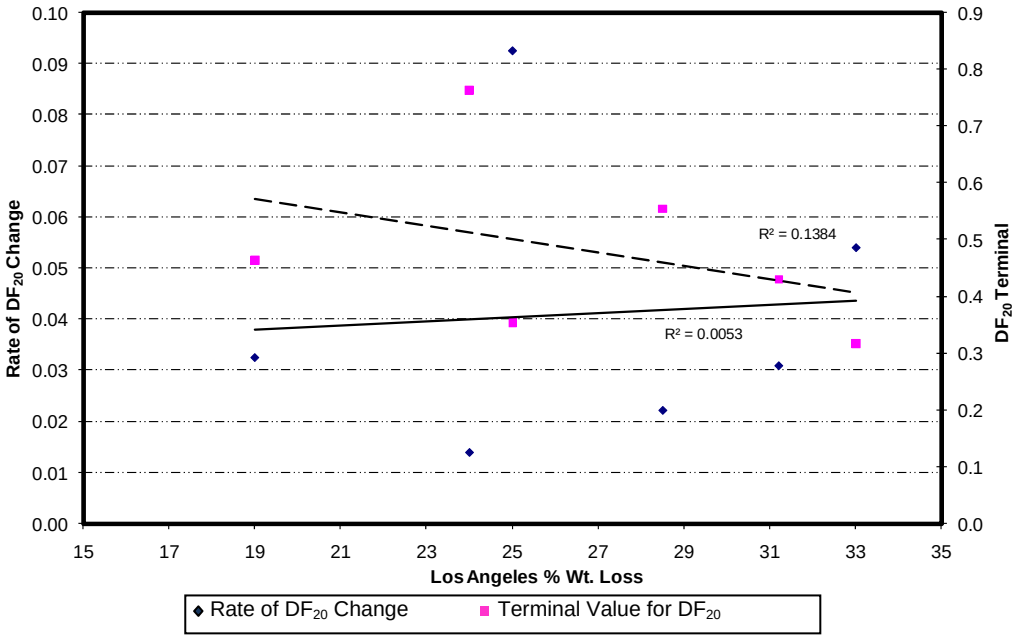

Figure 117. Rate of DF_{20} Change and Terminal Value vs. Los Angeles Percent Weight Loss for Type C Mix.

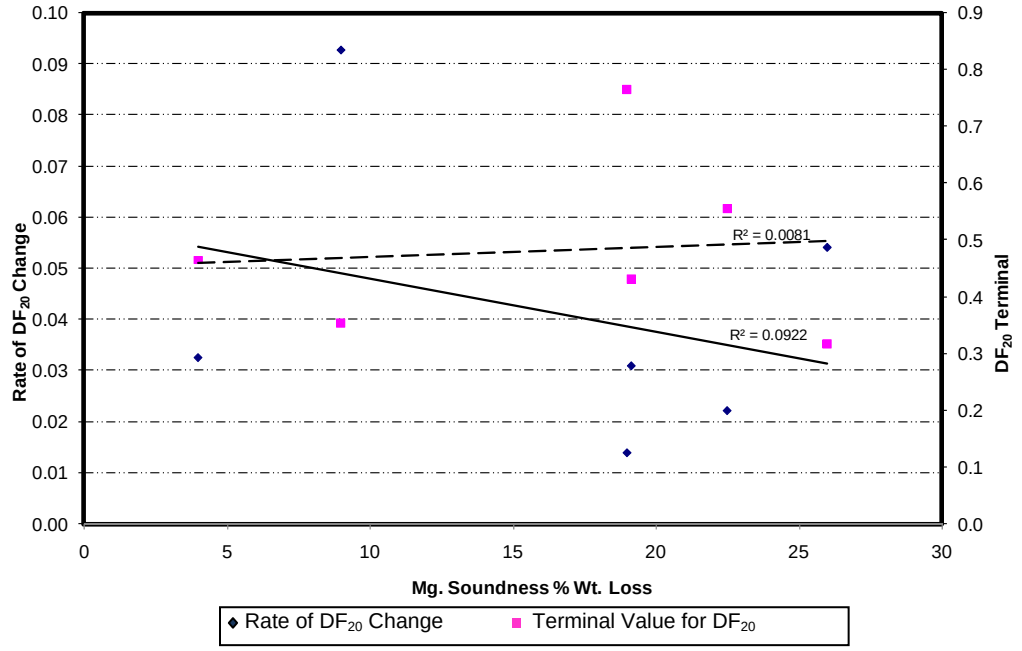

Figure 118. Rate of DF_{20} Change and Terminal Value vs. Mg Soundness for Type C Mix.

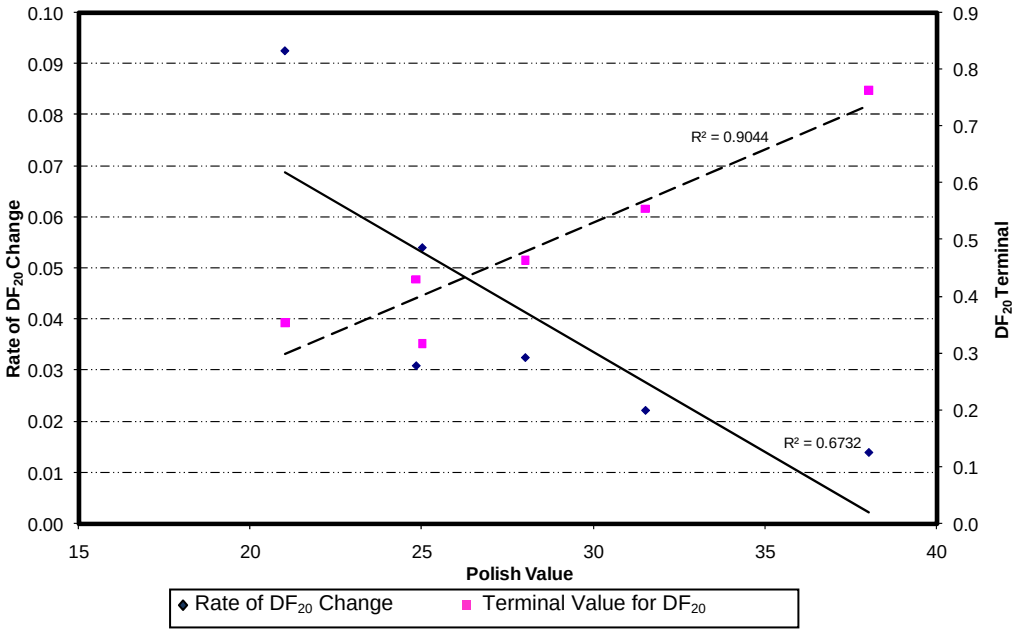

Figure 119. Rate of DF_{20} Change and Terminal Value vs. Polish Value for Type C Mix.

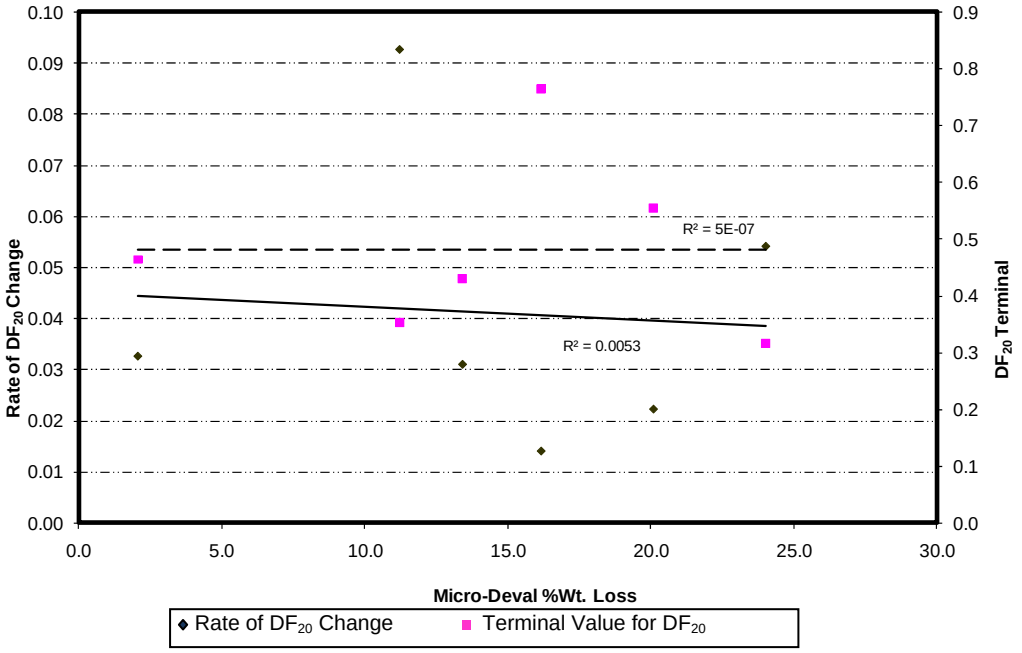

Figure 120. Rate of DF_{20} Change and Terminal Value vs. Micro-Deval Percent Weight Loss for Type C Mix.

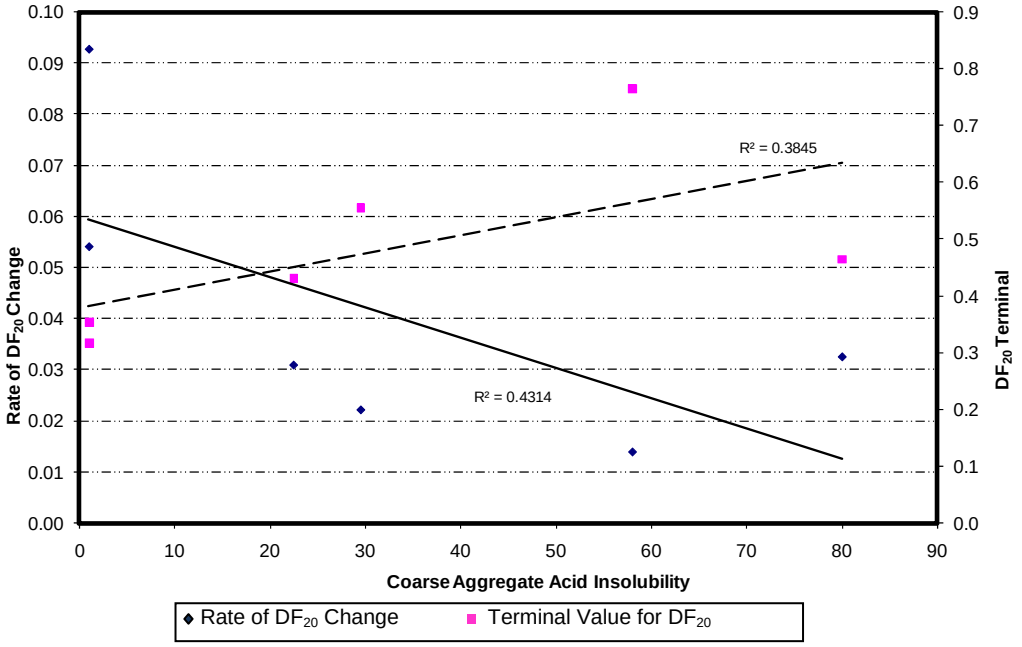

Figure 121. Rate of DF_{20} Change and Terminal Value vs. Coarse Aggregate Acid Insolubility for Type C Mix.

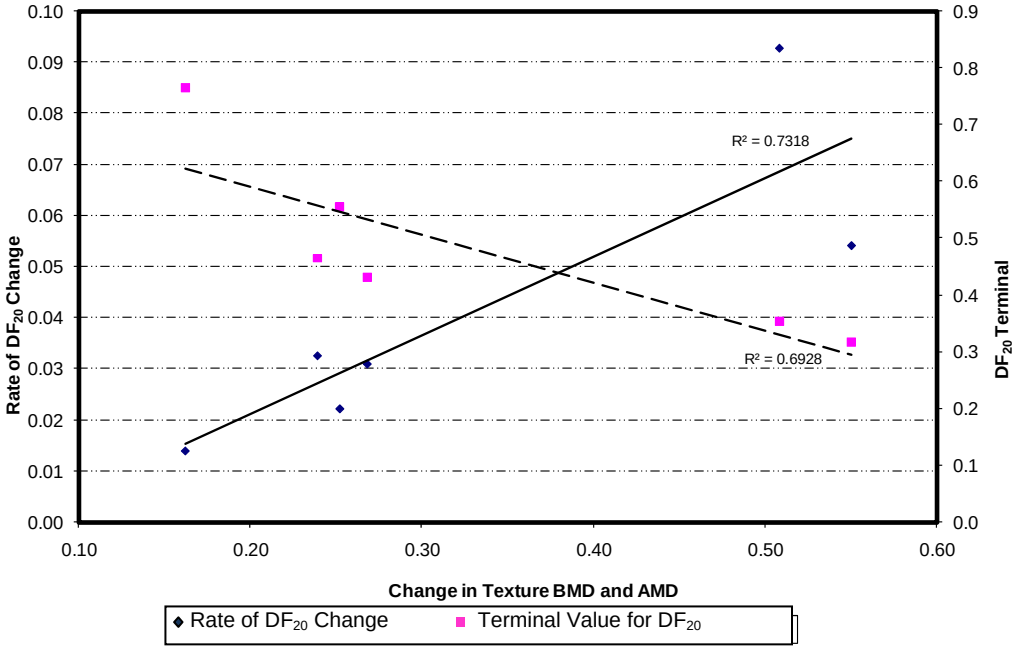

Figure 122. Rate of DF_{20} Change and Terminal Value vs. Change in Texture BMD and AMD for Type C Mix.

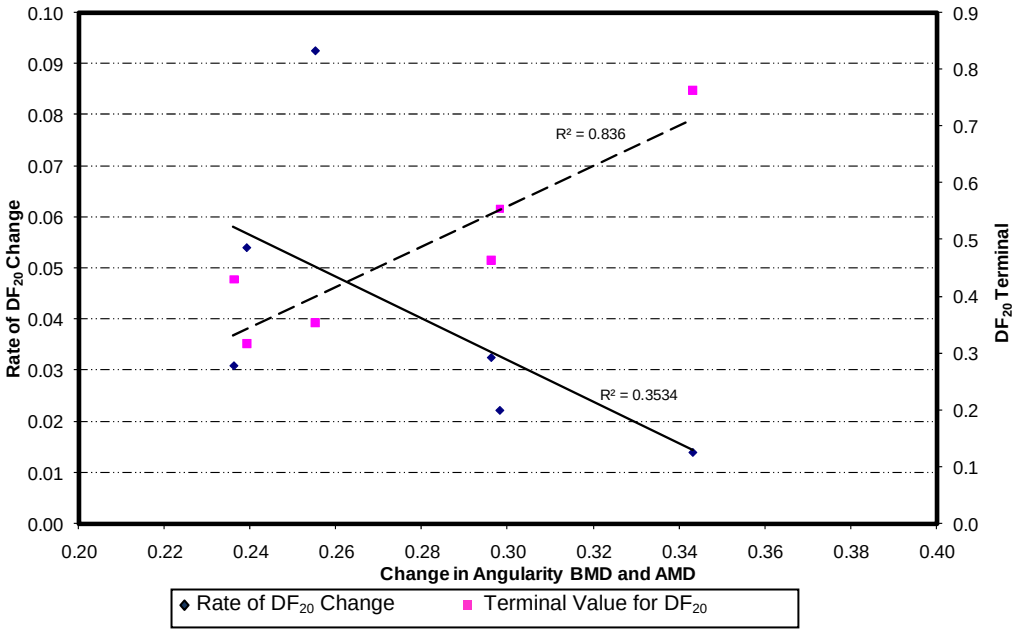

Figure 123. Rate of DF_{20} Change and Terminal Value vs. Change in Angularity BMD and AMD for Type C Mix.

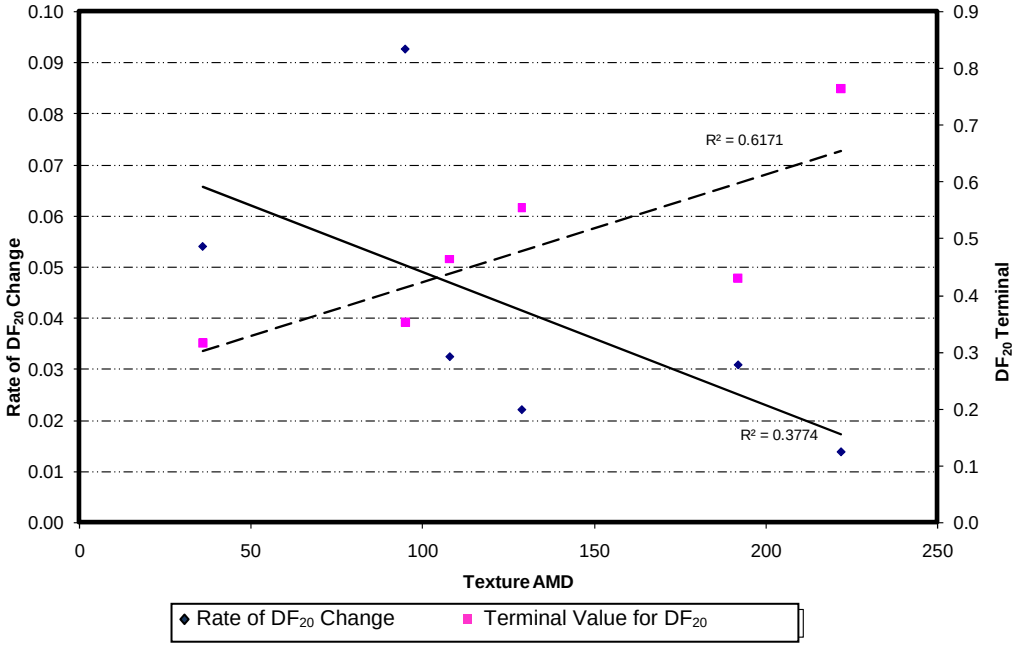

Figure 124. Rate of DF_{20} Change and Terminal Value vs. Texture AMD for Type C Mix.

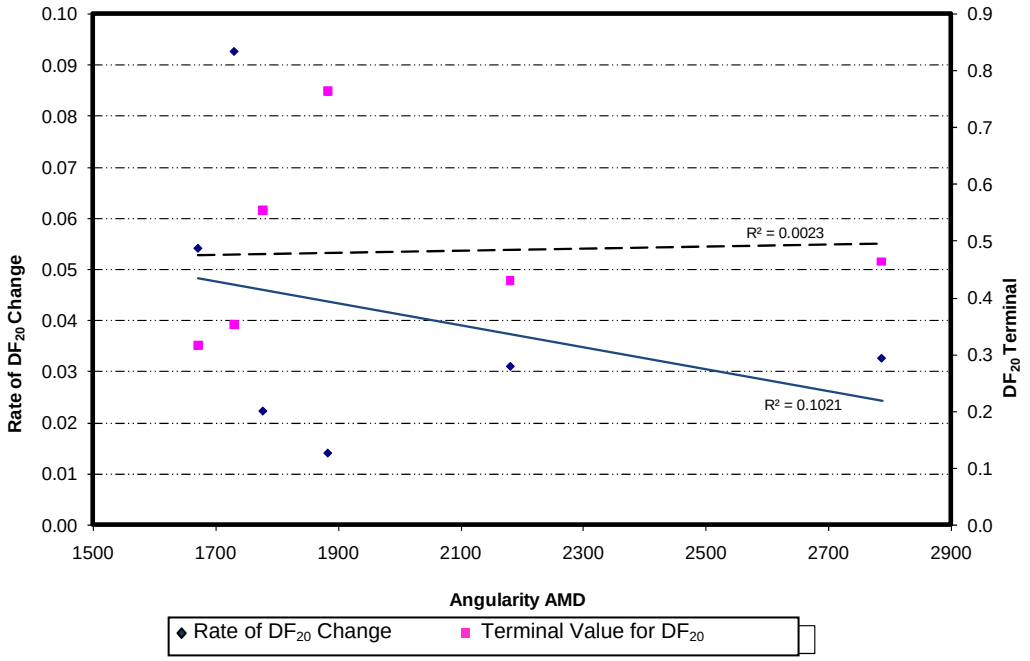

Figure 125. Rate of DF_{20} Change and Terminal Value vs. Angularity AMD for Type C Mix.

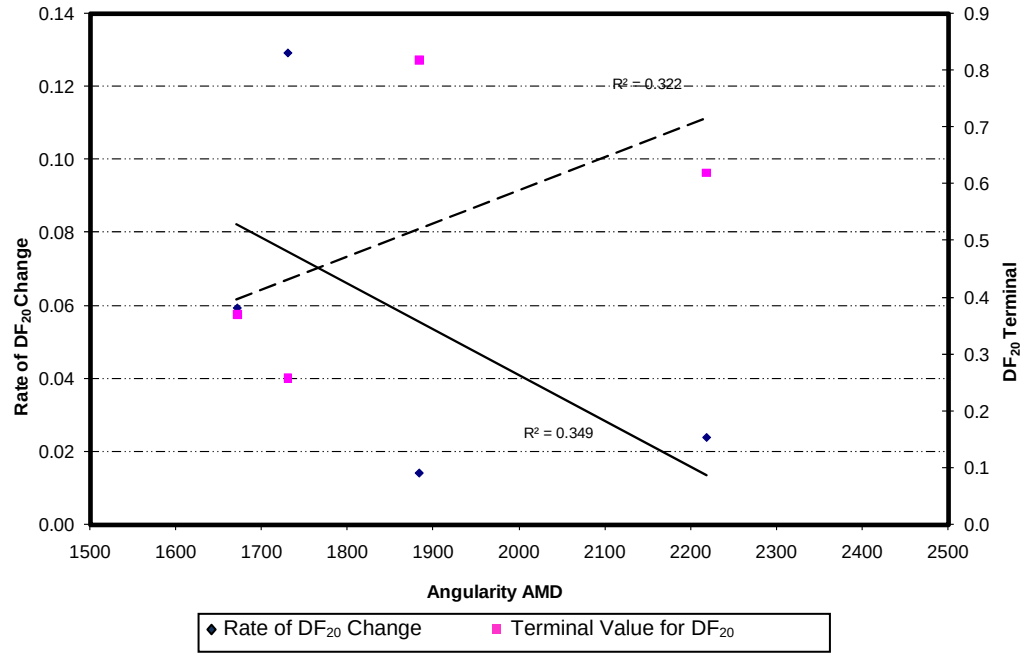

Figure 126. Rate of DF_{20} Change and Terminal Value vs. Angularity AMD for PFC Mix.

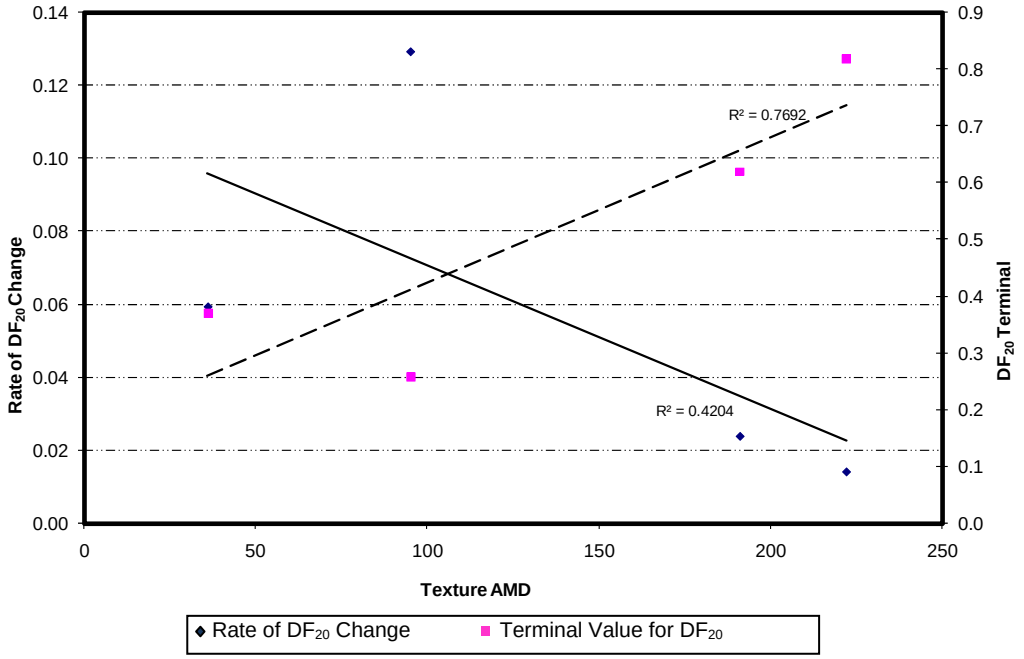

Figure 127. Rate of DF_{20} Change and Terminal Value vs. Texture AMD for PFC Mix.

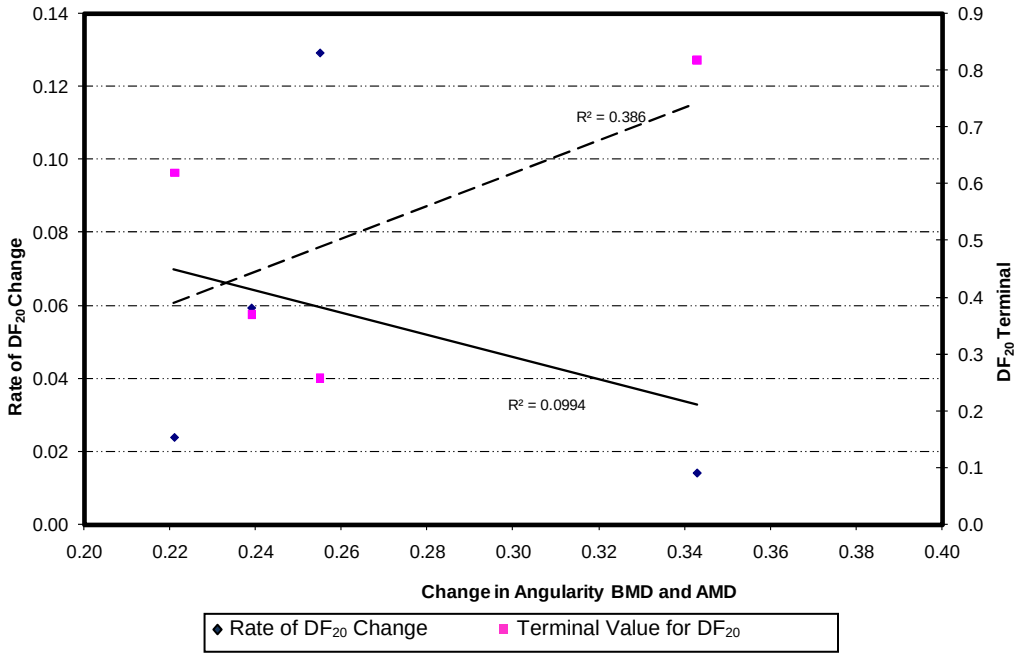

Figure 128. Rate of DF_{20} Change and Terminal Value vs. Change in Angularity BMD and AMD for PFC Mix.

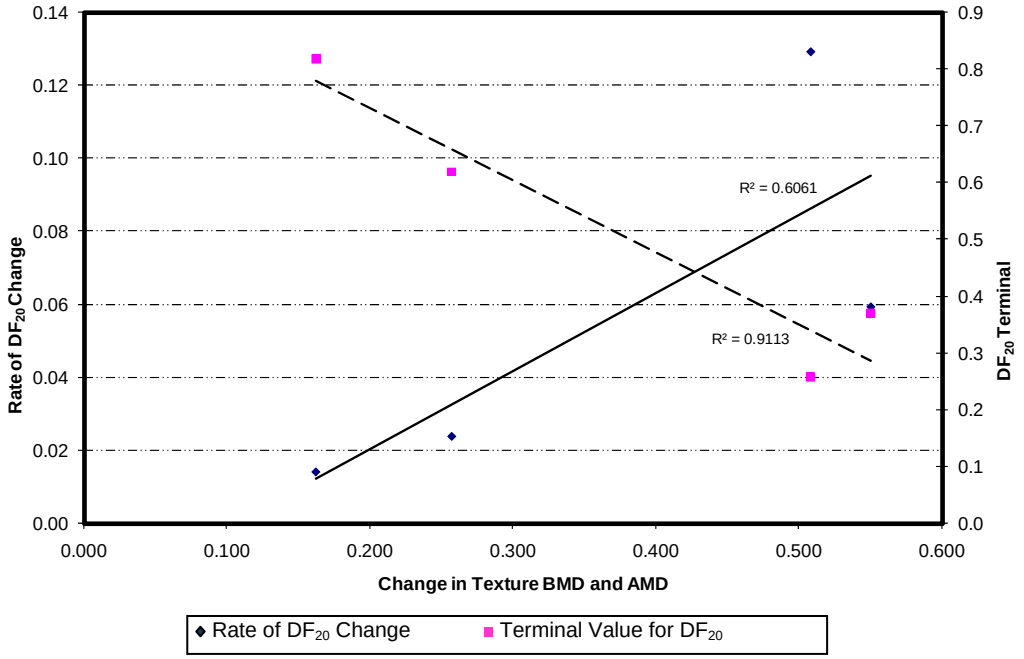

Figure 129. Rate of DF_{20} Change and Terminal Value vs. Change in Texture BMD and AMD for PFC Mix.

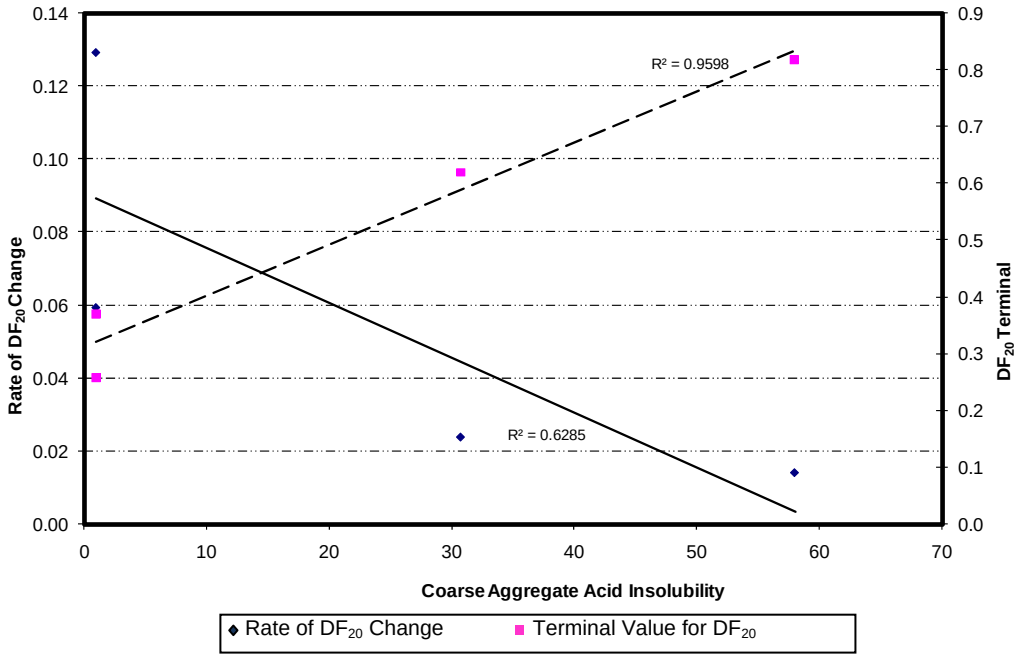

Figure 130. Rate of DF_{20} Change and Terminal Value vs. Coarse Aggregate Acid Insolubility for PFC Mix.

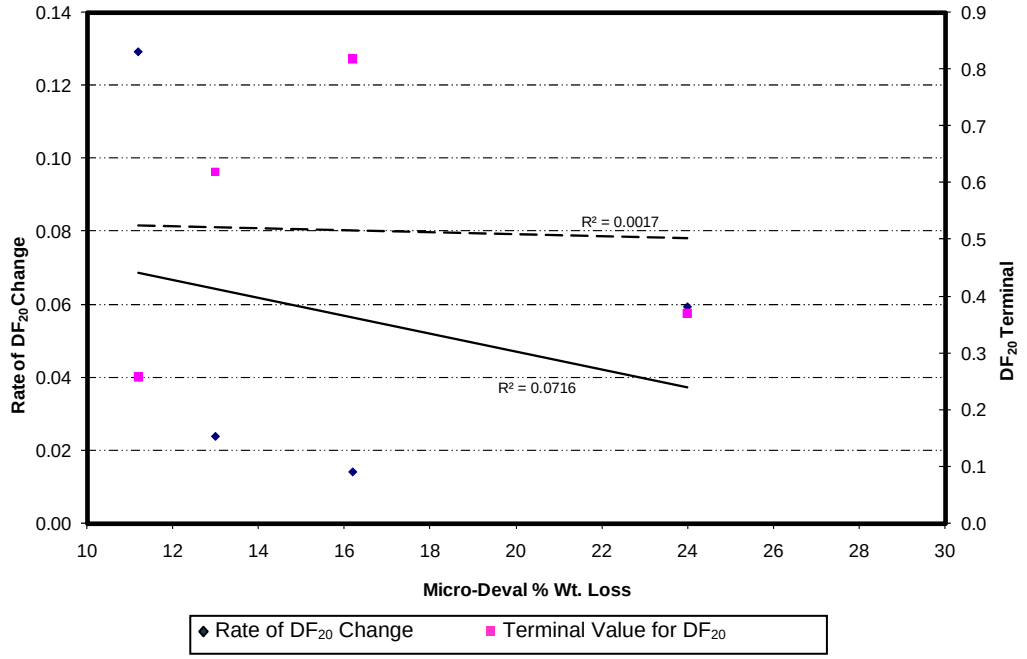

Figure 131. Rate of DF_{20} Change and Terminal Value vs. Micro-Deval Percent Weight Loss for PFC Mix.

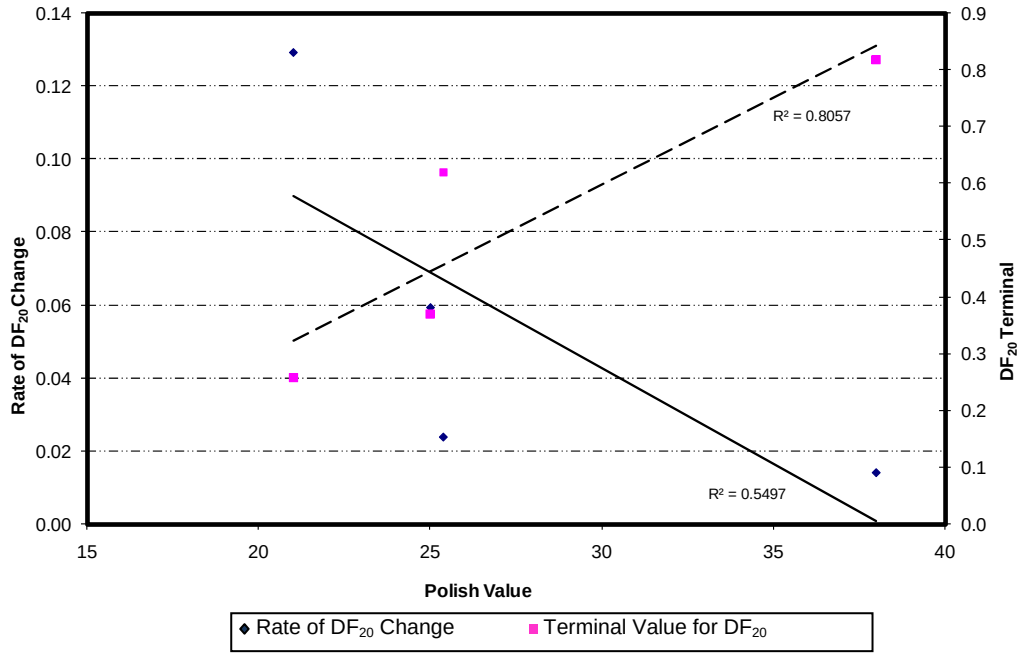

Figure 132. Rate of DF_{20} Change and Terminal Value vs. Polish Value for PFC Mix.

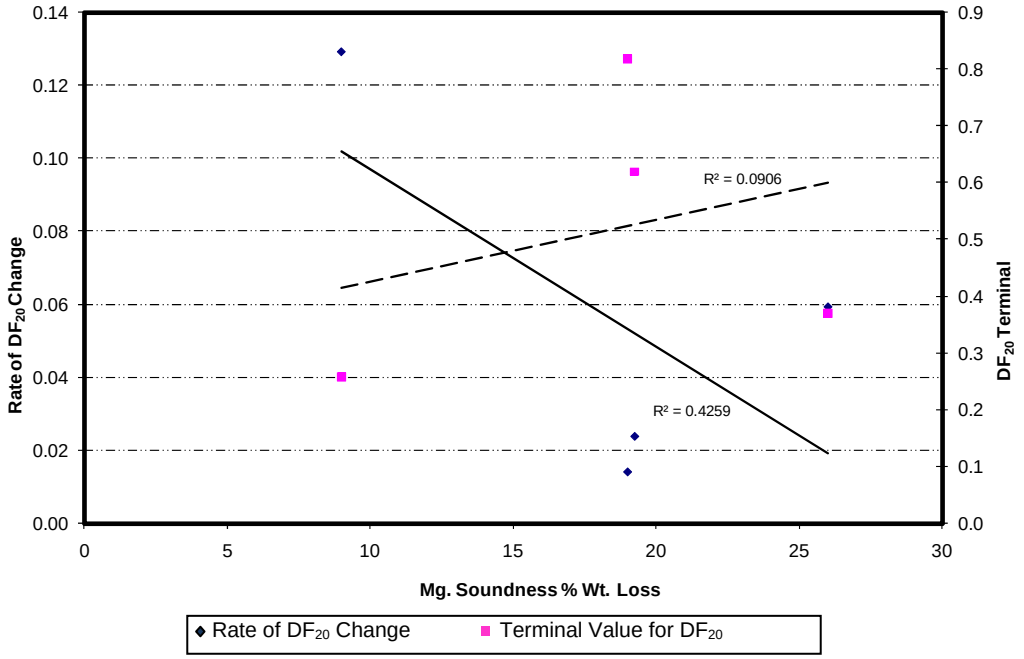

Figure 133. Rate of DF_{20} Change and Terminal Value vs. Mg. Soundness for PFC Mix.

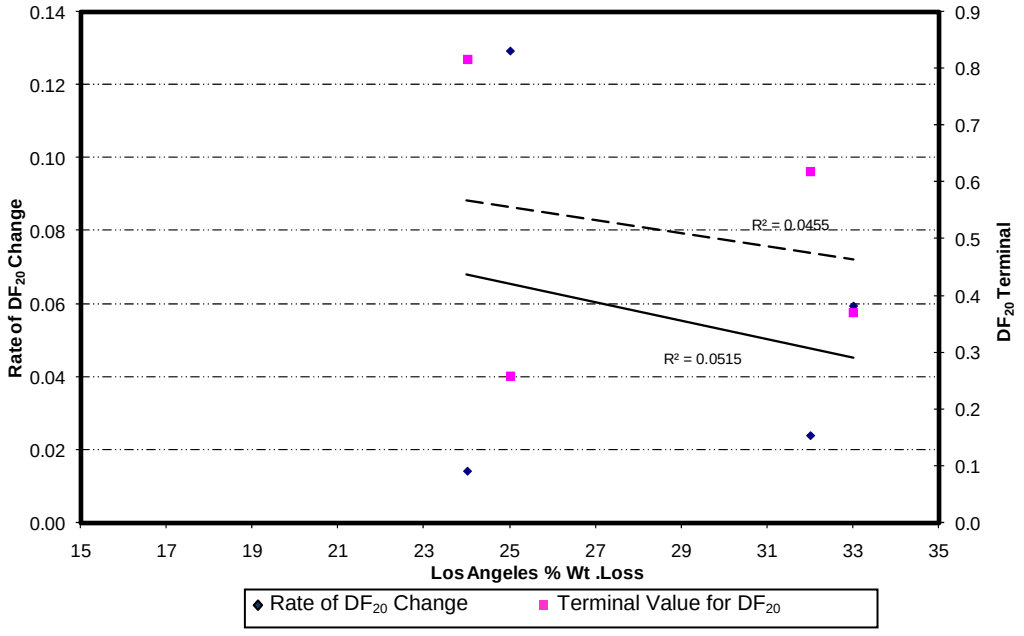

Figure 134. Rate of DF_{20} Change and Terminal Value vs. Los Angeles Percent Weight Loss for PFC Mix.

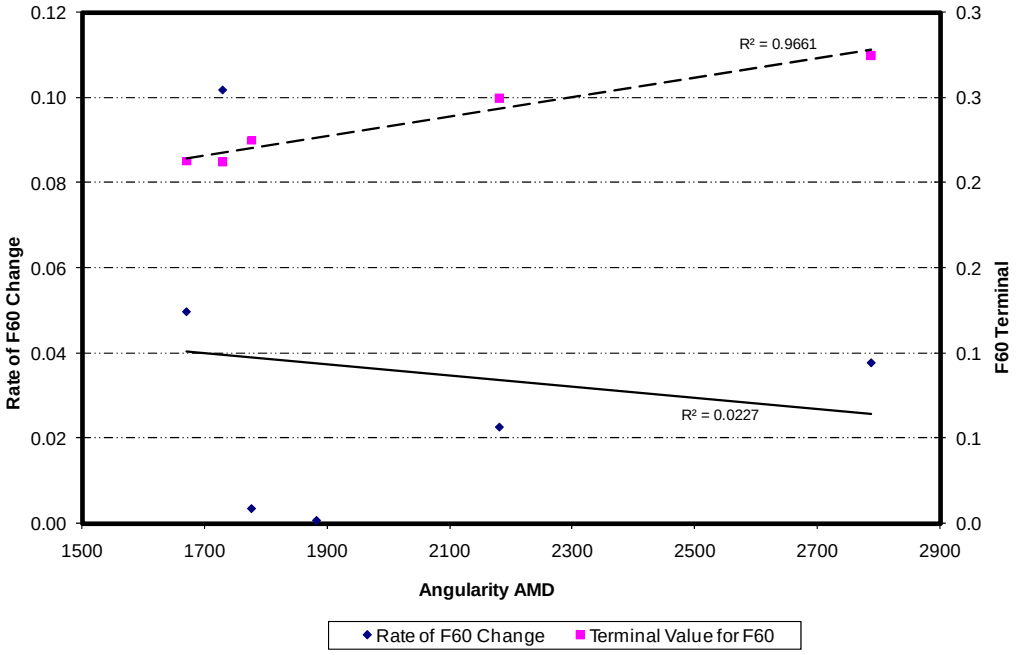

Figure 135. Rate of F60 Change and Terminal Value vs. Angularity AMD without Brownlee.

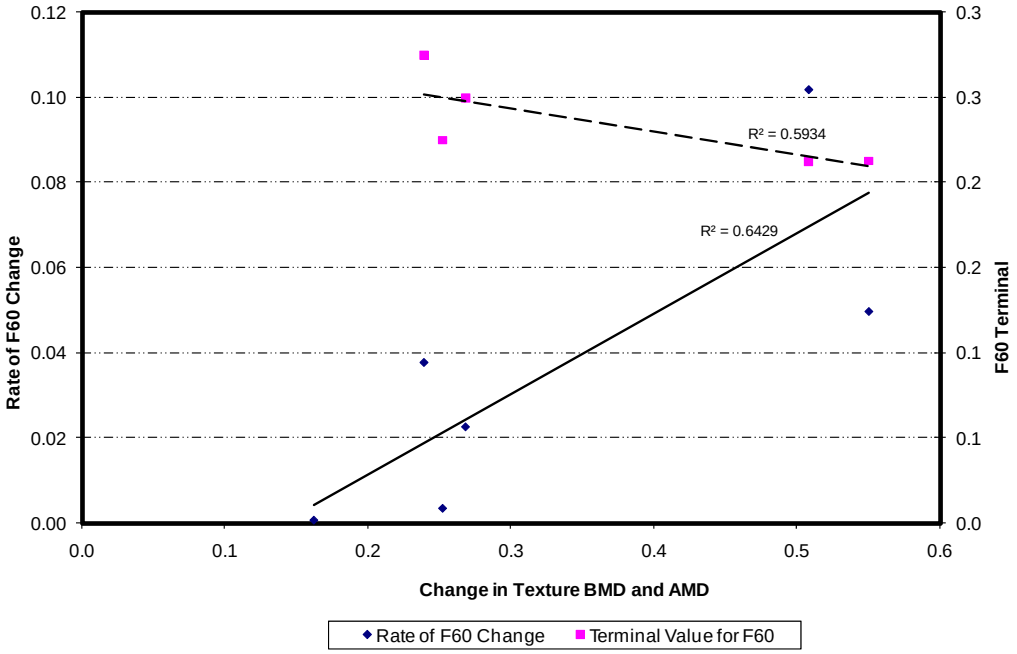

Figure 136. Rate of F60 Change and Terminal Value vs. Change in Texture BMD and AMD without Brownlee.

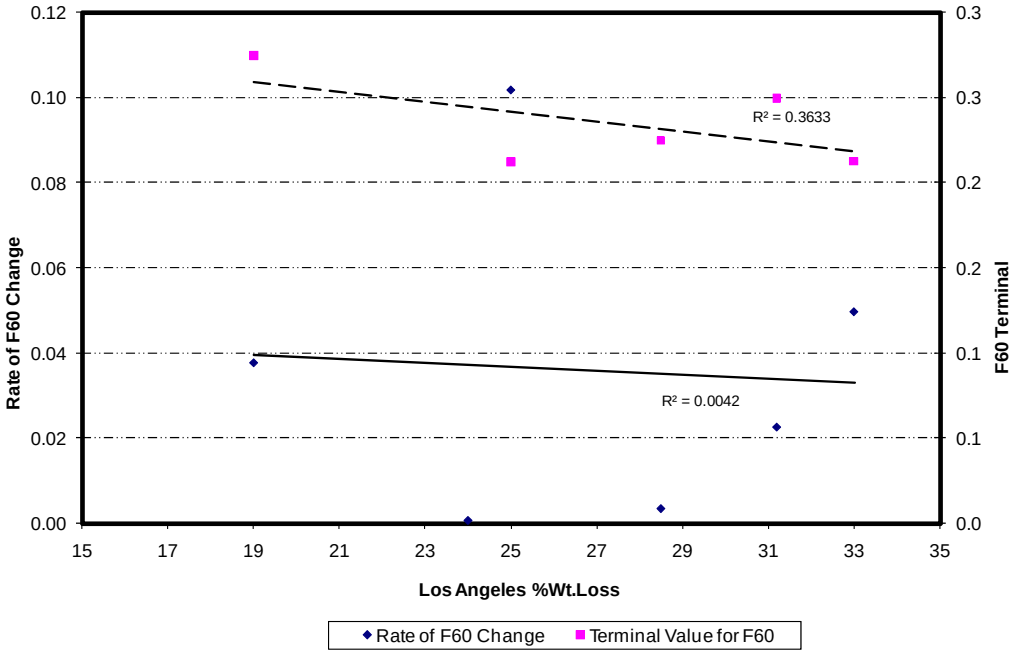

Figure 137. Rate of F60 Change and Terminal Value vs. Los Angeles Percent Weight Loss without Brownlee.

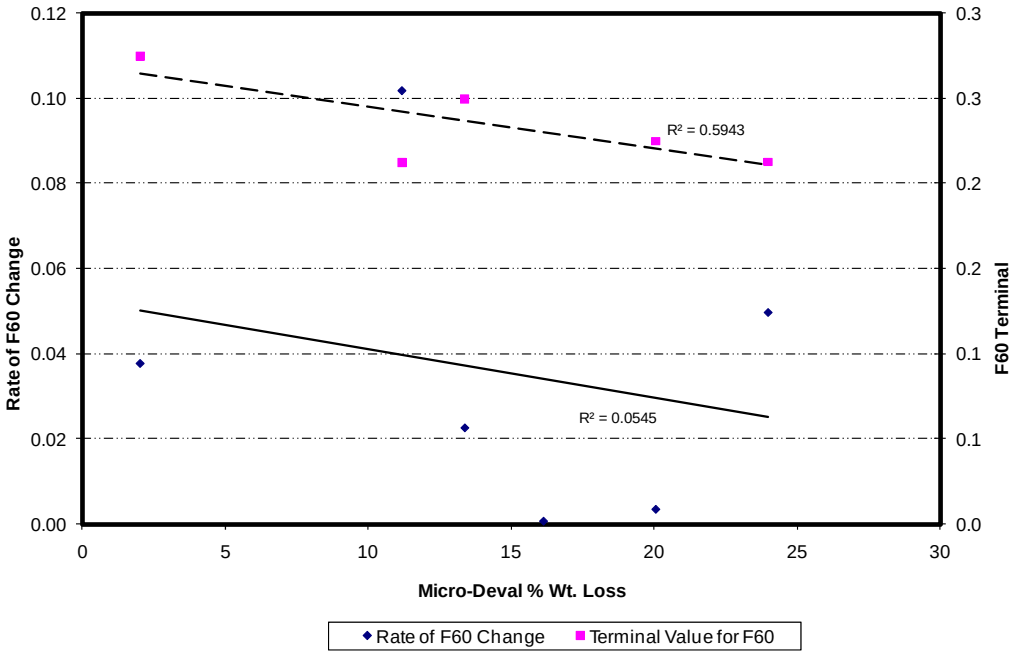

Figure 138. Rate of F60 Change and Terminal Value vs. Micro-Deval Percent Weight Loss without Brownlee.

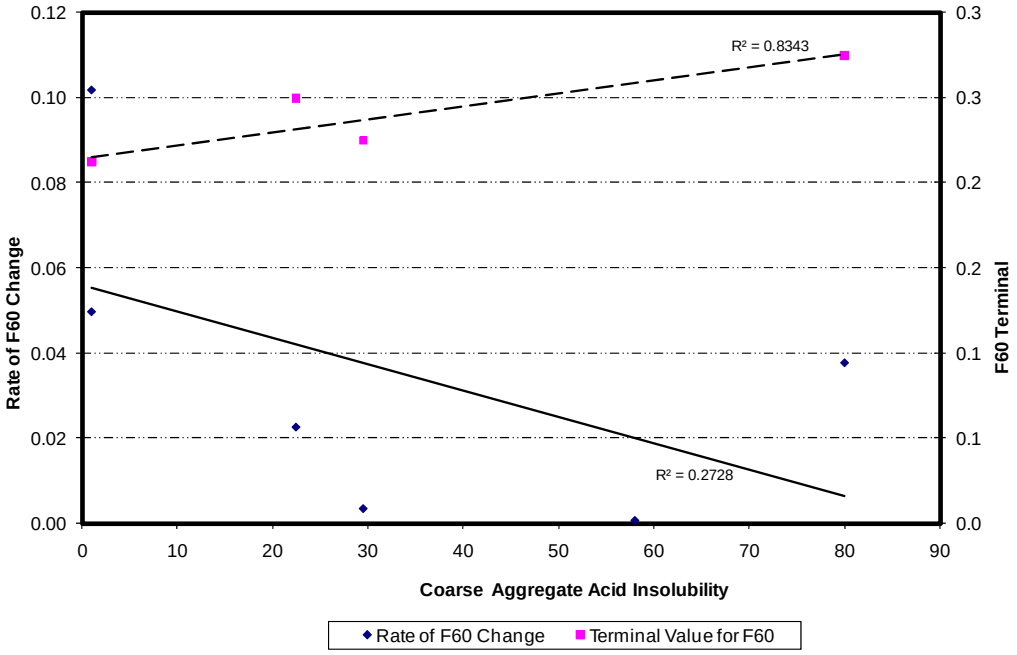

Figure 139. Rate of F60 Change and Terminal Value vs. Coarse Aggregate Acid Insolubility without Brownlee.

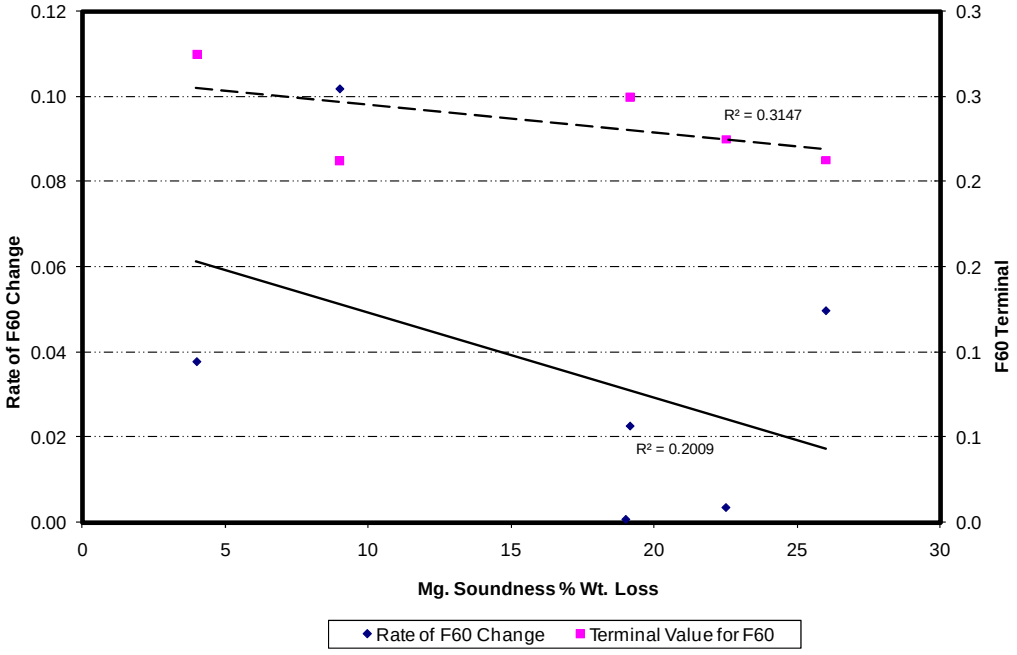

Figure 140. Rate of F60 Change and Terminal Value vs. Mg Soundness without Brownlee.